Engineering Institute of Porto

Department of Electrical Engineering

Energy Resource Management in Smart Grids Considering an Intensive use of Electric Vehicles

by

Tiago André Bastos de Sousa

A thesis presented in partial fulfillment of the requirements for the degree of Master of Science in Electrical Power Systems

Supervisor: Professor Zita Vale, Ph.D.

Co-Supervisor: Research Assistant Hugo Morais, MSc.

November 2011

Dedicated to my parents

"Logic will get you from A to B.
Imagination will take you everywhere"
(Albert Einstein)

Acknowledgements

I want to start by thanking Professor Zita Vale and Hugo Morais, my supervisor and co-supervisory respectively. I would like to express my gratitude to their dedication, support, guidance and mainly to their constant ideas and opinions about this work, which were in a big part responsible for the successful conclusion of this thesis. To professor Zita, I have a special thank you, not only concerning the supervisory, but also as GECAD director, for all the time that I spent in studying and working during my master degree course. During these 2 years, I had to spend a lot of time studying for my course, and I did not dedicate the same time in my GECAD tasks, this fact had a big impact in my performance as researcher. Even knowing that, Professor Zita did not warn me as a normal Director would do in this situation. Even without directly talking to me about my master course I knew that she supports me to study more and more in all the courses. I owe this to her, without her care and compassion I could not achieve this high performance, which I did not imagine that was possible in the beginning of this master degree.

I sincerely need to thank my co-supervisory Hugo Morais. Hugo was the first person who believed that I have the profile to be a GECAD researcher, and contribute in GECAD's projects. He was responsible by changing my perspectives of the future, and from his invite to be a researcher in GECAD at a class of SELE 1 in December 2007, I realized that researching is an interesting field. More recently, with his advice to move on my studies to a PhD course, I entirely realized that this was my future. During these years in GECAD, he has been a model to me, an example as a teacher, a researcher, a worker, a friend and a man. It has been a pleasure to work with him and if I become an infinitesimal part of what he is now, for me it will be a truly objective of life. I have to say that without my two supervisors, not only this work could not achieve this level but also I could not be in the level that I am right now.

Now I want to thank to GECAD workers, I am not the first and I will not be the last one to have this opinion about the GECAD workers, but I have to register here my thank you to a special family that GECAD workers are. In GECAD we constantly have discussions about the behaviors of some workers on GECAD, and we conclude that the first requirement to hire a researcher to GECAD is that person should have some "craziness", otherwise he/she would not be a good GECAD worker. I have to say that I could not agree more with this opinion, but it is this "craziness" that makes GECAD workers so special. Even in a future I have to work in another place I know for sure that GECAD is the best place I will ever work in. We can be crazy some times, but when cooperation is required to conclude any kind of articles or projects, everybody is there helping each other, and that is what makes us special and at the same time "crazy". That is why I do not get tired of working as many hours as necessary to help a colleague in achieving an individual objective, even if it means working during off office hours, such as Saturday and Sunday.

During the development of this thesis some GECAD workers helped me a lot in finishing my work. That is why I would like to express my gratitude and admiration for the following people: Bruno Canizes, Joana Neves, Marco Silva, Pedro Faria, Pedro Oliveira and Tiago Pinto. I would specially like to thank Tiago Pinto for all his great help and contribution to this thesis, and mainly for his friendship. During these last months of thesis writing you helped me in some many ways that I do not have the right words to thank you for all your support. You did not just review my thesis but you also

contributed to improving this document, and this document has parts of you! I hope that someday, maybe in your PhD I can repay my debt to you, MY FRIEND! I also want to express my admiration to Marco Silva; he did not just support me in this document but during my work in GECAD since March 2008. Marco always helped me in many ways, and I admire him for all the availability to help others without even care about his own work. For your master thesis, I will help in everything I can to repay all your help and friendship.

Continuing in the GECAD universe, I would like to express my gratitude to all the players of the GECAD futsal team. Being the manager of the team was a pleasure to me, even though my only role in the team was yelling and insulting the referee. Sincerely, it was a pleasure to wake up early all the Saturdays and assist our games. My thank you to all players: Antero Henriques, Bêbado, Costa, Discípulo, Filas, Filipão, Laranjeira, Luca Toni, Messi, Reyes, Ronaldo, Sérgio.

I have to express my gratitude and thank to a family that shared so many things with me along these about 5 years in ISEP. I am talking about the friends that I made during my bachelor and master courses. Without you I could not be the person that I am now, I have learned so many things with you. Unfortunately, I am an only child, but I could say that, for me, you are my brothers, and I am very fortunate to have met you all: Fininho, Gondomar, Lucho, Madeiras, Manteigas, Martins, Rafael, Ricardo, Pedro.

I would like to express my deepest gratitude to Rui Moreira, Helena Agante and João Duarte for their wise advices about my decision in PhD course, mainly to Rui Moreira and his constant incentives to continue my studies to PhD. I am truly grateful to Rui Moreira and his total availability during these months. I am very blessed to have you as my best friend.

To my high school friends: Bruno Costa, Bruno Fátima, Luís Castro and Rui Campos. I am grateful for all the friendship and I am sorry for my absence during these 5 years. Even in my absence they always supported me to keep going with my studies and shared with me my successes and victories during this journey.

Last but not least, a sincerely and deserved thank you goes to my mother - Maria de la Salete Sousa, my father - Anselmo Sousa, and my neighbor - Rosa Enes. To my parents I owe everything; my character is totally influenced by their attitudes. Without their education I would not be the man that I became, I know that is a cliché but they are the best parents and the persons that I most admire in the entire world. This work is totally dedicated to my parents.

Abstract

The introduction of electricity markets and integration of Distributed Generation (DG) have been influencing the power system's structure change. Recently, the smart grid concept has been introduced, to guarantee a more efficient operation of the power system using the advantages of this new paradigm. Basically, a smart grid is a structure that integrates different players, considering constant communication between them to improve power system operation and management. One of the players revealing a big importance in this context is the Virtual Power Player (VPP).

In the transportation sector the Electric Vehicle (EV) is arising as an alternative to conventional vehicles propel by fossil fuels. The power system can benefit from this massive introduction of EVs, taking advantage on EVs' ability to connect to the electric network to charge, and on the future expectation of EVs ability to discharge to the network using the Vehicle-to-Grid (V2G) capacity. This thesis proposes alternative strategies to control these two EV modes with the objective of enhancing the management of the power system. Moreover, power system must ensure the trips of EVs that will be connected to the electric network. The EV user specifies a certain amount of energy that will be necessary to charge, in order to ensure the distance to travel.

The introduction of EVs in the power system turns the Energy Resource Management (ERM) under a smart grid environment, into a complex problem that can take several minutes or hours to reach the optimal solution. Adequate optimization techniques are required to accommodate this kind of complexity while solving the ERM problem in a reasonable execution time.

This thesis presents a tool that solves the ERM considering the intensive use of EVs in the smart grid context. The objective is to obtain the minimum cost of ERM considering: the operation cost of DG, the cost of the energy acquired to external suppliers, the EV users payments and remuneration and penalty costs.

This tool is directed to VPPs that manage specific network areas, where a high penetration level of EVs is expected to be connected in these areas. The ERM is solved using two methodologies: the adaptation of a deterministic technique proposed in a previous work, and the adaptation of the Simulated Annealing (SA) technique. With the purpose of improving the SA performance for this case, three heuristics are additionally proposed, taking advantage on the particularities and specificities of an ERM with these characteristics.

A set of case studies are presented in this thesis, considering a 32 bus distribution network and up to 3000 EVs. The first case study solves the scheduling without considering EVs, to be used as a reference case for comparisons with the proposed approaches. The second case study evaluates the complexity of the ERM with the integration of EVs. The third case study evaluates the performance of scheduling with different control modes for EVs. These control modes, combined with the proposed SA approach and with the developed heuristics, aim at improving the quality of the ERM, while reducing drastically its execution time. The proposed control modes are: uncoordinated charging, smart charging and V2G capability. The fourth and final case study presents the ERM approach applied to consecutive days.

Keywords

Electric Vehicles, Energy Resource Management, Heuristic optimization, Simulated Annealing, Smart Grid, Virtual Power Player.

Resumo

A introdução dos mercados de electricidade e integração da produção distribuída tem causado alterações na estrutura e no modo de operação dos sistemas eléctricos de energia. Recentemente, o conceito de *SmartGrid* foi introduzido com o objectivo de garantir uma operação mais eficiente dos sistemas eléctricos de energia. Basicamente, uma *SmartGrid* é uma estrutura que envolve as diferentes entidades, e considera uma constante interacção e comunicação entre as mesmas, para melhorar a operação do sistema eléctrico de energia. Umas das entidades com grande relevância neste contexto são os *Virtual Power Players* (VPP).

Os Veículos Eléctricos (VE) têm surgido no sector dos transportes como uma alternativa aos veículos convencionais abastecidos por combustíveis fósseis. O sistema eléctrico de energia pode beneficiar dessa introdução massiva de VEs, aproveitando a sua capacidade de ligação à rede eléctrica para a carga dos veículos, e numa perspectiva mais vanguardista para descarga, fornecendo energia à rede. Nesta tese são propostas estratégias de gestão das cargas/descargas do VE com o objectivo de melhorar a operação do sistema eléctrico de energia. No processo de gestão de recursos, o operador da rede ou agregadores deverão considerar as necessidades dos utilizadores dos VEs, nomeadamente garantir a existência de energia suficiente nas baterias para que os utilizadores possam efectuar as viagens que tem programadas.

A introdução dos veículos eléctricos nos sistemas eléctricos de energia torna a gestão de recurso energéticos num ambiente de *SmartGrid*, um problema complexo que pode levar vários minutos ou horas para se obter uma solução. Considerando o período para o qual é necessário efectuar o escalonamento, que normalmente é para o dia seguinte ou para os 15 minutos seguintes no caso de escalonamento em tempo real, é necessário desenvolver algoritmos que permitam a resolução dos problemas em tempos muito razoáveis.

Nesta tese é apresentada uma ferramenta que permite a resolução do problema do escalonamento de recursos, considerando o uso intensivo de VEs no contexto das *SmartGrid*. O objectivo é obter o custo mínimo de operação, considerando: o custo de operação da produção distribuída, o custo da energia adquirida a fornecedores externos, a remuneração do uso de VEs e os custos associados ao incumprimento de condições contratuais.

A ferramenta desenvolvida é direccionada para a utilização pelos VPPs que gerem áreas de rede específicas, com um nível de penetração elevado de VEs. O escalonamento de recursos é resolvido usando duas metodologias: a adaptação de uma técnica determinista proposta em trabalhos anteriores, e a adaptação da técnica de *Simulated Annealing*, sendo propostas três abordagens para melhorar a solução obtida através da técnica de *Simulated Annealing*.

Diversos casos de estudo são apresentados, considerando uma rede de distribuição com 32 barramentos e cenários de evolução da penetração de VE até 3000 veículos. O primeiro caso de estudo, usado como um caso de referência para comparações com as abordagens propostas, resolve o escalonamento de recursos sem considerar VEs. O segundo caso avalia a complexidade do escalonamento de recursos com a integração de VEs, permitindo testar as técnicas propostas. O terceiro caso avalia o desempenho do escalonamento com diferentes modos de controlo de EVs. O quarto caso de estudo apresenta a abordagem aplicada ao escalonamento de recursos em diversos dias consecutivos.

Acronyms

Notation		Description
AI	-	**A**rtificial **I**ntelligence
BCG	-	**B**oston **C**onsulting **G**roup
BEV	-	**B**attery **E**lectric **V**ehicle
BIBC	-	**B**us-**I**njection to **B**ranch-**C**urrent
BMS	-	**B**attery **M**anagement **S**ystem
CI	-	**C**ompression **I**gnition
CO_2	-	Carbon dioxide
CONOPT	-	**Con**tinuous global **Opt**imizer
CPLEX	-	Simplex algorithm and C programming
DER	-	**D**istributed **E**nergy **R**esource
DG	-	**D**istributed **G**eneration
DICOPT	-	**Di**screte and **C**ontinuous **Opt**imizer
DM	-	**Dom**estic consumer
DNO	-	**D**istribution **N**etwork **O**perator
DSPFAP	-	**D**istribution **S**ystems **P**ower **F**low **A**nalysis **P**ackage
EHV	-	**E**xtra **H**igh **V**oltage
ERM	-	**E**nergy **R**esource **M**anagement
ERMaS	-	**E**nergy **R**esource **Ma**nagement in **S**mart Grid
EV	-	**E**lectric **V**ehicle
f/d	-	**f**orward/**b**ackward
FCV	-	**F**uel **C**ell **V**ehicle
FD	-	**F**ast **D**ecoupled
GAMS	-	**G**eneral **A**lgebraic **M**odeling **S**ystem
G-S	-	**G**auss-**S**eidel
GSM	-	**G**lobal **S**ystem for **M**obile
GVPP	-	**G**lobal **V**irtual **P**ower **P**layer
HEV	-	**H**ybrid **E**lectric **V**ehicle
ICE	-	**I**nternal **C**ombustion **E**ngine
IEA	-	**I**nternational **E**nergy **A**gency
IEC	-	**I**nternational **E**lectrotechnical **C**ommission
ISO	-	**I**ndependent **S**ystem **O**perator
JARI	-	**J**apan **A**utomotive **R**esearch **I**nstitutes
LC	-	**L**arge **C**ommerce
LFP	-	**L**ithium-Iron-**P**hosphate
LI	-	**L**arge **I**ndustrial

Li-ion	-	**Li**thium-**ion**
LMP	-	**L**ocational **M**arginal **P**rice
LSVPP	-	**L**arge **S**cale **V**irtual **P**ower **P**layer
LTO	-	**L**ithium-**T**itanate
MATLAB	-	**Mat**rix **Lab**oratory
MaxIter	-	**Max**imum number of **Iter**ations
MC	-	**M**edium **C**ommerce
MI	-	**M**edium **I**ndustrial
MINLP	-	**M**ixed-**I**nteger **N**on-**L**inear **P**rogramming
MIP	-	**M**ixed-**I**nteger **P**rogramming
MO	-	**M**arket **O**perator
NCA	-	Lithium-**N**ickel-**C**obalt-**A**luminum
NiMH	-	**Ni**ckel **M**etal-**H**ydride
NIST	-	**N**ational **I**nstitute of **S**tandards and **T**echnology
NLP	-	**N**on-**L**inear **P**rogramming
NMC	-	Lithium-**N**ickel-**M**anganese-**C**obalt
N-R	-	**N**ewton-**R**aphson
PHEV	-	**P**lug-in **H**ybrid **E**lectric **V**ehicle
PLC	-	**P**ower **L**ine **C**arrier
PSCAD	-	**P**ower **S**ystem **C**omputer **A**ided **D**esign
PVPP	-	**P**arallel **V**irtual **P**ower **P**layer
RAM	-	**R**andom-**a**ccess-**m**emory
SA	-	**S**imulated **A**nnealing
SAE	-	**S**ociety of **A**utomotive **E**ngineers
SC	-	**S**mall **C**ommerce
SCADA	-	**S**upervisory **C**ontrol **a**nd **D**ata **A**cquisition
SI	-	**S**park **I**gnition
Std Dev	-	**St**an**d**ard **Dev**iation
SVPP	-	**S**everal **V**irtual **P**ower **P**layer
TSO	-	**T**ransmission **S**ystem **O**perator
UNIFRND	-	**Unif**orm distributed **r**a**nd**om function in MATLAB
V2G	-	**V**ehicle-**to**-**G**rid
VPP	-	**V**irtual **P**ower **P**layer

Nomenclature

Notation		Description	Unit	
α	-	Cooling rate value from 0 to 1 applied to the geometric scheme of the simulated annealing	-	-
Δt	-	Elementary period	Hour	(h)
ΔI_i^k	-	Current mismatch to control the voltage magnitude for the bus *i* in iteration *k*	Ampere	(A)
ΔV_i^k	-	Voltage magnitude mismatch between the specific and calculated voltage magnitude for the bus PV *i* in iteration *k*	Volt	(V)
$\eta_{c(V)}$	-	Grid-to-Vehicle Efficiency	-	(%)
$\eta_{d(V)}$	-	Vehicle-to-Grid Efficiency	-	(%)
$\theta_{i(t)}$	-	Voltage angle at bus *i* in period *t*	Radians	(rad)
θ_i^{max}	-	Maximum voltage angle at bus *i*	Radians	(rad)
θ_i^{min}	-	Minimum voltage angle at bus *i*	Radians	(rad)
$\theta_{j(t)}$	-	Voltage angle at bus *j* in period *t*	Radians	(rad)
avpp	-	Average vehicles per period	-	-
B_{ii}	-	Imaginary part of the element in admittance matrix corresponding to the *i* row and *i* column	Siemens	(S)
B_{ij}	-	Imaginary part of the element in admittance matrix corresponding to the *i* row and *j* column	Siemens	(S)
$\overline{B_L^k}$	-	Current of branch *L* in polar form at iteration *k*	Ampere	(A)
$c_{A(DG,o,t)}$	-	Fixed cost coefficient of offer *o* for the *DG* unit in period *t*	Monetary unit	(m.u.)
$c_{B(DG,o,t)}$	-	Linear cost coefficient of offer *o* for the *DG* unit in period *t*	Monetary unit per Watt	(m.u./W)
$c_{C(DG,o,t)}$	-	Quadratic cost coefficient of offer *o* for the *DG* unit in period *t*	Monetary unit per square Watt	(m.u./W^2)
$c_{Charge(V,t)}$	-	Charge price of electric vehicle *V* in period *t*	Monetary unit per Watt	(m.u./W)
$c_{Discharge(V,t)}$	-	Discharge price of electric vehicle *V* in period *t*	Monetary unit per Watt	(m.u./W)
$c_{Discharge\_StepA(V,t)}$	-	Discharge price of step A of vehicle *V* in period *t*	Monetary unit per Watt	(m.u./W)
$c_{Discharge\_StepB(V,t)}$	-	Discharge price of step B of vehicle *V* in period *t*	Monetary unit per Watt	(m.u./W)
$c_{Discharge:StepC(V,t)}$	-	Discharge price of step C of vehicle *V* in period *t*	Monetary unit per Watt	(m.u./W)
$c_{EAP(DG,t)}$	-	Excess available power cost of *DG* unit in period *t*	Monetary unit per Watt	(m.u./W)
$c_{NSD(L,t)}$	-	Non-supplied demand cost of load *L* in	Monetary	(m.u./W)

		period *t*	unit per Watt	
$c_{Supplier(S,o,t)}$	-	Market energy price of offer *o* for the external supplier *S* in period *t*	Monetary unit per Watt	(m.u./W)
$E_{BatteryCapacity(V)}$	-	Battery energy capacity of electric vehicle *V* (Wh)	Watt hour	(Wh)
$E_{Initial(V)}$	-	Energy stored of the electric vehicle *V* in the beginning of period 1 (initial value)	Watt hour	(Wh)
$E_{MinCharge(V,t)}$	-	Minimum stored energy to be guaranteed at the end of period *t*, for electric vehicle *V*	Watt hour	(Wh)
$E_{Stored(V,t)}$	-	Energy stored in vehicle *V* at the end of period *t*	Watt hour	(Wh)
$E_{Trip(V,t)}$	-	Energy consumption during a trip of the electric vehicle *V* in period *t*	Watt hour	(Wh)
f	-	Objective function value	Monetary unit	(m.u)
F	-	Fitness function value of the proposed simulated annealing	-	-
f_1	-	Objective function part that handles the operation cost of the distributed generation	Monetary unit	(m.u)
f_2	-	Objective function part that handles the price exchange with the external suppliers	Monetary unit	(m.u)
f_3	-	Objective function part that handles the payments with the electric vehicle users	Monetary unit	(m.u)
f_4	-	Objective function part that handles the penalization cost	Monetary unit	(m.u)
G_{ii}	-	Real part of the element in admittance matrix corresponding to the *i* row and *i* column	Siemens	(S)
G_{ij}	-	Real part of the element in admittance matrix corresponding to the *i* row and j column	Siemens	(S)
$\overline{I_i^k}$	-	Injected current in bus i at iteration *k*	Ampere	(A)
$\overline{I_{ij(t)}}$	-	Current in the line that connect the bus *i* and *j* in polar form at period *t*	Ampere	(A)
$\overline{I_{sh\_i(t)}}$	-	Current in the shunt admittance of line connected to the bus *i* in polar form at period *t*	Ampere	(A)
L^i	-	Set of lines connected to bus *i*	-	-
M	-	Set of loads connected to line *L*	-	-
N_B	-	Total number of buses	-	-
N_{DG}	-	Total number of distributed generators	-	-
N_{DG}^i	-	Total number of *DG* units for the bus *i*	-	-
N_{DG}^O	-	Total number of offers for the *DG* unit	-	-
N_K	-	Total number of lines	-	-
N_L	-	Total number of loads	-	-

N_L^i	-	Total number of *L* loads for the bus *i*	-	-
N_{MINLP}	-	Total number of variables used in the proposed mixed-integer non-linear programming	-	-
$nopp$	-	Total number of off-peak periods	-	-
N_{PV}	-	Total number of PV buses	-	-
N_S	-	Total number of external suppliers	-	-
N_S^i	-	Total number of *S* external suppliers for the bus *i*	-	-
N_S^O	-	Total number of offers *o* for the *S* external suppliers	-	-
N_{SA}	-	Total number of variables used in the proposed simulated annealing	-	-
N_V	-	Total number of electric vehicles	-	-
N_V^i	-	Total number of electric vehicles for the bus *i*	-	-
$P_{Charge(V,t)}$	-	Active power charge of electric vehicle *V* in period *t*	Watt	(W)
$P_{Charge(V,t)}^i$	-	Active power charge of electric vehicle *V* at bus *i* in period *t*	Watt	(W)
$P_{ChargeLimit(V,t)}$	-	Maximum active power charge of vehicle *V* in period *t*	Watt	(W)
$\overline{P_{ChargeLimit(nopp)}}$	-	Average maximum active power charge of all vehicle in the off-peak periods	Watt	(W)
$P_{DG(DG,o,t)}$	-	Active power generation of offer *o* for the *DG* unit in period *t*	Watt	(W)
$P_{DG(DG,o,t)}^i$	-	Active power generation of offer *o* for the *DG* unit at bus *i* in period *t*	Watt	(W)
$P_{DGMaxLimit(DG,o,t)}$	-	Maximum active power generation of offer *o* for the *DG* unit in period *t*	Watt	(W)
$P_{DGMinLimit(DG,o,t)}$	-	Minimum active power generation of offer *o* for the *DG* unit in period *t*	Watt	(W)
$P_{Discharge(V,t)}$	-	Active power discharge of electric vehicle *V* in period *t*	Watt	(W)
$P_{Discharge(V,t)}^i$	-	Active power discharge of electric vehicle *V* at bus *i* in period *t*	Watt	(W)
$P_{DischargeLimit(V,t)}$	-	Maximum active power discharge of electric vehicle *V* in period *t*	Watt	(W)
$P_{Discharge\_StepA(V,t)}$	-	Power discharge in step A of vehicle *V* in period *t*	Watt	(W)
$P_{Discharge\_StepB(V,t)}$	-	Power discharge in step B of vehicle *V* in period *t*	Watt	(W)
$P_{Discharge\_StepC(V,t)}$	-	Power discharge in step C of vehicle *V* in period *t*	Watt	(W)
$P_{Di(t)}$	-	Active power demand at bus *i* in period *t*	Watt	(W)
$P_{EAP(DG,t)}$	-	Excess available power by *DG* unit in period *t*	Watt	(W)
$P_{EAP(DG,t)}^i$	-	Excess available power by *DG* unit at bus *i* in period *t*	Watt	(W)
$P_{Gi(t)}$	-	Active power generation at bus *i* in period *t*	Watt	(W)

$P^{i}_{Load(L,t)}$	-	Active power demand of load *L* at bus *i* in period *t*	Watt	(W)
$P_{NSD(L,t)}$	-	Active power non-supplied demand for load *L* in period *t*	Watt	(W)
$P^{i}_{NSD(L,t)}$	-	Active power non-supplied demand for load *L* at bus *i* in period *t*	Watt	(W)
$P_{Supplier(S,o,t)}$	-	Active power generation of offer *o* for the external *S* supplier in period *t*	Watt	(W)
$P^{i}_{Supplier(S,o,t)}$	-	Active power generation of offer *o* for the external supplier *S* at bus *i* in period *t*	Watt	(W)
$P_{SupplierLimit(S,o,t)}$	-	Maximum active power of offer *o* for the external supplier *S* in period *t*	Watt	(W)
$P_{Vehicle(V,t)}$	-	Active power charge/discharge of electric vehicle *V* in period *t* of proposed simulated annealing	Watt	(W)
$Q_{DG(DG,o,t)}$	-	Reactive power generation of offer *o* for the *DG* unit in period *t*	Volt-ampere reactive	(VAr)
$Q^{i}_{DG(DG,o,t)}$	-	Reactive power generation of offer *o* for the *DG* unit at bus *i* in period *t*	Volt-ampere reactive	(VAr)
$Q_{DGMaxLimit(DG,o,t)}$	-	Maximum reactive power generation of offer *o* for the *DG* unit in period *t*	Volt-ampere reactive	(VAr)
$Q_{DGMinLimit(DG,o,t)}$	-	Minimum reactive power generation of offer *o* for the *DG* unit in period *t*	Volt-ampere reactive	(VAr)
$Q_{Di(t)}$	-	Reactive power demand at bus *i* in period *t*	Volt-ampere reactive	(VAr)
$Q_{Gi(t)}$	-	Reactive power generation at bus *i* in period *t*	Volt-ampere reactive	(VAr)
$Q^{i}_{Load(L,t)}$	-	Reactive power demand of load *L* at bus *i* in period *t*	Volt-ampere reactive	(VAr)
$Q_{NSD(L,t)}$	-	Reactive power non-supplied demand for load *L* in period *t*	Volt-ampere reactive	(VAr)
$Q^{i}_{NSD(L,t)}$	-	Rective power non-supplied demand for load *L* at bus *i* in period *t*	Volt-ampere reactive	(VAr)
$Q_{Supplier(S,o,t)}$	-	Reactive power generation of offer *o* for the external supplier *S* in period *t*	Volt-ampere reactive	(VAr)
$Q^{i}_{Supplier(S,o,t)}$	-	Reactive power generation of offer *o* for the external supplier *S* in period *t*	Volt-ampere reactive	(VAr)
$Q_{SupplierLimit(S,t)}$	-	Maximum reactive power of the external supplier *S* in period *t*	Volt-ampere reactive	(VAr)
$\overline{S_{Di}}$	-	Apparent power demand at bus *i* in period *t*	Volt-ampere	(VA)
$\overline{S_{Gi}}$	-	Apparent power generation at bus *i* in period *t*	Volt-ampere	(VA)
$\overline{S_{i}}$	-	Injected apparent power at bus *i* in period *t*		
$S_{ij(t)}$	-	Apparent power flow through the line that connect the bus *i* and *j*	Volt-ampere	(VA)
S^{max}_{Lk}	-	Maximum apparent power flow	Volt-ampere	(VA)

		established in line *k* that connect the bus *i* and *j*		
T	-	Total number of periods	-	-
T_k	-	Temperature level in iteration *k*	-	-
$\overline{U_{i(t)}}$	-	Voltage at bus *i* in polar form in period *t*	Volt	(V)
$\overline{U_i^k}$	-	Voltage at sending bus *i* in polar form in iteration *k*	Volt	(V)
$\overline{U_{j(t)}}$	-	Voltage at bus *j* in polar form in period *t*	Volt	(V)
$\overline{U_j^k}$	-	Voltage at receiving bus *i* in polar form in iteration *k*	Volt	(V)
$V_{i(t)}$	-	Voltage magnitude at bus *i* in period *t*	Volt	(V)
V_i^{max}	-	Maximum voltage magnitude at bus *i*	Volt	(V)
V_i^{min}	-	Minimum voltage magnitude at bus *i*	Volt	(V)
$V_{j(t)}$	-	Voltage magnitude at bus *j* in period *t*	Volt	(V)
$W\left(\theta_i^{violated}\right)$	-	Penalty function considering all $\theta_{i(t)}$ violation	-	-
$W\left(S_{ij}^{violated}\right)$	-	Penalty function considering all $S_{Li(t)}$ violation	-	-
$W\left(V_i^{violated}\right)$	-	Penalty function considering all $V_{i(t)}$ violation	-	-
$X_{Charge(V,t)}$	-	Binary variable of vehicle *V* related to power charge in period *t*	-	-
$X_{Discharge(V,t)}$	-	Binary variable of vehicle *V* related to power discharge in period *t*	-	-
$X_{DG(DG,o,t)}$	-	Binary variable of *DG* unit related to accept the offer *o* in period *t*	-	-
X_{max}	-	Maximum value for a generic variable *X*	-	-
X_{min}	-	Minimum value for a generic variable *X*	-	-
$\overline{Y_{ij}}$	-	Series admittance of line that connect the bus *i* and *j* in polar form	Siemens	(S)
$\overline{Y_{Sh\_i}}$	-	Shunt admittance of line connected in the bus *i* in polar form	Siemens	(S)
$\overline{Y_{Sh\_j}}$	-	Shunt admittance of line connected in the bus *j* in polar form	Siemens	(S)
$\overline{Z_L}$	-	Series impedance of line *L* that connect the bus *i* and *j* in polar form	Ohm	(Ω)
Z_{sen}^{-1}	-	Sensitivity matrix which size depends on the number of PV buses	Siemens	(S)

Contents:

List of Figures

List of Tables

Chapter 1

Introduction

1. Introduction

1.1. Background and Motivation

In recent years, the power system paradigm has been changed and new players are now operating in this field [1]. Power system deregulation, introduction of competitive electricity markets and integration of increasingly large amounts of Distributed Energy Resources (DERs), namely Distributed Generation (DG), are the main changes. The increase of DG based on renewable sources has been encouraged by funding policies, in opposition to what happened in the traditional power system paradigm characterized by the existence of large power plants. Part of Portugal's obligation to the European Union 2020 targets (20-20-20 targets) [2-3] is to meet the 31% target of renewable energy consumption. In the electric sector, the Portuguese goal is to meet a target of 45% of energy production by renewable sources and 60% in 2020 [4].

The smart grid concept appears as a suitable solution to guarantee the power system operation in this new electricity paradigm [1, 5]. It is possible to find several definitions to the smart grid concept, but at this moment there is no complete consensus about it [6-8]. Essentially, the smart grid can be understood as a structure that has the main purpose to integrate different players, technologies and resources that act in this new power system context.

As it has been mentioned, this new power system paradigm has introduced new players with different objectives from the players that existed in the traditional paradigm. The National Institute of Standards and Technology (NIST) proposed in 2009 [9] a framework for the communication between the players of a smart grid. Figure 1.1 presents the NIST proposal smart grid framework. This figure includes the following players based on references [9-10]: Producers, Consumers, Independent System Operator (ISO), Market Operator (MO), Transmission System Operator (TSO) and Distribution Network Operator (DNO).

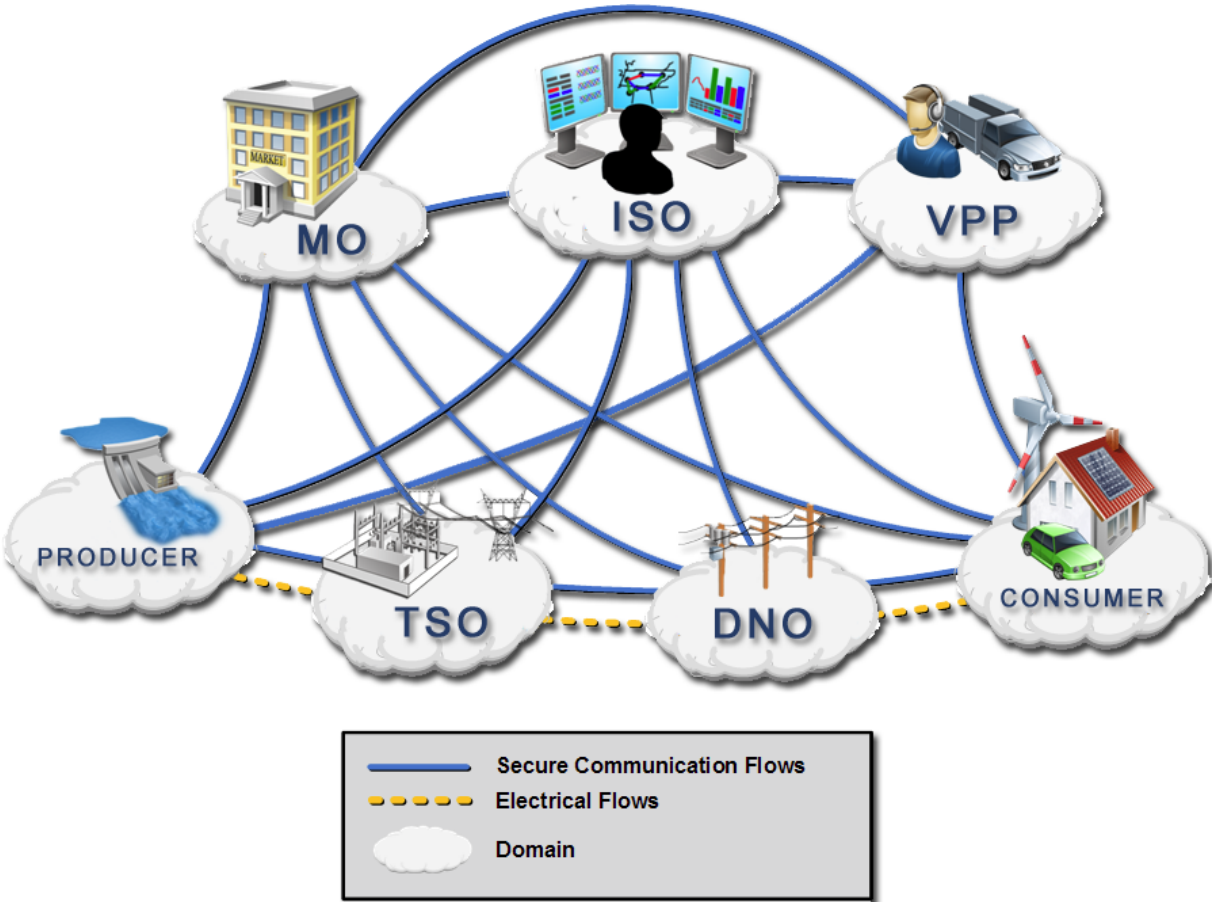

Figure 1.1 – Smart grid structure and domains (adapted from [9]).

The market operator is responsible to manage the negotiation in the electricity market; it will inform the independent system operator about the results of these negotiations. The independent system operator has the responsibility of operating, planning and maintaining the electric network, including the transmission and distribution levels [10]. It is responsible for the technical validation of the results sent by the market operator. The transmission system operator acts in the transmission network and distribution network operator only acts in the distribution network [10]. These two players can have the responsibility to operate and plan the respective networks. Producers have the responsibility to generate the required energy that has been negotiated in the electricity markets. On the other hand, consumers will consume the energy that has been negotiated in the electricity markets.

Virtual Power Players (VPPs) is other player that is represented in Figure 1.1. This player aggregates several energy resources, mainly in the distribution level [11]. The aggregation of DERs can be seen as an important strategy to improve the management of these resources.

The massive introduction of several types of DERs into the electric network, not only DG but also demand response, storage systems, and, more recently, the Electric Vehicles (EVs) is one of the reasons of the changes that occurred in power systems.

Recently, the increasing petroleum price and environmental concerns have forced governments to consider the adoption of alternative transportation solutions [12]. Electric vehicles appear as a reliable alternative in the transportation sector, and they could also represent a good available resource to the electrical sector. It is predicted that most EV models will require an electric network connection with the purpose of fully or partially charging their batteries, but EVs might also have the capability of injecting energy in the network. This approach can turn electric vehicles into an essential resource for the good management of the network in different control levels [13]. The gridable capability of injecting energy in the network is commonly referred as Vehicle-to-Grid (V2G). With a massive use of electric vehicles, the control of charge and discharge periods will be an important decision to improve the management of the available resources. On the one hand, it will be necessary to control the charge to prevent critical events in the electric network due to excessive load caused by EVs simultaneous charge. On the other hand, the V2G capability can be used as another energy resource that can be used to supply the demand, in certain periods, instead of using more expensive resources to generate energy.

Energy Resource Management (ERM) has the purpose to obtain the best scheduling of the aggregated DERs, this thesis is mainly focused on this management in the scope of a VPP [14]. Electric vehicles should be considered for this scheduling considering that EVs can behave as a load (charging mode) or as a generator (discharge mode). Typically, the VPP tries to minimize the costs associated with the scheduling of the DERs, operation costs, greenhouse gases emissions costs or active power loss costs. This optimal resource scheduling can turn into a large combinatorial problem, due to the huge number of involved DERs [14]. In a future scenario, a VPP can manage a large quantity of DG units, can have several demand response programs with each aggregated consumer and can have a large number of electric vehicles in its network area.

In order to improve DER management adequate tools are required to determine a satisfactory scheduling in terms of cost and execution time. A player in a smart grid, namely VPP, needs a tool to determine a good scheduling solution that, at the same time, maximizes its profit and is obtained in a reasonable execution time.

Some works have presented methodologies to determine the ERM solution in a smart grid context, considering different types of DERs [14]. However, the introduction of electric vehicles brings new challenges to this field, and only few works address the energy resource management problem considering EVs. These works use simplified models, such as the detailed trip profile, simple battery models or even the simplification in the electric network model. Current works in this area have only addressed parts of the whole problem. The present state of the art does not yet allow to develop an adequate tool to evaluate the real impact of electric vehicles in the network, and to determine the optimal energy resource scheduling.

1.2. Objectives

In the future energy resource management will have to handle a large amount of data required by the intensive use of electric vehicles. This can turn into a complex, hard and large combinatorial optimization problem. An optimization problem with these characteristics requires high quality computational resources, in terms of memory and processing velocity. In a smart grid environment it is expected that the energy resource management problem can be solved in a reasonable amount of time, able to cope with operation constraints and to enable the analysis of alternative scenarios.

The main objective of this work is the development of adequate methodologies to address the ERM problem previously characterized. The conceived methodologies should be computationally implemented and result in a tool that efficiently solves the energy resource management. The proposed methodologies will be integrated in the Energy Resource Management in Smart grid (ERMaS) tool that has as main purpose to determine the DERs scheduling for a specific multi-period problem, namely for day-ahead scheduling [15].

This main objective requires to address the following topics as intermediate objectives to be achieved in this work:

- Developing an energy resource management methodology, considering an intensive use of electric vehicles with the capability of both charging and discharging into the electric network;
- Implementing and analyzing the performance of deterministic methods, e.g. mixed-integer non-linear programming; and heuristic approaches, e.g. simulated annealing, envisaging the proposed energy resource management problem;
- Evaluating the impact of different penetration levels of electric vehicles in the distribution network, considering different EV control modes;
- Determining the optimal amount of energy stored in EV batteries at the end of the scheduling period considering the influence of successive days;
- Developing a tool which combines all the previously referred work.

1.3. Contributions of the Thesis

The main contributions of this thesis are the proposed methodologies to support the energy resource management of a VPP in a smart grid environment, considering an intensive used of EVs and V2G. Another important contribution is to implement the proposed methodologies upgrading the ERMaS tool to support the decision of VPP to solve the energy resource management, considering the intensive use of EVs and V2G.

The proposed methodologies aim at obtaining the optimal scheduling with an adequate balance between the execution time, solution quality and scheduling model

accuracy. In this context, the developed tool is distinct from the other energy resource management tools because it considers both technical and business models in an accurate way. The architecture of the ERMaS tool with these enhancements is presented in Figure 1.2. The proposed ERMaS tool will be explained ahead in section 3.2.

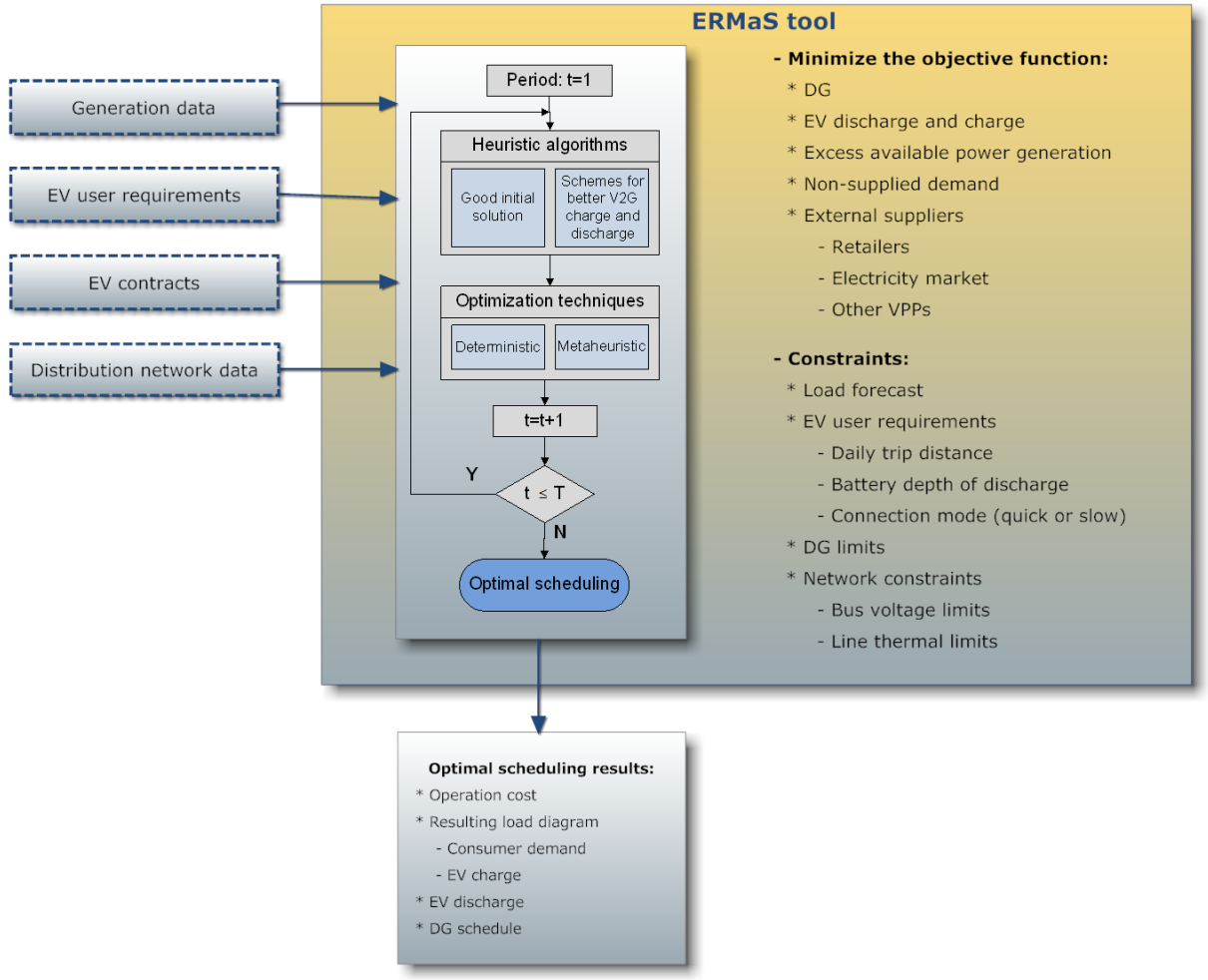

Figure 1.2 – Proposal diagram for the ERMaS tool.

The work developed in the scope of this thesis was supported by several projects funded by FCT "*Fundação para a Ciência e a Tecnologia*", in the scope of the Knowledge Engineering and Decision Support Research Centre – GECAD. The regarded projects are:

- ViP-DiGEM - VIrtual power Producers and DIstributed Generation trading in Energy Markets (PTDC/ 72889);
- ID-MAP - Intelligent Decision Support for Electricity Market Players (PTDC/EEA-EEL/099832/2008);
- FIGURE – Flexible and Intelligent Grids for Intensive Use of Renewable Energy Sources (PTDC/SEN-ENR/099844/2008).

The developed work has resulted in several scientific papers. Some of which have already been published and/or accepted for publication. From this, the following should be referred:

One scientific paper in **journals**:

- Tiago Sousa, Hugo Morais, Zita Vale, Pedro Faria and João Soares, "Intelligent Energy Resource Management Considering Vehicle-to-Grid: A Simulated Annealing Approach", Accepted for Publication on IEEE Transaction on Smart Grid, Special Issue on Transportation Electrification and Vehicle-to-Grid Applications, 2011.
  This paper presents an early version of simulated annealing methodology in sub-section 3.4.3 to solve the energy resource management considering an intensive use of electric vehicles with V2G capacity.

One scientific paper in top ISI[1] **conferences** of the research area:

- João Soares, Tiago Sousa, Hugo Morais, Zita Vale and Pedro Faria, "An Optimal Scheduling Problem in Distribution Networks Considering V2G", IEEE Symposium Series on Computational Intelligence, CIASG 2011, April 11-15, 2011.
  This paper addresses the problem of energy resource scheduling with an intensive use of V2G. A proposed particle swarm optimization approach is compared with a reference methodology based on mixed integer non-linear programming.

These scientific contributions support the relevance of the work developed in the scope of this thesis to the scientific community.

[1] *Conference Proceedings Citation Index* ®; http://thomsonreuters.com/products_services/science/science_products/a-z/conf_proceedings_citation_index/

1.4. Thesis Overview

This section has the purpose to give a brief explanation of the five chapters that compose this thesis. This chapter presents the background and the main motivation for the work of this thesis and points out the aimed objectives for the research work. The other chapters are described in the following topics:

- Chapter 2 – Electric Vehicles

This chapter introduces the concept of smart grid and the role of virtual power players in this context. Afterwards, the characteristics and differences of several types of EVs are described. The concept of energy resource management is explained and an overview of the developed works considering energy resource management with electric vehicles is presented. This chapter finishes with the presentation of several batteries technologies and charging connections that can be expected between EVs and the electric network.

- Chapter 3 – Energy Resource Management considering Vehicle-to-Grid

Chapter 3 starts with the presentation of the mathematical formulation use in ERMaS tool to solve the ERM problem. The two proposed methodologies used for the ERM to obtain the optimal scheduling are described considering the mathematical formulation presented in this chapter. In this chapter is explained the different steps of the implementation of the two proposed methodologies, mainly of the SA technique.

- Chapter 4 – Cases Studies

The chapter 4 illustrates a set of cases studies. The 32 bus distribution network is used in the set of case studies. The first case study considers a scenario without EVs penetration in the network. The second case study demonstrates the difference in the solution quality of the ERM problem considering two different approaches and regarding the cluster of EVs.

The third case study presents the results of several ERM considering different control modes between EVs and the VPP. These control modes are firstly explained in section 2.5. The fourth case study presents an ERM result considering the influence of consecutive days in the scheduling of a particular day.

- Chapter 5 – Conclusions and Future Research

This chapter summarizes the thesis and presents its main conclusions and also the envisaged future work in the field. The main contributions of this thesis are discussed.

Chapter 2

Electric Vehicles

2. Electric Vehicles

2.1. Introduction

Power system operation paradigm has been changing, with the successive introduction of Distributed Energy Resources (DERs) and with the introduction of competitive electricity markets. In this new context, the power system structure needs to change in order to maintain the security of its operation [1]. The traditional power system structure was based on large power plants (typically thermoelectric or hydroelectric) distant from the demand centers. Considering the challenges of the new paradigm, this traditional structure is not suitable any longer [16].

The traditional architecture of Supervisory Control and Data Acquisition (SCADA) system cannot support the intensive integration of DER, mainly Distributed Generation (DG) based on renewable resources [4]. The new paradigm requires modifications in the SCADA system [1, 15], such as a decentralized control decision. In 2010, the European Commission suggested the use of four hierarchy levels for power system control [17]; in the same year, Morais proposes a structure of six level hierarchy control [15].

Smart grids are seen as the paradigm able to accommodate these new challenges of power systems. In the smart grid structure, Virtual Power Players (VPPs) play a major role, managing DERs and negotiating as buyers and/or sellers in electricity markets [18]. A VPP is a player that aggregates small and medium scale several resources with the responsibility of managing efficiently the DERs, e.g. DG units, demand response, storage systems, and Electric Vehicles (EVs). VPP deals with several DERs mainly at the distribution network level. All the mentioned DERs have to be considered in the management of the power system, consequently considering their characteristics and requirements [19]. An adequate Energy Resource Management (ERM) by the VPP is important to maintain the network standards operation [20].

The transportation sector is shifting from conventional vehicles, propelled by fossil fuels, to electric vehicles. The majority of these vehicles will require a network connection to charge the battery in order to support users' trips. Few investments in EVs' components can also enable the discharge of energy to the network [21]. This capability is known as Vehicle-to-Grid (V2G). V2G enables EVs to be seen as another available DER to be used in the smart grid context which can help to achieve a more efficient management of the resources. The choice of use the charging or discharging mode can be made by the VPP with the agreement of the EV user. The VPP must guarantee that a minimum amount of energy, required for a user's travel, is always available [22-23].

Recently, automobile manufacturers have announced Battery Electric Vehicle (BEV) and Plug-in Hybrid Electric Vehicle (PHEV) models with the ability to charge their battery directly from electric network [24-25]. The interest in EVs use has been increased in several

countries, mainly in Europe, Japan, United States and China due to their high dependence of petroleum and concern about Carbon dioxide (CO_2) emissions [12]. Governments have started to implement some financial incentives for companies and private users to replace their conventional vehicles [26]. Figure 2.1 presents the different pathways of transition in the transportation sector from an Internal Combustion Engine (ICE) solution to a full electric vehicle solution [27]. In the next years, the conventional vehicles will dominate the transportation sector with two different solutions, gasoline powered Spark Ignition (SI) and diesel powered Compression Ignition (CI). The electrification of transportation sector can be achieved through two pathways, the first one is to change from conventional vehicles to Hybrid Electric Vehicles (HEVs) and afterwards to EVs, and the second one is to change from conventional vehicles to Fuel Cell Vehicles (FCVs). The gradual change from conventional vehicles to HEVs and afterwards to EVs is the most predicted scenario [27-28].

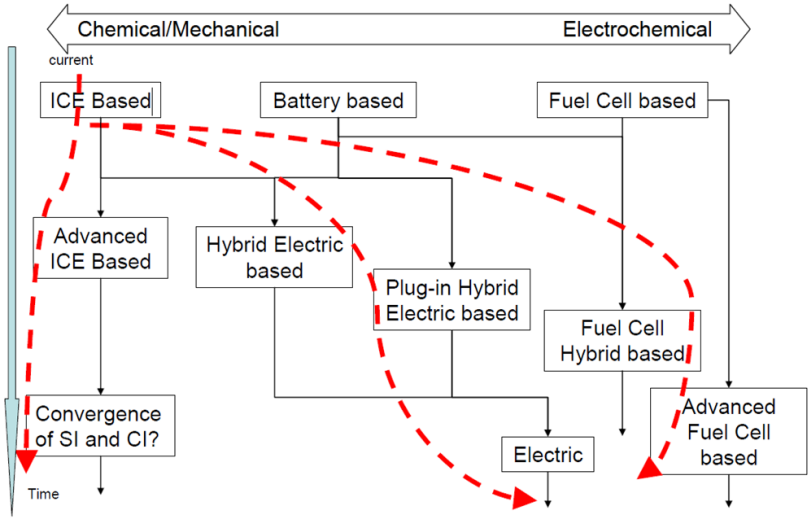

Figure 2.1 – Possible vehicle system pathways [27].

Governmental incentives, petroleum price and public opinion about environmental issues can be considered as the most relevant factors for the acceleration of the electrification of transportation sector. Figure 2.2 depicts a possible EV sales evolution in the next years, based on the 2009 transportation roadmap of the International Energy Agency (IEA) [29].

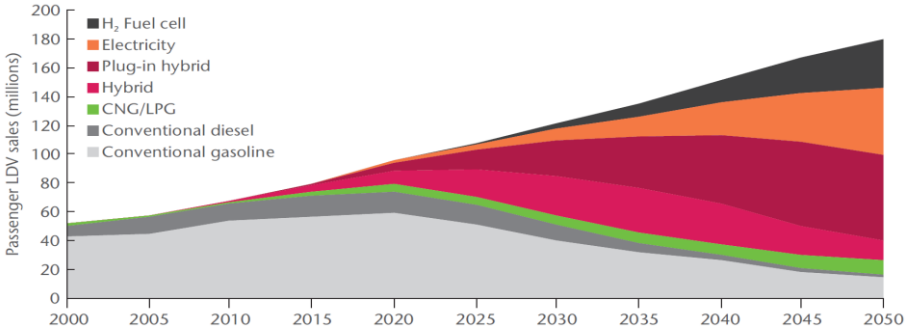

Figure 2.2 – Annual vehicle sales by technology type from IEA [29].

After the present introduction section, sections 2.2, 2.3 and 2.4 will present an explanation about the concepts of smarts grid, VPPs, and EVs respectively. Energy resource management in power systems is addressed in section 2.5. Section 2.6 shows the explanation about several types of batteries, and the charge systems. Section 2.7 presents the conclusions concerning the themes of this chapter.

2.2. Smart Grids

The smart grid concept appears as a response to the new power system challenges, considering the decentralization of the whole power system management, with different hierarchy levels of a decentralized SCADA system [1, 30]. The traditional power system structure proved to be not suitable for these new challenges [16]. The definition of a smart grid has been evolving over the years, including active networks and micro grids. Different authors and government entities have been considering several meanings for the smart grid concept over the recent years [6, 31].

Currently, one can say that a smart grid has the purpose of integrating the different players acting in electricity markets and in power system in order to guarantee a sustainable, reliable and secure delivery of electricity to the end-user [32-33]. The smart grid can be seen as a dispersed control center that will communicate with different players and take actions to improve the efficiency of the power system. Therefore, the practical implementation of the smart grid requires advanced technology with the purpose of achieving intelligent control, using reliable communication networks and measurement systems (smart metering) [5]. Figure 2.3 illustrates the different steps of the power system evolution from a centralized control to the smart grid implementation.

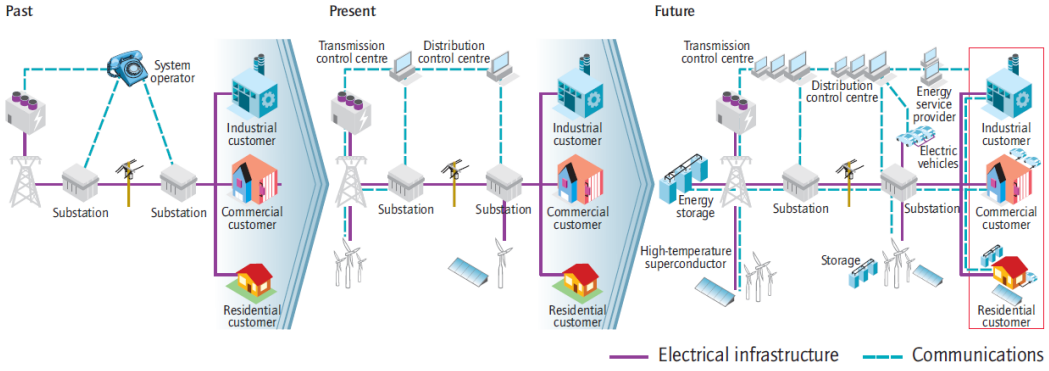

Figure 2.3 – Evolutionary process of the power system [32].

The main difference between the steps of the power system evolution in Figure 2.3 is the number of communications used. In the past, the centralized control required less communications and a simpler structure than in the present scenario. Nowadays it is possible to see more control systems, mainly in the Transmission System Operator (TSO) with the transmission control centre and Distribution Network Operator (DNO) with

distribution control centre. In the future is expected a more complex structure with more communication between the players, in order to achieve this purpose Morais [15] proposed a power system control with six levels (Figure 2.4).

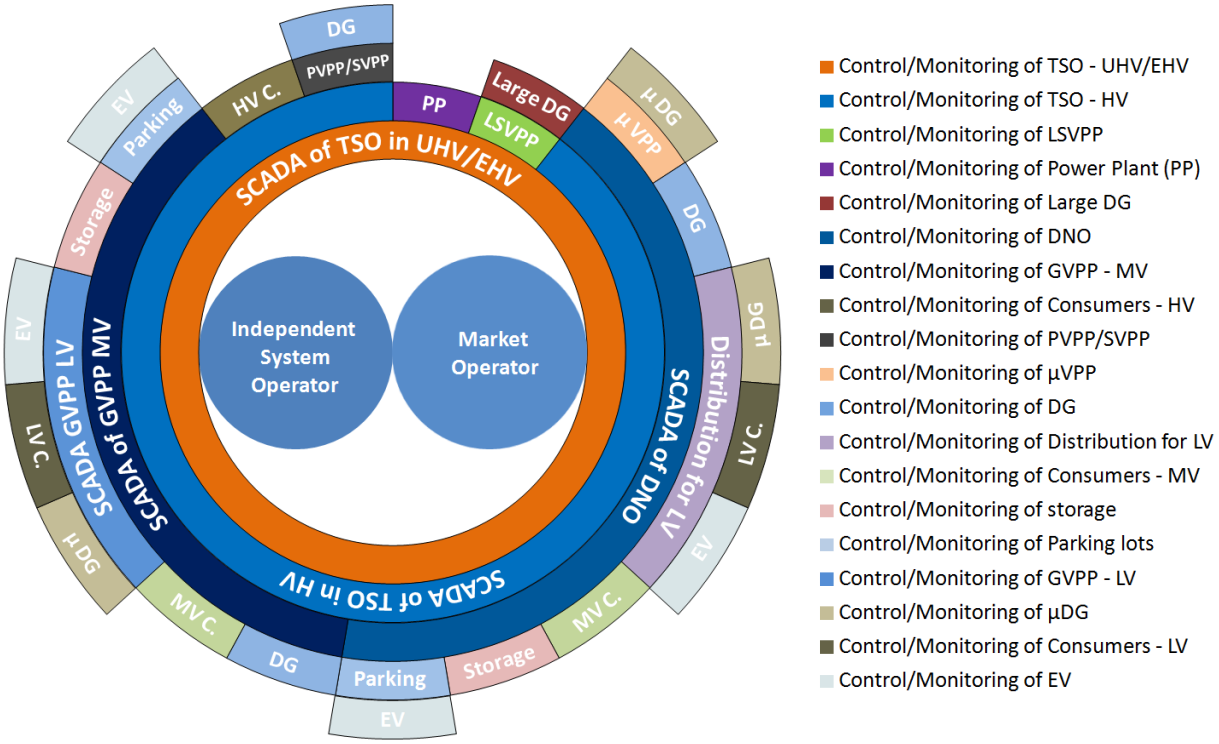

Figure 2.4 – Power system with a six level hierarchy control [15].

It is pointed in Figure 2.4 a decentralized control system and the players that will operate in this control system. In this figure is used a classification of VPPs that follows the reference [34]. The 1st level will be occupied by the market operator and the independent system operator; the TSO will be in the 2nd level to control the transmission system [15] with a rated voltage higher than 220 kV, denominate by Extra High Voltage (EHV)[2]. The 3rd level will be also controlled by the TSO using a SCADA system. In this level there are some players connected to the transmission system with rated voltage equal to 150 kV, such as power plants and the Large Scale Virtual Power Player (LSVPP) [15]. LSVPP can directly communicate with the TSO due to the characteristics of the LSVPP, which will be explained ahead in section 2.3.

DNO will occupy the 4th level to manage the distribution system, and in distribution level it appears others players that will cooperate with distribution network operator and transmission system operator. Parallel Virtual Power Player (PVPP) and Several Virtual Power Player (SVPP) can directly communicate with TSO in representation of some DG

[2] Consulted in November 2011: http://www.electricalengineering-book.com/voltagesystems.html

units [15]. The Global Virtual Power Player (GVPP) can aggregate several DERs that are in lowest levels, and manage some parts of the electric network. The GVPP can communicate with TSO and DNO to improve the management of the network.

In the 5th level will be occupied by VPPs and DERs [15]. Some VPPs manage the DERs that are located in the 6th level, because these DERs have a low capacity and these VPPs are located on a single transformer of the distribution system. In the 5th level appears DERs that can respond to the 4th level, such as storage system, or group of consumers or a parking lot that aggregates several EVs. The final level (6th level) contains the DERs with the lower capacity at will connect in different points of the network. It is important to refer that in a lower level will be more distributed the control than a higher level. This decentralized control system will improve the communication between the players in order to achieve a better efficiency of the power system in a smart grid environment.

2.3. Virtual Power Players

DER can be characterized as resources with a low installed power geographically dispersed in the network. Currently, the main type of DER implemented in power system is DG, due to the financing incentives that have been put into practice to achieve energy policy targets [2, 4, 35-36]. The use of distributed storage systems tends to increase in order to support the operation of DG based on renewable resources, due to the intermittent behavior of this type of generation [4]. Other important DER that should be considered in the context of smart grids is the demand response [37-39]. Electric vehicles [13] should also be seen as DERs connected to the network.

A VPP can be defined as a virtual agent that aggregates several energy resources in a specific network with the objective of gaining an amount of power larger than the one considering each energy resource individually [15]. DERs are especially important in this aggregation philosophy. The VPP can represent the aggregated resources in the electricity market [34, 40], and also provide them with an improved management, allowing to increase their profits.

Similarly to the smart grid concept, the VPP concept has also been changing over the years. In the beginning, the VPP was seen as an aggregator of DG units [41-43], but with the introduction of demand response programs, storage systems and EVs, the concept of VPP has been changed to a more general one [11, 44].

Depending on the characteristics of a VPP, it can be in the 3rd, 4th, 5th level of control presented in Figure 2.4. The LSVPP at 3rd level will manage DERs with large installed capacity that are connected in a transmission system [15]. For this reason it is necessary a VPP in this level. For instance, if there is a large quantity of wind farms connected to the transmission system it is required a player that aggregates them to improve the

management at this level. This VPP can communicate directly with TSO to determine the amount of energy acquired by TSO. In the 4th level is possible to identify more VPPs to control, such as GVPP, PVPP/SVPP. These VPPs will manage essentially the DERs that will be connected in the distribution level [15]; these VPPs will be the player that represents the DERs with the TSO and LSVPP. The VPPs at the 5th level will manage the DERs that are installed in the end-user, in a level lower than the distribution level that was mentioned before. At this level a player that will only manage a fleet of EVs appears; some authors suggested this approach to aggregate several vehicles in parking lots [45].

In the scope of this thesis, a VPP is seen as an aggregator of energy resources which can be of any type of the already referred ones. Figure 2.5 shows a schematic representation of a VPP in a smart grid environment. The communication can be established in different ways: Power Line Carrier (PLC) or by the Global System for Mobile (GSM) communication technologies.

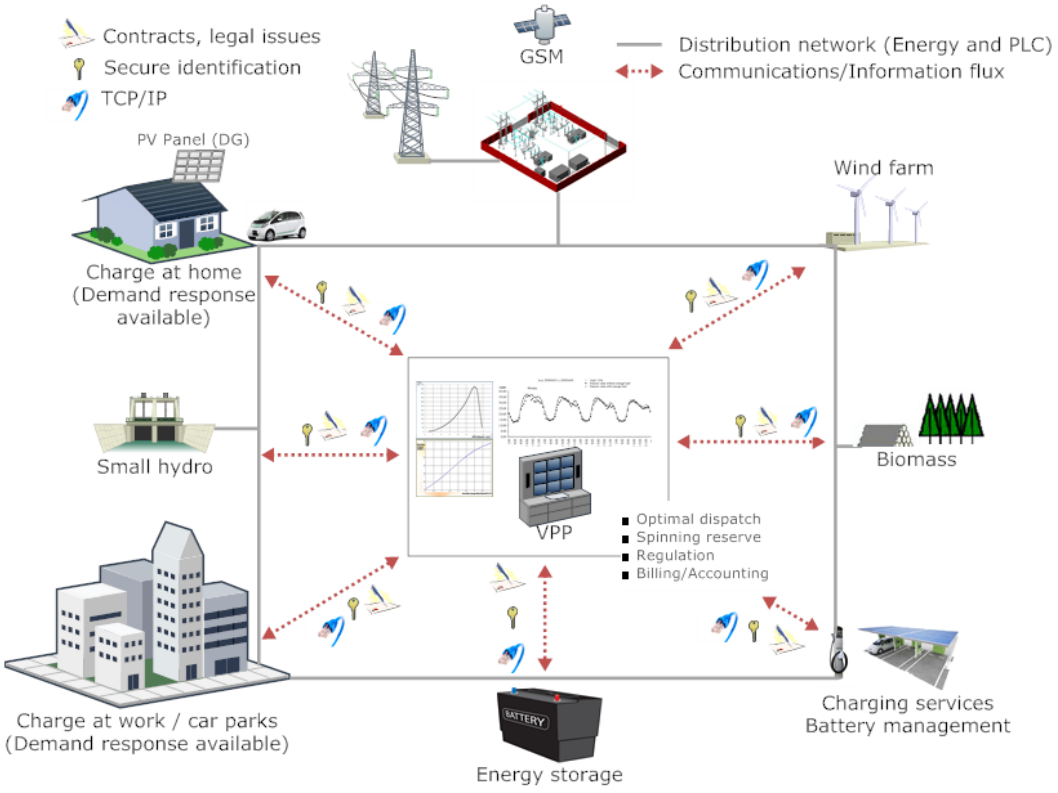

Figure 2.5 – VPP interaction in a smart grid environment (adapted from [23]).

The VPP will communicate with the different available resources to be used. Effective communications are very important to the VPP in order to achieve an efficient management of the available DERs. The massive introduction of EVs could imply more complexity to the VPP management, because it is required to communicate with each EV user to know his/her requirements in terms of trips. Particularly, EVs have a flexible behavior, and are potentially capable of enhancing the efficiency of other DERs [46]. In order to improve system security

and avoid these problems, the VPP can control the charging at preferred periods and afterwards can register data about vehicle use and user behavior [23].

Communications can also be used by the VPP to use the amount of energy that an EV can discharge in the network. VPP needs to communicate with each user to know if they accept to discharge the required amount of energy. So, bidirectional information between the VPP and EV users are required to support that kind of operation. The communication structure must be prepared to cope with the required amount of information between the VPP and each user. This can correspond to hard requirements due to the large number of envisaged EV users.

The communication infrastructure is very important, because it makes possible to control charge and discharge of EVs as well as to know when the user wants its vehicle ready to use and what is the required autonomy. Using the SCADA system, the VPP can control EVs charge and discharge. Knowing the periods of time in which customers need their vehicles charged, the whole dispatch can be optimized including this new resource.

2.4. Electric Vehicle Technologies

Electric vehicles can be defined as vehicles which use an electric motor to provide mechanical shaft power, allowing to drive the wheels. The main difference between EVs and conventional vehicles is the energy source used to supply the engine. Conventional vehicles use an internal combustion engine supported by fuel (namely gasoline or diesel) to activate the engine. EVs have been presented as a suitable solution for the transportation sector in the 19th century [47]. However, till the present, conventional vehicles have dominated this sector. In terms of driving performance (acceleration time and maximum speed) the EV presents a better performance than the conventional vehicles, but the massive use of conventional vehicles happened with the discovery of petroleum [48].

In many articles, EVs are divided into three categories, depending on the type of on-board energy source [13, 48-50]: battery electric vehicle, plug-in hybrid electric vehicle, fuel cell vehicle.

Battery Electric Vehicle

Battery electric vehicles use the battery as main power source. However, some BEVs use extra systems to support the batteries, such as the ultracapacitor [49]. The BEV contains an electric motor, batteries and power electronics. The power electronics control and measure the electric motor/battery [48], e.g. the accelerating/braking moments and the interface with the network to charge/discharge the battery. Figure 2.6 shows the typical BEV structure, including the battery, which is able to charge from the network or supply energy, in V2G mode.

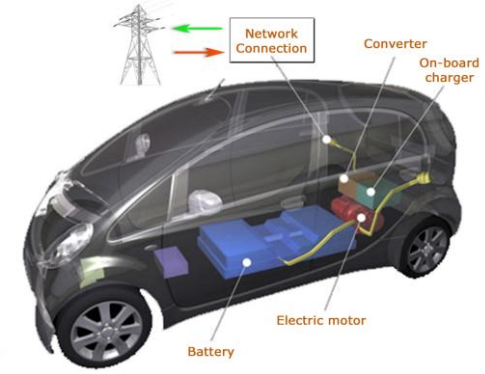

Figure 2.6 – Architecture of a BEV (adapted from [51]).

Plug-in Hybrid Electric Vehicle

A hybrid electric vehicle uses two or more energy supplies/sources to propel the vehicle, being one of these sources an electrical energy engine [52-53]. The HEV has the goal of achieving consumptions and CO_2 emissions lower than conventional vehicles. The HEV can have four configurations: series, parallel, series-parallel and complex [52-53]. The concept of PHEV emerges when a similar model to the HEV is developed, with the possibility of connecting it to the electric network [54]. Figure 2.7 illustrates the different operation types for HEV and PHEV. The "combined mode" joins the power from ICE and from the electric motor. The "braking mode" uses the energy from braking to charge the battery. In parking mode, the "recharge mode" charges the battery and the "V2G mode" injects energy in the power network.

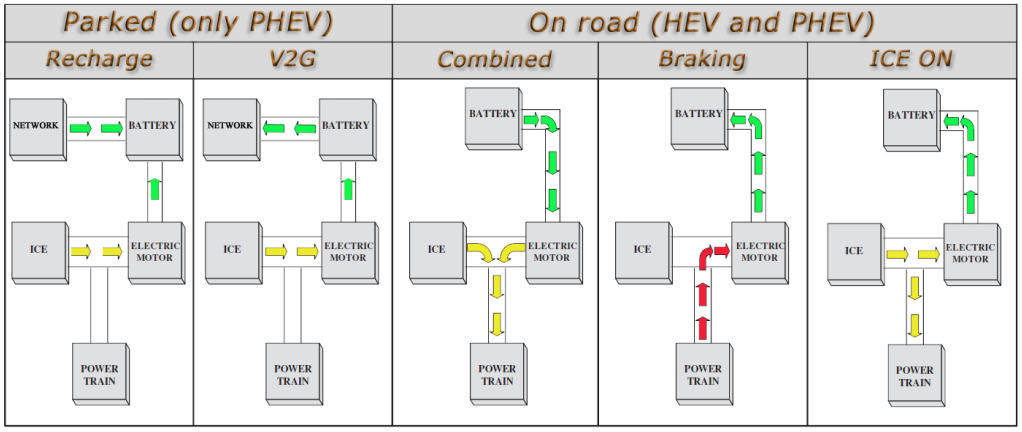

Figure 2.7 – The conceptual design modes of an HEV/PHEV (adapted from [53]).

Fuel Cell Vehicle

A fuel cell unit is used to generate power either to supply the electric motor or to store energy in the battery. FCVs are less likely to be competitive in a near future, when compared to BEV and PHEV, because fuel cell units and are currently very expensive [13]. In the future, FCVs can play an important role. However, in order to achieve a more relevance role in the transportation sector it is required that, fuel cells become more competitive in terms of hydrogen cost and on-board security [55].

In this thesis, the term EV refers to both BEV and PHEV vehicles FCV is not considered. Table 2.1 summarizes the main features of the three types of EVs, and their main advantages and disadvantages.

Type of EVs	BEV	HEV/PHEV	FCV
Propulsion	Electric motor	Electric motor	Electric motor
		ICE	
Energy system	Battery	Battery	Fuel cell
	Ultracapacitor	Ultracapacitor	
		Fossil fuel tank	
Energy source and infrastructure	Electric grid charging facilities	Gasoline stations	Hydrogen
		Electric grid charging facilities for PHEV	Hydrogen production and transportation infrastructures
Characteristics	Zero emission and high energy efficiency	Very low emission	Zero emission or ultra low emission
		The increase in fuel economy and reduction of emissions, depending on the power level of motor and battery	High energy efficiency
	Independence from fossil fuels	Higher fuel economy	Independence from fossil fuels, if not used to produce hydrogen
		Dependence on fossil fuels for HEV	
	Relatively short range	Long driving range	Satisfying driving range
	High initial cost	Higher cost than CV	High cost and under development
	Commercially available	Commercially available	
Major issues	Battery and its management	Multiple energy sources management and optimization	Fuel infrastructure and cost
	Charging facilities	Battery sizing and management	Fuel life cycle and reliability
	Vehicle Cost		

Table 2.1 – Characteristics of different types of EVs [13].

2.5. Energy Resource Management

The energy resource management has the purpose to determine the best operation point of the available DERs, considering generation units, storage systems, demand response and EVs. The energy resource management can be characterized as an optimization process used to manage the DERs with global objectives. ERM can consider different objectives to determine the optimal scheduling of the available energy resources. The aimed objectives can include the minimization of the operation costs, of the greenhouse gases emissions, of the active power loss of the network, and the maximization of the players' profits.

The ERM can be undertaken by a diversity of players, including network operators, single players owning energy resources and VPPs. ERM is especially important in the case of VPPs operating in the smart grid context. These VPPs can aggregate a large quantity of DERs, increased when EV penetration increases.

Considering the ERM definition, it is possible to obtain an optimal scheduling that only minimizes the operation costs of the generation units. This approach is commonly referred by several authors as economic dispatch. An economic dispatch is a ERM that obtains the optimal scheduling with a global objective of minimizing the total operation costs of generation units, subjected to supply the demand and to power system operation constraints [56]. The economic dispatch is typically executed in operation environment, for which the operation constraints concerning the thermal limit of lines and voltage limits are important [57].

Traditionally, the economic dispatch approaches are centralized and only optimize the generation of power plants with more impact in the operation costs, such as large thermoelectric power plants based on coal or nuclear and large hydroelectric power plants [56]. Smaller generators based on renewable sources [4] were not considered in the optimization process or were simply subtracted from the demand. However, in the context of an intensive use of DG this approach is not acceptable. On the one hand, this is due to the relevant participation of DG in demand satisfaction. On the other hand, a decentralized resource management is required for the present and future power system.

Therefore, new adequate optimization methods are required for this purpose. These methods should be able to deal with problems with a large number of variables and constraints. Moreover, solutions should be developed in a way they can provide solutions rapidly, in order to cope with operation time constraints. The massive use of EVs can improve the ERM, because the EV can be seen as a controlled load or a controlled generator (with V2G capacity). Additionally, EVs can also help reducing CO_2 emissions in the electric sector. The combination of EVs with other renewable resources can help reducing the use of traditional thermoelectric power plants based on fossil fuels.

An approach to include PHEV in ERM and to determine the optimal dispatch with PHEV that can charge or discharge energy, is presented in [58]. The main purpose of this report [58] is to present a methodology that is able to intelligently allocate the charges and discharges of the PHEVs in order to optimize the operation cost from the point of view of the network operator. The authors tried to control the PHEV charging in precise times, when the demand is at the minimum level, therefore not overloading the network. The report also considers the discharge of PHEVs to the network in order to provide power in load peak periods. These two approaches can be considered as the main opportunities that can be explored concerning the electric vehicles connected to network. The use of EVs to charge during periods with minimum demand level is commonly associated to load leveling. The EVs discharging in periods with a peak demand is commonly referred as peak shaving.

Several authors [46, 59-60] present applications of EVs with V2G capacity to support the use of renewable sources. These articles propose cost and CO_2 emission optimization in order to schedule the V2G sources, while taking into account renewable resources. Saber and Venayagamoorthy [46, 60] use this strategy to combine renewable and EV resources in a "smart grid model". This approach considers emissions from thermoelectric power plants and EVs. Emissions of EVs depend on the number of miles the of trip. The authors compare the results of scheduling for three strategies: the use of EVs without any control, the use of EVs for load leveling, and the use of the smart grid model.

The use of EVs as another DER can bring more problems to the network, namely for distribution networks. Several authors point out that a large amount of EVs in charging mode can have a negative influence in distribution networks. It is possible that new power demand peaks appear in inappropriate periods, and that the voltage drops increase. Several studies evaluate the performance of the distribution network considering three types of strategies [61]:

1. Uncoordinated charging;
2. Smart charging;
3. Smart charging/discharging.

The uncoordinated charging occurs when vehicles connect to the distribution network and start immediately to charge until they achieve the battery's maximum capacity. The smart charging and discharging consists in the network operator controlling the time and the power of EVs charging/discharging. The network operator will decide on when the most suitable periods of charging/discharging occur and the amount of power. The EV user will indicate the energy that should be stored in the battery at specific periods. This smart control will be integrated in the smart grid, and EVs can be simply controlled to charge in off-peak periods, resulting in the increase of the demand. They can additionally be used as generators, to reduce the demand in peak periods.

In the mid-nineties, the first studies about the impact of the EV in the distribution network appeared, mainly regarding the impact of EVs in the load diagram [62-64]. These studies suggested that the most appropriate control mode is the smart charging which allows operating with low degradation of the distribution network performance. Clement-Nyns *et al.* [65-66] present the impact of EVs charging and discharging in the distribution network. Hartmann *et al.* [67] evaluate the impact of EVs in the German network in 2030, considering different control modes for EVs charging. The use of smart charging with the objective of using the load leveling (i.e. increasing the load factor) and reducing the active power loss is proposed by Sortomme *et al.* [68-69].

2.6. Energy Storage

Electric vehicles use electrochemical batteries [48, 70] and/or ultracapacitors as energy storage systems. The manufacturers have increased their financial investments, so that they can improve the battery performance and life span [49, 71]. The BEV cost is largely influenced by the high cost of the battery [72].

The storage system of EVs will play a major role in the success of the electrification of transportation sector, namely the electrochemical battery. Currently, the battery has a big impact in the performance of the EVs, because it influences the autonomy of the vehicle. The common user cannot peacefully accept the change from conventional vehicles to EVs. It is pointed that the most predicted scenario will be a gradual change from conventional vehicles to HEVs and afterward to EVs [27-28]. During this transition, it is expected that the batteries performance will increase and that their cost will decrease.

2.6.1. Battery technologies

Batteries are classified according to the materials that are used in the chemical process. Battery manufacturers point out three main battery types as the most suitable for the EV requirements: the lithium ion (Li-ion), the nickel metal-hybride (NiMH) and Molten salt. The Li-ion batteries are composed by lithium and are considered the most promising battery type for EVs [73-74]. The battery manufacturers are making enormous improvements in what concerns the Li-ion battery capacity. The Li-ion polymer battery belongs to the Li-ion battery group, presenting a lower performance and cost than the typically Li-ion battery used in electronic applications [73]. The NiMH batteries were introduced in the final of the 1980s and are composed by nickel and hydrogen [75-76]. They have been used in the Prius model of Toyota. Another suitable battery for EVs is composed by molten salt material [76] - the Th!nk EV model [77-78] uses the molten salt battery. The materials of the last two battery types present the advantage of them reserve being much larger than the reserves of lithium.

The ultracapacitor is a recent energy storage system, presenting better specific power and life span than a battery. However, it provides less specific energy[3] than a battery [49, 71]. The ultracapacitor presents high power capacity, with quick response; and the battery presents a higher capacity. A hybrid storage system with the ultracapacitor and battery can improve the performance of EVs [79-83], using the advantages and mitigate the disadvantages of each storage system. EVs use a Battery Management System (BMS) to control and monitor the battery. The BMS controls the charge/discharge process to maintain the battery within its parameters and prevent the battery reaches its limit. Therefore, the user will take advantages with the BMS, because it can extend the battery life span [84].

A report from the Boston Consulting Group (BCG) [74] in collaboration with manufacturers points out six characteristics to evaluate batteries in terms of performance: safety, life span, performance, specific energy, specific power and cost. It is possible to see with more detail these battery characteristics in reference [74].

Figure 2.8 depicts the performance of several energy storage systems, considering the amount of specific energy and power [85-87].

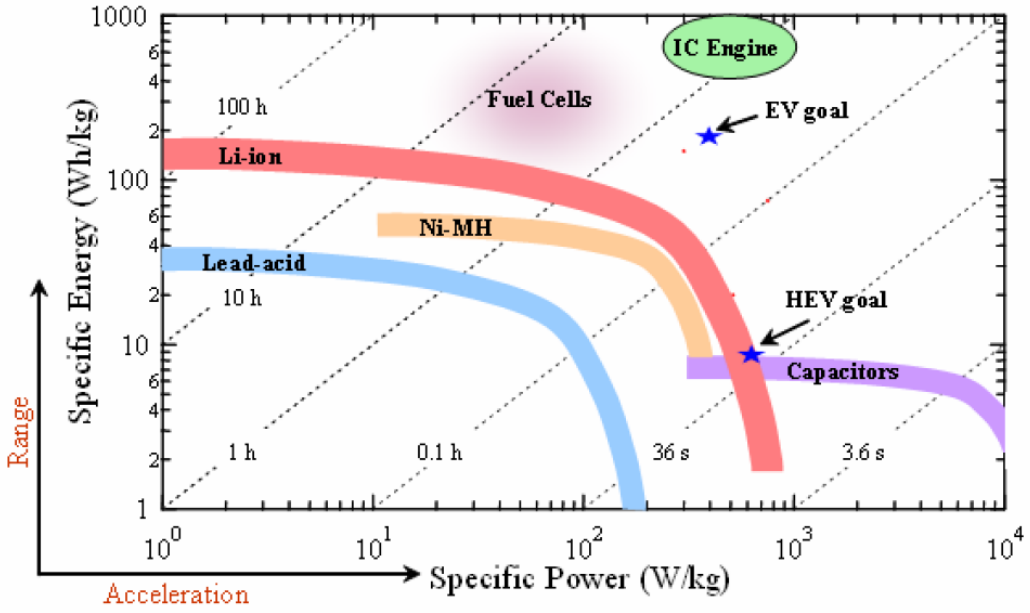

Figure 2.8 – Specific energy and power plot of the batteries [85-87].

Li-ion and NiMH batteries present a good performance that allows meeting the users' desires in terms of driving range. Currently, the automobile manufacturers choose the NiMH battery, due to its higher durability, safety, lower cost and maturity when compared to the Li-ion battery. One of the Li-ion battery main problems is its degradation along the successive use of the vehicle [74, 87-88]. NiMH batteries do not present such problem.

[3] The specific energy (or energy density) is the capacity for storing energy per kilogram of weight (Wh/kg) or per volume (Wh/m^3)

Some authors suggest that NiMH will be used in the first EV models, as an interim step, while the Li-ion technology is not competitive enough [74, 87-88].

From Figure 2.8 it is perceptible that the specific energy and power of the ICE (gasoline or diesel) is the combination that presents the higher success. The goal is to perform successive improvements in batteries and electric motor, so that the electric vehicle can achieve the same or closer performance to the conventional vehicles.

Figure 2.9 presents the performance of the five main Li-ion battery technologies, as presented in the BCG report [74]. As one can see, none of the five technologies shows a good performance regarding the six characteristics. The Lithium-Nickel-Cobalt-Aluminum (NCA) battery and the Lithium-Nickel-Manganese-Cobalt (NMC) battery achieve a good performance in what concerns the specific energy and power, but they present safety issues and a relatively high cost.

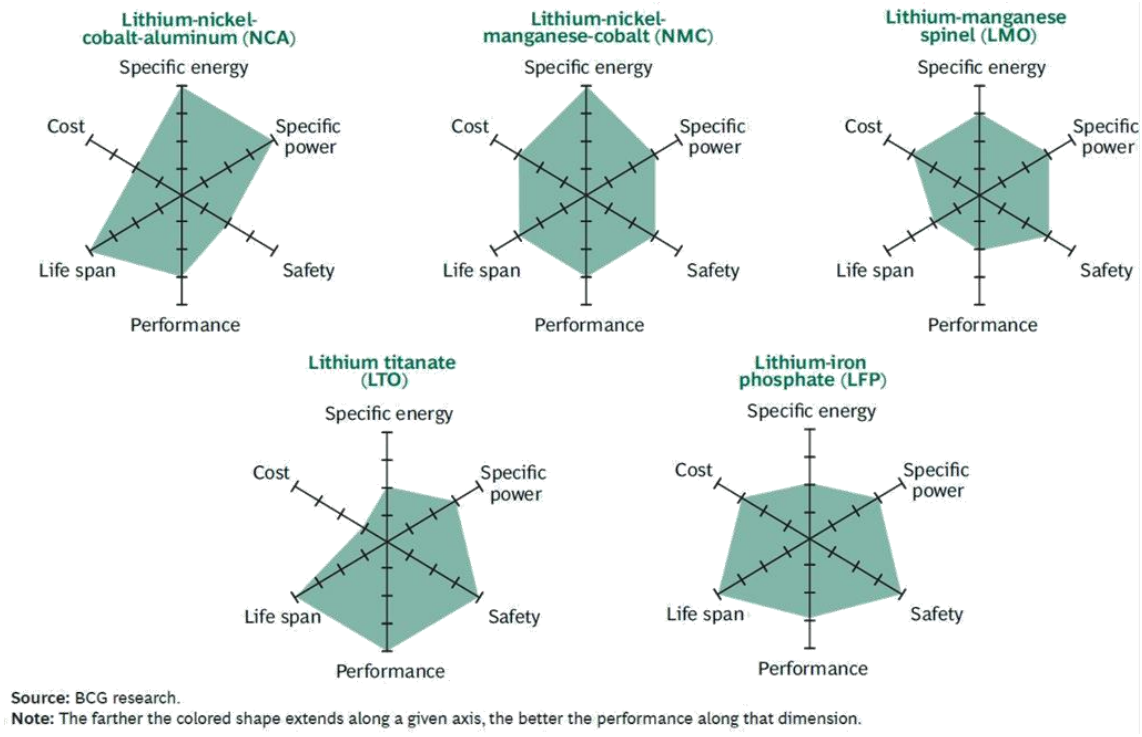

Figure 2.9 – Performance of the lithium-ion battery technologies [74].

As referred before, a massive use of Li-ion batteries in the EVs is expected in the future. Therefore, it becomes crucial to understand if the Li-ion battery has potential for technological improvements and for the reduction of production costs. These two factors are the biggest problems in what concerns the full usage of Li-ion batteries. The Li-ion battery should improve in safety, life span and reduce the production costs.

Figure 2.10 depicts the Li-ion battery cost evolution from 2009 to 2020, based on the BGC report [74]. This analysis suggests that the battery cost will decline between 60 to 65 percent. A Li-ion battery will cost around US$360 to US$440 per kWh, and the price for the consumer will be fixed in US$570 to US$700 per kWh [74].

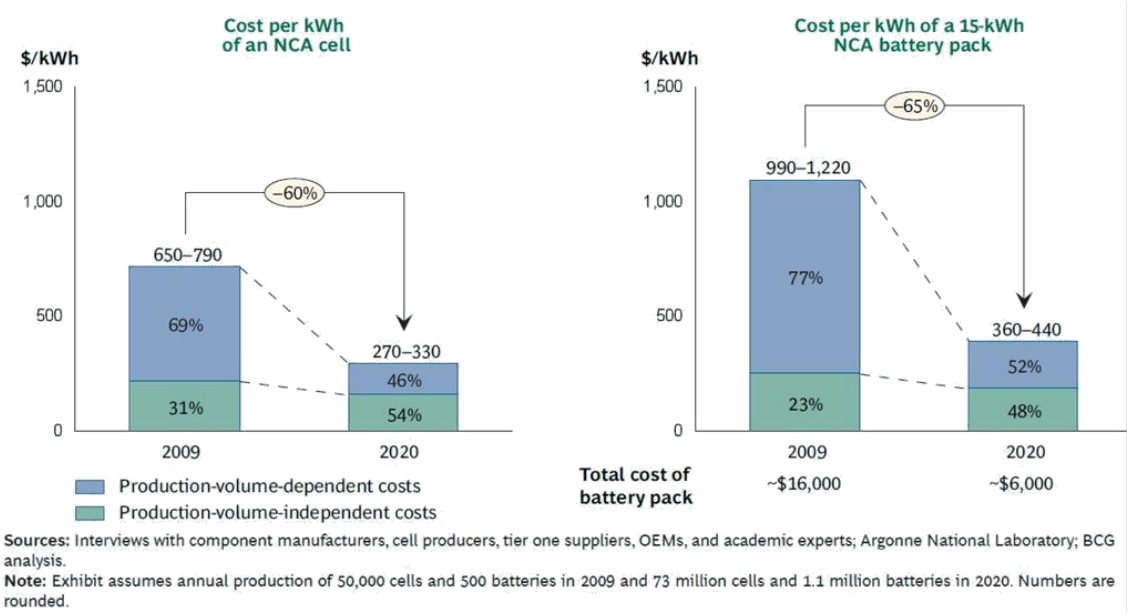

Figure 2.10 – Battery costs evolution since 2009 to 2020 [74].

2.6.2. Charge Systems

In the beginning of the electrification of the transportation sector, the vehicle batteries' charge was one of the big issues to be solved in order to sustain the widespread of EVs. The connection of EVs with the electric network will be the most used system to charge the batteries. It is important to refer the existence of other systems, such as switch battery system that will be detailed ahead in this section.

The charge system must be cheap, flexible for the manufacturers and simple and fast for the users. The system must be as flexible as possible, so that it allows manufacturers to sell in different regions, since different connection types are used in different regions. At the same time, the charge system shall not present a highly complicated handling for the user, as this would difficult the adoption of EVs by the public. If the system used for EVs is similar to the charging system of conventional vehicle (gas station), a rapid change of the transportation sector can be achieved [89].

Standard organizations, mainly the International Electrotechnical Commission (IEC)[4] among other organizations, have established several technical committees since 1970s with the objective of discussing the charge system and establishing a final standardization process [90-91]. The IEC 61851 family indicates the requirements for all the charging infrastructure [91], from conductive connection (IEC 61851-21) [92] to the charging station (IEC 61851-22) [93]. This standard defines four distinct charging modes [76, 89, 94-96]:

- Mode 1: Standard socket without communication (slow charging with a maximum current of 16 A);

[4] www.iec.ch

- Mode 2: Standard socket with in-cable pilot cable control (quick charging with a maximum current of 32 A);
- Mode 3: Dedicated socket with a permanent pilot cable control (fast charging with a maximum current of 250 A);
- Mode 4: DC off-board charger connection (ultra fast charging with a maximum current of 400 A).

The Society of Automotive Engineers (SAE) J1772 [97] defines 3 levels of charging in U.S., which are very similar to the IEC 61851. Level 1 is the slow charge in AC, level 2 is the quick charge in AC and level 3 is the fast charge in DC [96, 98]. The Japan Automotive Research Institutes (JARI) have defined their own standards - the DC charging (mode 4) will be adopted. The reference [99] indicates the different standards that can be applied for the components of the charging system of EVs.

The IEC 62196 [100] family defines the main characteristics of the network connectors. These standards are based not only on the IEC 61851 but also on other standards, e.g. IEC 60309 [101]. The IEC 62916 [100] family contains three types of connector that shall be used in the charge system:

- Type 1: is proposed by the Yazaki manufacturer and by the SAE J1772 (uses the specifications of mode 2);
- Type 2: is proposed by the Germany manufacturer Mennekes, and by the VDE-AR-E-2623-2-2 (uses the specifications of mode 3);
- Type 3: is proposed by the EV plug Alliance, formed by Schneider, Legrand and SCAME 2 (uses the specifications of mode 3);
- DC Charging: is proposed by the CHAdeMO Japanese association, and by JARI (uses the specifications of mode 4).

Figure 2.11 depicts the predicted usage of type 1 and 2 connectors in the world. Type 1 is going to be adopted mainly in the U.S., Japan and Western Europe; and used by Japanese and some European automobile manufacturers, such as Nissan, Mitsubishi and Citroen. Type 2 is going to be applied mainly in Europe and South America. The main users are European automobile manufacturers, such as BWM or Mercedes. This connector is able to use 1 or 3 phases, and allows charging an EV in slow or fast rate. The reference [102] shows the technical differences between types 1 and 2.

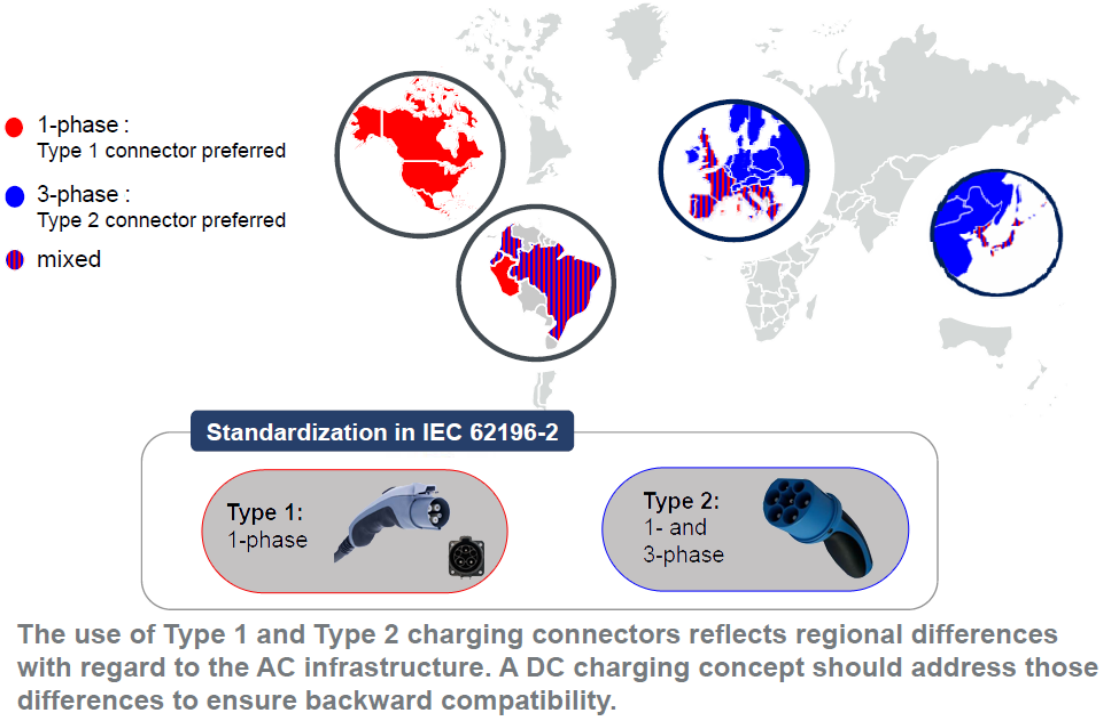

Figure 2.11 – World location of EV connectors [99].

The Portuguese manufacturer EFACEC will introduce several charging stations with both connectors (type 1 and type 2) in the Portuguese EV charging network (MOBI.E[5]). Figure 2.12 shows the different connectors that are going to be used in the charge system [103].

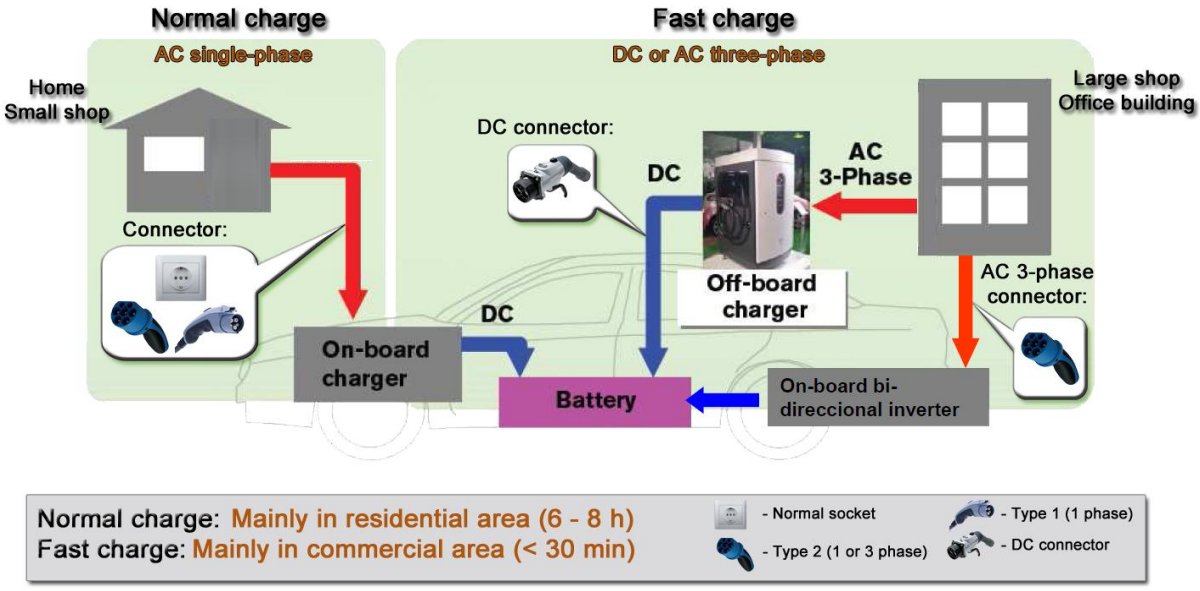

Figure 2.12 – Different charging methods (adapted from [103]).

[5] www.mobie.pt/en/homepage

Figure 2.12 shows a typical house or residential building using a normal socket, type 1 and type 2. In outside places the use of type 2 or DC charging will be necessary.

The switch battery mode is another concept in the charge systems of EVs. This mode consists in changing an empty battery for a fully charged one in just a few minutes. This concept would solve some problems with the fast charging of batteries. The fast charging of the batteries guarantees only the charge of a battery until 80 percent of its capacity, in order to prevent the decrease of life span and performance. This system has been proposed by a manufacturer called Better Place [104]. The system starts in a simple gasoline station:

1. The EV enters the station;
2. A robot changes the empty battery for a fully charged battery;
3. The EV returns to the street;
4. The empty battery will be connected to the network to charge in slow rate.

Using this process enables the user to charge the EV in less than 5 minutes. This pilot project should be implemented in several countries so that standards can be quickly established, as has happened with the connectors.

2.7. Conclusions

The new power system paradigm has been subjected to constant changes in whole power system. The DERs brings new challenges to the power system, because it is required some changes in the power system structure to better accommodate these kind of energy resources, mainly the DERs based on renewable sources. The electricity market brings additional challenges to a structure that in the past worked in a centralized way. Different organizations have been proposed the solution of smart grids to deal with this new paradigm. The SG concept is based on an intelligent network that tries to improve the management, operation and control of power system in this new paradigm. With the arising of SG concept, new players are defined, which that will be responsible for different services in the power system.

VPP is one of the players that, in a SG context, will play an important role. VPP is a representative player of several DERs, and with this aggregation the VPP can have more impact in a SG than an individual DER. This player is not only important to negotiate in the electricity market, but also to manage the aggregated DERs in a specific network area in order to supply the demand. VPP can aggregate different types of DERs, such as DG units, demand response, storage systems and EVs.

EVs are emerging as the appropriate solution for overcoming the increasingly prominent problems caused by fossil fuel propelled vehicles. Conventional vehicles have been controlling this sector for a long time; however, the interest of several countries in

finding an alternative solution has increased, due to the countries' high dependence on petroleum and also due to the CO_2 emissions issue.

In fact, financial incentives are already being implemented by governments, so that countries gradually move towards the change to EVs. These governmental incentives, the petroleum prices and public opinion on environmental issues clearly indicate that the change to EV will occur smoothly. The main arrangements for the welcoming of EVs in a large scale are currently being performed all around the world. A large variety of studies and pilot implementations regarding EV charge systems, types of batteries and technologies for EV motors are under development. This chapter presents an overview on these issues and a discussion on the implications of the inclusion of a vehicle with such characteristics in the power system.

Power system will have to be prepared to deal with such an evolving environment, with the large scale inclusion of EVs. However, the issues that will have to be dealt, can and should be looked at as opportunities, for so many are the advantages of using this type of vehicle's characteristics for the power system's benefit. VPP and SG are two concepts that are directly related to the efficient EV management issue. These concepts aim at providing the means to effectively take the best possible advantage out of the new context that arises with the EV integration in power system.

The efficient and intelligent management of EVs' implications in power systems is also the purpose of this thesis, aiming at providing support to the controlling entities, in what concerns this type of management. Chapter 3 presents the proposed methodology, implemented to optimally solve this problem, considering the intensive use of EVs.

Chapter 3

Energy Resource Management considering Vehicle-to-Grid

3. Energy Resource Management considering Vehicle-to-Grid

3.1. Introduction

The proposed Energy Resource Management in Smart Grids (ERMaS) tool aims at optimizing the management of Distributed Energy Resources (DERs) that are available in a smart grid managed by a Virtual Power Player (VPP), considering an intensive use of Electric Vehicles (EVs). The goal of the resource scheduling is to satisfy demand and EV users' requirements, while respecting all the involved constraints, aiming at obtaining the minimum operation cost. ERMaS has the purpose of helping a VPP with the Energy Resource Management (ERM) of the available DERs, contributing to the surpassing of VPPs' need of adequate tools to handle the different DERs that are considered under the new power system paradigm. These tools must incorporate detailed and accurate models concerning DERs specifications, while providing quick responses, able to cope with operation requirements.

Energy resource management turns into a large combinatorial problem when a huge number of DERs are connected to the grid [23]. It is necessary to use optimization techniques in order to obtain the best ERM solution, which presents the minimum operation cost of the available DERs, while supplying the demand [105]. ERM can be classified as a Mixed-Integer Non-Linear Programming (MINLP) problem. A MINLP problem is a large combinatorial and complex problem that can require a huge amount of computation resources [106]. Achieving the optimal solution of the envisaged problem can take several minutes or even hours. Therefore, it is necessary to select the most adequate optimization techniques to address the ERM problem. In order to solve a MINLP problem, it is possible to use deterministic techniques (traditional optimization techniques) or Artificial Intelligence (AI) techniques [107].

Due to non-convexity and non-linearity of the MINLP problem, there are multiple local optima in the search region. The optimization technique has to handle this complexity and avoid being "trapped" in a local optimal [108]. The large number of local optimal solutions contributes to the huge amount of time taken to find the optimal solution. In a problem such as the ERM, the execution time is exacerbated due to the large number of DERs to be handled; hence the execution time becomes a crucial factor when determining the optimal solution of an ERM problem. Therefore, a suitable optimization technique should obtain a satisfactory solution in a reasonable execution time.

Deterministic techniques ensure the global optimal solution; however, as mentioned before, the use of this type of techniques to solve a MINLP problem can take several hours. Recently, AI techniques have been used to solve problems in the power system field, replacing deterministic techniques [109-110]. AI techniques, mainly based on metaheuristic algorithms, are effective in exploring the search region of problems in which this space is

large. Metaheuristic techniques cannot guarantee the global optimal solution. These techniques search for local optima and incorporate a biological process to escape from local optimal solution, finding new local optimum. The main advantage of a metaheuristic approach to deal with optimization problems is the requirement of less computational resources than a deterministic technique [107, 111], mainly in what concerns the execution time and memory allocation. Heuristic optimization, namely genetic algorithms, particle swarm optimization, and Simulated Annealing (SA) have been largely used in power system problems with good results.

In this thesis, the use of the SA technique is proposed to address ERM, due to its suitability to the requirements of the ERM problem. SA is able to obtain a satisfactory solution in a low execution time. Additionally, a deterministic technique has also been implemented to solve the ERM problem, in order to compare its results with the one of the SA. The proposed SA approach has been implemented in the Matrix Laboratory (MATLAB) [112] software, and the deterministic technique has been modeled in the General Algebraic Modeling System (GAMS) [113] software. The MATLAB has also been used as interface with GAMS. This way, GAMS is only responsible for modeling the deterministic technique, and MATLAB organizes the input data and results.

The objective of this chapter is to present the mathematical formulation of the envisaged ERM problem and to detail the proposed SA methodology to address this problem. Moreover this chapter provides a detailed description of the ERMaS tool.

3.2. ERMaS tool structure

This section presents the ERMaS structure and the steps used to determine the ERM scheduling result. The ERMaS structure is shown in Figure 3.1.

In the scope of ERMaS it is assumed that a VPP is able to operate different DERs in a specific network area. The VPP must respect the contracts established with the available DER in order to achieve a good scheduling solution. The ERMaS tool uses historical data and daily forecasted data to support energy resource management. These data can be seen in the left side of Figure 3.1, concerning the identification of the different DER that may be available in the network. The data base contains the forecasted values for each hour referring to the following periods, concerning namely the DG capacity, EV travelling requirements and bus location, and network configuration.

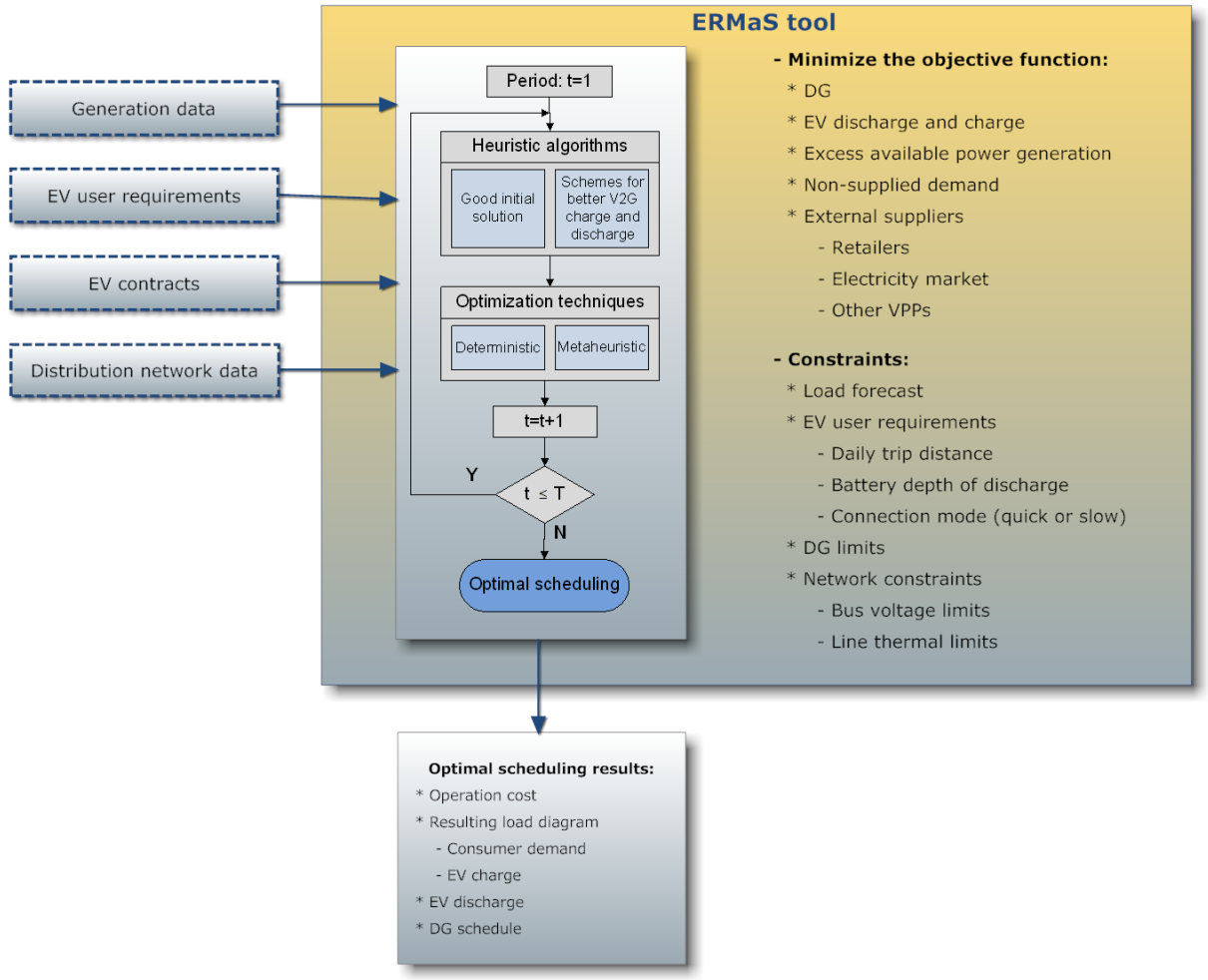

Figure 3.1 – ERMaS tool structure.

DG data includes the generation limits (active and reactive), the selling price, and h the DG "take or pay" contracts, obligating the VPP to dispatch the power of these DG resources. EV data includes the travelling requirements, specifying the timings of each travel, and the energy that each of these travels will require. It also indentifies the bus in which each EV will be connected to the network. The VPP also detains the information regarding the selling price of EVs that have V2G capacity.

The objective of ERM in the ERMaS tool is the operation cost minimization, considering the topics presented in the right hand side of Figure 3.1. The constraints regarding the available DERs and concerning the network must be considered. The use of the ERMaS tool results on an optimal scheduling. ERMaS provides the user with the means to consult the resulting load diagram, including the demand of consumers, EVs charging, and the scheduling of the generation. Section 3.3 presents the mathematical formulation of the ERM, which has been implemented using the deterministic and metaheurisitic proposed techniques.

The main component of the ERMaS tool is the algorithm used to determine the ERM for the next periods. This thesis is focused on conceiving, implementing and improving this

algorithm to determine the optimal resource scheduling. The ERM is determined for different periods until it reaches the maximum number of envisaged periods (*T*). Typically, the ERM is executed for a period of 24 hours of the next day. The ERM can be performed, in the scope of the ERMaS tool, using deterministic and metaheurisitic techniques. Both methodologies have been developed in this thesis. The main goal is finding adequate techniques to solve the ERM, considering both deterministic and metaheuristic methods. The deterministic technique was based on a previous work directed to smart grid [15]. The deterministic model proposed in the referred work has been improved and adapted to the ERMaS tool, considering an intensive use of EVs. Additionally, the ERMaS tool includes the SA approach proposed in the scope of the present thesis to solve the ERM problem.

3.3. Mathematical Formulation

This section describes the mathematical formulation of energy resource management problem. The ERM problem is formulated as a mixed-integer non-linear programming problem due to the VPP's capability of using resources (integer variables) and managing the amount of energy for each resource (continuous variables). Regarding the proposed methodology, it has been considered that the VPP establishes contracts for managing the DER aggregated in the VPP's network area. In order to supply the consumers' required energy demand the VPP is able to use several DER:

- The installed DG, and remunerate its owners with a established price;
- The discharge of EVs with V2G capacity, and remunerate their owners;
- External suppliers outside of its network area, namely retailers, the electricity market pool and other VPPs.

3.3.1. Objective Function

The objective function represents all the VPP objectives that present a mathematical significance. The VPP must be able to obtain a minimum cost or a maximum profit through a mathematical representation (objective function) of the involved objectives. In terms of the optimal resource scheduling, the most common approach is developing an objective function that makes it possible to minimize the DER operation costs. In the scope of this thesis an objective function that minimizes the operation cost has been considered. Therefore, the objective function can be divided into 4 sub-functions:

- Operation costs with DG (f_1 in equation 3.1);
- Cost of the energy acquired to the external suppliers (f_2 in equation 3.1);
- EV users payments and remuneration (f_3 in equation 3.1);
- Penalty costs (f_4 in equation 3.1).

Function f (3.1) represents the four costs that the proposed methodology will minimize. This model is based on a previous methodology proposed by Morais [15], aiming at finding the minimum operation cost for the VPP.

$$minimize\ f = f_1 + f_2 + f_3 + f_4 \tag{3.1}$$

Function f_1 (3.2) represents all the VPP operation costs with DG in a specified time period (from period t=1 to t=T). f_1 is a quadratic function, as it is usually used for generators based on fossil fuel [114-115]. Figure 3.2 illustrates an example of generation cost function considering the cost coefficients a, b and c (C(P)= a + bP + cP^2).

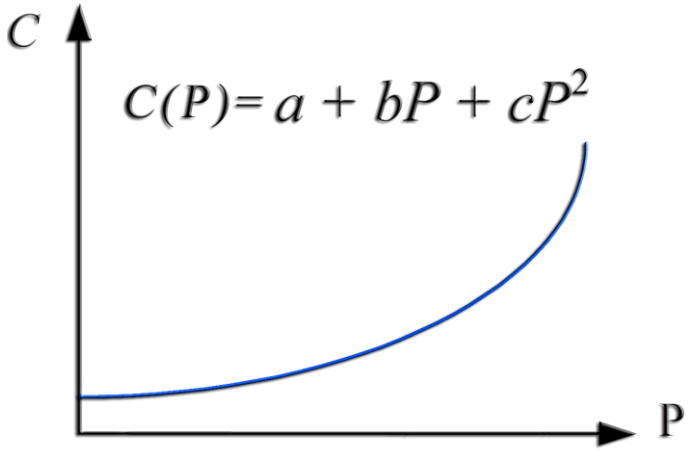

Figure 3.2 – Generation cost function (adapted from [116]).

In order to formulate f_1 as a quadratic polynomial function, the cost coefficients $c_{A(DG,o,t)}$, $c_{B(DG,o,t)}$ and $c_{C(DG,o,t)}$ (see equation 3.2) are used. Regarding DG units based on other primary energy types (e.g. wind or solar source), the DG owner and the VPP can establish the unitary energy price (Wh/m.u.) and incorporate that payment in the linear cost coefficient $c_{B(DG,o,t)}$. Using this function makes the ERM problem flexible enough to consider DG units with different cost function. For generators with fossil fuel the three coefficients can be used; for generators with linear cost functions, the coefficient ($c_{B(DG,o,t)}$) is the only one required.

$$f_1 = \sum_{t=1}^{T} \sum_{DG=1}^{N_{DG}} \sum_{o=1}^{N_{DG}^{O}} c_{A(DG,o,t)} \times X_{DG(DG,o,t)} + c_{B(DG,o,t)} \times P_{DG(DG,o,t)} + c_{C(DG,o,t)} \times P^2_{DG(DG,o,t)} \tag{3.2}$$

Function f_2 (3.3) represents the VPP costs with the energy bought from external suppliers. These costs concern the amount of bought energy from such suppliers for a specified time period (from period t=1 to t=T). Retailers, the electricity pool and other VPPs can be classified as external suppliers. An external supplier offer is established with an energy price ($c_{Supplier(S,o,t)}$) and a maximum active power ($P_{SupplierLimit(S,o,t)}$). Usually, these players are located outside of the VPP network area. The maximum active power supplied

by an external supplier will be limited by the capacity of interconnection of the VPP network with the rest of the network, and by the maximum active power of the external supplier ($P_{SupplierLimit(S,o,t)}$).

$$f_2 = \sum_{t=1}^{T}\sum_{S=1}^{N_S}\sum_{o=1}^{N_S^O} c_{Supplier(S,o,t)} \times P_{Supplier(S,o,t)} \quad (3.3)$$

Figure 3.3 depicts the negotiation curve considering several external suppliers. Offers are organized in an ascendant order, so that the cheaper ones can be selected, in order to fulfill the required demand.

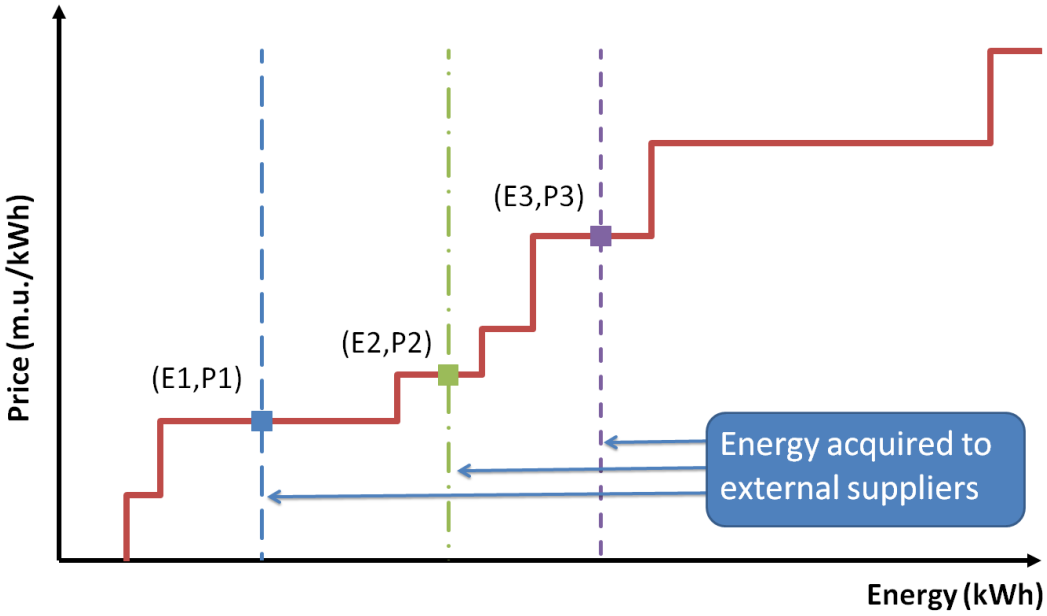

Figure 3.3 – Example of a set of offers from external suppliers.

When a higher value of energy is acquired to external suppliers, the VPP will have to support a higher price. For instance, if it is determined that the amount of energy (E1) must be acquired, instead of energy amount (E3), the resulting price (P1) will be lower than price (P3).

Function f_3 (3.4) represents the payments that occur between the VPP and EV users. These payments also consider a specified time period (from period t=1 to t=T). This function is divided into two terms. When the EV user buys a certain energy amount to charge the EV; and when the VPP uses some energy from the EV (discharge) to supply the network. EV discharges represent a cost to the VPP, and the charges bring benefits and profit for the VPP. The amount of energy stored in EVs batteries can be seen as an opportunity for the VPP to supply the energy demand in other periods.

$$f_3 = \sum_{t=1}^{T}\sum_{V=1}^{N_V} c_{Discharge(V,t)} \times P_{Discharge(V,t)} - c_{Charge(V,t)} \times P_{Charge(V,t)} \quad (3.4)$$

Considering that the constant use of batteries to charge and discharge can decrease their life span, it is possible to adapt function f_3 to consider this kind of behavior. Another

approach considers that function f_3 (3.5) can be formulated to consider three discharge price steps, depending on the battery level of the EV. This approach aims at establishing a fair remuneration scheme, which prevents unnecessary battery deterioration. The first price is applied to EV discharge power regarding the interval between 100% and 70% of the battery capacity. The second price is activated when the first price step reached 70% of battery capacity. The new interval of EV discharge is from 70% to 40% of the battery capacity. The third price is only active when the EV has stored at most 40% of the battery capacity, meaning that the first and second steps were used in previous periods. This step is used on the interval from 40% to 20% of the battery capacity. The first step price has been defined as the lowest value, the second step presents a mid-term price value and the third step corresponds to the highest price of all three price steps.

$$f_3 = \sum_{t=1}^{T}\sum_{V=1}^{N_V}\left(\begin{array}{l} c_{Discharge\_StepA(V,t)} \times P_{Discharge\_StepA(V,t)} + c_{Discharge\_StepB(V,t)} \times P_{Discharge\_StepB(V,t)} + \\ c_{Discharge\_StepC(V,t)} \times P_{Discharge\_StepC(V,t)} - c_{Charge(V,t)} \times P_{Charge(V,t)} \end{array}\right) \quad (3.5)$$

Function f_4 (3.6) represents the costs with excess available power ($P_{EAP(DG,t)}$) and non-supplied demand ($P_{NSD(L,t)}$). The goal is to achieve a robust mathematical formulation, and deal with different situations in the network. The excess available power is important because the VPP can establish "take or pay" contracts with some DG resources, for instance with producers based on renewable sources. In these situations, when the load is lower than this generation, the value of excess available power will be the difference between both. The non-supplied demand is activated when the supply is not enough to balance the load demand. In this case, the price of non-supplied demand should differ ($c_{NSD(L,t)}$), considering the priority of each consumer.

$$f_4 = \sum_{t=1}^{T}\sum_{L=1}^{N_L} c_{NSD(L,t)} \times P_{NSD(L,t)} + \sum_{t=1}^{T}\sum_{DG=1}^{N_{DG}} c_{EAP(DG,t)} \times P_{EAP(DG,t)} \quad (3.6)$$

3.3.2. Constraints

In general, an optimization problem needs, not only an objective function that mathematically expresses the purpose of the problem (in terms of minimization or maximization), but it also requires several constraints to limit the search space of the decision variables [117]. This section presents the constraints of the ERM problem. The constraints were divided into groups in order to better organize the corresponding organization and to ease the reading. The minimization of the ERM objective function is subjected to the following constraint groups:

- Network equality and inequality constraints;
- DG and external suppliers inequality constraints;
- EVs equality and inequality constraints.

Network equality and inequality constraints

This couple of constraints has the goal of modeling the network, and traducing its influence on the optimal resource scheduling. The optimal resource scheduling should use an accurate model of the network with the objective of achieving a feasible scheduling. The model has to consider the active/reactive power losses in each network line, and verify if the power flow in the lines is higher than their thermal limits[6].

For this purpose, during the optimization process, an ac power flow [114] is executed, to determine the power flow and power loss in each line. The active (3.7) and reactive (3.8) power balance traduces the application of the Kirchhoff's current law (or node rule) [114] in each bus. The power injected in a bus *i* is defined as the sum of the power flow through the lines that connect bus *i* to other buses, or to the ground[7]. The injected power is equal to the power generation minus the power demand in each bus [114].

In this model, the voltage magnitude and angle are considered as influent variables to the calculation of the power flow in each line. The maximum and minimum limits for the voltage magnitude (3.9) and voltage angle (3.10) are verified for each bus of the network. A slack bus is previously selected in the network, and fixed voltage magnitude and angle are specified for it. As referred before, the line power flows must be determined, so that they can be compared to the thermal limit of each line (3.12).

- The network active (3.7) and reactive (3.8) power balance with power loss at bus *i* in period *t*:

$$V_{i(t)}^2 \times G_{ii} + V_{i(t)} \times \sum_{j \in L^i} V_{j(t)} \left(G_{ij} \cos\left(\theta_{i(t)} - \theta_{j(t)}\right) + B_{ij} \sin\left(\theta_{i(t)} - \theta_{j(t)}\right)\right) = P_{Gi(t)} - P_{Di(t)}$$

$$\begin{aligned} P_{Gi(t)} &= \sum_{DG=1}^{N_{DG}^i} \sum_{o=1}^{N_{DG}^O} P_{DG(DG,o,t)}^i - \sum_{DG=1}^{N_{DG}^i} P_{EAP(DG,t)}^i + \sum_{S=1}^{N_S^i} \sum_{o=1}^{N_S^O} P_{Supplier(S,o,t)}^i + \sum_{V=1}^{N_V^i} P_{Discharge(V,t)}^i \\ P_{Di(t)} &= \sum_{L=1}^{N_L^i} P_{Load(L,t)}^i + \sum_{V=1}^{N_V^i} P_{Charge(V,t)}^i - \sum_{L=1}^{N_L^i} P_{NSD(L,t)}^i \end{aligned} \quad (3.7)$$

$$\forall t \in \{1,\ldots,T\}; \forall i \in \{1,\ldots,N_B\}$$

$$V_{i(t)} \times \sum_{j \in L^i} V_{j(t)} \left(G_{ij} \sin\left(\theta_{i(t)} - \theta_{j(t)}\right) - B_{ij} \cos\left(\theta_{i(t)} - \theta_{j(t)}\right)\right) - V_{i(t)}^2 \times B_{ii} = Q_{Gi(t)} - Q_{Di(t)}$$

$$\begin{aligned} Q_{Gi(t)} &= \sum_{DG=1}^{N_{DG}^i} \sum_{o=1}^{N_{DG}^O} Q_{DG(DG,o,t)}^i + \sum_{S=1}^{N_S^i} \sum_{o=1}^{N_S^O} Q_{Supplier(S,o,t)}^i \\ Q_{Di(t)} &= \sum_{L=1}^{N_L^i} Q_{Load(L,t)}^i - \sum_{L=1}^{N_L^i} Q_{NSD(L,t)}^i \end{aligned} \quad (3.8)$$

$$\forall t \in \{1,\ldots,T\}; \forall i \in \{1,\ldots,N_B\}$$

[6] *thermal limit:* means the maximum apparent power that can flow through a line without damaging it

[7] The lines are usually modeled in π circuit, with a series impedance (resistance and inductive reactance) and two shunt admittances (typically referred as susceptance)

- Voltage magnitude (3.9) and angle (3.10) limits at bus *i* in period *t*:

$$V_i^{min} \le V_{i(t)} \le V_i^{max} \quad ;\forall t \in \{1,...,T\};\forall i \in \{1,...,N_B\} \tag{3.9}$$

$$\theta_i^{min} \le \theta_{i(t)} \le \theta_i^{max} \quad ;\forall t \in \{1,...,T\};\forall i \in \{1,...,N_B\} \tag{3.10}$$

Equation (3.11) illustrates the power flow determination through a line *K,* connecting bus *i* to bus *j*. This equation is an example to allow a better comprehension of the constraint (3.12):

$$\begin{aligned} S_{ij(t)} &= \overline{U_{i(t)}} \times \left(\overline{I_{ij(t)}} + \overline{I_{Sh\_i(t)}}\right)^* \\ S_{ij(t)} &= \overline{U_{i(t)}} \times \left[\overline{y_{ij}} \times \left(\overline{U_{i(t)}} - \overline{U_{j(t)}}\right) + \overline{y_{sh\_i}} \times \overline{U_{i(t)}}\right]^* \end{aligned} \tag{3.11}$$

- Line thermal limit at line *k* in period *t*:

$$\begin{aligned} &\left|\overline{U_{i(t)}} \times \left[\overline{y_{ij}} \times \left(\overline{U_{i(t)}} - \overline{U_{j(t)}}\right) + \overline{y_{sh\_i}} \times \overline{U_{i(t)}}\right]^*\right| \le S_{Lk}^{max} \\ &\left|\overline{U_{j(t)}} \times \left[\overline{y_{ij}} \times \left(\overline{U_{j(t)}} - \overline{U_{i(t)}}\right) + \overline{y_{sh\_j}} \times \overline{U_{j(t)}}\right]^*\right| \le S_{Lk}^{max} \\ &\forall t \in \{1,...,T\};\forall i,j \in \{1,...,N_B\};i \ne j;\forall k \in \{1,...,N_K\} \end{aligned} \tag{3.12}$$

DG and external suppliers inequality constraints

The technical constraints of the DG and external suppliers are presented in this sub-topic. The inequality constraints essentially represent the limits for the active and reactive power generation. Two different situations were considered regarding DG units. In the first situation, the DG unit must keep its active and reactive power generation within its limits (3.13) and (3.15). These constraints are applied to DG units that can be dispatched or not, depending on the optimal scheduling decision (e.g. generation based on fossil fuel).

Regarding the second situation, the active power generation is equal to the maximum limit (3.14) and the reactive power generation is also equal to the maximum limit (3.16). The ERM problem is obligated to dispatch all the DG units that work under this second situation. This is applied to small scale intermittent resources [4] that do not represent a large impact on the optimal scheduling. This dispatch obligation is determined by energy policies determined by governments of several countries regarding the use of DER, e.g. an energy policy of Portuguese government[8]. The producers with renewable resources are one of these energy policies. Governments impose that the network operator fully dispatches this kind of producers.

[8] Consulted in November 2011: http://www.renovaveisnahora.pt

External supplier offers present a maximum limit, in terms of the active generation (3.17) and reactive generation (3.18):

- Active generation limit of offer *o* for the *DG* unit in each period *t*:

$$P_{DGMinLimit(DG,o,t)} \times X_{DG(DG,o,t)} \leq P_{DG(DG,o,t)} \leq P_{DGMaxLimit(DG,o,t)} \times X_{DG(DG,o,t)} \quad \forall t \in \{1,\ldots,T\}; \forall DG \in \{1,\ldots,N_{DG}\}; \forall o \in \{1,\ldots,N_{DG}^{O}\} \tag{3.13}$$

$$P_{DG(DG,o,t)} = P_{DGMaxLimit(DG,o,t)} \quad \forall t \in \{1,\ldots,T\}; \forall DG \in \{1,\ldots,N_{DG}\}; \forall o \in \{1,\ldots,N_{DG}^{O}\} \tag{3.14}$$

- Reactive generation limit of offer *o* for the *DG* unit in each period *t*:

$$Q_{DGMinLimit(DG,o,t)} \times X_{DG(DG,o,t)} \leq Q_{DG(DG,o,t)} \leq Q_{DGMaxLimit(DG,o,t)} \times X_{DG(DG,o,t)} \quad \forall t \in \{1,\ldots,T\}; \forall DG \in \{1,\ldots,N_{DG}\}; \forall o \in \{1,\ldots,N_{DG}^{O}\} \tag{3.15}$$

$$Q_{DG(DG,o,t)} = Q_{DGMaxLimit(DG,o,t)} \quad \forall t \in \{1,\ldots,T\}; \forall DG \in \{1,\ldots,N_{DG}\}; \forall o \in \{1,\ldots,N_{DG}^{O}\} \tag{3.16}$$

- Active generation limit of offer *o* for external supplier *S* , for each period *t*:

$$P_{Supplier(S,o,t)} \leq P_{SupplierLimit(S,o,t)} \quad \forall t \in \{1,\ldots,T\}; \forall S \in \{1,\ldots,N_{S}\} \forall o \in \{1,\ldots,N_{S}^{O}\} \tag{3.17}$$

$$Q_{Supplier(S,o,t)} \leq Q_{SupplierLimit(S,o,t)} \quad \forall t \in \{1,\ldots,T\}; \forall S \in \{1,\ldots,N_{S}\} \forall o \in \{1,\ldots,N_{S}^{O}\} \tag{3.18}$$

EVs equality and inequality constraints

The energy stored in EV batteries should be limited by its capacity (3.19). Three discharge power steps have been considered. The first discharge power step (3.20) is applied to the interval from 100% to 70% of the battery capacity. The second step (3.21) is used between 70% and 40% of the battery capacity. The third discharge power step (3.22) is only active in the interval of 40% at 20% of the battery capacity. Equation (3.23) adds the three discharge power steps. Equations (3.20) to (3.23) are only used when the remuneration scheme with three discharge steps is applied, using the equation (3.5).

The charge/discharge rates present their own maximum limit (3.24) to (3.27). In this formulation it was considered that the charge/discharge rate limit can change, depending on the different parts of the network the EV user is connected to. Each EV can be connected in a single phase (e.g. at home), with the rate limit being lower than when EVs are connected in three phases (e.g. a parking lot at the work). The charging ($\eta_{c(V)}$) and discharging ($\eta_{d(V)}$) efficiency battery are also used in the mathematical formulation. In this formulation two binary variables for each EV are used, to control the charge/discharge power, avoiding that the two operations occur at the same period (3.28).

- Battery capacity limit of electric vehicle *V* in period *t*:

$$E_{Stored(V,t)} \le E_{BatteryCapacity(V)} \quad \forall t \in \{1,\ldots,T\}; \forall V \in \{1,\ldots,N_V\} \tag{3.19}$$

- Discharge limit of step A, this step is activated until 70% of battery capacity:

$$0.7 \times E_{BatteryCapacity(V)} \le P_{Discharge\_StepA(V,t)} \le E_{Stored(V,t-1)} \quad \forall t \in \{1,\ldots,T\}; \forall V \in \{1,\ldots,N_V\} \tag{3.20}$$

- Discharge limit of step B, this step is activated until 40% of battery capacity:

$$0.4 \times E_{BatteryCapacity(V)} \le P_{Discharge\_StepB(V,t)} \le 0.7 \times E_{BatteryCapacity(V)} \quad \forall t \in \{1,\ldots,T\}; \forall V \in \{1,\ldots,N_V\} \tag{3.21}$$

- Discharge limit of step C, this step is activated until 20% of battery capacity:

$$0.2 \times E_{BatteryCapacity(V)} \le P_{Discharge\_StepC(V,t)} \le 0.4 \times E_{BatteryCapacity(V)} \quad \forall t \in \{1,\ldots,T\}; \forall V \in \{1,\ldots,N_V\} \tag{3.22}$$

- Add the discharge powers of step A, B and C for each vehicle:

$$P_{Discharge(V,t)} = P_{Discharge\_StepA(V,t)} + P_{Discharge\_StepB(V,t)} + P_{Discharge\_StepC(V,t)} \quad \forall t \in \{1,\ldots,T\}; \forall V \in \{1,\ldots,N_V\} \tag{3.23}$$

- Discharge limit of electric vehicle *V* in period *t*:

$$P_{Discharge(V,t)} \le P_{DischargeLimit(V,t)} \times X_{Discharge(V,t)} \quad \forall t \in \{1,\ldots,T\}; \forall V \in \{1,\ldots,N_V\}; X_{Discharge(V,t)} \in \{0,1\} \tag{3.24}$$

$$\frac{1}{\eta_{d(V)}} \times P_{Discharge(V,t)} \times \Delta t \le E_{Stored(V,t-1)} - E_{Trip(V,t)} \quad \forall t \in \{1,\ldots,T\}; \ \forall V \in \{1,\ldots,N_V\}; \ \Delta t = 1 \tag{3.25}$$

- Charge limit of electric vehicle *V* in period *t*:

$$P_{Charge(V,t)} \le P_{ChargeLimit(V,t)} \times X_{Charge(V,t)} \quad \forall t \in \{1,\ldots,T\}; \forall V \in \{1,\ldots,N_V\}; X_{Charge(V,t)} \in \{0,1\} \tag{3.26}$$

$$\eta_{c(V)} \times P_{Charge(V,t)} \times \Delta t \le E_{BatteryCapacity(V)} - E_{Stored(V,t-1)} - E_{Trip(V,t)} \quad \forall t \in \{1,\ldots,T\}; \forall V \in \{1,\ldots,N_V\}; \ \Delta t = 1 \tag{3.27}$$

- Vehicle charge and discharge are not simultaneous in electric vehicle *V* in period *t*:

$$X_{Charge(V,t)} + X_{Discharge(V,t)} \leq 1$$
$$\forall t \in \{1,...,T\};\ \forall V \in \{1,...,N_V\}; X_{Charge(V,t)}\ and\ X_{Discharge(V,t)} \in \{0,1\} \quad (3.28)$$

The typical daily travel profile of each EV user should be considered by ERM problem, as the VPP is obligated to guarantee the energy required for the EV user to travel in the time horizon of the optimization process. This energy consumption, through the travel ($E_{Trip(V,t)}$) has been considered in the mathematical formulation. In order to satisfy EV user requests, the VPP should use adequate forecast methods to learn the typical daily travel profile. This forecast is introduced in the battery balance using the variable $E_{Trip(V,t)}$. The VPP can combine the charge power $P_{Charge(V,t)}$ with the initial value of the battery ($E_{Initial(V)}$) in order to achieve the required $E_{Trip(V,t)}$. Equations (3.29) and (3.30) are used to determine the amount of energy stored at the end of period *t*. Equation (3.29) is only used for the first period, in order to consider the initial value of the battery. Equation (3.30) is applied in the other periods, considering the energy stored in the previous periods.

Constraint (3.31) assures that the battery of each vehicle *V* always contains a minimum amount of energy. It is predicted that some EV users will request that the battery never lowers from that minimum value. This can be seen as a reserve energy that can be used for an unexpected travel in each period.

- Battery balance of electric vehicle *V* in period *t*:

$$E_{Stored(V,t)} = E_{Initial(V)} + \eta_{c(V)} \times P_{Charge(V,t)} \times \Delta t - E_{Trip(V,t)} - \frac{1}{\eta_{d(v)}} \times P_{Discharge(V,t)} \times \Delta t \quad (3.29)$$
$$\forall t = 1;\ \ \forall V \in \{1,...,N_V\};\ \Delta t = 1$$

$$E_{Stored(V,t)} = E_{Stored(V,t-1)} + \eta_{c(V)} \times P_{Charge(V,t)} \times \Delta t - E_{Trip(V,t)} - \frac{1}{\eta_{d(v)}} \times P_{Discharge(V,t)} \times \Delta t \quad (3.30)$$
$$\forall t \in \{2,...,T\};\ \ \forall V \in \{1,...,N_V\};\ \Delta t = 1$$

- Minimum stored energy to be guaranteed in electric vehicle *V* at the end of period *t*:

$$E_{Stored(V,t)} \geq E_{MinCharge(V,t)}$$
$$\forall t \in \{1,...,T\}; \forall V \in \{1,...,N_V\} \quad (3.31)$$

3.3.3. Deterministic Technique

The GAMS software has been used to implement the deterministic technique, using the Discrete and Continuous Optimizer (DICOPT) solver to solve the MINLP problem. DICOPT [118] solves two sub-problems, the Non-Linear Programming (NLP) problem and the Mixed-Integer Programming (MIP) problem. DICOPT considers the sub-problems independently, using the most appropriate approach for each one, namely the Continuous global Optimizer (CONOPT) solver [119] to solve the NLP problem; and the simplex algorithm and C programming (CPLEX) [120], to solve the MIP problem.

The deterministic technique uses the following decision variables for each period:

- Active power generation of each DG unit - $P_{DG(DG,o,t)}$;
- Binary variable of each DG unit - $X_{DG(DG,o,t)}$;
- Active power generation of each external supplier - $P_{Supplier(S,o,t)}$;
- Active power discharge of each EV - $P_{Discharge(V,t)}$;
- Active power charge of each EV - $P_{Charge(V,t)}$;
- Excess available power of each DG unit - $P_{EAP(DG,t)}$;
- Non-supplied demand of each load - $P_{NSD(L,t)}$.

The mathematical formulation considers some additional variables for the deterministic technique, which, however, are not classified as decision variables:

- Reactive power generation of each DG unit - $Q_{DG(DG,o,t)}$;
- Reactive power generation of each external supplier - $Q_{Supplier(S,o,t)}$;
- Binary variable of vehicle *V* related to power charge - $X_{Charge(V,t)}$;
- Binary variable of vehicle *V* related to power discharge - $X_{Discharge(V,t)}$;
- Voltage angle at bus *i* - $\theta_{i(t)}$;
- Voltage magnitude at bus *i* - $V_{i(t)}$.

The number of variables used by the deterministic technique can be determined using the following expression (3.32):

$$N_{MINLP} = \left(N_{DG} \times \left(1 + 3 \times N_{DG}^{O}\right) + 2 \times N_S \times N_S^{O} + 4 \times N_V + N_L + 2 \times N_B\right) \times T \quad (3.32)$$

3.4. Simulated Annealing

SA is a metaheuristic inspired by the cooling process seen in metallurgy. This metaheuristic simulates the heat treatment of a metal, followed by the cooling process that reduces the temperature until the material achieves a crystallized state. This methodology

was proposed in 1983 by Kirkpatrick *et al.* [121-122]. The genesis of the SA was presented in 1953 by Metropolis *et al.* [123]. Kirkpatrick *et al.* realized that the annealing algorithm proposed by Metropolis *et al.* could be adapted to optimization problems.

In the initial state, the process becomes unstable, and consequently the atoms gain a larger possibility of finding new configurations. During the cooling process, the temperature is reduced and the atoms achieve new energy states with minimum values. At the end of the cooling process a crystallized state with a minimum energy is achieved [121, 124].

3.4.1. General SA Algorithm

This sub-section presents the most generic structure of the SA methodology. The parameters used by the SA technique and the mechanism used to avoid local optima are explained. The pseudo code of the SA methodology is shown in Figure 3.4.

```
Create initial solution s;
Set initial temperature T_0;
Set number of trials at each temperature level (level-length) L;
Set level count k ← 0;
while termination criterion not satisfied do
    for i=1 to L do
        Create new neighbor s' by applying an arbitrary / random move to s;
        Calculate cost difference ΔC between s' and s: ΔC = C(s') − C(s);
        if ΔC ≤ 0 then
            Switch over to solution s' (current solution s is replaced by s');
        else
            Create random number r ∈ [0, 1];
            if r ≤ exp(−ΔC/T_k) then
                Switch over to solution s' (current solution s is replaced by s');
            end
        end
    end
    Update best found solution (if necessary);
    Set k ← k + 1;
    Set / Update temperature value T_k for next level k;
end
return Best found solution;
```

Figure 3.4 – Simulated annealing algorithm [125].

The SA algorithm starts with an initial solution and temperature (s, T_0), typically the temperature is specified with a high value [122]. The fitness function of the initial solution ($C(s)$) is calculated, most of the times incorporating the objective function and penalty factors. The cooling process is initialized with the creation of a neighbor solution (s') [125]. Basically, the objective of this step is finding a new solution in the search space of

the optimization problem. The generic example presented in Figure 3.4 considers the execution of a random movement to obtain a new solution (*s'*), however, in some optimization problems an heuristic process is applied, in order to obtain a new better solution (*s'*) [126].

The following step evaluates the fitness function (*C(s')*) of the neighbor solution. Additionally, the difference (*ΔC*) between the fitness value of *s'* and the initial one (*s*) is determined. After this step, the next solution (*s*) for the next iteration (*k+1*) is selected based on two criteria [121-122]:

1. If *ΔC* is lower than zero, the current solution (*s*) is replaced by the neighbor solution (*s'*);
2. If *ΔC* is higher than zero, the acceptance probability of the neighbor solution (s') is determined. The acceptance probability depends on *ΔC* and on the temperature value. If this probability is higher than a randomly generated value, the current solution (*s*) is updated with the neighbor solution (*s'*).

The steps to create a new *s'*, to calculate the *ΔC* and to accept the *s',* are executed in a specific number of iterations (*L*). The temperature (T_K) is reduced after iteration *L* is reached. At the same time, iteration *k* is updated, becoming iteration *k+1*. The SA algorithm finishes when the termination criteria are achieved.

The SA algorithm is based on local search, but it is enhanced with the use of the annealing process, to avoid the local optima. This algorithm enables the acceptance of worse solutions, as a possible pathway for reaching better solutions. The SA algorithm has the advantage of requiring less computational resources when compared to population based algorithms (e.g. genetic algorithm and particle swarm optimization) because it is able to generate a single neighborhood solution [127-128]. This fact makes the SA algorithm promising to solve the ERM problem.

3.4.2. Simulated Annealing Parameters

The SA parameters influence the performance of the method, both in terms of accuracy and execution time. Adapting the SA algorithm for a specific optimization problem requires some necessary adjustments in the parameters. The literature presents some indications about the behavior of the parameters depending on the type of problem. Typically, the initial temperature should have a high value, and the cooling should be slow. The general SA algorithm includes three main parameters [121, 125]:

- Initial Temperature (T_0) — This parameter is used to control the acceptance probability, to avoid local optima;

- Number of iterations at constant temperature (L) — This parameter is used to find further solutions with the same probability, in order to increase the changes of escaping from a local optima;
- Cooling rate (α) — This parameter is used to decrease the initial temperature lowering the acceptance probability of worse solutions. This strategy enables the possibility of escaping from local optima.

3.4.2.1. Cooling Schedule

In the beginning of its execution, the cooling process (or annealing process) increases the possibilities of finding solutions with lower internal energy than the initial one. During the cooling process, the temperature will decrease in order to reduce the acceptance of worse solutions. This cooling process is the key to accept solutions with worse fitness function values than local optima. The cooling schedule influences the accuracy of the SA algorithm.

The cooling schedule can be based on several different approaches when decreasing the temperature, and must be adapted to the optimization problem. The majority of optimization problems that use SA present generic cooling schedules. It is possible to find two or three generic cooling schedules in the literature [125].

Linear scheme

The linear scheme (3.33) is commonly used in the SA algorithm. It requires a good adjustment in the constant c to control the reduction of the temperature [125]. In this scheme the reduction is constant, which is found to be enough to control the cooling process in some optimization problems. At the beginning, it can be found to be necessary to maintain the temperature in a high level, and in a certain specific iteration k, the temperature can reduce rapidly to limit the number of accepted worse solutions.

$$T_{k+1} = T_k - c \tag{3.33}$$

Geometric scheme

The geometric schedule (3.34) is one of the most used schemes in SA applications. This scheme has been used in the SA methodology proposed in this thesis [125]. The cooling rate (α) controls the reduction of the temperature. This parameter can assume a value from 0 to 1, being typically close to 1. Considering a high value makes the temperature decrease slowly.

$$T_{k+1} = T_k \times \alpha \tag{3.34}$$

Logarithmic annealing schedule

The logarithmic schedule (3.35) [129] can be applied to the SA algorithm. It is necessary to specify the *C* and *d* constants, typically *C* has a high value and *d* is 1. This scheme originates a slower temperature decrease than the other two schemes, but it is able to achieve a good accuracy in the optimization problem.

$$T_{k+1} = \frac{C}{\log(k+d)} \tag{3.35}$$

A comparison between the cooling schedules and hybrid schedules is performed in several works [130-131].

3.4.2.2. Acceptance Probability

Function *p* (3.36) is used to determine the acceptance probability, and it is based on the Boltzman distribution [121, 125]. This function depends on the temperature value, and on the difference between the fitness functions of the current solution and of the previous solution. Using this function ensures that the acceptance probability will depend on the annealing process during the iterations.

Figure 3.5 illustrates the behavior of the acceptance probability.

$$p = e^{-\frac{\Delta F_k}{k \times T_k}} \tag{3.36}$$

$$\Delta F_k = \left| f(x_{k+1}) - f(x_k) \right|$$

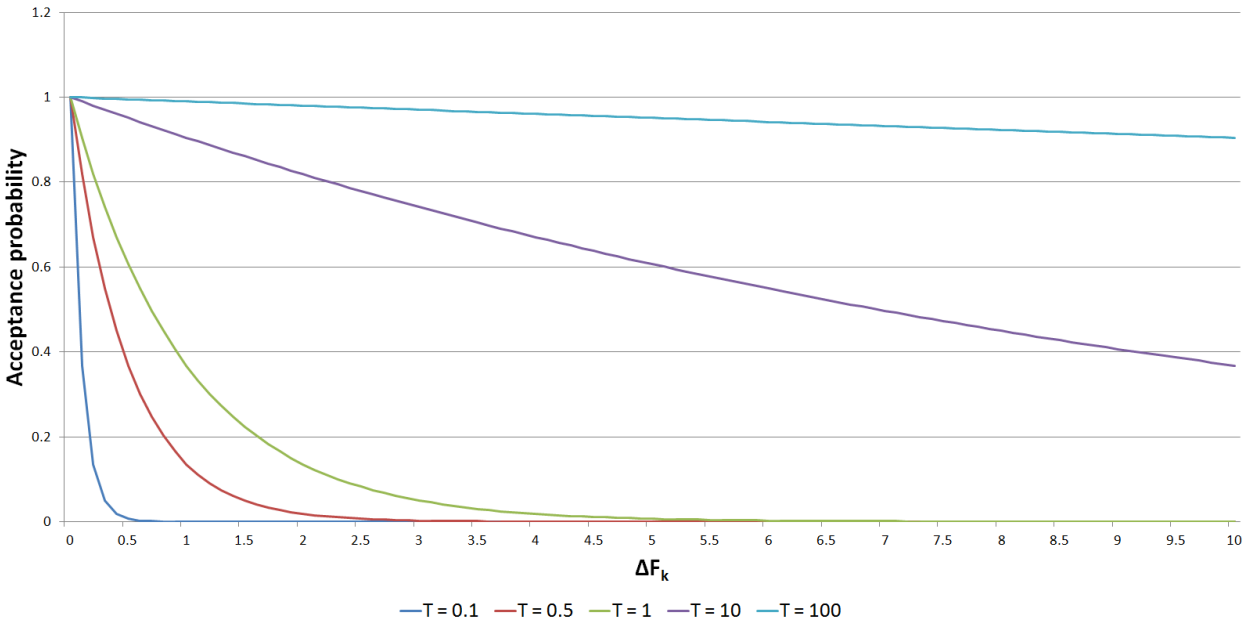

Figure 3.5 – Acceptance probability evolution to different temperature values.

For a given value of temperature (T_k), a high difference in the fitness function (ΔF_k) results in a low acceptance probability, meaning that the current solution cannot be accepted. A low ΔF_k increases this probability. However, the acceptance probability of a solution, independently of its ΔF_k , will be close to 1 for high values of T_k. On the other hand if the temperature is too low, the acceptance probability will be close to 0. In the beginning of the annealing process, the probability of accepting worse solutions is higher, due to the high level of temperature. When the temperature starts decreasing, with the cooling process, the acceptation probability of worse solutions will also decrease.

3.4.2.3. Termination criteria

The termination criteria present a direct influence over the execution time of the SA algorithm. Several criteria can be used to stop the optimization process. Typically the following criteria are used [125]:

- Reaching of a minimum value of temperature;
- Reaching of a maximum number of iterations;
- The best fitness function presenting no improvement during a specific number of iterations.

3.4.3. Proposed Simulated Annealing Methodology

The proposed simulated annealing methodology is based on an adaptation of the generic SA algorithm. With the purpose of being used as an adequate optimization technique directed to the ERMaS tool, the proposed methodology presents some changes regarding the generic version of the SA algorithm [23]. The proposed methodology considers the geometric cooling scheduling for temperature decreasing. The main changes were introduced on:

- Neighborhood scheme;
- Fitness function;
- Constraint control strategy;
- Termination criteria.

These changes will be explained ahead in detail. Figure 3.6 shows the flowchart of the proposed SA methodology.

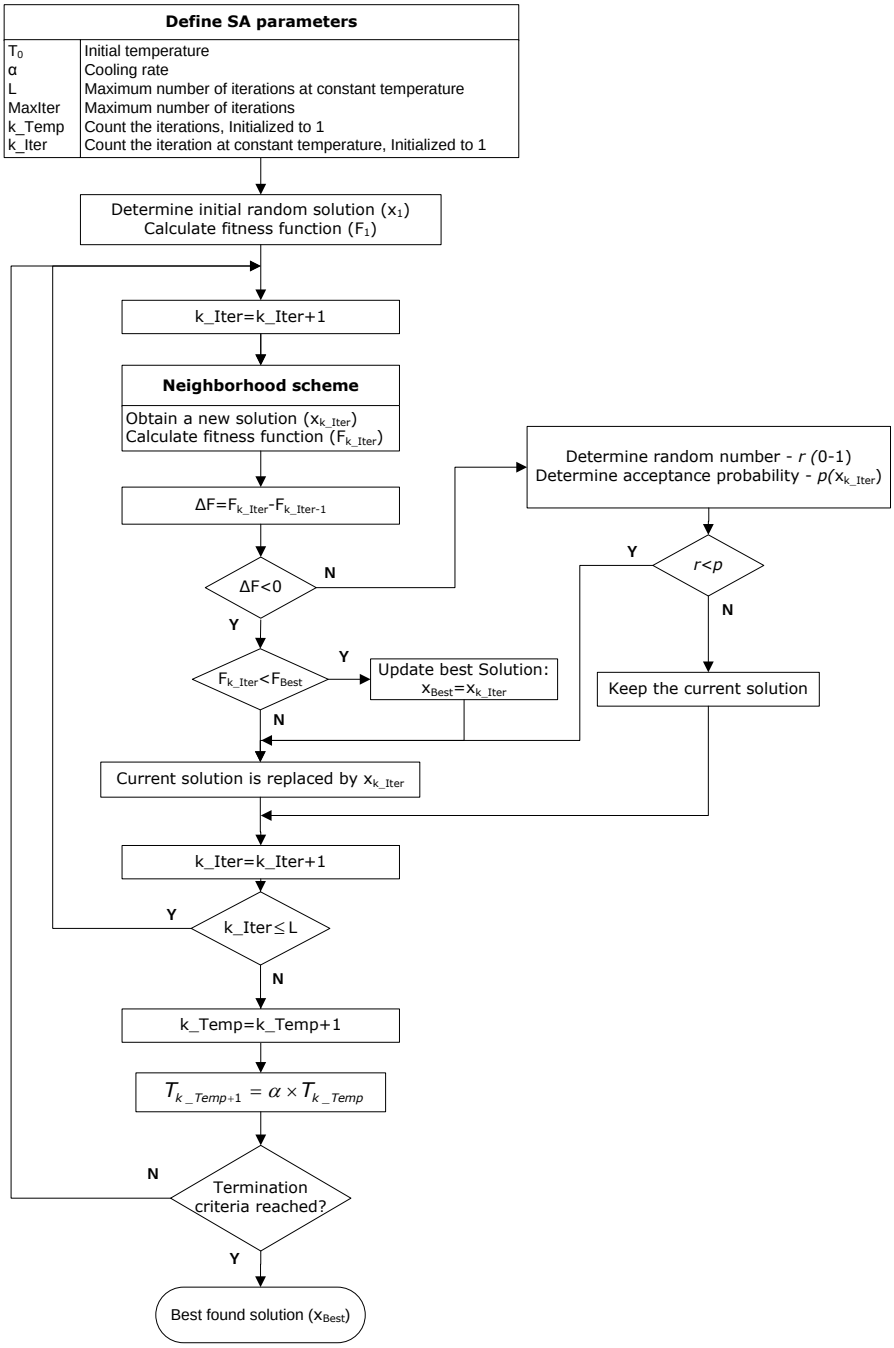

Figure 3.6 – Flowchart of the proposed SA methodology.

3.4.3.1. Decision Variables

The proposed SA methodology considers the following decision variables for each period:

- Active power generation of each DG unit - $P_{DG(DG,o,t)}$;
- Binary variable of each DG unit - $X_{DG(DG,o,t)}$;
- Active power generation of each external supplier - $P_{Supplier(S,o,t)}$;
- Active power discharge of each EV - $P_{Discharge(V,t)}$;

- Active power charge of each EV - $P_{Charge(V,t)}$;
- Excess available power of each DG unit - $P_{EAP(DG,t)}$;
- Non-supplied demand of each load - $P_{NSD(L,t)}$.

For a single EV, the active power charge ($P_{Charge(V,t)}$) and discharge ($P_{Discharge(V,t)}$) are considered as one variable. The following constraint (3.37) represents the way that the charge and discharge limits have been considered in the proposed SA methodology.

$$-P_{DischargeLimit(V,t)} \leq P_{vehicle(V,t)} \leq P_{ChargeLimit(V,t)} \quad \forall t \in \{1,...,T\};\ \forall V \in \{1,...,N_V\} \tag{3.37}$$

Instead of using two continuous variables ($P_{Charge(V,t)}$, $P_{Discharge(V,t)}$) and two integer variables ($X_{Charge(V,t)}$, $X_{Discharge(V,t)}$) for each EV, the proposed SA methodology tries to determine the active power using one variable ($P_{vehicle(V,t)}$). This modification decreases the number of variables used by this methodology. The computation resources benefit from this modification, mainly in what concerns the reduction of memory allocation. This means that the deterministic methodology uses four variables allocated to a single EV for each period, while the proposed SA methodology only uses one variable for each vehicle for each period.

Other variables from the mathematical formulation have also been considered by the proposed SA methodology, not being classified as decision variables:

- Reactive power generation of each DG unit - $Q_{DG(DG,o,t)}$;
- Reactive power generation of each external supplier - $Q_{Supplier(S,o,t)}$.

The number of variables used by the proposed SA methodology can be determined by the following expression (3.38):

$$N_{SA} = \left(N_{DG} \times \left(1 + 3 \times N_{DG}^{O}\right) + 2 \times N_S \times N_S^O + N_L + N_V\right) \times T \tag{3.38}$$

The number of variables used in this methodology is much lower than in the deterministic technique.

3.4.3.2. Termination Criteria

The proposed SA methodology uses two criteria that were previously presented:

- Reaching of a maximum number of iterations;
- The best fitness function presenting no improvement during a specific number of iterations.

Considering the flowchart in Figure 3.6, a maximum number of iterations (*MaxIter*) is established. When iteration (*k*) reaches the maximum number of iterations *MaxIter*, the algorithm stops. The SA methodology can stop through another criterion, considering the fitness function evolution. In each iteration *k* an evaluation is performed, regarding the improvement of the best fitness function. Firstly, the error *ε*, and a maximum number of iterations for the best fitness evolution (iter_ *ε*) are determined. The difference from the best fitness function found between iteration *k* and *k-1* is determined. If this difference is lower than the error *ε* then a count variable is incremented at 1, when this variable reaches iter_ *ε,* the algorithm stops.

For instance, if the error *ε* is established as 0.01, and iter_ *ε* as 10; the best fitness function in iteration *k* is 1000 and in iteration *k+1* it is also 1000; then the difference is equal to 0. Being lower than 0.01, the variable is incremented by 1. This process can go on until reaching the maximum number of 10. If during this process the difference between the current and the best fitness function is higher than *ε,* the count variable is initialized at 0.

3.4.3.3. Neighborhood Scheme

Heuristic processes have been implemented in order to improve the selection of new better solutions. The heuristic processes have been used for the variables: $P_{DG(DG,o,t)}$, $P_{Supplier(S,o,t)}$, $P_{vehicle(V,t)}$.

DG units and external suppliers heuristic

The heuristic process used in the proposed SA methodology is denominated as order of merit heuristic [132]. This heuristic determines a new solution for the active power generation of DG and external supplier, which can be described as follows:

1. The operation cost of each DG unit and external supplier for the previous solution is determined, using the f_1 (3.2) and f_2 (3.3) functions;
2. The operation cost is sorted by ascendant order;
3. The first half of generators (including DG and external suppliers) are randomly determined based on a uniform distribution between the respectively previous solution and the generators' maximum active power;
4. The other half of generators is randomly determined by a uniform distribution between the previous solution and the minimum active power.

The random generation of numbers, based on the uniform distribution, is performed using the UNIFRND function of MATLAB.

EVs heuristics

Two heuristic processes have been developed with the purpose of allocating the charge and discharge of EVs in the neighborhood scheme.

- **Consecutive EVs allocation**

The first heuristic process is called consecutive EVs allocation, and has already been used in one of the articles published during the development of this thesis work [23]. The flowchart of the consecutive EVs allocations is shown in Figure 3.7.

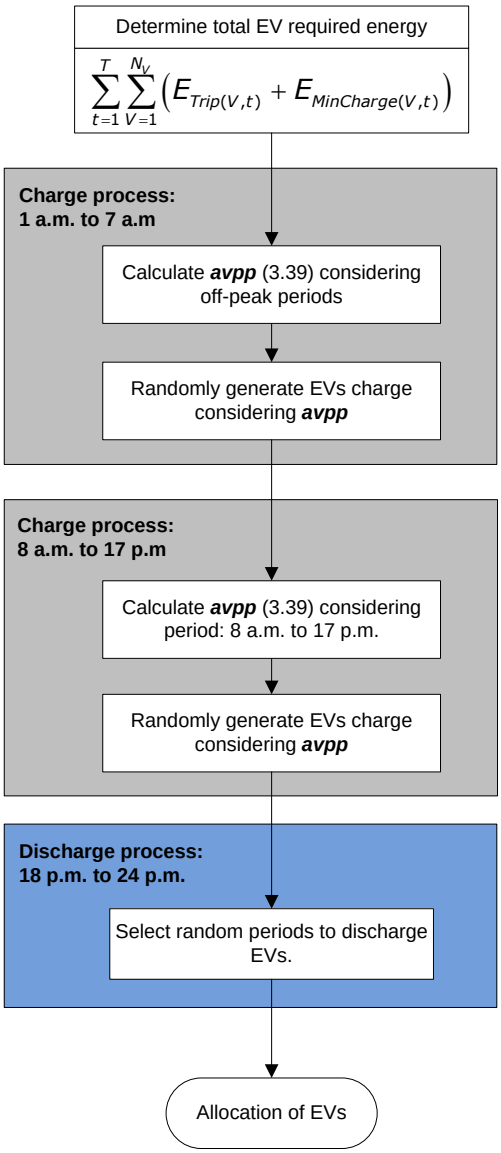

Figure 3.7 – Proposed heuristic process denominated consecutive EVs allocation.

The proposed heuristic tries to allocate the EVs considering three steps. The first step allocates the charge of EVs in off-peak periods. This process starts by determining the total energy that EVs will need to use in the next periods, i.e. considering the energy with trips ($E_{Trip(V,t)}$) and the minimum stored energy that must be guaranteed ($E_{MinCharge(V,t)}$).

Using this energy the average vehicle per period (*avpp*) is determined through expression (3.39):

$$avpp = \frac{\sum_{t=1}^{T}\sum_{V=1}^{N_V}\left(E_{Trip(V,t)} + E_{MinCharge(V,t)}\right)}{nopp \times \overline{P_{ChargeLimit(nopp)}}} \tag{3.39}$$

where *nopp* is the number of off-peak periods, and $\overline{P_{ChargeLimit(nopp)}}$ is the average EVs charge limit for the set of off-peak periods.

Expression (3.39) is used to allocate the number of EVs by period, during off-peak periods. If one considers an *avpp* of 10, then 10 vehicles will be allocated for each off-peak period. As an example, considering seven hours of off-peak periods and 75 EVs, we will have 70 EVs allocated in off-peak periods, and the remaining 5 EVs will be randomly allocated to off-peak periods. A random number between 0 and $P_{ChargeLimit(V,t)}$ is generated to define $P_{vehicle(V,t)}$.

The second step uses a similar methodology, but it is applied to charge EVs between 8 a.m. and 17 p.m. This step also starts by determining the total energy that EVs will need, but only the energy during the previous mentioned periods (8 a.m. to 17 p.m.). *avpp* is determined using expression (3.39), but, this time, using the previous energy. These periods are also selected to charge, because one of the most common EVs behaviors is that they will be parked in working places during the period from 8 a.m. to 17 p.m.

The third step allocates the discharge in other periods. The discharge process is obtained by selecting the periods in which EVs do not charge. During these periods, the discharge power of each EV is randomly generated, considering numbers between 0 and the minimum limit of $-P_{DischargeLimit(V,t)}$. These random values may possibly be changed to zero during the calculation of the fitness function, with the use of the constraint control strategy.

This heuristic allocates the charge and discharge of all EVs in just one loop. It is also a more suitable heuristic for ERM problems with a small number of EVs.

- **Intelligent EVs allocation**

The second heuristic process is called intelligent EVs allocation. This process tries to allocate EVs to charge during periods with a low demand value. Allocating the EVs charge in periods with low demand helps the minimization of the operation cost, because these periods consider a higher availability of DER at a low cost.

In terms of discharge power allocation, the intelligent EVs allocation heuristic process uses a similar process. Selecting the best periods to discharge means an intelligent allocation of EVs during peak periods, when load demand achieves high values. During

these periods, in order to supply the demand, the VPP may have to use more expensive DERs, and the EVs discharging may help in minimizing the operation cost.

The flowchart of the intelligent EVs allocations is shown in Figure 3.8.

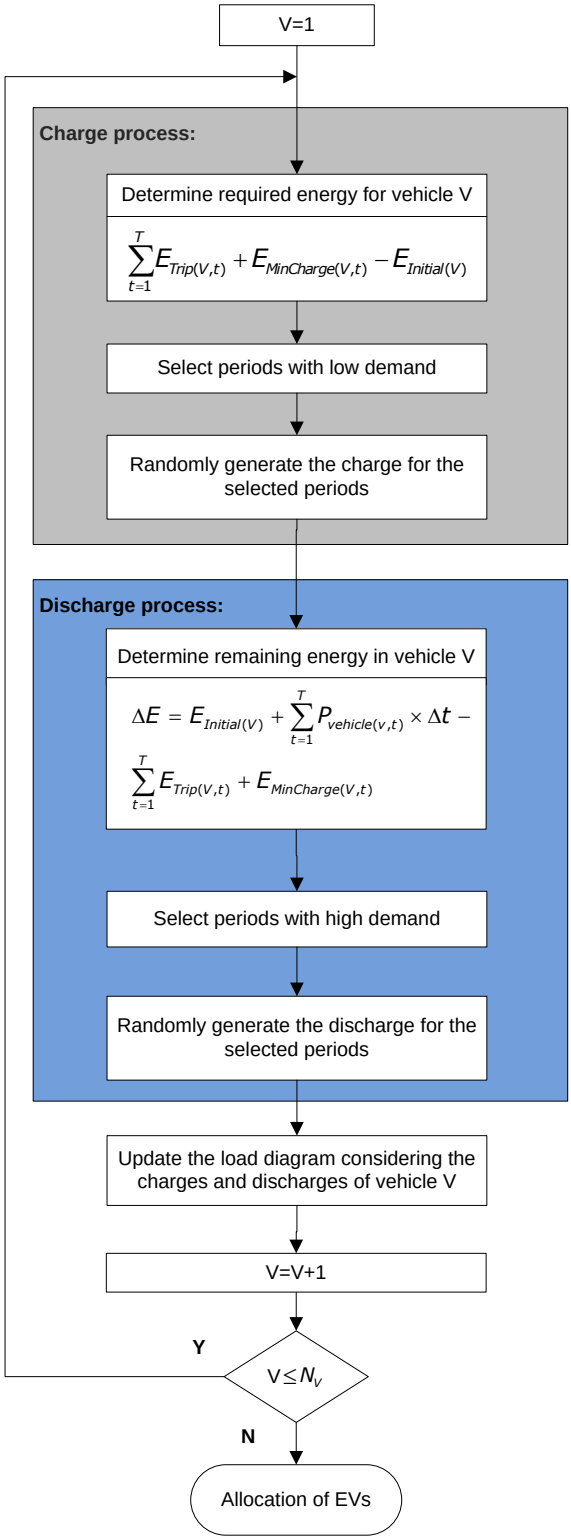

Figure 3.8 – Proposed heuristic process denominated intelligent EVs allocation.

It is necessary to consider the load demand reduced by the DG generation power that the VPP is obligated to dispatch (see equation 3.14). This process is executed for each vehicle until it reaches the maximum number of EVs (N_V), and it is divided into two steps.

The first step selects the best periods to charge the vehicle. In the first part of this step the energy that the vehicle will require in the next periods is determined. This is done by calculating the energy used for the trips during the day minus the initial value of the battery (see the bottom part of Figure 3.8). In order to select the periods with low demand, where the vehicle *V* will charge so that it achieves the required energy, it is necessary to determine the required time to charge. This is done by dividing the previous energy value by the slow charge rate of vehicle *V*. The selected set of periods during which vehicle *V* will charge, is a set of periods found to have low demands. This selection is always made considering a load demand sorted in ascendant order.

The randomly generation of the charge power for the selected periods is the last part of this step. A random number between 0 and $P_{ChargeLimit(V,t)}$ is generated using the UNIFRND function of MATLAB. This charge process is repeated more than one time, in order to increase the charge of the vehicle *V* and to achieve the required energy of the vehicle.

The second step is characterized by a selection of the best periods to discharge the vehicle, which will be the periods with a high load demand. Considering the charge power randomly generated in the previous step, the remaining energy of vehicle *V* is determined (see the expression in Figure 3.8, determining ΔE). The charging power is added to the initial battery value, minus the energy used for the trips during the day (see Figure 3.8). The time to discharge is determined by dividing this energy value by the slow discharge rate of vehicle *V*. This will be used to select the periods to discharge the vehicle in the next part of this step. The periods with a high demand value will be selected, and the step finishes with the random generation of numbers between $-P_{DischargeLimit(V,t)}$ and 0 for the selected periods to discharge.

After these two steps, the load diagram value in each period is updated. The load diagram value is added to the charge power, or reduced when considering the discharge power. Executing this update in each iteration of this loop will prevent the massive allocation of EVs in the same periods, because the load diagram will gradually increase when high charges are allocated in the some periods. The same happens with the discharge, but decreasing the load diagram.

This heuristic will finish when variable *V* reaches the total number of EVs. This heuristic works well if it is executed in an iterative process, due to the requirement of changing the load diagram, considering the charge and discharge that are determined for each vehicle. For this reason, the execution time of this heuristic process is higher than the first one (consecutive EVs allocation). This heuristic presents better results when solving

ERM problems with a large number of EVs, because this heuristic gradually allocates the charge and discharge considering the load demand value in each period. Annex B presents a more detailed explanation about the use of consecutive and intelligent EVs allocations in the neighborhood scheme.

3.4.3.4. Fitness Function

The fitness function of the proposed SA methodology incorporates the objective function (3.1), and penalty factors that represent the deviation of the constraints. This is a common strategy to handle the constraints of an optimization problem. The penalty factors must be adjusted to suit the optimization problem.

Several penalization functions were studied before using the chosen ones. The penalty factors used in this proposed SA methodology have been used in a previous work [132]. The requirements to choose a good penalization function were: for low deviations the function should grow quickly; however, with higher deviations, the function should not grow too much, as can be seen in Figure 3.9. Figure 3.9 shows the penalization function for a thermal line limit deviation (3.42).

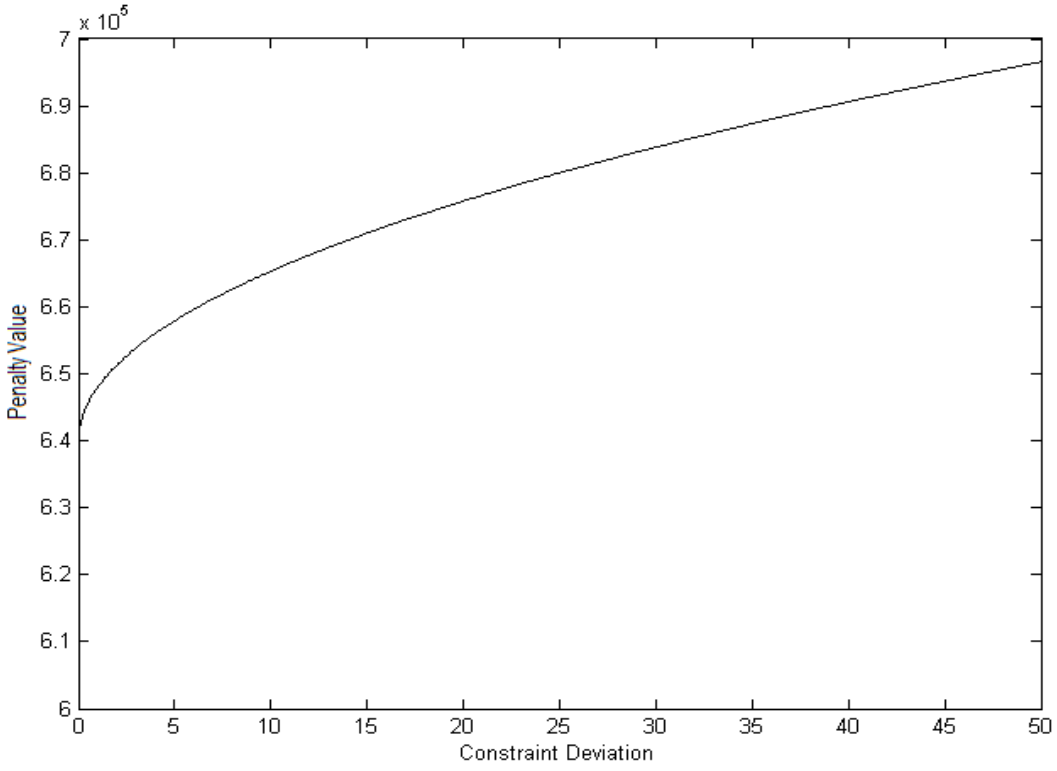

Figure 3.9 – Penalization function evolution.

Using this strategy, the SA algorithm is able to maintain the solutions without constraint violations. When a solution violates the constraints, the objective function assumes a higher value. In the proposed SA methodology, the thermal line limit (3.42) has more relevance than other constraints.

The following penalty factors try to control the deviation of the network constraints:

- Voltage magnitude limits (3.40) violated (maximum or minimum)

$$w\left(V_i^{violated}\right) = \sum_{t=1}^{T}\left(100 \cdot \left(\sum_{i \in N_B}^{violated}\left(V_i^{\min} - V_{i(t)}\right)^2 + V_i^{\min} - V_{i(t)}\right) + 100 \cdot \left(\sum_{i \in N_B}^{violated} V_{i(t)} - V_i^{\max}\right)\right) \quad (3.40)$$

- Voltage angle limits (3.41) violated (maximum or minimum)

$$w\left(\theta_i^{violated}\right) = \sum_{t=1}^{T}\left(10 \cdot \left(\sum_{i \in N_B}^{violated} \theta_i^{\min} - \theta_{i(t)} + \sum_{i \in N_B}^{violated} \theta_{i(t)} - \theta_i^{\max}\right)\right) \quad (3.41)$$

- Thermal line limit (3.42) violated

$$w\left(S_{ij}^{violated}\right) = \sum_{t=1}^{T}\left(f^2 + 10 \times f \times \sqrt{\sum_{k \in N_K}^{violated} S_{ij(t)} - S_{Lk}^{\max}}\right) \quad (3.42)$$

The fitness function (3.43) used to evaluate the solution of the proposed SA methodology is formulated as follows:

$$\min F = f + w\left(V_i^{violated}\right) + w\left(\theta_i^{violated}\right) + w\left(S_{Li}^{violated}\right) \quad (3.43)$$

3.4.3.5. Constraint Control Strategy

The constraint control strategy has the purpose of guaranteeing that any solution violates the constraints of the mathematical formulation. The used deterministic technique is implemented on GAMS software, and the DICOPT solver guarantees that the constraints are not violated. In the proposed SA methodology it is also necessary to use a strategy to control the constraints of the mathematical formulation.

The proposed constraint control strategy is supported by two different controls. The first one consists in maintaining the decision variables in their limits, see equations 3.13, 3.14, 3.17, and 3.37. A uniform distributed random function in MATLAB (UNIFRND command) has been used to randomly generate numbers between the limits of each variable. With this MATLAB command it is possible to define the maximum and minimum limit, e.g. X=unifrnd(X_{min}, X_{max}) returns a matrix of random numbers on the interval from X_{min} to X_{max}. The binary variables of the DG units are randomly generated between 0 a 1 as continuous variables and the results are rounded to 0 or 1. The $P_{EAP(DG,t)}$ and $P_{NSD(L,t)}$ decision variables are initialized as 0 and, in case of their use being required to guarantee the network active power balance (see equation 3.7), the values of these variables are set according to the respective costs. This first strategy helps to maintain a SA solution as a feasible solution of the ERM problem. This strategy is executed in the neighborhood scheme

of Figure 3.6 when a new solution is obtained, and it is also applied in the initial solution of the proposed SA methodology.

The second strategy is based on direct repair of the solution with the purpose of satisfying all the constraints. This strategy is applied during the calculation of the fitness function in the neighborhood scheme (Figure 3.6). Before the calculation of the fitness function, the constraints are checked and the solution is repaired according to the constraints. This direct repair is used in the following situations:

- The EV battery balance and technical specifications are controlled in each neighborhood solution, see equations 3.19, 3.25, 3.27, 3.29, 3.30, and 3.31;
- The active power balance (equation 3.7) of the system is matched in each neighborhood solution. This match is calculated without knowing the value of the active power loss. When there is a surplus of generation power, the DG units or EVs discharge with higher costs are reduced or disconnected until active power balance is achieved. A similar scheme is used in the case of lack of generation power. In this case the DG units or EVs discharging with lower costs are chosen;
- The next step uses a power flow algorithm to determine the power flow and voltage profile of the SA solution. The previous step is used to select the DG units and EVs that should not be considered to match the active power balance. This power flow algorithm is a second validation of the active (3.7) and reactive (3.8) power balance, considering in this case the active and reactive power loss. This algorithm included additional calculations to consider a more detailed DG unit model;
- After determining the power flow and voltage profile, the penalization function that was presented in the fitness function topic is applied. The penalization function has been considered to control the constraints (3.9), (3.10) and (3.12).

The power flow analysis has the objective to determine the voltage magnitude and angle at all buses of the network and the power flow that pass in each line of the network. The Newton-Raphson (N-R), Gauss-Seidel (G-S) and Fast Decoupled (FD) are the conventional iterative algorithms used to determine the power flow [114], but in distribution networks these algorithms present poor convergence characteristics. Typically, the distribution network is characterized to have a radial topology, a high level of R/X ratio and feeds unbalanced loads. The power flow at the distribution level is seen as an ill conditioned problem that requires robust and efficient iterative algorithms to solve this problem. The conventional algorithms (N-R, G-S and FD) can work well in transmission

networks, where the R/X ratio achieves a low value and typically operates in meshed topology.

Instead of using conventional power flow algorithms, several authors have been presented alternative algorithms to solve ill conditioned distribution networks. The works developed can be divided into two groups [133]. The first one presented the conventional algorithms (N-R, G-S and FD) with modifications for distribution networks. The second group is based on forward and/or backward sweep algorithms using Kirchhoff's laws or making use of the well-known bi-quadratic equation. This second group is also based on iterative process. The forward and/or backward sweep process is simple and presents good performance, in terms of accuracy and efficiency. A typical radial topology of the distribution network is represented in Figure 3.10.

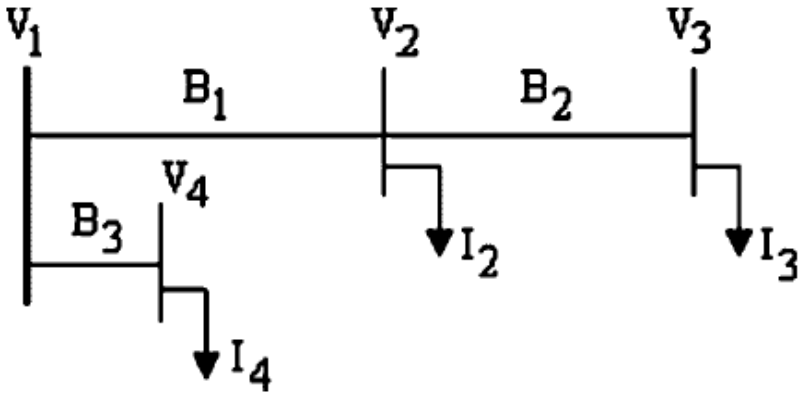

Figure 3.10 – Radial topology of a distribution network from [134].

This type of distribution network has a topology that considers few supplying buses or sending buses. Typically a distribution network has one sending bus that feeds to the rest of the network, as it is possible to see in the previous figure.

There are several forward/backward (f/b) approaches with different modifications, but the principle is centered in the Kirchhoff' laws. The different f/b approaches have in common the following steps to determine the power flow:

1. **Calculation of current in buses:** It is determined the current that is injected in each bus of the distribution network. It is necessary to divide the apparent power injected by the voltage in each bus, using the equation (3.44). The injected power is equal to the power demand minus the power generation, and these values should be specified. In the mathematical formulation has been indicated an opposite expression to determine the power injected, but in the f/b method the reduction of the generation power in the demand power is considered. The symbol * is used to represent the complex conjugate operator;

$$\overline{I_i^k} = \left(\frac{\overline{S_i}}{\overline{U_i^{k-1}}} \right)^* - \overline{y_{sh\_i}} \times \overline{U_i^{k-1}}$$

$$\overline{S_i} = \overline{S_{Di}} - \overline{S_{Gi}} \qquad (3.44)$$

$$e.g. \quad \overline{I_3^k} = \left(\frac{\overline{S_3}}{\overline{U_3^{k-1}}} \right)^* ; \quad \overline{I_4^k} = \left(\frac{\overline{S_4}}{\overline{U_4^{k-1}}} \right)^*$$

$$\forall i \in \{1,\ldots,N_B\}$$

2. **The backward sweep process**: it consists in determining the current of all lines starting for the far end bus until reaching the sending bus. In each line is applied the Kirchhoff's first law (or node rule). In this process the current or the apparent power that pass in the lines can be determined. The equation (3.45) can be used to determine the current in each line *L*;

$$\overline{B_L^k} = \sum_{i \in M} \overline{I_i^k}$$

$$e.g. \ \overline{B_3^k} = \overline{I_4^k} \ ; \ \overline{B_1^k} = \overline{I_2^k} + \overline{I_3^k} \qquad (3.45)$$

$$\forall L \in \{1,\ldots,N_K\}$$

where, *M* is the set of loads connected to the *L* line. Instead of using the current, this equation could be easily adapted to consider apparent power that passes in the lines.

3. **The forward sweep process:** it consist in determining the voltage in all buses starting from the sending end bus until reaching the far end bus. It is applied the Kirchhoff's second law (or mesh rule). In this step, the line currents that were determined in the previous backward step will be used. The equation (3.46) is used to determine the voltage in all buses. In the sending bus it is not required to determine the voltage, because the voltage magnitude is known and the voltage angle is typically 0.

$$\overline{U_j^k} = \overline{U_i^k} - \overline{z_L} \times \overline{B_L^k} \qquad (3.46)$$

$$\forall i, j \in \{1,\ldots,N_B\}; \forall L \in \{1,\ldots,N_K\}$$

where, *i* is the sending bus of the *L* line and *j* is the receiving bus of the *L* line. z_L is the series impedance of the *L* line.

These three steps are iteratively executed until the algorithm reaches a termination criterion, namely a tolerance value. It is necessary to specify an initial value for the voltage in all buses, and typically the voltage magnitude is specified as 1 and the voltage angle as 0 value. The different f/b proposed methods considered these three steps, and they include some modifications, mainly in the termination criteria and in the modeling of the demand load. Shirmohamadi *et al.* [135] considered the f/b method to solve power flow for distribution networks with termination criteria based on the active and reactive power mismatches in all bus. These mismatched should be lower than a tolerance. Thurkaram *et al.* [136] used the f/b method, but considering the mismatches of the voltage in all buses.

The f/b method requires to know the buses that each line feeds, in order to determine the currents. It is necessary to use auxiliary techniques to number and mark the buses that each line feeds. For instance, in Figure 3.10 the line 1 feeds the loads in bus 2 and 3, and line 2 only feeds the bus 3.

The power flow of the proposed SA methodology has been supported by the Distribution Systems Power Flow Analysis Package (DSPFAP) in the reference [134]. In this package is used a Bus-Injection to Branch-Current (BIBC) matrix to identify the buses that each line feeds. This package uses several f/b algorithms that are presented in the literature, that can be seen in the reference [133]. It has been adopted a f/b sweep algorithm proposed by Thukaram *et al.* in 1999 [136]. The f/b flowchart is presented in Figure 3.11.

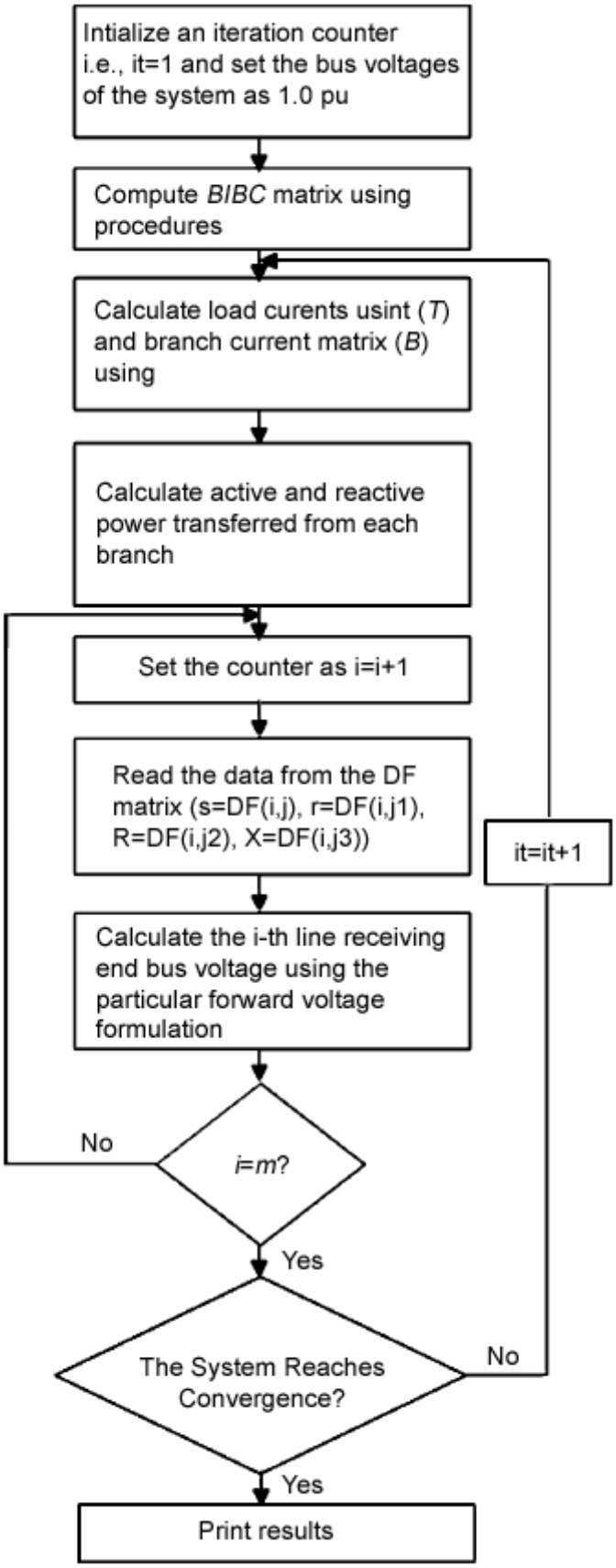

Figure 3.11 – Flowchart of the DSPFAP algorithm [134].

In order to consider a better model of DG it has been required to include additional features in the f/b method of the proposed SA methodology. The DG units introduce new challenges in the distribution network, and one of the changes is seen in the power flow algorithms. The power flows for distribution network are modeled with a single supply bus, or even a few points to supply. With a massive introduction of DG units and EVs there will be several buses with generation power and this will result in bidirectional power flow in the lines. It is required to adapt the power flow to consider the DG units.

In the power flow analysis, the buses with DG units can be classified as PV buses [114], because the DG can inject a certain amount of generation power. Several authors have been proposed different approaches of f/b to consider the PV buses. In reference [133] are indicated three different approaches to include PV buses in distribution networks:

- Secant method proposed by Shirmohamadi *et al.* [135] in 1988;
- Power injections proposed in the references [137] and [138];
- Shunt capacitor method by Augugliaro *et al.* [139] in 2008.

DG units can have two classifications based on the DG power capacity. The bus with DG can be seen as a PQ bus, when a small DG is used (small generation capacity). On the other hand, the bus with a large DG can be seen as a PV bus [140-141]. In the first type, the bus will be model as a normal PQ bus and in the demand power is reduced the generation power from the DG. In the second type, the voltage magnitude and active generation power of DG are specified and the reactive generation power of DG will be determined from power flow.

The power injections method presented in the reference [141] has been used, considering the impact of DG, which is based on the references [137-138]. In this thesis has been considered the same model for a distribution network with balanced loads. The power injections method has been adopted because it presents a better performance to control the voltage in the PV buses [137-138]. The secant method can take several iterations to determine the reactive generation power for the specified voltage of PV buses.

The power injection method [141] starts when the f/b method converges. The first step is to determine the mismatch between the specific voltage value and voltage calculated in the PV buses. If the mismatch was higher than a tolerance it is necessary to determine the reactive current required using the equation (3.47).

$$\Delta I_i^k = Z_{sen}^{-1} \times \Delta V_i^k \qquad (3.47)$$

$$\forall i \in \{1,\ldots,N_{PV}\}$$

where, the Z_{sen} is the sensitivity matrix which size depends on the number of PV buses N_{PV} .

The diagonal elements results from the sum of the series line impedance between each PV node *i* and the sending bus, considering the absolute value of the series impedance. The other elements are determined adding the common series line impedance between the two PV buses (*i* and *j*) and the sending bus [137-138, 141]. If does not exist any common series line impedance the matrix element is equal to zero. The DG could operate in lagging or leading power factor according to the signal of the ΔV_i^k. If ΔV_i^k is positive, then the reactive power is supplied by DG and the ΔI_i^k has a negative signal. Otherwise, the DG will consume reactive power and ΔI_i^k has a positive signal when the ΔV_i^k is negative [141].

This current will be added to the injected current (3.48) of bus *i* in order to use in the iteration the new value of the injected current.

$$I_i^k = I_i^k + \Delta I_i^k \qquad (3.48)$$

$$\forall i \in \{1,\ldots,N_{PV}\}$$

During this process it is necessary to verify if the reactive generation power of the DG violates its limits (3.15). When a reactive limit is achieved, the bus *i* changes from PV bus to PQ and the respective line and column of that bus are removed from Z_{sen} matrix.

In this proposed SA methodology and deterministic technique, the DG units based on co-generation, biomass or waste to energy were considered large DG. Therefore, the buses where these DG units will be connected are classified as PV buses. It will be necessary to define a specific value for voltage magnitude, and if during the power flow algorithm the reactive limit of the DG is achieved, this bus changes to PQ bus (with reactive power fixed to its limit). The rest of DG unit technologies were considered small DG and the respective buses are classified as PQ buses.

In the mathematical formulation has been considered that reactive generation power will be equal to its maximum limit in the small DG, such as in the equation (3.16). The voltage magnitude will be specified in the buses where large DG units are located. The reactive generation power will be determined from the power flow algorithm without violating its limits on (3.15).

3.5. Conclusions

This chapter presented in detail the proposed models to implement in ERMaS tool. The proposed ERMaS tool aims at helping the management of DERs, considering an intensive use of EVs. The core of the ERMaS tool is to determine the scheduling for a specific number of periods, with adequate and reliable models of DG and EVs resources. A

VPP can use the ERMaS tool to solve the ERM problem, obtaining a satisfactory solution for the scheduling.

Due to the huge number of resources connected to a distribution level, the management of these DERs can turn into a complex problem. The massive use of EVs will increase the complexity of the ERM problem. In a smart grid context, the ERM problem should be solved in a reasonable amount of time, and it should incorporate adequate models of DERs in the power system. These two problems are essential to make the tool suitable for a player (namely a VPP) in a smart grid environment. With the introduction of EVs in the electric network, it is required that the tools solving ERM problems should consider a reliable model of EVs that incorporate the influence of EVs into the scheduling.

The proposed ERMaS tool tries to solve these two problems. Firstly it considers an accurate EVs model in the ERM, and it uses optimization techniques that solve the ERM problem in a reasonable execution time. In what concerns the EV model, the ERMaS tool assumes as input data: the trip distance in energy, the bus location, the charge rate and discharge rate in each period. It is also possible to indicate a minimum amount of energy that the EV user wants that the VPP guarantee in its battery. Considering these characteristics of EVs, mainly the indication of the trips distance and the minimum stored energy to be guaranteed, the ERMaS tool becomes stricter than other tools presented in the literature.

The ERMaS tool also tries to solve the problem concerning the complexity of the ERM optimization problem. Two optimization techniques are incorporated in the ERMaS tool, with the purpose of solving the ERM problem in a reasonable amount of time. A deterministic technique has been adopted to solve the ERM problem, in order to compare the results with the proposed SA methodology. The deterministic model has been based on a previous work of Morais [15].

An adaptation of the SA technique is also adopted in the ERMaS tool. SA is presented in the literature as an adequate technique to solve hard optimization problems in a satisfactory execution time. It is expected that the proposed SA methodology achieves a near optimal solution, determined by the deterministic technique, in a much lower execution time. In the proposed SA methodology the use of a power flow algorithm for distribution networks was required. The reasons have been pointed out in sub-section 3.4.3.5. The power flow was modified to include a better model of DG units. They are divided into two behaviors. The first one includes the buses with small DG units that are classified as PQ buses. The second one includes the buses with large DG units that are classified as PV buses.

Chapter 4 presents the test cases that support the effectiveness of both methodologies to solve the ERM problem in a smart grid environment.

Chapter 4

Case Studies

4. Case Studies

4.1. Introduction

This chapter presents a set of case studies, which intend to assess the applicability and adequacy of the methodologies proposed in the scope of this thesis, and described in chapter 3. In this chapter the deterministic technique will be denominated as Mixed-Integer Non-Linear Programming (MINLP) methodology. The simulated annealing will be denominated as Simulated Annealing (SA) methodology. This introduction section presents the organization of this chapter and the input data used in the case studies.

The first presented case study (section 4.2) does not consider the use of Electric Vehicles (EVs) for the optimal resource scheduling, rather only the inclusion of DG units and external suppliers. This case study is used as reference for the following ones, which consider electric vehicles.

The second case study is presented in section 4.3. This case study presents seven scenarios that were solved by the MINLP methodology. Considering the high complexity and large dimension of these optimization problems, it can be concluded that the basis Mixed-Integer Non-Linear Programming (MINLP) is not suitable to support the Energy Resource Management (ERM) considering an intensive use of electric vehicles. Three different alternatives are used to address this issue, aiming at reducing the execution time. The first one uses the relaxation of some networks constraints. The second one uses EVs clustering to reduce the problem dimension. Finally, the third one uses the SA based methodology, proposed in chapter 3.

Section 4.4 presents the third case study, concerning the performance of different control modes used by a Virtual Power Player (VPP) when considering EVs for ERM. This case study considers three scenarios with different penetration levels of EVs. For each scenario three EVs control modes have been used: uncoordinated charging, smart charging and Vehicle-to-grid (V2G). In this section the MINLP and SA approaches are used to solve the scheduling problem for the three control modes of EVs, and the results of both methodologies are compared.

The fourth case study is presented in section 4.5. For this case study the objective is to solve the ERM considering the influence of successive days in the envisaged problem. The ERM problem is determined considering different time horizons, 24, 30, 36, 42 and 48 hours. The case study considers three scenarios to determine the ERM. The first one is for two regular week days, the second one is for Friday and Saturday and the third one is for Sunday and Monday.

Finally, section 4.6 presents the main conclusions regarding the four case studies of this chapter.

Table 4.1 presents the characteristics and specifications of each case study. It summarizes the characteristics of the considered case studies and presents the most relevant information about the scenarios. The number of EVs used in each scenario is presented in the second column of Table 4.1. A small description concerning the specifications of each case study has been included in the third column for better understanding of the objectives of the case studies.

The fourth column indicates the acronym that identifies each scenario of the case studies. This information is used in the next sections to make the presentation of the results obtained for a specific scenario of each case study. The optimization techniques used in each scenario is indicated in the last column.

Case Study	Number of EVs	Description	Label	Optimization technique
1	Without EV	Reference scenario	-	MINLP
2	500	Analyzing the complexity and results of ERM considering different penetration levels of EVs	-	MINLP and SA
	750			
	1000			
	1500			
	2000			
	2500			
	3000			
3	1000	Uncoordinated charging	1000_EV_UnC	MINLP
		Smart charging	1000_EV_SC	MINLP and SA
		V2G	1000_EV_V2G	
	2000	Uncoordinated charging	2000_EV_UnC	MINLP
		Smart charging	2000_EV_SC	MINLP and SA
		V2G	2000_EV_V2G	
	3000	Uncoordinated charging	3000_EV_UnC	MINLP
		Smart charging	3000_EV_SC	MINLP and SA
		V2G	3000_EV_V2G	
4	1000	ERM for two week days	1000_EV_ERM_WeWe	MINLP
		ERM for Friday and Saturday	1000_EV_ERM_FrSa	
		ERM for Sunday and Monday	1000_EV_ERM_SuMo	

Table 4.1 – Case studies.

The case studies presented in this chapter use a distribution network with 32 bus that can be found in [142-143]. Figure 4.1 shows the projection of 32 bus distribution network in 2040 with Distributed Generation (DG) spread over the network [142]. In this

figure, the solid lines represent the branches that are used, and the dashed lines represent the branches that can be used in a reconfiguration scenario.

In Annex A, Table A.1 presents the resistance, inductance and thermal limit of each branch used in this distribution network.

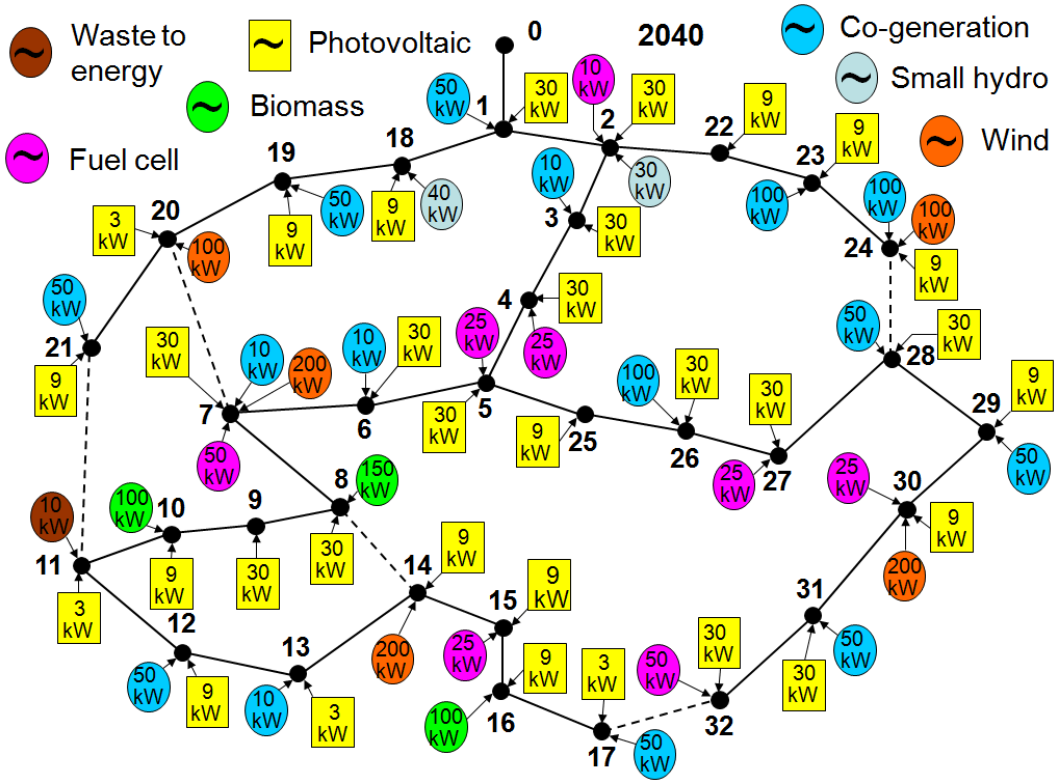

Figure 4.1 – Distribution network configuration in 2040 scenario [142].

In Figure 4.1 the DG units are represented by different colors, which identify the used generation technology. Additionally, the installed power is indicated. For the year 2040, this network includes 66 DG units (32 photovoltaic, 15 co-generation, 8 fuel cell, 5 wind farm, 3 biomass, 2 small hydro and 1 waste to energy). For the case studies presented in this chapter, it is considered that the VPP has the obligation of buying all the generation power from photovoltaic units.

Additionally, external suppliers which supply electrical energy to the consumers of this network are considered in the case studies. These external suppliers are connected to bus 0. Table 4.2 presents the ten offers from external suppliers that the VPP can use in these case studies. Table A.2 in Annex A presents additional information regarding DG and these external suppliers.

External supplier					
No.	**Power offer (kW)**	**Price offer (m.u./kWh)**	**No.**	**Power offer (kW)**	**Price offer (m.u./kWh)**
1	400	0.06	**6**	500	0.11
2	400	0.07	**7**	400	0.12
3	400	0.08	**8**	400	0.13
4	500	0.09	**9**	500	0.14
5	700	0.10	**10**	2000	0.15

Table 4.2 – External suppliers' information.

It has been established that the VPP will serve 218 consumers with a total peak demand around 4.2 MW. The load diagram of the consumers is shown in Figure 4.2.

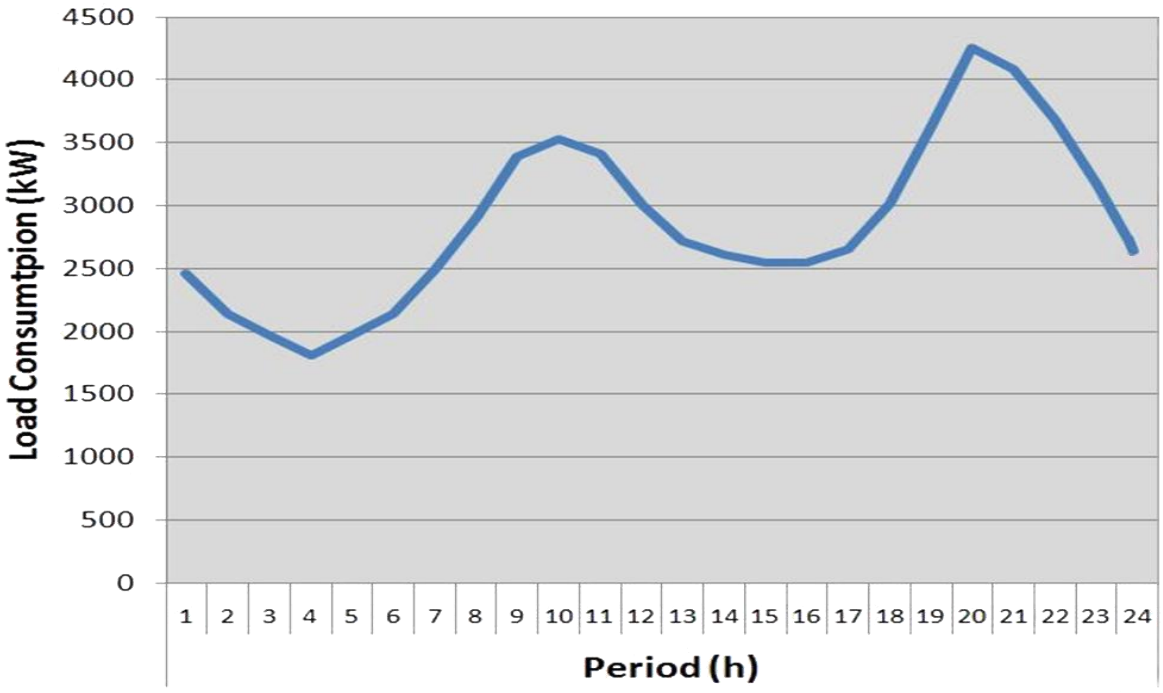

Figure 4.2 – Total load diagram of the 218 consumers [144].

The 218 consumers are divided into 6 groups [144]: domestic consumers, small commerce, medium commerce, large commerce, medium industrial and large industrial. The number of consumers and corresponding demand power have been based on reference [144]. The 218 consumers have been grouped depending on the bus to which they are connected, resulting in one representative load in each bus (32 loads). A more detailed description is presented in Table A.3 and Table A.4 of Annex A.

The case studies consider 11 types of electric vehicles. The technical information regarding each type of vehicle has been obtained from automobile manufacturers [145-151] and it is presented in Table 4.3. This table also presents the charge and discharge rate for two charging modes - slow mode and fast mode (see sub-section 2.6.2).

The slow and fast charge rates are based on the automobile manufacturers' information. The fast mode guarantees the charge of the battery until 80% of its capacity. The automobile manufacturers do not present information about the discharge rate. It is assumed that the slow discharge rate will be used when the EV is connected at a consumer's home, and the power supported by an outlet is approximately 3.7 kW (corresponding in Europe to 230 V and 16 A). Regarding the fast charge rate, it was established that the EVs will only discharge until 70% of its capacity, so that the wearing out of the battery is not accelerated.

Vehicle type		Battery		Charge rate (% of battery capacity/h)		Discharge rate (% of battery capacity/h)	
		Capacity (kWh)	Range (km)	Slow	Fast	Slow	Fast
T1	**MiEV**	16.0	160	0.14	1.6	0.21	0.7
T2	**C-Zero**	16.0	150	0.17	1.6	0.21	0.7
T3	**Fluence**	22.0	160	0.13	1.6	0.15	0.7
T4	**Leaf**	24.0	160	0.14	1.6	0.14	0.7
T5	**Kangoo**	15.0	160	0.13	1.6	0.22	0.7
T6	**Zoe**	15.0	160	0.25	1.6	0.22	0.7
T7	**iOn**	16.0	160	0.14	1.6	0.21	0.7
T8	**Prius**	4.4	20	0.67	-	0.64	-
T9	**Ampera**	16.0	60	0.33	-	0.21	-
T10	**Volt**	16.0	54	0.15	-	0.21	-
T11	**V60**	12.0	50	0.28	-	0.28	-

Table 4.3 – EV technical information [145-151].

The daily travel profile of EV users is important for the ERMaS tool to determine the required amount of energy used to travel. The travel profile considered in the case studies has been based on a travelling report of the U.S. Department of Transportation [152], which indicates the distribution of vehicles and the traveled distance. It is pointed out that the average trip length is between 35 and 40 miles. This report has been used to develop the scenarios of EVs used in this thesis, using the trip lengths, both in terms of distance and time. Figure 4.3 depicts the distribution of vehicles presented in the report of the U.S. Department of Transportation.

The energy that EVs will use to travel is determined by using this travel profile. This information is introduced in the variable $E_{Trip(V,t)}$ of the mathematical formulation (see equation 3.26).

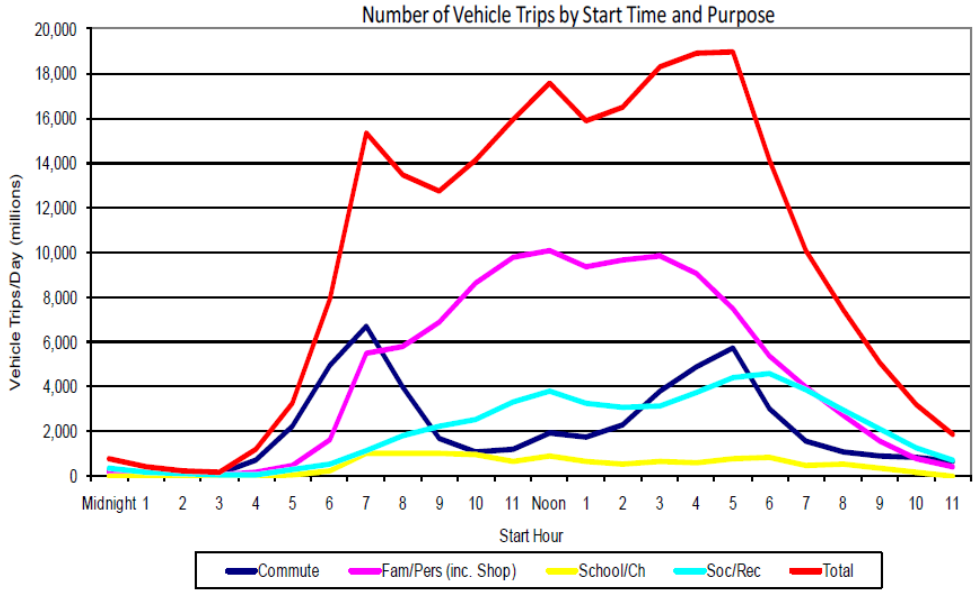

Figure 4.3 – Distribution of vehicles by trip purpose and start time from [152].

The U.S. report [152] also indicates the percentage of travels regarding the destination, for instance a travel between home and work. Three areas have been defined, concerning the 32 bus distribution network, and are presented in Figure 4.4.

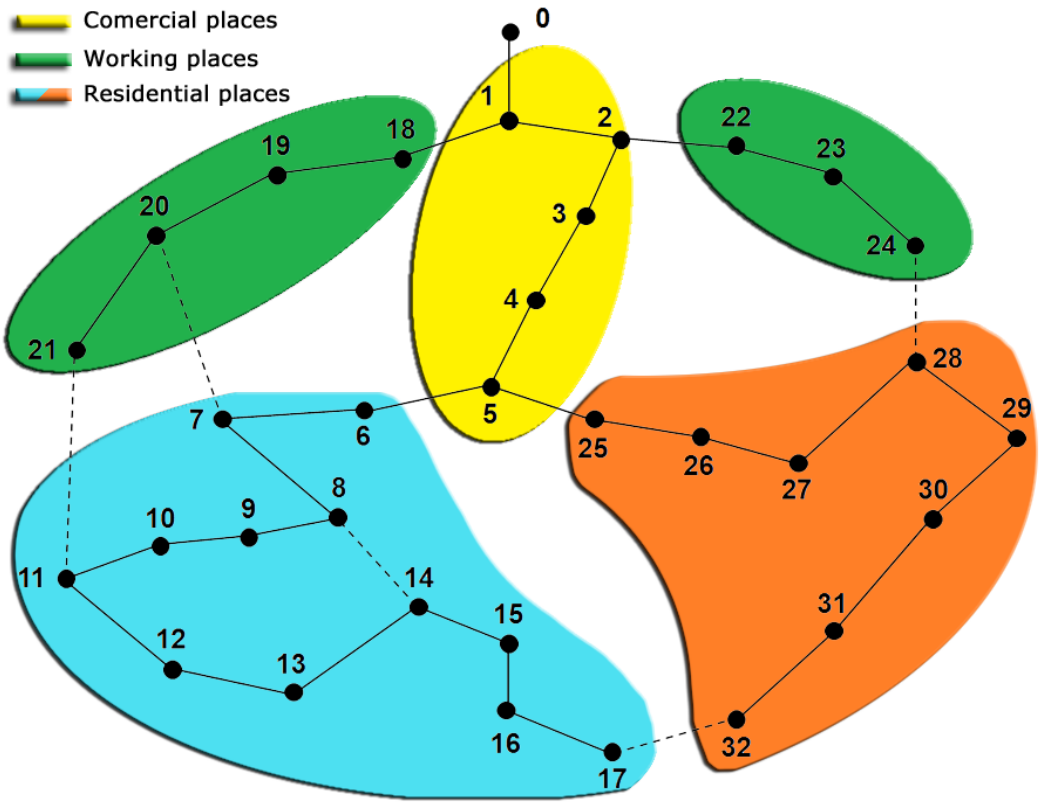

Figure 4.4 – EV areas in the distribution network.

It is important to identify the bus number to which each EV will be connected after the trip, and the type of charging/discharging that is used in each area. In residential places

only the use of slow mode is considered. However, in the working and commercial sites, it is possible to use both fast and slow modes. The scenarios of EVs considered for the case studies presented in this thesis were created using a tool, which is proposed in reference [153]. This tool allocates EVs in the distribution network and establishes the trip distance of each EV, considering the travelling profiles depicted in Figure 4.3.

The case studies have been tested on a computer with two processors Intel® Xeon® W3520 2.67 GHz, each one with two cores, 3GB of random-access-memory (RAM) and Windows 7 Professional 64 bits operating system.

4.2. Energy Resource Management without EVs

The case study presented in this section does not consider the use of EVs for the optimal resource scheduling, rather only the inclusion of DG units and external suppliers. It is important to simulate a case study without EVs, so that after obtaining results for the cases which consider this type of DER, conclusions can be taken regarding EVs' influence on the distribution network. The VPP will obtain the optimal resource scheduling in order to supply the load diagram presented in Figure 4.2. The optimal resource scheduling leads to an operation cost of 6,002.80 m.u., and the MINLP methodology solved the problem in approximately 51 seconds. Figure 4.5 illustrates the optimal resource scheduling, presenting the DG and external suppliers' power. In this case study the demand has been completely supplied, so it was not necessary to impose any non-supplied demand to maintain the stability of the power system.

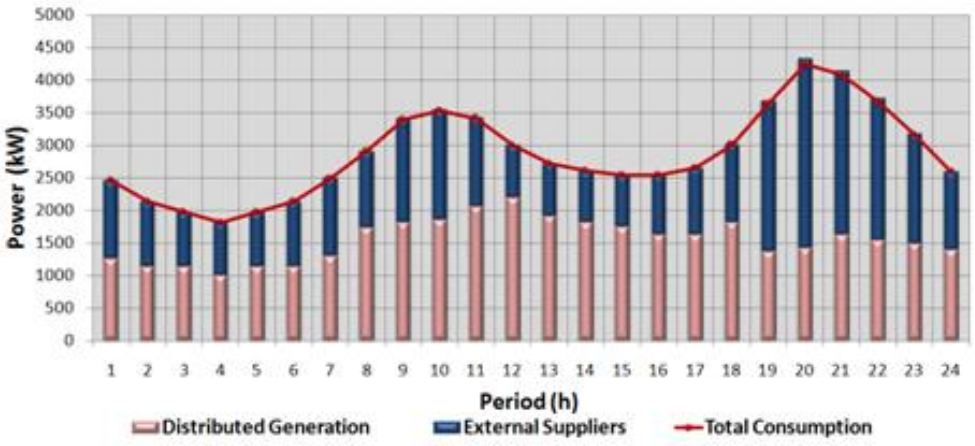

Figure 4.5 – Optimal resource scheduling for the case study without electric vehicles.

Figure 4.6 shows the VPP costs with the DG units and with the acquisition of energy to external suppliers. In terms of costs, the DG units present a higher impact than the external suppliers.

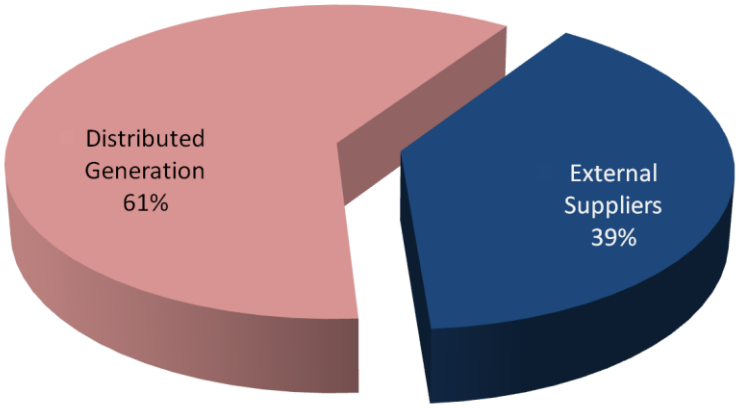

Figure 4.6 – Cost balance for the case study without vehicles.

Figure 4.7 and Figure 4.8 present the resource scheduling and costs, respectively, for each type of DER and for the external suppliers.

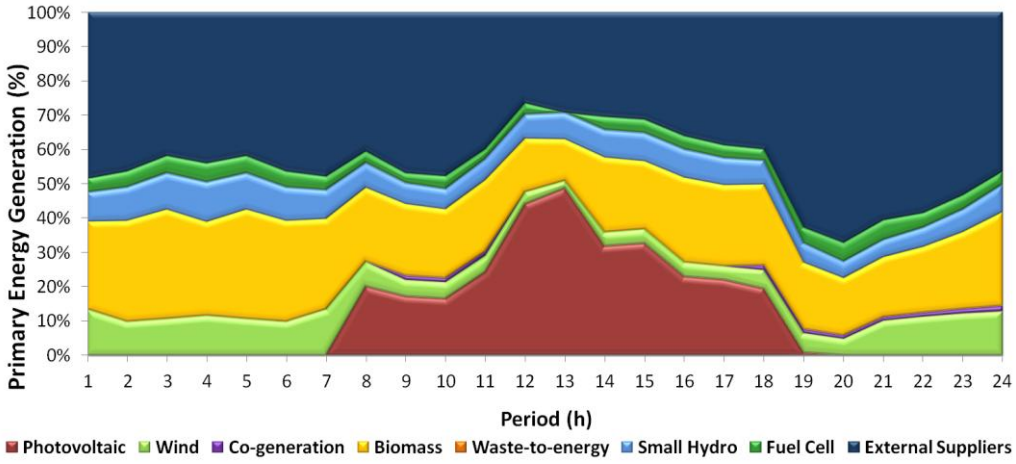

Figure 4.7 – Generation scheduling, regarding each type of DER.

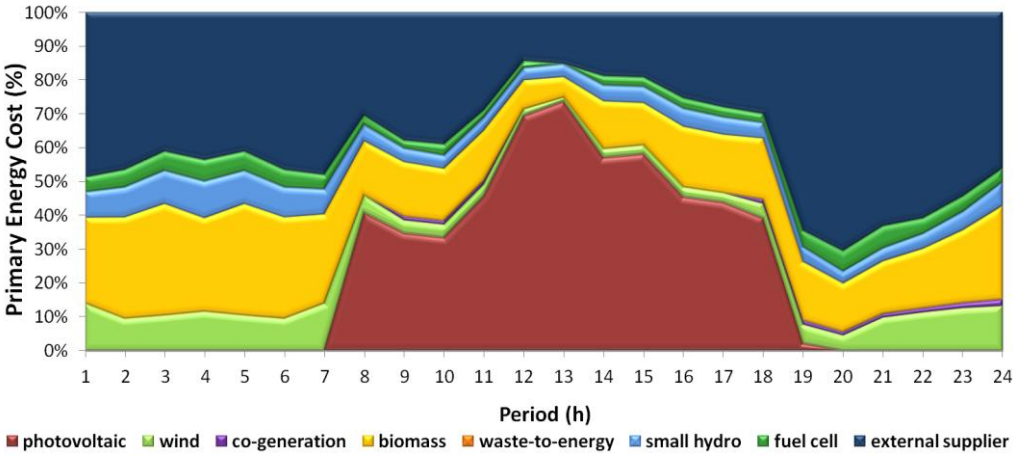

Figure 4.8 – Generation cost, regarding each type of DERs.

Analyzing these figures, one can conclude the photovoltaic DG units have more impact on the VPP costs than the other resources, due to the obligation that the VPP has to buy all the power generated by photovoltaic units.

4.3. Energy Resource Management with EVs – Methods Performance Evaluation

This section has the purpose to demonstrate the complexity of the ERM problem, considering a large amount of DERs, including EVs. The performance of the proposed methodologies will be analyzed in terms of solution quality and execution time.

Firstly, it was used MINLP methodology to determine the optimal scheduling for seven scenarios. These scenarios use different penetration levels of EVs, beginning with 500 vehicles until 3000 vehicles. With the introduction of more vehicles, the ERM problem turns into a harder optimization problem for which it can take several hours to determine the optimal scheduling.

Table 4.4 shows the execution time required by the MINLP methodology to determine the optimal scheduling for the seven scenarios. It this table also indicates the number of decision variables used by MINLP for each scenario.

Number of EVs	Number of decision variables						Execution time (hours)
	DGs	Suppliers	Loads	Buses	EVs	Total	
500	6,336	480	768	1,584	48,000	57,168	0.73
750					72,000	81,168	3.99
1000					96,000	105,168	5.71
1500					144,000	153,168	14.37
2000					192,000	201,168	28.87
2500					240,000	249,168	68.54
3000					288,000	297,168	74.32

Table 4.4 – Results of the variables and execution time of the MINLP methodology.

The execution time exponentially grows with the introduction of more EVs. In the first scenario the MINLP approach takes less than one hour to solve the ERM problem, but for the remaining scenarios it takes several hours or even days to solve the scheduling problem. In the case of 1000 and 1500 EVs, it is required many hours to solve the problem, i.e. it takes approximately 6 and 14 hours respectively to find an optimal solution. For the scenarios with more than 2000 EVs it is necessary more than one day to determine the solution for the ERM problem using the MINLP methodology. The scenario with 3000 EVs requires the highest execution time; it takes approximately 74 hours (more than 3 days) to determine an optimal solution for the scheduling.

It is important to note that the VPP needs energy resource scheduling for the next day. So, the ERMaS tool using the MINLP methodology could never take more than a day to solve the optimal scheduling. However, for this scenario with 3000 EVs it takes 3 days to

obtain an optimal solution. These execution times are unacceptable to a player that operates in a competitive environment, such as a smart grid. It is required to use methodologies that find a satisfactory solution for the scheduling but in a reasonable execution time.

Table 4.4 indicates the number of decision variables for each scenario, and it can be concluded that the number of EVs influences directly the growth of the number of decision variables. It is possible to see the big difference between the number of variables in the scenario with 3000 and 500 EVs. Dividing the two numbers of variables (297,168 for 3000 EVs and 57,168 for 500 EVs) the result is approximately 5. If we make similar calculations for the execution times, the result will be approximately 102. So, an increase of 5 times in the number of variables resulted in an increase of 102 times in the execution time.

The execution time evolution is shown in Figure 4.9. It has been included a regression analysis to determine the relation between the execution time and the number of EVs. The regression type more suitable for this behavior is the polynomial regression of quadratic degree.

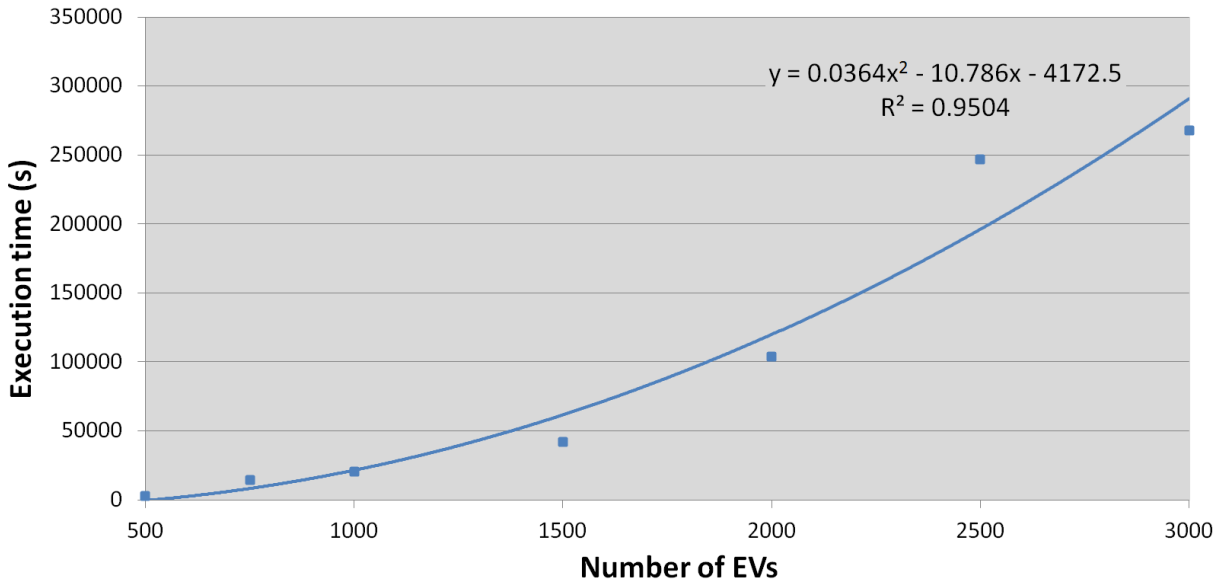

Figure 4.9 – Execution time evolution of the MINLP methodology.

Considering the results of the MINLP approach with execution times higher than the ones that can be acceptable, this section also presents three solutions to solve the same seven scenarios but in a much lower execution time. The following solutions have been used to be compared with the results of MINLP approach:

- MINLP methodology without considering the network constraints (sub-section 4.3.1);
- MINLP methodology with EVs clusters (sub-section 4.3.2);
- SA methodology (sub-section 4.3.3).

4.3.1. Relaxation of the ERM Problem

This sub-section presents a solution for which the network constraints have been simplified in order to relax the ERM problem. In this solution the network constraints are relaxed, the line thermal limit is not considered and the active and reactive power balance are matched in a much simpler expression than the ones presented in the section mathematical formulation of ERM (see sub-section 3.3.2). This approach with the relaxations will be executed by the MINLP methodology.

Firstly, the constraints of voltage magnitude (3.9), of voltage angle (3.10) and of lines thermal limit (3.12) have not considered. The second step was to relax the network constraints of active power balance (3.7) and reactive power balance (3.8). The network active (4.1) and reactive (4.2) power balance without power loss in period *t* can be expressed as follows:

$$\sum_{DG=1}^{N_{DG}}\sum_{o=1}^{N_{DG}^{O}} P_{DG(DG,o,t)} - \sum_{DG=1}^{N_{DG}} P_{EAP(DG,t)} + \sum_{S=1}^{N_S}\sum_{o=1}^{N_S^{O}} P_{Supplier(S,o,t)} + \sum_{V=1}^{N_V} P_{Discharge(V,t)} = \sum_{L=1}^{N_L} P_{Load(L,t)} + \sum_{V=1}^{N_V} P_{Charge(V,t)} - \sum_{L=1}^{N_L} P_{NSD(L,t)} \quad (4.1)$$

$$\forall t \in \{1,\ldots,T\}$$

$$\sum_{DG=1}^{N_{DG}}\sum_{o=1}^{N_{DG}^{O}} Q_{DG(DG,o,t)} + \sum_{S=1}^{N_S}\sum_{o=1}^{N_S^{O}} Q_{Supplier(S,o,t)} = \sum_{L=1}^{N_L} Q_{Load(L,t)} - \sum_{L=1}^{N_L} Q_{NSD(L,t)} \quad (4.2)$$

$$\forall t \in \{1,\ldots,T\}$$

Table 4.5 depicts the execution time for the MINLP approach with relaxation in the mathematical formulation; it is possible to compare these times with the MINLP approach.

Number of EVs	Execution time (seconds)	
	Basis approach (MINLP)	Relaxation approach (MINLP)
500	2,645.09	3.31
750	14,350.52	5.43
1000	20,559.21	7.76
1500	42,086.73	12.74
2000	103,945.70	17.46
2500	246,742.36	23.09
3000	267,547.61	31.97

Table 4.5 – Execution time results of the MINLP methodology with relaxation solution.

With the relaxation in the optimization process, the execution time has been significantly reduced in comparison with the execution time of the basis approach. For the scenario of 3000 EVs, the execution time dropped from 267,547.61 seconds (74.32 hours) to 31.97 seconds. In the other scenarios the difference is still high; for instance in the scenario of 1000 EVs, the execution time drops from 20,559.21 to 7.76 seconds.

This difference in the execution time is causes by the way in which the network constraints are considered (see from equation 3.7 to 3.12). The network constraints bring a large non-linearity to the ERM problem, mainly due to the equations 3.7, 3.8 and 3.12. Removing the equation line thermal limit (3.12) and using a linear equation for the power balance (4.1 and 4.2) this turns the ERM problem into a mixed-integer linear programming problem.

In terms of execution time, this relaxation brings advantages to the ERMaS tool, but it does not consider the line thermal limit and the power losses. So, the solutions of this approach do not represent the real solution of the optimal scheduling.

4.3.2. EVs clustering Approach

The use of vehicle clusters can help in the reduction of execution time, without a significant loss in the solution quality. In this sub-section the MINLP methodology will be used to solve the same seven scenarios considered in the basis approach, but considering the EVS grouped in several clusters.

In this case, the EVs have been grouped in 10 vehicles, obtaining seven scenarios that have 50, 75, 100, 150, 200, 250 and 300 EVs, respectively. This EV clustering approach aggregates vehicles that have the same type of battery characteristics and have similar behavior in terms of trip profile and bus location. For instance, if we have two vehicles with the same battery capacity but they have a trip distance of 35 km and 36 km respectively. They can be considered similar enough to be grouped in the same cluster. 10 vehicles have been selected for each cluster, with the only objective of demonstrating the effectiveness of the proposed approach. Using appropriate techniques, directed to determining the number of clusters, and the type of vehicles contained in each of these clusters could improve the objective function results, while at the same time reducing the execution time.

This EV cluster approach will be compared with the results obtained by the basis approach presented in the beginning of this section 4.3. The obtained execution time and operation cost are shown in Table 4.6.

Number of EVs	Operation cost (m.u.)		Execution time (seconds)	
	Basis approach (MINLP)	EV clusters approach (MINLP)	Basis approach (MINLP)	EV clusters approach (MINLP)
500	6,252.78	6,250.37	2,645.09	107.91
750	6,384.56	6,381.18	14,350.52	179.24
1000	6,555.03	6,550.17	20,559.21	282.07
1500	6,655.98	6,647.17	42,086.73	574.45
2000	6,940.95	6,933.17	103,945.70	662.43
2500	7,269.71	7,264.51	246,742.36	1328.88
3000	7,325.26	7,317.85	267,547.61	1445.45

Table 4.6 – Operation cost and execution time results of the MINLP methodology with EV cluster approach.

The clustering approach presents approximately the same result in terms of operation cost but with a much lower execution time than the basis approach. The difference in the operation cost is not very relevant when compared with the difference in the execution time. The execution time of the EV cluster approach is much lower than the execution time of the basis approach, because in this approach the number of decision variables is decreased with the use of EVs clusters.

For instance, in the 500 EVs scenario the basis approach takes approximately 44 minutes and the EV cluster approach only takes 107.91 seconds (approximately 2 minutes). By dividing the execution times of the EV cluster and basis approaches, the result will be approximately 25. In the 3000 EVs scenario, if we make similar calculation, the result will be approximately 185.

For each situation, when undertaking day ahead scheduling, the VPP is likely to have to test several scenarios with differences in the EVs data, such as trip distance and EV bus location. The EV cluster approach could help the ERM for the next day, because it can test several scenarios without losing a significant solution quality. With the basis approach, if we want to test several scenarios the required execution times are unacceptable, even for the scenario with 500 EVs.

For the scenarios with 2000 or more EVs, it is necessary more than one day to determine the optimal scheduling considering the basis approach. Using the EV clustering approach, the same scenario requires only 10 minutes. For these scenarios, the EV clustering approach is essential to achieve a solution for the ERM of the next day.

The difference in the operation cost is much lower than the difference in the execution time. The difference in the operation cost of the EV clustering approach is around 0.04% and 0.13%. For this reason, the EV clustering approach should be adopted to

determine the scheduling in a reasonable execution time, because using the basis approach is impractical to solve with a large number of EVs.

4.3.3. Simulated Annealing Approach

This sub-section presents a comparison between the proposed SA methodology and the results of the basis approach. In the SA methodology, the consecutive EVs allocation scheme (see neighborhood scheme topic in sub-section 3.4.3) has been adopted for the scenarios with 500, 750 and 1000 EVs. The consecutive EVs allocation scheme presents good results in scenarios with a low number of EVs. The intelligent EVs allocation scheme (see neighborhood scheme topic in sub-section 3.4.3) has been used for the scenarios with 1500, 2000, 2500 and 3000 EVs, because this heuristic presents good results for scenarios with a large number of EVs (see Annex B). It has been executed a sensitivity analysis to determine the best values for the SA parameters. These analyses are presented in Annex B.

Table 4.7 presents the worst solution, mean solution and the Standard Deviation (Std Dev) of the SA methodology. The best, worst and mean solutions have been obtained after a total of 100 runs for SA. Table 4.7 also indicates the number of runs that violate any constraint of the mathematical formulation.

Number of EVs	Approach	Operation cost (m.u.)				Mean execution time (s)	Trial violations
		Best	Worst	Mean	Std Dev		
500	**MINLP**	6,252.78	-	-	-	2,645.09	-
	SA	6,365.41	6,378.84	6,373.63	5.78	5.78	0/100
750	**MINLP**	6,384.56	-	-	-	14,350.52	-
	SA	6,537.41	6,553.67	6,546.67	3.62	17.37	0/100
1000	**MINLP**	6,555.03	-	-	-	20,559.21	-
	SA	6,727.75	6,745.62	6,737.97	3.90	10.70	0/100
1500	**MINLP**	6,655.98	-	-	-	42,086.73	-
	SA	6,795.98	6,800.96	6,799.52	0.78	31.58	0/100
2000	**MINLP**	6,940.95	-	-	-	103,945.70	-
	SA	7,146.52	7,151.67	7,149.49	1.04	52.25	0/100
2500	**MINLP**	7,269.71	-	-	-	246,742.36	-
	SA	7,554.31	7,563.46	7,559.71	1.93	79.80	0/100
3000	**MINLP**	7,325.26	-	-	-	267,547.61	-
	SA	7,637.22	7,643.65	7,640.51	1.33	80.51	0/100

Table 4.7 – Results of the MINLP and SA methodologies using the individual EV approach.

The SA approach determined the ERM problem in much less time than the basis approach. These scenarios can demonstrate the effectiveness of the proposed SA methodology to solve large combinatorial and complex scheduling problems considering EVs. The SA approach achieves a solution in an execution time lower than the MINLP with EV clustering approach presented in the previous section. The operation cost difference between the SA and the MINLP methodologies is around 2 to 4%. When compared with the difference between the execution times, it is possible to conclude the advantage of using the proposed SA methodology to solve ERM problems.

4.4. Evaluation of different control modes of EVs

This section presents the results of different control modes of EVs in the smart grid context. Three scenarios with different penetration levels of EVs are used in this section. The scenarios consider penetration levels of about 1000, 2000 and 3000 EVs respectively, in the 32 bus distribution network. The penetration levels have been based on the forecasting studies [29] presented in section 2.1. Table 4.8 shows the penetration levels for the three scenarios.

<table>
<tr><th colspan="3" rowspan="2">EVs penetration</th><th colspan="7">Consumers in the network</th></tr>
<tr><th>DM</th><th>SC</th><th>MC</th><th>LC</th><th>MI</th><th>LI</th><th>Total</th></tr>
<tr><td colspan="3">Number of consumers</td><td>117</td><td>44</td><td>23</td><td>13</td><td>8</td><td>13</td><td>218</td></tr>
<tr><td rowspan="3">Vehicle/ consumer</td><td>Sc. 1</td><td rowspan="3">2</td><td rowspan="3">5</td><td>20</td><td>70</td><td rowspan="2">50</td><td rowspan="2">70</td><td rowspan="3">-</td></tr>
<tr><td>Sc. 2</td><td rowspan="2">60</td><td rowspan="2">200</td></tr>
<tr><td>Sc. 3</td><td>150</td><td>150</td></tr>
<tr><td rowspan="3">Sc. 1</td><td colspan="2">PHEV (%)</td><td>25</td><td>23</td><td>28</td><td>28</td><td>20</td><td>20</td><td>-</td></tr>
<tr><td colspan="2">BEV (%)</td><td>5</td><td>5</td><td>12</td><td>11</td><td>6</td><td>9</td><td>-</td></tr>
<tr><td colspan="2">PHEV + BEV</td><td>70</td><td>62</td><td>184</td><td>355</td><td>104</td><td>264</td><td>1039</td></tr>
<tr><td rowspan="3">Sc. 2</td><td colspan="2">PHEV (%)</td><td>25</td><td>23</td><td>28</td><td>28</td><td>23</td><td>24</td><td rowspan="2">-</td></tr>
<tr><td colspan="2">BEV (%)</td><td>10</td><td>10</td><td>12</td><td>11</td><td>8</td><td>10</td></tr>
<tr><td colspan="2">PHEV + BEV</td><td>82</td><td>73</td><td>552</td><td>1014</td><td>124</td><td>309</td><td>2154</td></tr>
<tr><td rowspan="3">Sc. 3</td><td colspan="2">PHEV (%)</td><td>35</td><td>25</td><td>20</td><td>36</td><td>30</td><td>29</td><td rowspan="2">-</td></tr>
<tr><td colspan="2">BEV (%)</td><td>10</td><td>17</td><td>10</td><td>11</td><td>14</td><td>10</td></tr>
<tr><td colspan="2">PHEV + BEV</td><td>105</td><td>92</td><td>414</td><td>1222</td><td>528</td><td>761</td><td>3122</td></tr>
</table>

Table 4.8 – Penetration levels for the EVs scenarios.

The EV clustering approach will be used in the MINLP methodology. Therefore, each EV referred in these tests using the MINLP approach represents a group of 10 EVs, and the considered number of clusters for the tests are 100, 200 and 300, respectively for 1, 2 and

3 scenario leading to 1000, 2000 and 3000 EVs which are close enough to the EV numbers presented in Table 4.8.

In terms of travel profile, different trip profiles for each vehicle have been generated for the three scenarios. As mentioned before, the travel profiles were based on the U.S. national traveling report [152] and the scenarios have been generated using the tool presented in [153].

It has been assumed that the energy stored in each EV battery (one per vehicle) must be always equal or higher than 20% of its capacity to prevent a premature degradation of the batteries. In order to achieve this goal, the value of 20% of each EV battery's capacity has been specified in the variable $E_{MinCharge(V,t)}$ of the mathematical formulation (see equation 3.25).

It is also imposed that, at the end of the day, each EV battery should have at least 40% of its capacity in order to ensure a stored energy amount for the next day. Several studies undertaken in the scope of this thesis have shown that the scheduling for the following day becomes more difficult if it is not imposed that a minimum energy must be guaranteed at the end of the day (between 30 and 40% of the battery capacity). This will be further explored in section 4.5.

Random numbers between 20 and 100% have been generated for the three scenarios. These random numbers were multiplied by the capacity of each EV battery in order to establish the initial value of these batteries.

The simulated situations in this section have been based on the three types of control modes presented in section 2.5:

1. Uncoordinated charging;
2. Smart charging;
3. Vehicle-to-Grid.

The first control mode does not consider the possibility of controlling the charge periods of EVs, starting immediately to charge when the EV is connected to the network. With this strategy, the EVs behave as the other loads, placing problems in what concerns the system performance (mainly regarding voltage deviation and active loss) and increase the operation cost. This control mode could lead to insufficient power to supply the load in several periods of the day.

With the smart charging strategy it is possible to control the charging process. The VPP controls the EV charge as any other available resource, taking into account the periods in which each EV is connected to the network, and the trip requirements.

The third control mode considers the control of the charging process, and the use of the V2G capacity of the EVs that have gridable capacity. This allows the VPP to discharge the energy stored in EV batteries into the network, preventing it from higher operation

costs due, for instance, from the need to use more expensive generation resources or to curtail loads.

4.4.1. Uncoordinated Charging

The scenarios concerning this control mode have been simulated with the MINLP methodology using the GAMS software. The SA methodology has not been used in this section because the main purpose is to present the impact of the EV charging without any type of control.

This control mode simulates the EVs charge until they reach their maximum battery capacity. This situation could compromise the security and stability of the network, because the amount of energy required to charge the EVs can significantly increase the load diagram and lead to the thermal line limit violation. Moreover, the available power may be insufficient to supply the increased demand. Figure 4.10 depicts the EV charging requirements for the three scenarios (1000_EV_UnC, 2000_EV_UnC and 3000_EV_UnC) considering the uncoordinated charging until the maximum capacity.

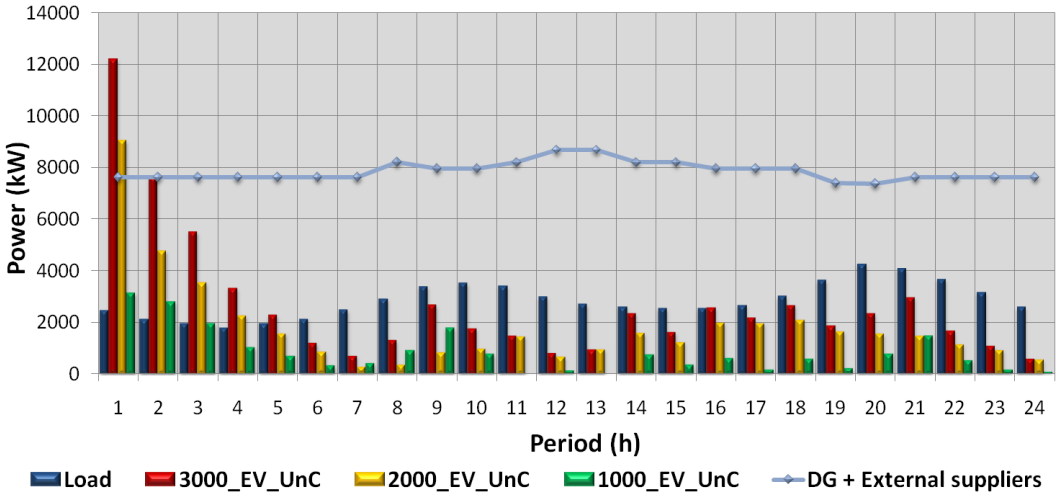

Figure 4.10 – EV charge requirements in the uncoordinated charging.

Using this strategy, the first three hours are the most critical ones. In the 2000_EV_UnC and 3000_EV_UnC scenarios the DG and external suppliers do not have the capacity to supply the required demand. The 1000_EV_UnC scenario does not present any problem in terms of supply capacity. Some basic proceedings in what concerns the solving of this problem have been considered:

- Shifting of EVs charge;
- EVs charge to a specific value indicated by the users.

Shifting of EVs charge

The shifting of EVs charge it corresponds to the re-scheduling of the EVs charge from periods of high value than generation capacity (hour 1 and 2) to other periods. The MINLP approach has been used to solve the 1000_EV_UnC and 2000_EV_UnC under this solution, because these two scenarios were enough to show the impact of the uncoordinated charging.

Table 4.9 indicates the results of the MINLP approach for the 1000_EV_UnC and 2000_EV_UnC. The operation cost for the VPP is largely affected by the introduction of EVs in uncoordinated charging strategy.

Scenario	Operation cost (m.u.)	Generation (kWh)		Load (kWh)	EV charge (kWh)	Non-supplied demand (kWh)
		External suppliers	DG units			
1000_EV_UnC	8,111.65	48,446.15	41,633.80	68,710.21	19,996.86	-
2000_EV_UnC	11,055.78	69,356.75	45,249.89	68,679.13	43,666.17	31.09

Table 4.9 – Results of the uncoordinated charging to shift EVs charge solution.

The operation cost without vehicles is 6,002.80 m.u., the EV charging originates a considerable increase in the VPP operation cost. The operation cost of the 1000_EV_UnC and 2000_EV_UnC was 8,111.65 m.u. and 11,055.78 m.u. respectively. Even in the scenario 1000_EV_UnC with less EVs the operation cost is much higher than the case study without vehicles, and the difference of cost is 2,108.85 m.u representing approximately 35% of the initial cost.

Figure C.1 and Figure C.2 show the load diagram for the 1000_EV_UnC and 2000_EV_UnC scenarios respectively. Figure C.3 shows the power that VPP bought from the external suppliers in the two scenarios. Figure C.3 also shows the Locational Marginal Price (LMP) in bus 0.

EVs charge to a specific value indicated by the users

Still concerning the uncoordinated charging, another possible solution has been tested. This solution considers the possibility of the EV charging right from the start, but stopping when reaching a specific value indicated by the user. This is a possible solution that could be adopted in the beginning of the electrification of the transportation sector. Let us assume that, after connecting the electric vehicle to the electric network, the user is able to indicate the amount of energy that he/she wants in the battery. The mechanism can be incorporated in the connection with the network or in the vehicle, and when the battery reaches the required amount of energy the vehicle is unplugged from the network. To take this possibility into account, a situation where the EVs will charge until they reach the energy required for the trips during the day has been considered.

The 1000_EV_UnC, 2000_EV_UnC and 3000_EV_UnC scenarios have been used to test this uncoordinated charging solution, in this solution the network could support the EVs charging without compromising the security and stability. It is also been used the MINLP approach to determine the optimal scheduling and the results are presented in Table 4.10.

Scenario	Operation cost (m.u.)	Load (kWh)	EV charge (kWh)	Execution time (s)
1000_EV_UnC	6,692.27	68,710.21	6,744.84	59.22
2000_EV_UnC	6,921.81	68,710.21	9,631.69	79.22
3000_EV_UnC	7,709.13	68,710.21	15,962.37	146.40

Table 4.10 – Results of the uncoordinated charging to satisfy the trip profiles.

Considering a specific value to achieve in each EV battery, the operation cost for the VPP does not present the same impact as the previous uncoordinated charging situations with the shifting of EVs charge. In the 3000_EVs_UnC the operation cost increases, i.e. the difference for the operation cost without vehicles is around 28%.

Figure 4.11 shows the load diagram and EVs' charge in each hour for the three scenarios. From Figure 4.11 it is possible to identify when EVs start to charge. The massive introduction of EVs without any kind of control could generate a new peak of power demand in hours in which such a high amount of power is not expected. The load diagram is significantly changed, mainly in hours 1 and 2, for the three scenarios. In these hours EVs are charging at their maximum charge rate, increasing significantly the demand power. Therefore, the VPP was obligated to use off-service generators to support this new load diagram. These off-service generators are more expensive than the ones usually in service; therefore they are not turned on unless it is strictly necessary, as in this case. This fact increases the operation cost of the VPP. In hours 20 and 21 a larger amount of EVs are charging, mainly in the 3000_EV_UnC scenario, to guarantee that the EVs achieve the targeted 40% of the battery capacity (see Figure 4.11 c)).

a)

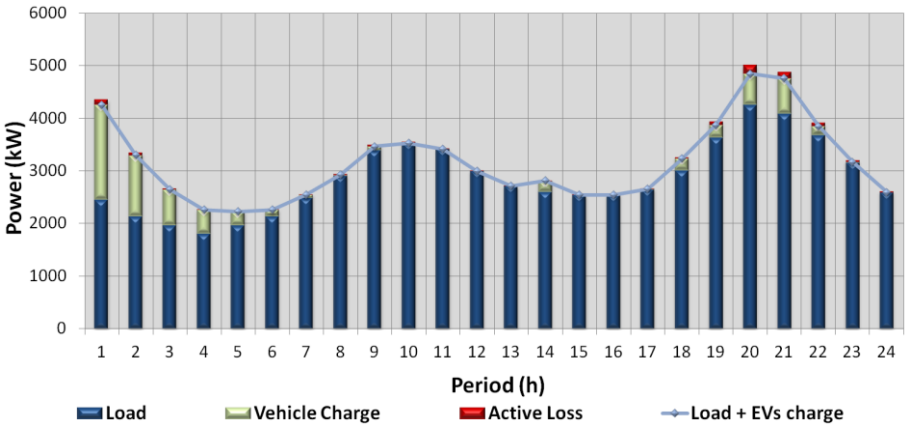

b)

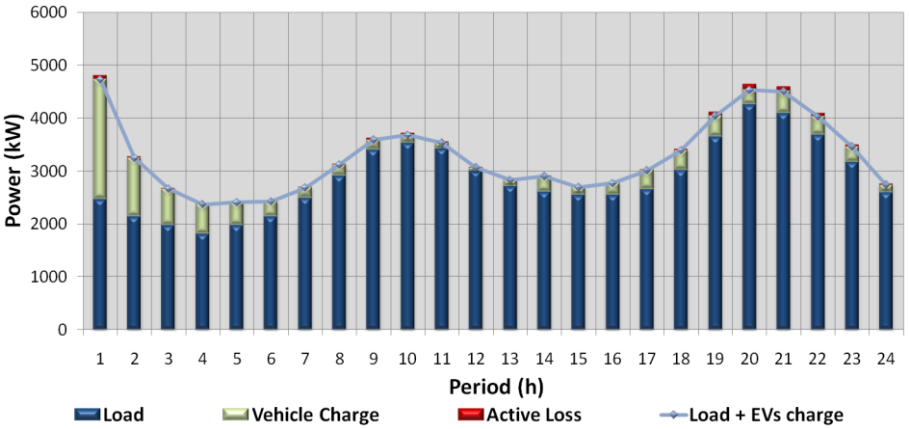

c)

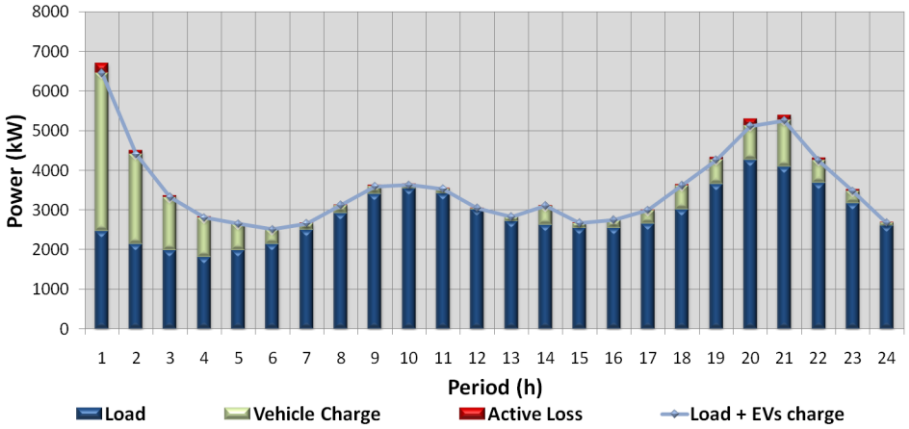

Figure 4.11 – Load diagram of uncoordinated charging to satisfy the trip profiles for scenario: a) 1000_EV_UnC, b) 2000_EV_UnC, c) 3000_EV_UnC.

Figure 4.12 shows the power that the VPP bought from the external suppliers. In this figure the thermal line limit from bus 0 to bus 1 is indicated. In section 4.1 it has already been referred that this line connects the distribution network with a substation. The acquisition from external suppliers is limited to the value defined by this line, because it is the only connection that the VPP has with the main network.

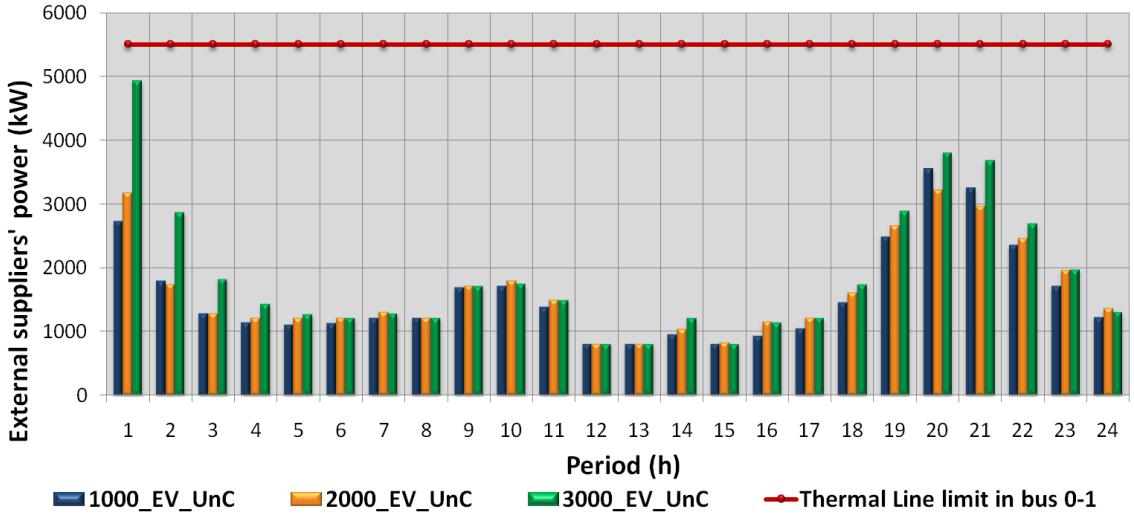

Figure 4.12 – External suppliers' power for the uncoordinated charging to satisfy the trip profiles.

In the 3000_EV_UnC scenario, the VPP almost reaches the thermal limit line in hour 1. Concerning hours 20 and 21, the VPP was obligated to use the external suppliers with higher intensity, in order to ensure the specific value of 40% of battery capacity in each vehicle.

Figure 4.13 shows the VPP cost with the acquisition of energy from external suppliers.

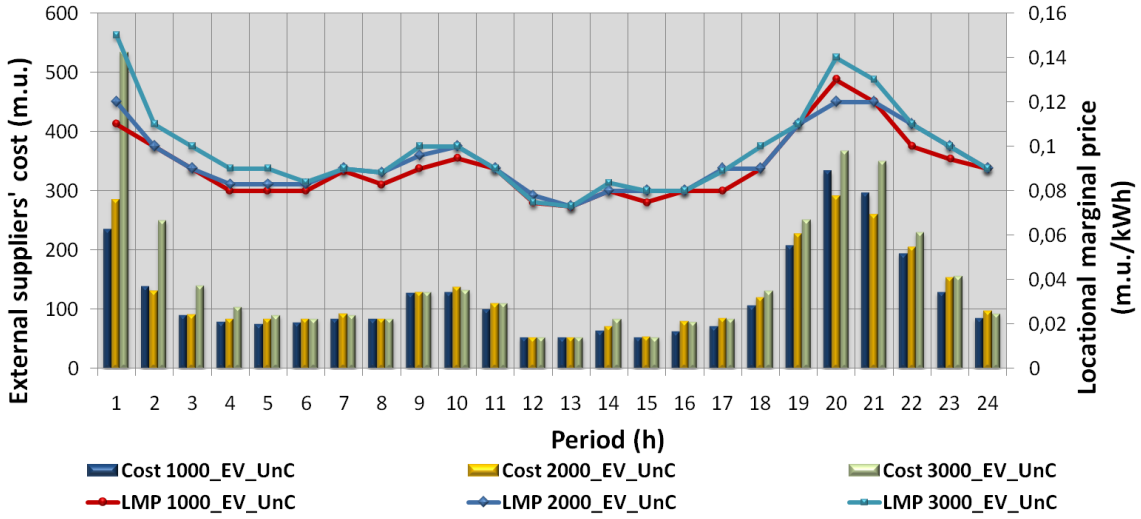

Figure 4.13 – External suppliers' cost for the uncoordinated charging to satisfy the trip profiles.

Figure 4.13 also shows the LMP in bus 0. It is possible to identify the hours with higher price resulting from the large amount of energy required to charge the EVs. The LMP achieves the higher values in hours 1, 20 and 21. For instance, in the 3000_EV_UnC scenario, the LMP achieves 0.15 m.u./kWh in the hours with the highest required energy from the EVs, as it is possible to conclude from Figure 4.12. The LMP achieves the maximum of 0.15 m.u./kWh because the VPP had to use all the external suppliers, even the more expensive one, which presents an offer of 0.15 m.u./kWh (see Table 4.2).

4.4.2. Smart Charging

The smart charging mode aims at providing the VPP with better management capabilities, in what concerns the objective of decreasing operation costs. In this case, the VPP will try to find the periods with the lower costs, without compromising the trip profile of EVs. This strategy applies the SA and the MINLP methodology to solve the ERMaS problem and find the minimum operation cost. The MINLP performance will be compared to the performance of the SA methodology.

The smart charging mode increases the complexity of the ERMaS optimization problem, mainly with the inclusion of further decision variables. Therefore, the minimum operation cost is not the only important value for the evaluation of SA and MINLP approaches; the execution time also arises as an equally important factor of evaluation. Metaheuristic techniques are crucial for this type of problems, as they allow solving the problem in a significantly reduced amount of time. However, the increase in the efficiency of the problem solving has implications in what concerns the quality of the objective function value. The achieved solutions are always expected to be slightly worse than the ones obtained by deterministic techniques.

The metaheuristic approach used to solve this problem was the SA, presented in chapter 3. The SA parameters have been chosen according to the results of a sensitivity analysis. The SA algorithm has been run several times with different parameter values, until the SA algorithm obtained a constant and low value for the fitness function (3.34). Details about these tests are presented in Annex B where it is possible to see the best values for the SA parameters. Table 4.11 shows the SA parameters values used for the smart charging case studies.

The proposed consecutive EVs allocation scheme used by the SA, explained in sub-section 3.4.3, has been used to allocate EVs charging for the 1000_EV_SC scenario. This proposed EVs allocation is used in the neighborhood scheme of the proposed SA methodology. In what concerns the 2000_EV_SC and 3000_EV_SC scenarios, the intelligent EVs allocation scheme was used in the neighborhood scheme of the proposed SA methodology. This scheme considers the allocation of EVs charging in hours with low demand consumption (see sub-section 3.4.3). Intelligent EVs allocation scheme presents better performance in 2000_EV_SC and 3000_EV_SC scenarios. Annex B presents a more detailed explanation about the use of consecutive and intelligent EVs allocations in the neighborhood scheme of the proposed SA methodology.

SA parameters	Case study scenarios		
	1000_EV_SC	2000_EV_SC	3000_EV_SC
Maximum number of iterations	90	70	70
Iterations at constant temperature – *L*	8	10	10
Initial temperature – T_0	2100	3200	3200
Cooling rate – α	0.90	0.88	0.88
Tolerance error for the best fitness evolution	5.10^{-4}	5.10^{-4}	5.10^{-4}
Maximum number of iterations for the best fitness evolution	20	20	20

Table 4.11 – SA parameters for the smart charging mode.

Table 4.12 depicts the results of the operation cost for the three scenarios (1000_EV_SC, 2000_EV_SC and 3000_EV_SC). Both MINLP and SA methodologies have been used in order to evaluate the operation cost results. The SA solution corresponds to the best solution between a total of 100 runs for each scenario. Table 4.12 shows the worst solution, mean solution and the standard deviation for the SA methodology. This table also indicates the number of runs that violate any constraint of the mathematical formulation.

Scenario	Approach	Operation cost (m.u.)				Mean execution time (s)	Trial violations
		Best	Worst	Mean	Std Dev		
1000_EV_SC	**MINLP**	6,564.85	-	-	-	223.78	-
	SA	6,788.19	6,841.51	6,814.93	10.11	9.92	0/100
2000_EV_SC	**MINLP**	6,789.35	-	-	-	480.57	-
	SA	7,058.79	7,121.64	7,094.42	11.80	47.90	0/100
3000_EV_SC	**MINLP**	7,405.47	-	-	-	967.16	-
	SA	7,682.39	7,707.51	7,697.66	4.7183	77.85	0/100

Table 4.12 – Results of the smart charging mode for the three EVs scenarios.

As expected, the operation cost decreased using the smart charging mode, when compared to the uncoordinated charging mode. The SA methodology achieves a similar operation cost for the three scenarios, when compared to the MINLP methodology. The costs difference between the SA and the MINLP methodologies is about 3 to 4%. The execution time of the SA methodology is much lower than the MINLP methodology. Since the SA operation cost is only slightly different from the MINLP methodology, the execution time is the most important factor to analyze. With a much quicker approach to solve the

ERMaS, it is possible to test different scenarios in terms of trip length, EVs requirements and DG capacity.

Figure 4.14 depicts the convergence of best fitness function for the best solution of SA methodology, as seen on the left side of the figure. On the right side of the figure is shown the objective function value over 100 runs.

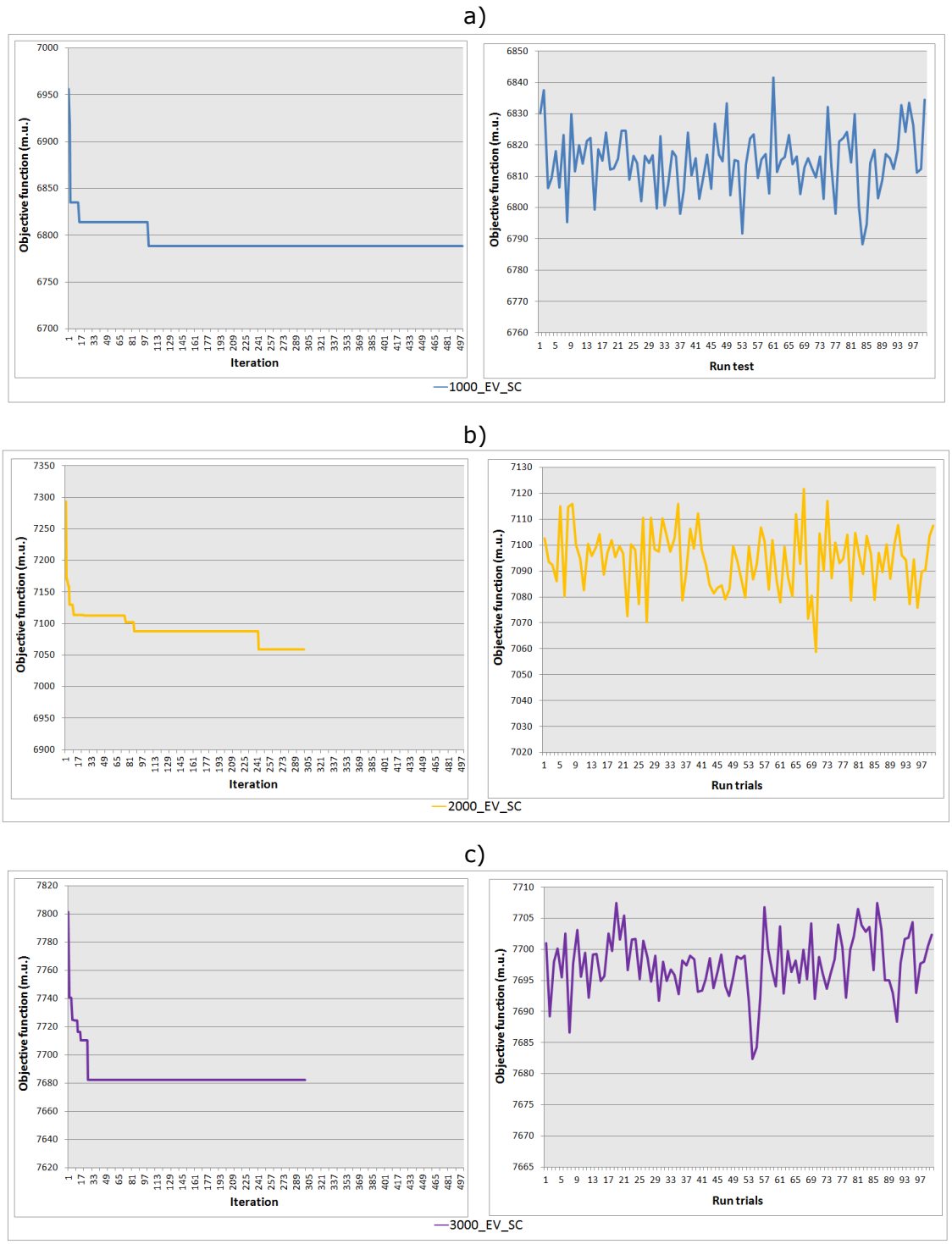

Figure 4.14 – Performance of SA methodology for smart charging: a) 1000_EV_SC, b) 2000_EV_SC, c) 3000_EV_SC.

The SA methodology demonstrated a fast convergence in the three scenarios, finding the best solution in the first iterations, but in 2000_EV_SC presents a different behavior. In this case, the SA approach found the best solution in the last iterations. In terms of objective function evolution over the 100 runs, the SA shows a great variability over the 100 runs.

Figure 4.15 shows the resulting load diagram considering the demand of consumers (represented by blue bars) and the EVs charging (green bars). These results have been obtained from the MINLP methodology for the three scenarios.

The smart charging contributes to a better scheduling what is made clear, when comparing Figure 4.15 with Figure 4.11, which presents the load diagram of uncoordinated charging for the three scenarios. Using the smart charging mode, the VPP intelligently manages the charge of EVs in order to schedule this additional demand to periods when the resources' offers are lower than in other hours. For this reason, the VPP uses the off-peak hours with the lower demand to allocate the EVs charging, e.g. in hours 3, 4, 5, 12, 13 and 14.

The MINLP approach tries to maintain a constant demand in off-peak hours, between hours 1 and 7, using the EVs charging to create a resulting load diagram without variations between hours. This makes the scheduling of generation simpler and improves the regulation of generators, as the load diagram is fixed in a constant value. During the midday hours, the VPP allocates a large amount of EVs to charge, since photovoltaic units start generating during this period.

Figure 4.16 shows the generation cost for the 1000_EV_SC scenario, and the LMP in the bus 0 where the external suppliers are located.

a)

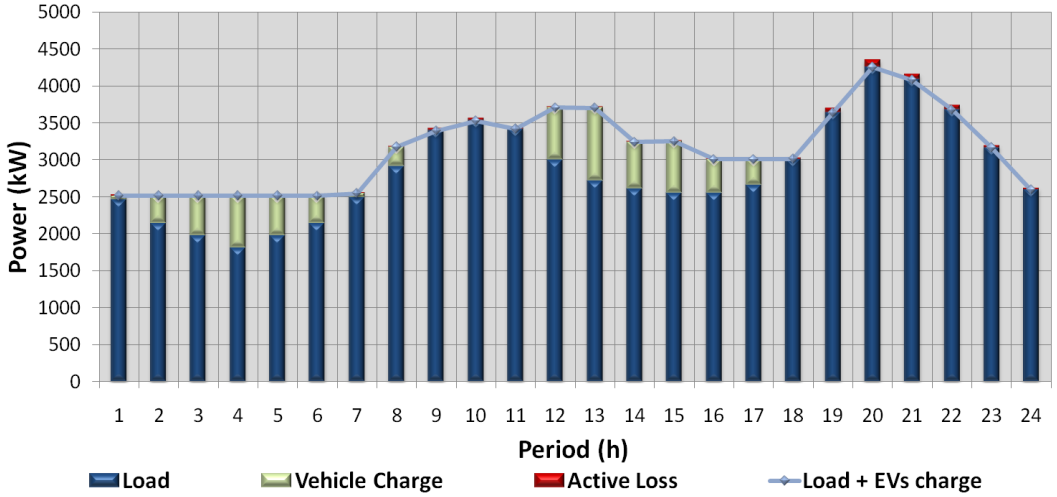

b)

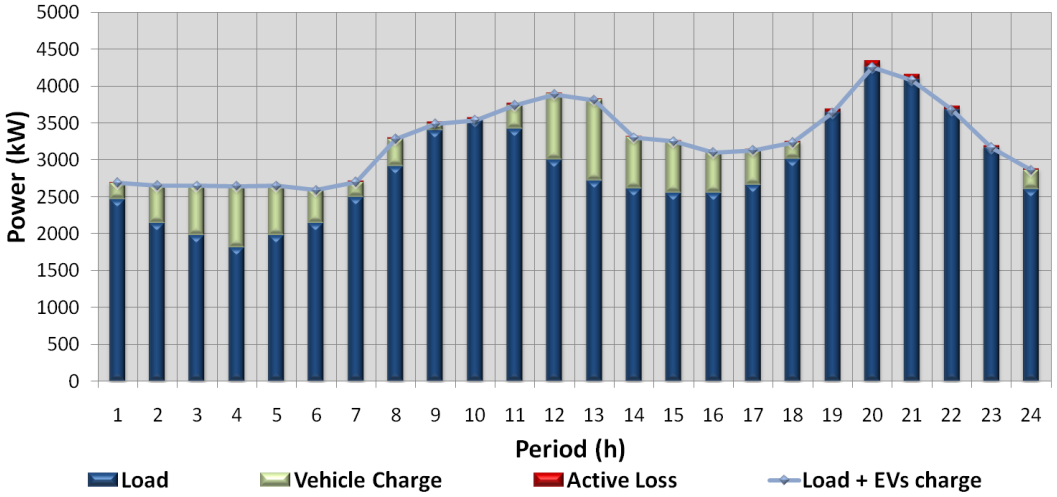

c)

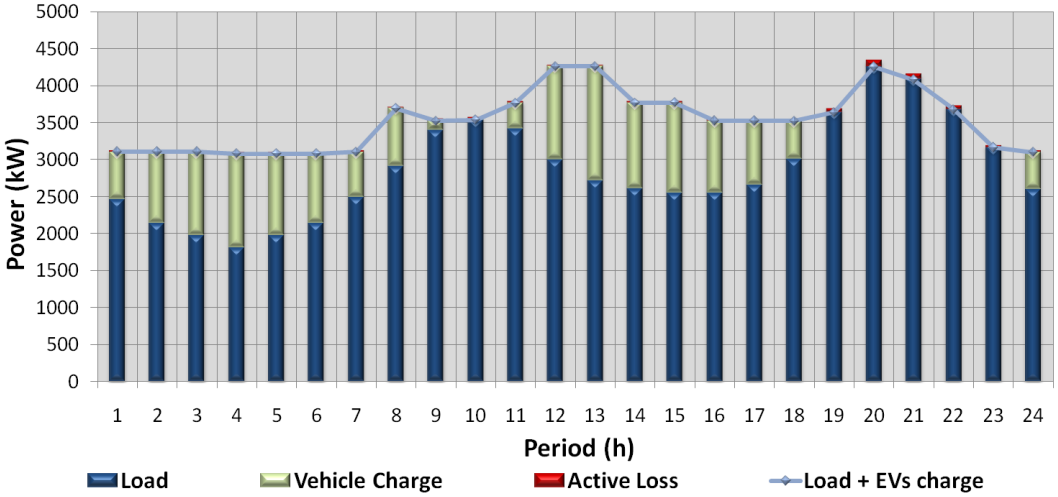

Figure 4.15 – Load and EVs charging power of smart mode using MINLP methodology for: a) 1000_EV_SC, b) 2000_EV_SC, c) 3000_EV_SC.

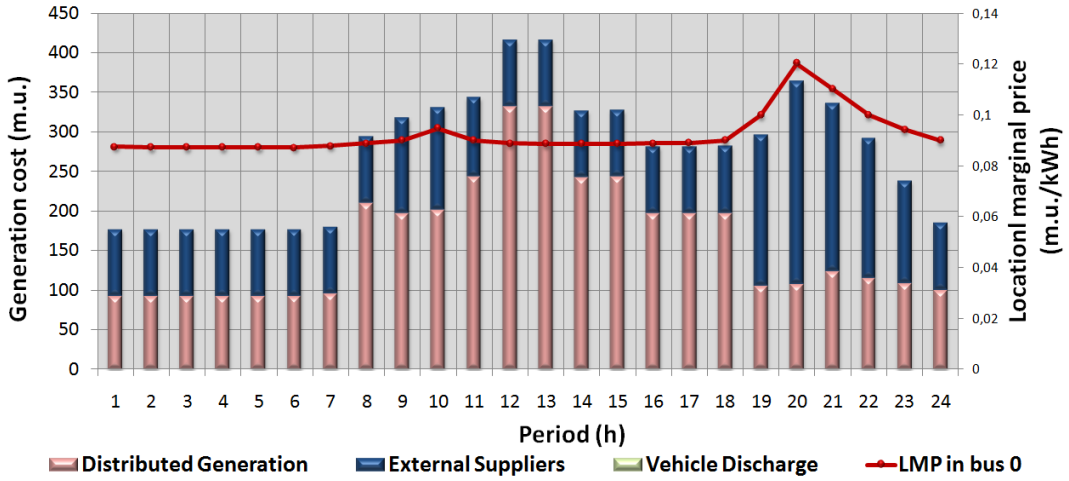

Figure 4.16 – Generation cost of smart charging mode for MINLP methodology, for the 1000_EV_SC.

From hour 8 to hour 18, the VPP cost with the DG units increases, mainly due to the obligation of the VPP in buying generation power from photovoltaic units. The photovoltaic units start generating in hour 8; hence the VPP uses this power to charge the EVs instead of allocating them in other periods with higher costs. Analyzing the LMP profile in bus 0, it is possible to conclude that the LMP maintains a value around 0.09 m.u./kWh even during midday, when an intensive charging of EVs occurs. The external supplier cost during the period from hour 8 to 18 (when the photovoltaic generated power is used) is similar to the cost during off-peak hours (between hours 1 and 7). For this reason, the LMP is kept around the same value. This behavior is consistent for the other scenarios - the hours when the photovoltaic generation is available are used to charge EVs.

In the uncoordinated charging mode, the VPP was obligated to buy more expensive resources during off-peak hours instead of using the available power from the photovoltaic units because it is not possible to control the charge in this mode. The LMP profile for the 1000_EV_SC scenario, using the uncoordinated charging mode, presented in Figure 4.12, is much more inconstant than the LMP using the smart charging mode. During the first hours of the day, the LMP increases its value, and in the remaining hours it is reduced. Using the smart charging mode, the LMP is kept almost constant, due to the control over the EVs charging process.

Figure 4.17 shows the load diagram, with the demand of the consumers and the EVs charging for the three scenarios using the SA approach. Figure 4.17 can be compared with Figure 4.15, so that the differences in terms of EVs charging allocation for the three scenarios can be analyzed.

a)

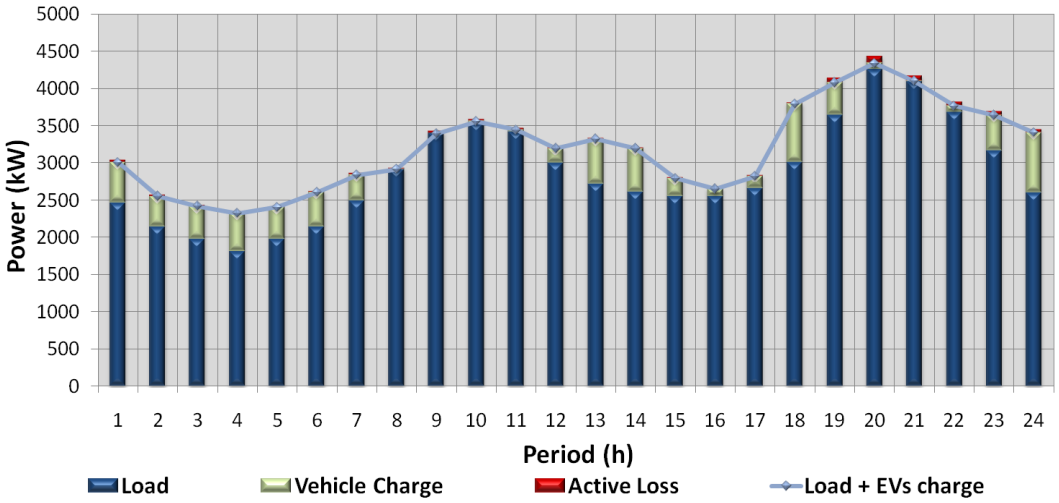

b)

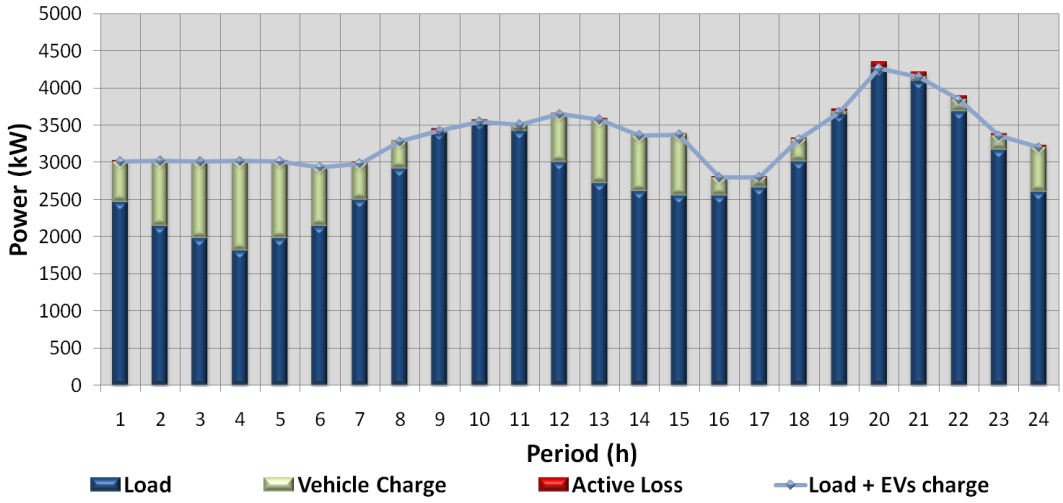

c)

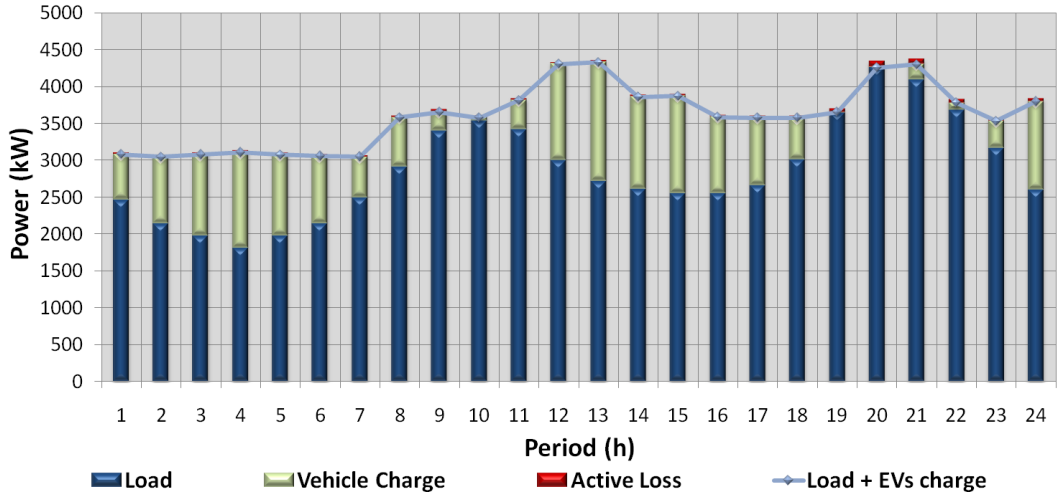

Figure 4.17 – Load and EVs charging power of smart mode using SA methodology for: a) 1000_EV_SC, b) 2000_EV_SC, c) 3000_EV_SC.

The SA methodology allocates EVs in hours with the lower resources' cost, in order to reduce the VPP's operation cost. The solution for the 1000_EV_SC scenario, presented in Figure 4.17 a), uses a more dispersed allocation of the EVs charging, instead of concentrating the charges in the off-peak hours and midday period. The same occurs for the 2000_EV_SC and 3000_EV_SC scenarios, presented in Figure 4.17 b) and Figure 4.17 c), respectively.

As seen in Figure 4.17 a), the random EV charging allocation methodology, used by the neighborhood generation scheme, improves the allocation of the EVs charging during the off-peak hours, but this process is still more random and disperse than the result of the MINLP methodology (see Figure 4.15 a)). As seen in Figure 4.17 b) and Figure 4.17 c), the EVs charging allocation during hours with low demand consumption obtains a better scheduling of EVs charging. The load diagram of both scenarios is similar to the load diagram of Figure 4.15 b) and Figure 4.15 c), respectively.

The proposed SA methodology uses the same strategy of the MINLP approach, i.e. allocating the EVs in the hours with lower resources' costs, in order to reduce the operation cost for the VPP. SA uses the EVs charge more intensely in the same hours than the MINLP approach. The main difference between the SA and the MINLP solutions is the disparity after hour 20, due to the minimum stored energy to be guaranteed in hour 24 (equation 2.25). The MINLP approach charges EVs more often during off-peak hours, in order to guarantee that after the use of the battery (during the day) the EVs will have enough stored energy, not requiring further EVs' charge until hour 24.

4.4.3. Vehicle-to-Grid

In this sub-section, the V2G capacity will be considered as a scheduling option for the EVs that present that capacity and for the VPP that could use as another energy resource. It is assumed that all the vehicle models used in these case studies have the capacity of injecting energy into the network. Some models have the possibility of injecting energy in fast and slow mode, while other models are only able to use the slow mode to discharge. The fast or slow discharge mode will be assumed in the same periods that were considered for the smart charging mode.

It will be used the function f_3 (3.4) to determine the remuneration scheme between the VPP and EVs users. The charging price will be maintained at zero, in order to compare the results of this V2G mode with the ones presented in the previous sub-sections. The discharge price has been fixed in 0.025 m.u./kWh for all vehicles, which represents the profit that each user expects with the discharge process. In fact, a charging and discharging price should be considered, but since the charging price is equal to zero, the discharging price will be the mentioned profit. Another reason for using the user's profit in the

discharging process is the purpose of minimizing the operation cost, and the charging process may not be included because the VPP can consider a fixed tariff for the charge as it happens for consumers. The fixed tariff is the income of the VPP when the required energy is supplied to the loads, and the charging of EVs is seen typically as another load to the VPP. Using the discharge price as the profit for the EV user it makes easier the comparison with the other two control modes of uncoordinated charging and smart charging. Even considering only the discharge price, the ERMaS tool has the possibility to included a charge and discharge price for each EV user.

The inclusion of V2G capacity makes the scheduling a more complex optimization problem than when using the smart charging mode. SA and MINLP will be used to solve the optimal scheduling for the same three scenarios used in the previous sub-sections.

The same parameters used in the previous section for the smart charging mode have been used in this case study. Table 4.13 shows the SA parameters values used for smart charging case studies.

SA parameters	**Case study scenarios**		
	1000_EV_SC	**2000_EV_SC**	**3000_EV_SC**
Maximum number of iterations	90	70	70
Iterations at constant temperature – *L*	8	10	10
Initial temperature – T_0	2100	3200	3200
Cooling rate – α	0.90	0.88	0.88
Tolerance error for the best fitness evolution	5.10^{-4}	5.10^{-4}	5.10^{-4}
Maximum number of iterations for the best fitness evolution	20	20	20

Table 4.13 – SA parameters for the V2G mode.

Table 4.14 presents the results concerning the operation cost for the three scenarios using the SA and MINLP methodologies. In these case studies the best solution of the SA approach is determined after a total of 100 runs for each scenario. In what regards the heuristics about EVs allocation (consecutive and intelligent EVs allocation), the neighborhood scheme is the same used in the previous sub-section – using the smart charging mode. The control of EVs discharge process has been based on the constraints control strategy of choosing the best period to discharge the EVs, explained in sub-section 3.4.3.5.

Scenario	Approach	Operation cost (m.u.)				Mean execution time (s)	Trial violations
		Best	Worst	Mean	Std Dev		
1000_EV_V2G	MINLP	6,555.86	-	-	-	240.76	-
	SA	6,701.61	6,754.07	6,722.82	10.27	9.81	0/100
2000_EV_V2G	MINLP	6,709.37	-	-	-	758.18	-
	SA	6,901.57	6,915.48	6,910.93	2.43	46.92	0/100
3000_EV_V2G	MINLP	7,317.85	-	-	-	1,212.15	-
	SA	7,631.92	7,672.18	7,651.47	6.53	78.13	0/100

Table 4.14 – Results of the V2G mode for the three scenarios.

Using this V2G mode, the SA achieved a worse operation cost for the three scenarios when compared with the MINLP methodology, however with a much lower execution time. In the 1000_EV_V2G scenario, the SA methodology obtains a solution with a cost of 6,701.61 m.u. in 9.81 seconds; MINLP obtains a solution with a cost of 6,555.86 m.u. in 240.76 seconds. In what concerns the execution time, the SA methodology takes approximately 4% of the MINLP's execution time. Regarding the 2000_EV_V2G scenario, the SA methodology achieves a similar operation cost when compared to the MINLP result, in a much smaller execution time. In the 2000_EV_V2G and 3000_EV_V2G scenarios, the SA achieves a solution in approximately 2% of the MINLP's execution time, and the difference in the operation cost is around 4%.

For the three scenarios, the operation cost using the V2G capacity decreases when compared to the same scenarios using the smart charging mode, as presented in the previous sub-section. The same is verified in what regards the individual performance of both the MINLP and SA. Both approaches achieve lower values when compared to the application in the smart charging mode (comparing Table 4.14 with Table 4.12). The inclusion of the V2G capacity improves the management performance of the VPP, by allowing the use of energy from EVs batteries instead of deciding to use an expensive generator. As referred in section 2.5, regarding the applications of EVs in smart grid, should be intelligently controlled with the purpose of using their charge/discharge when it is economically and technically viable.

Figure 4.18 depicts the convergence of best fitness function for the best solution of SA methodology as seen on the left side of the figure. On the right side of the figure is shown the objective function value over 100 runs.

The SA methodology demonstrated again a fast convergence in the three scenarios. The SA quickly finds a good solution, and considering this behavior the termination criteria could be improved (see sub-section 3.4.3.2). The proposed SA methodology uses two criteria to stop the algorithm, the maximum number of iterations and best fitness function presenting no improvement. It could be included another criterion regarding the number of

iterations that the best fitness function maintains at the same value. If the fitness function remains the same during a specific number of iterations the SA methodology will stop.

a)

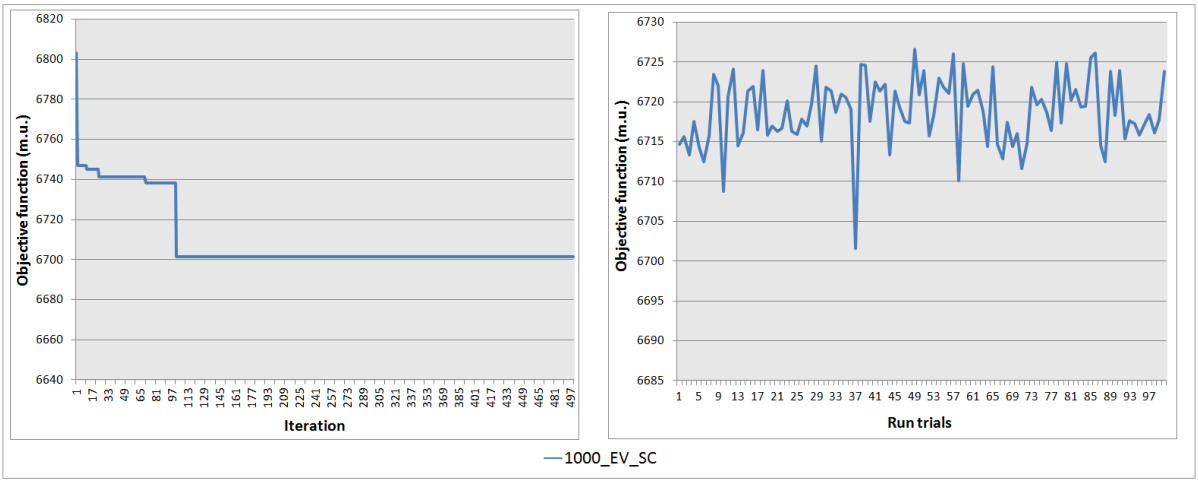

b)

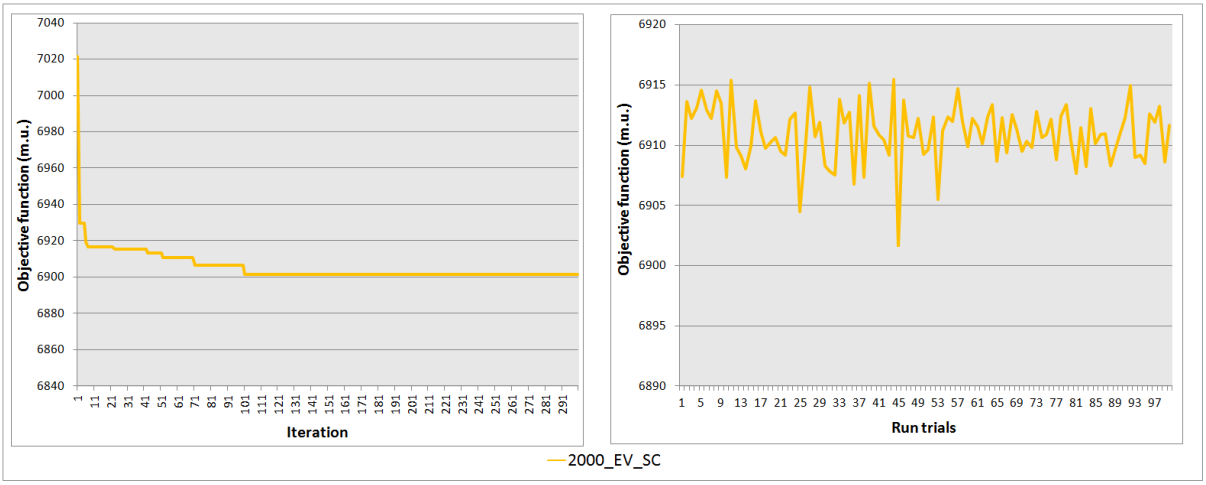

c)

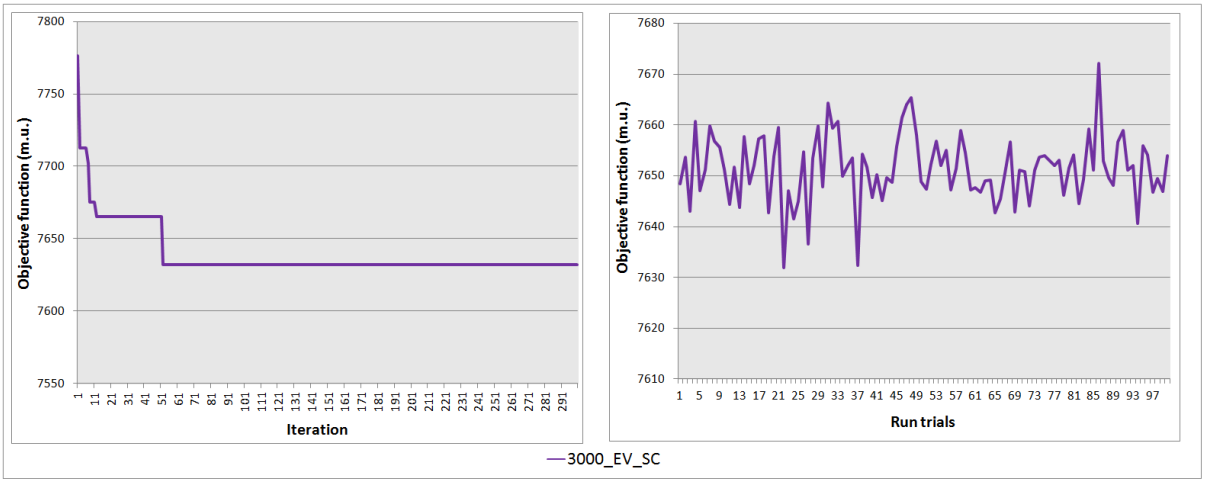

Figure 4.18 – Performance of SA methodology for V2G: a) 1000_EV_SC, b) 2000_EV_SC, c) 3000_EV_SC.

Figure 4.19 shows the obtained scheduling for the three scenarios, using the MINLP methodology.

a)

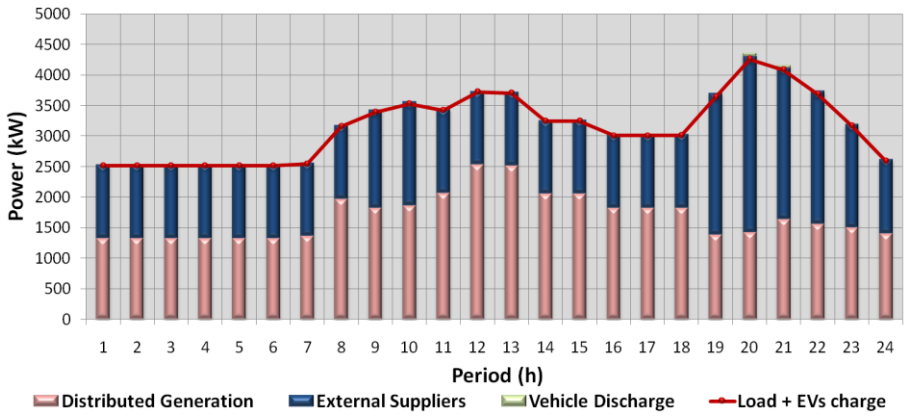

b)

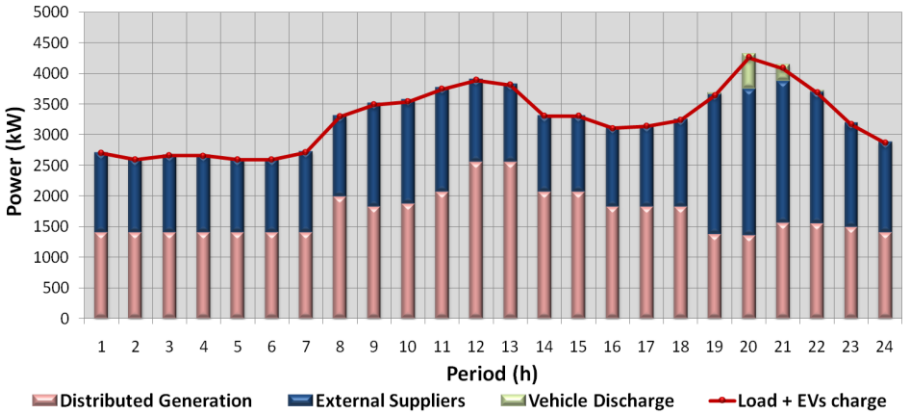

c)

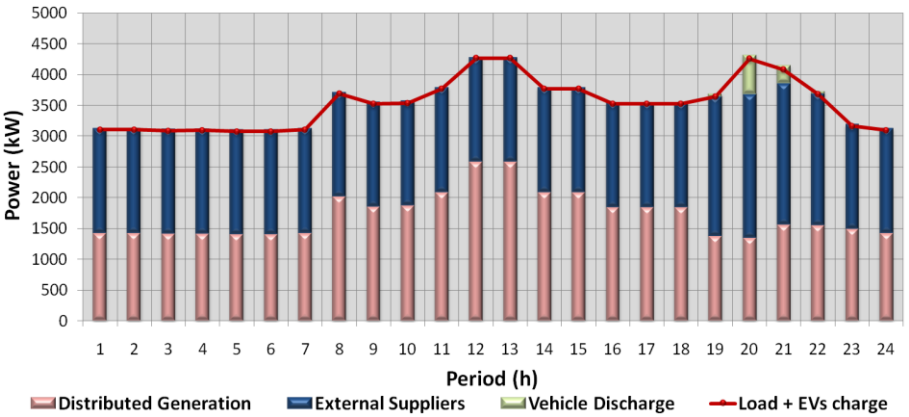

Figure 4.19 – Optimal resource scheduling of V2G mode using MINLP methodology for: a) 1000_EV_V2G, b) 2000_EV_V2G, c) 3000_EV_V2G.

Concerning the 1000_EV_V2G scenario, the V2G capacity has low impact in the scheduling. However, in the other two scenarios it is possible to see an increasing use of EVs to discharge. The discharges occur in hours 20 and 21, due to the high generation costs verified in these two periods.

Figure 4.20 shows the scheduling for the three scenarios using the SA methodology.

a)

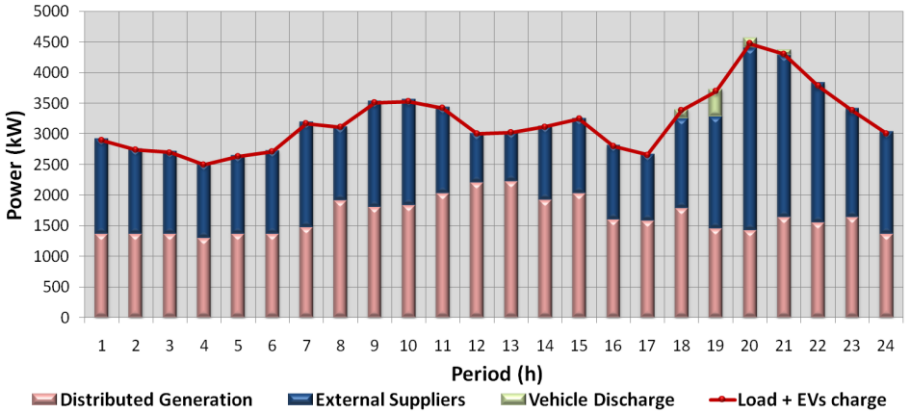

b)

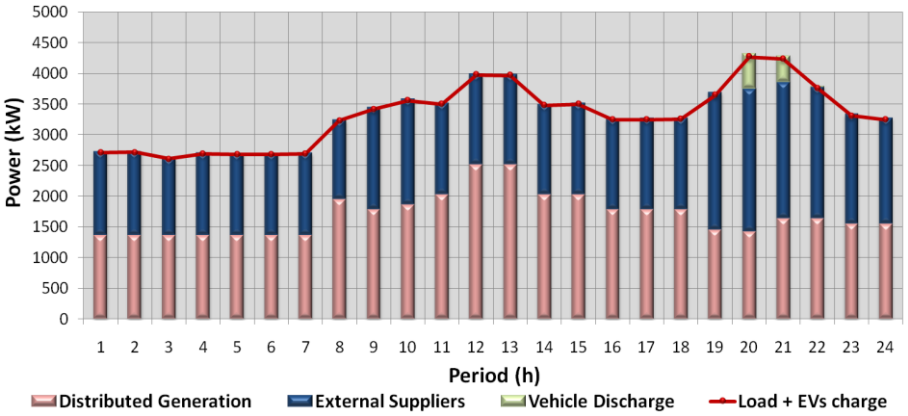

c)

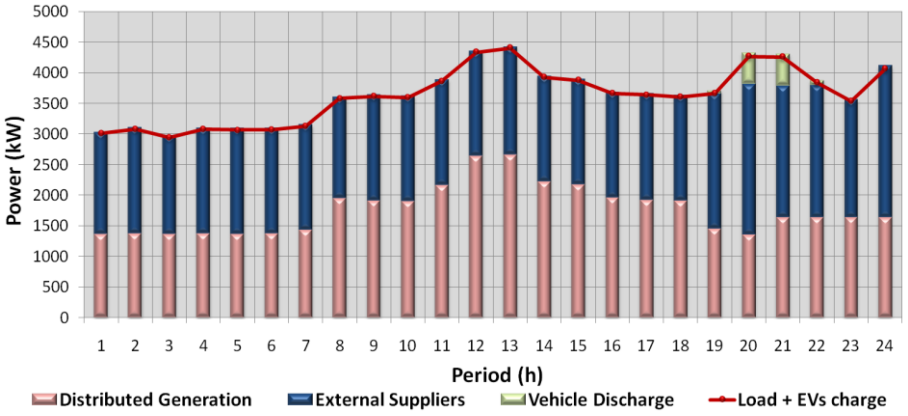

Figure 4.20 – Optimal resource scheduling of V2G mode using SA methodology for: a) 1000_EV_V2G, b) 2000_EV_V2G, c) 3000_EV_V2G.

Comparing Figure 4.20 with Figure 4.19, it is possible to see that, regarding the 2000_EV_V2G and 3000_EV_V2G scenarios, the periods in which EV are discharged are the same, using SA and MINLP – periods 20 and 21. In what concerns the 1000_EV_V2G scenario, SA uses the discharging capability of EVs in period 19, which does not occur when using the MINLP.

Figure 4.21 presents the load diagram and the total EVs charge for the three scenarios. These results were determined using the MINLP methodology. The blue line indicates the load diagram considering the demand of consumers, the total EVs charge and the reduction effect achieved through the use of EV discharge.

a)

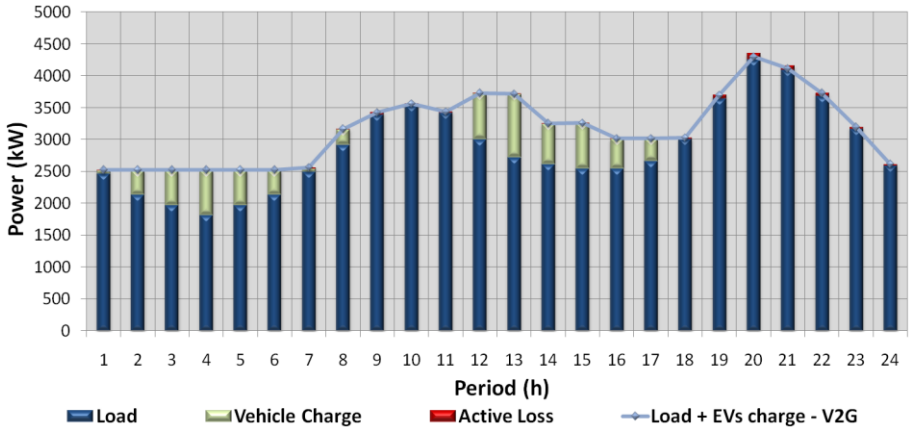

b)

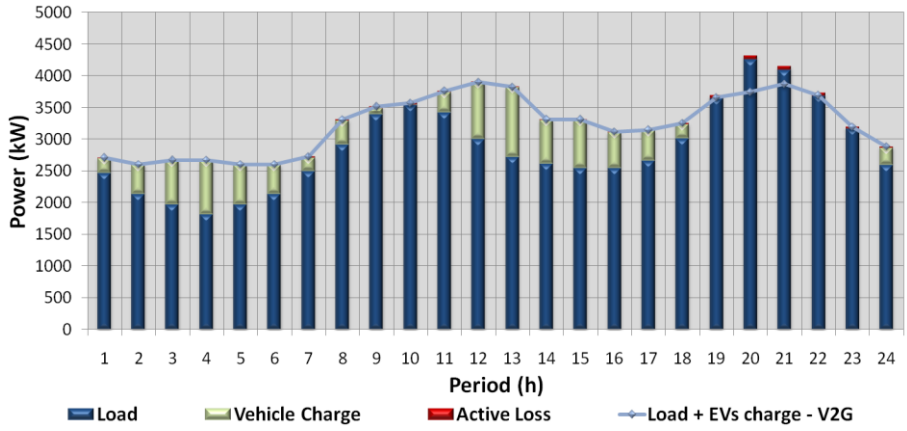

c)

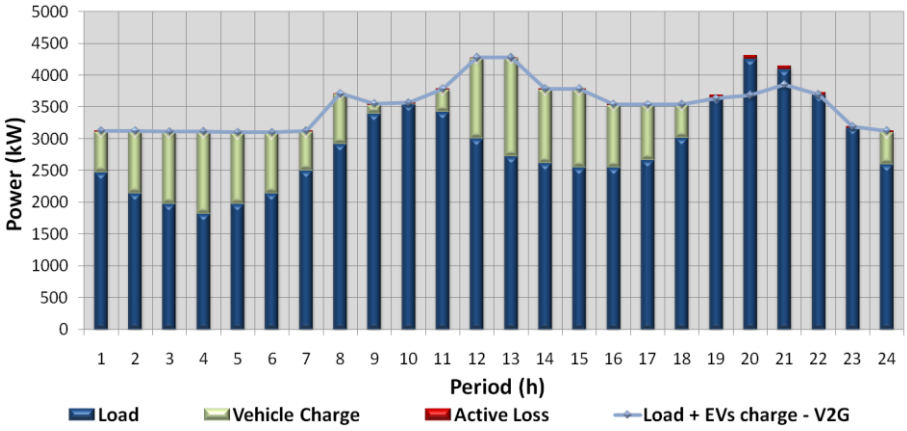

Figure 4.21 – Load and EVs charging power of V2G mode using MINLP methodology for: a) 1000_EV_V2G, b) 2000_EV_V2G, c) 3000_EV_V2G.

From Figure 4.21 it is possible to see that the load diagram decreases when EV discharges are used in peak hours (hours 20 and 21). Considering the logic of minimizing the operation cost, the VPP allocates EVs charges in the off-peak periods (from hours 1 to 6), for the same reason presented in the smart charging section.

Figure 4.22 shows the load diagram obtained with the use of the SA methodology for the three scenarios. This figure presents the consumer demand, the total EVs charge, and the load reduction obtained using the EVs discharge.

a)

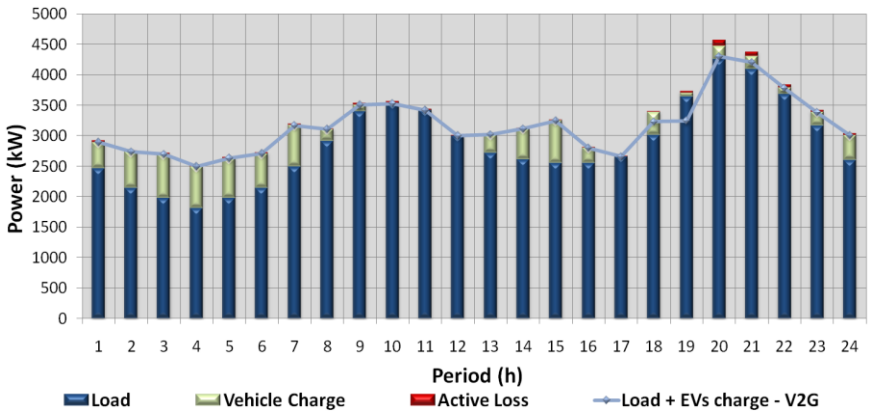

b)

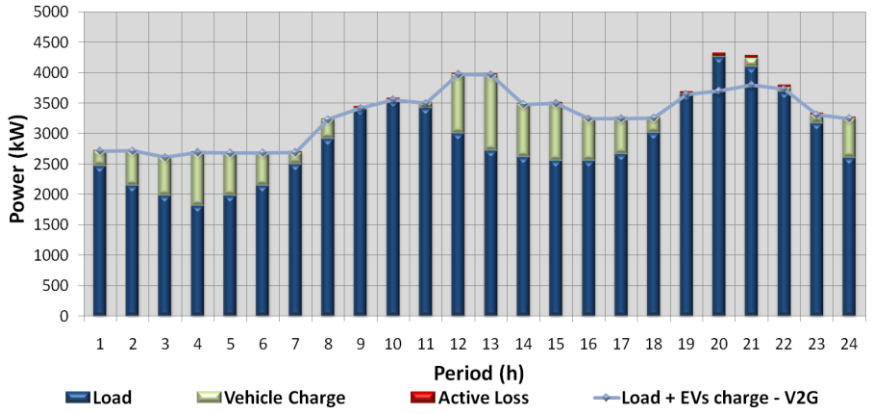

c)

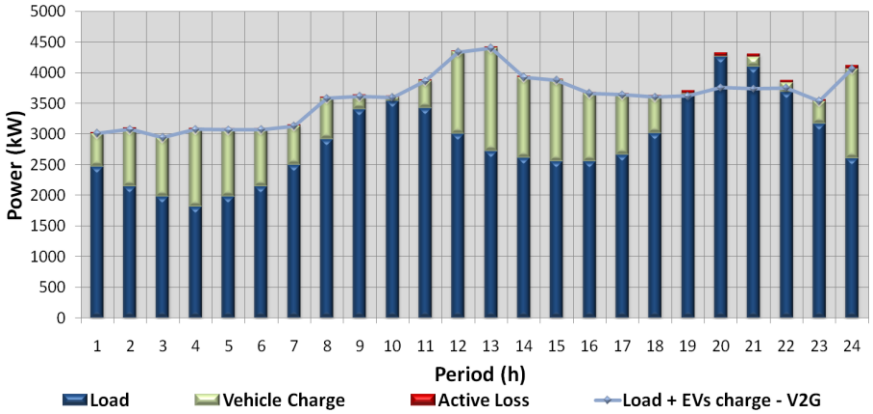

Figure 4.22 – Load and EVs charging power of V2G mode using SA methodology for: a) 1000_EV_V2G, b) 2000_EV_V2G, c) 3000_EV_V2G.

Analyzing Figure 4.22, it is possible to see that the SA methodology achieves a similar load diagram to the MINLP. The main discrepancy between the SA and the MINLP solutions is after hour 20, due to SA's higher charging, making the necessary adjustments to ensure that the battery is at least at 40% of its capacity in hour 24.

4.5. Energy Resource Management considering successive days scenarios

The case studies presented in this section considers the influence of successive day scenarios in the ERM problem. In fact, although the objective is to solve the scheduling of the available energy resources for the next day, the scenarios that will become effective on the successive days will influence the optimization. Another important result from the scheduling is to know the energy stored in the EVs batteries at the end of the day (hour 24). In the other case studies it is assumed a specific value for the battery energy stored at hour 24, but in this section this will be determined by the ERM problem considering the influence of successive days.

It is assumed that in principle the EV owners' only are committed to provide the VPP with their requirements on a day ahead basis, but more information about the subsequent days may be available. It is also considered the use of EVs model with control charge and discharge (V2G capacity) with three discharge prices steps, using the Equation (3.5) in sub-section 3.3.2. The first price has been fixed in 0.02 m.u./kWh and it is used between 100% and 70% of the battery capacity. The second price has been defined in 0.04 m.u./kWh and it is used from 70% to 40% of the battery capacity. The third price has been fixed in 0.06 m.u./kWh and it is used from 40% to 20% of the battery capacity.

The MINLP methodology has been used to solve the optimal resource scheduling for five scenarios (scenarios A, B, C, D and E). Each scenario considers the 24 hour periods that correspond to the day ahead planning and a number of additional periods to consider the successive day influence on the resource scheduling for the first day. The number of additional periods differs from scenario to scenario. The main purpose is to obtain the best time horizon of the five scenarios that corresponds to the lowest operation cost in the two successive days.

Scenario A considers a simulation horizon of 48 hours. These 48 hours correspond to the day-ahead 24 hour periods and to the consecutive day, which is considered to take into account the successive day influence.

Scenario B considers a simulation horizon of 42 hours, corresponding to the 24 day-ahead periods, plus 18 additional hours for considering the successive day influence. After this simulation, the energy stored in each EV at the end of the 24^{th} hour is used as the initial state for another 24 hours simulation. The total operation cost for the two days is the

sum of the costs obtained for the first 24 hours in the first simulation with the cost obtained for the second simulation.

Scenario C considers a simulation horizon of 36 hours, corresponding to the 24 day-ahead periods plus 12 additional hours for considering the successive day influence. The energy stored in the end of the 24th hour is used as the initial state of the second simulation of 24 hours.

Scenario D is simulated for 30 hours, corresponding to the 24 hours of the next day and to 6 additional hours for considering the successive day influence. The energy stored in the end of the 24th hour is used as the initial state of the second simulation of 24 hours.

Scenario E is simulated for 24 hours only, in order to allow taking conclusions concerning the advantages of using an additional simulation period to consider the influence of the successive day impact, when compared with a single optimization considering only the 24 hourly periods of the day ahead.

4.5.1. Two Successive Days of Week

The five scenarios referred above consider the same behavior of the EV driving patterns for regular week days. Load and EV requirements for the second day are considered equal to the ones for the first day, for sake of data simplicity. In all scenarios it is assumed that all EVs start with 30% charge of their battery capacity. These values are assumed as equal for all the considered vehicles for the case study. A global value equal to 30% of the total battery capacity, considering the whole set of vehicles, is imposed at the final of the total simulation periods. It is assumed a case study with 1000 EVs in the 32 bus distribution network.

Table 4.15 shows the operation cost for days *D* and *D+1* for scenarios A, B, C, and D. The operation costs for day *D* are the costs obtained for the first 24 hours of the first simulation. The operation costs for day *D+1* are the costs obtained for the 24 periods of the second simulation, which is run considering as initial state the EV batteries state at the end of the 24th hour of the first simulation.

Table 4.16 summarizes the scheduling results of days *D* and *D+1* for all five scenarios. It is indicated the execution time for each scenario, and the difference in terms of operation cost, where the scenario A is considered as reference because this scenario presents the minimal total operation cost for the two days.

Sc.	Day D					
	DG and External suppliers cost (m.u.)	Discharge Cost (m.u.)			Operation cost (m.u.)	24th hour EVs battery state (%)
		Step A (100-70 %)	Step B (70-40 %)	Step C (40-20 %)		
A	6,546.80	8.88	14.94	30.80	6,570.90	30.80
B	6,235.42	0.17	3.64	39.69	6,278.92	12.05
C	6,188.50	1.49	2.78	63.62	6,256.39	9.38
D	6,125.13	0	0	73.27	6,198.40	5.22
E	6,067.96	44.07	0	0.91	6,112.94	0.68
Sc.	**Day D+1**					
A	6,519.63	10.96	19.28	9.12	6,558.99	30
B	6,858.53	3.19	6.72	3.36	6,871.80	30
C	6,913.70	0	2.66	0	6,916.36	30
D	6,986.50	0	2.48	1.32	6,990.30	30
E	No feasible solution					

Table 4.15 – Results comparison for the energy resource scheduling of 1000_EV_ERM_WeWe.

Sc.	Execution time (s)	Operation cost (m.u.)			Difference cost	
		Day *D*	Day *D+1*	Total	m.u.	%
A	4,731.50	6,570.90	6,558.99	13,129.89	-	-
B	3,492.17	6,278.92	6,871.80	13,150.72	20.83	0.16
C	2,758.70	6,256.39	6,916.36	13,172.75	42.86	0.33
D	2,158.70	6,198.40	6,990.30	13,188.70	58.81	0.45
E	1,832.29	6,112.94	No feasible solution		-	-

Table 4.16 – Total operation cost for the ERM of 1000_EV_ERM_WeWe.

The scenario A results correspond to the lowest operation cost. This scenario corresponds to the maximum considered successive day influence period which has been a complete day. This corresponded to a first simulation for 48 hours, from which the results for day ahead scheduling are the results for the first 24 hours. The scenario A obtains a feasible solution for the considered days, with a cost of 13,129.89 m.u. in 4,731.50 seconds (1.3 hours). In this scenario the overall battery charge remains slightly above 30% of the total V2G battery capacity at the end of the 24th hour, helping the scheduling for the next day (Day *D+1*) and achieving a operation cost lower than the others scenarios.

In the scheduling for the first day (day *D*), scenarios B, C and D achieved lower costs than scenario A, due to a lower value of energy stored in EV batteries at the end of the 24th

hour. For these three scenarios the energy stored in the EV batteries at the end of the 24th hour is equal to 12.05%, 9.38% and 5.22%, respectively for scenario B, for scenario C and for scenario D. These lower stored energy values make the scheduling for the next day (*D+1*) more costly for the VPP, being necessary to use more expensive energy to guarantee the required trip distances. For scenario E it was not possible to find a solution for the next day (*D+1*), because the energy stored in the V2G batteries at the end of the first day (0.68%) is too low. The analysis of these results shows that the consideration of a complete day to consider the influence of the successive day (Scenario A) in the day ahead scheduling led to the best solution.

Figure 4.23 depicts the resulting energy resource scheduling over 48 hours for scenario A.

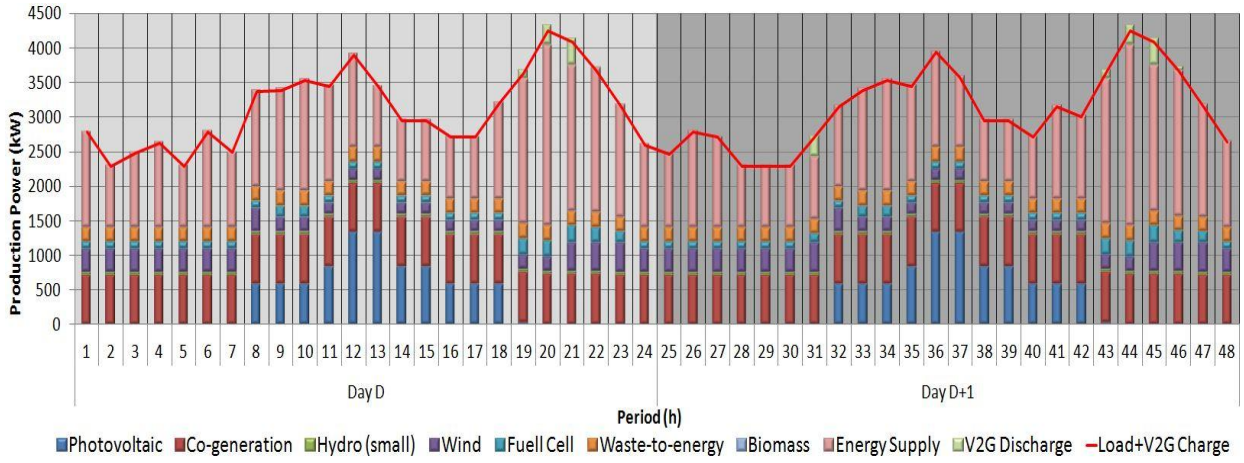

Figure 4.23 – Energy resource scheduling for the scenario with 48 hours of 1000_EV_ERM_WeWe.

Figure 4.24 illustrates the load diagram and the total V2G charge for the 48 hour periods of scenario A.

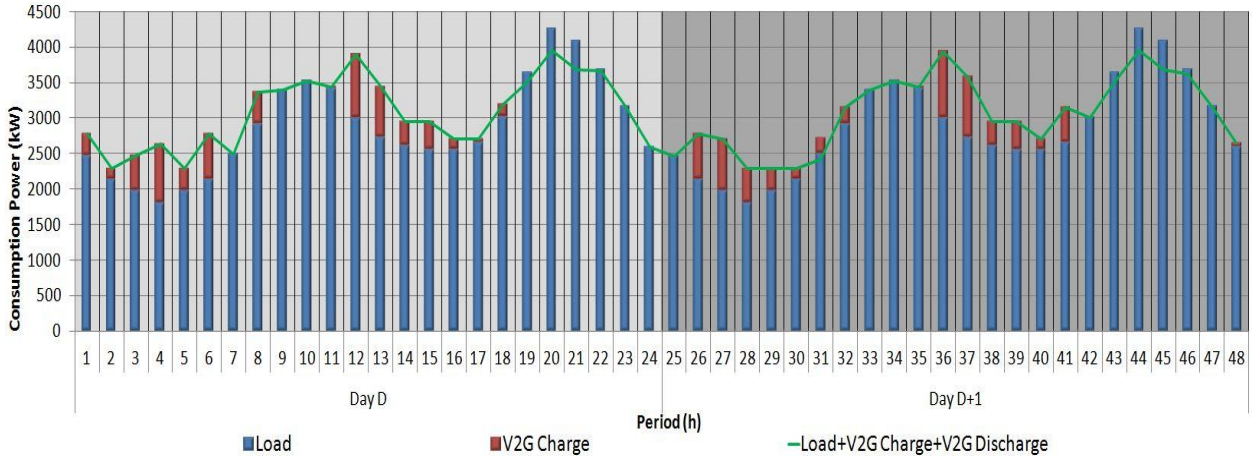

Figure 4.24 – Load diagram for the scenario with 48 hours of 1000_EV_ERM_WeWe.

It can be concluded from Figure 4.23 that EV discharge has been allocated in the peak periods (hours 19, 20, 21, 43, 44, 45 and 46). This is a good strategy for cost

minimization due to the fact that in these periods the V2G discharge has lower cost than the other available resources. The solid line represents the sum of the load demand and the EV charge. The difference between the displayed bar height and this line, for each period, corresponds to the power losses.

Figure 4.24, the solid line represents the resulting load diagram considering the demand, EV charge and the load reduction effect achieved through the use of EV discharge. The EV charges are allocated in the off-peak periods (from hour 1 to hour 6 and from hour 25 to hour 32), because the charging costs are lower than in the other periods.

Figure 4.25 shows the total EV charge and discharge results obtained for scenario A, being possible to see the amount of energy that is used to discharge in each considered price step (step A, B and C).

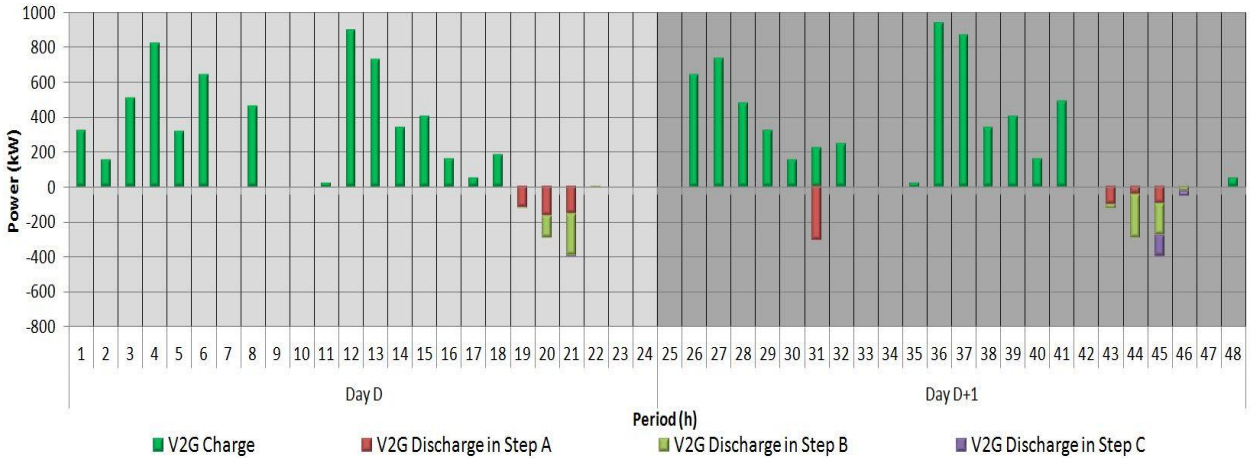

Figure 4.25 – Total charge and discharge profile for the scenario with 48 hours of 1000_EV_ERM_WeWe.

4.5.2. Friday to Saturday Transition

In this case study Friday and Saturday are considered in order to determine the ERM for Friday considering the influence of Saturday behavior. This sub-section relates the experience of using five scenarios considering Friday and Saturday profiles, in terms of consumers and EV driving pattern. The first day of this simulation uses the profiles of a typical Friday, and in the second day the consumers and EV requirements have been simulated according to a typical Saturday behavior.

The load diagram of the consumers is different for the two days. Figure 4.26 presents the total load diagram for these two days inspired on the data from the Portuguese transmission operator[9]. Figure 4.27 shows the total used with trips for these two days. The load diagram was based on the 18th and 19th of March 2011.

[9] Consulted in October 2011: http://www.centrodeinformacao.ren.pt/en/Pages/CIHomePage.aspx

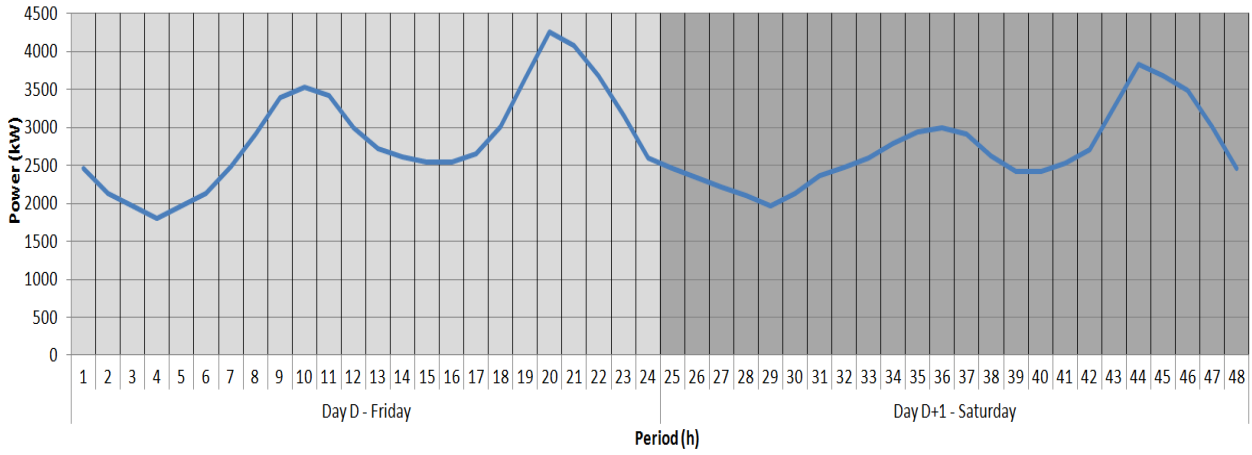

Figure 4.26 – Total load diagram for the 1000_EV_ERM_FrSa case study.

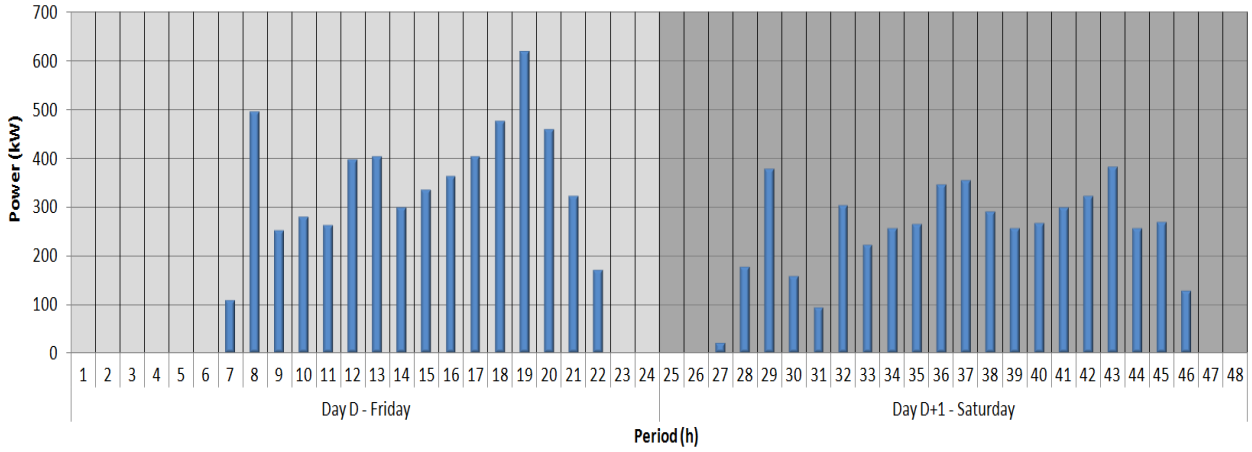

Figure 4.27 – Total energy with trips for the 1000_EV_ERM_FrSa case study.

In terms of EV driving pattern, this case study is different from the previous ones. In day *D* (Friday) the EVs have the same profile as a regular day in the afternoon, but in the evening the EVs tend to travel more (hours 20, 21 and 22). In day *D+1* (Saturday) the EVs have less travels in the morning than in a regular day, but in the evening EVs have a similar behavior as in day *D* (hours 44, 45 and 46).

It is also assumed that all EVs start with 30% charge of their battery capacity. These values are assumed as equal for all the considered vehicles for the case study. A global value equal to 30% of the total battery capacity, considering the whole set of vehicles, is imposed at the end of the total simulation periods. It is used the same number of EVs as in the previous case study.

The operation costs for days *D* and *D+1* are presented in Table 4.17, which shows the results for the five scenarios. This case study uses the same approach as the previous case study. In day *D+1* the initial state of EV batteries is equal to the result of the batteries state at the end of the 24th hour of day *D*.

Sc.	Day D					
	DG and External suppliers cost (m.u.)	Discharge Cost (m.u.)			Operation cost (m.u.)	24th hour EVs battery state (%)
		Step A (100-70 %)	Step B (70-40 %)	Step C (40-20 %)		
A	6,557.80	8.69	0	0	6,566.49	27.71
B	6,278.73	1.11	3.61	35.20	6,318.65	11.49
C	6,258.87	0.66	2.59	48.12	6,310.24	10.28
D	6,164.66	34.83	5.46	3.97	6,208.92	4.49
E	6,105.04	39.67	5.28	3.95	6,153.94	0.65
Sc.	**Day D+1**					
A	6,187.45	1.44	2.88	1.44	6,193.21	30
B	6,469.61	1.44	2.88	1.44	6,475.37	30
C	6,494.79	0	0	0	6,494.79	30
D	6,595.38	0	0	0	6,595.38	30
E	6,663.77	0	0	0	6,663.77	30

Table 4.17 – Results comparison for the ERM of 1000_EV_ERM_FrSa.

The operation cost of the two successive days achieves the lowest value for scenario A, because it is considered the total simulation horizon of 48 hours. On the other hand, scenario E presents the highest value in terms of operation cost for the two days. The scenario A result for day *D* is 6,566.49 m.u. and for day *D+1* is equal to 6,193.21 m.u. The resulting cost is 12,759.70 m.u. and these two operation costs only differ by 373.28 m.u.

In scenario E it is possible to see more difference between the two operation costs of day *D* and day *D+1*. In day D, the cost was 6,153.94 m.u. and in day *D+1* was 6,663.77 m.u. The difference between the two operation costs is 509.83 m.u., resulting in a total cost of 12,817.71 m.u. The difference between the two operation costs happened due to the energy stored in the EVs batteries at the end of hour 24 of day D. The energy stored in scenario E is only 0.65% of the total capacity of all 1000 EVs for this case study. This means that most of the EVs in day *D* had their batteries totally discharged until zero; only a few EVs remained with a certain amount of energy in the battery. In the next day D+1, the scheduling starts with the EVs battery closer to zero, what results in more charges of EVs to maintain the trip profile of the next day. Due to this fact the resulting operation cost increased significantly.

In scenario A, the difference in the operation cost between the two successive days is not significant, because in hour 24 of day *D* the energy stored is much higher than in scenario E. In this case, the energy stored at hour 24 achieves approximately 28% of the total capacity of EV batteries. This fact makes less costly the scheduling for the next day

D+1. The more available energy in the batteries helps managing the ERM of the next day and in day *D+1* is not necessary a large amount of energy to charge EVs. The trip distance of day *D+1* will be sustained jointly by the energy stored in day *D* (28% of the total capacity) and the charges of EVs in day *D+1*. Although, scenario A achieves the highest operation cost in day *D*, because in this day was necessary to charge more the EVs to increase the energy stored at the end of hour 24.

Another important fact in the scheduling of these two successive days is the increase of operation cost in day *D* when it is used a bigger simulation horizon, such as in the case of scenario A with 48 hours. Scenario A achieves the highest operation cost in day *D*, and scenario B achieves the second higher value in the operation cost in day *D*. The same happens in scenario C, where this scenario is the third higher value. The quantity of energy stored in the EVs at the end of day D influences the operation cost value of day *D*.

The influence of successive days in the scheduling changes the amount of power used with the EVs discharges. In day *D*, the EVs discharge more when is used a small simulation horizon, such as in scenario C and E, because the time horizon decreases and the Saturday trip profile becomes less important and the resulting scheduling maximizes the usage of EVs to discharge.

Table 4.18 presents the operation cost for day *D* and *D+1* of each scenario. It shows the difference in terms of operation costs. Scenario A is considered as reference because, this scenario achieves the best operation cost.

Sc.	Execution time (s)	Operation cost (m.u.)			Difference cost	
		Day *D*	Day *D+1*	Total	m.u.	%
A	7,998.70	6,566.49	6,193.21	12,759.70	-	-
B	5,386.20	6,318.65	6,475.37	12,794.02	34.32	0.27
C	5,143.03	6,310.24	6,494.79	12,805.03	45.33	0.36
D	4,834.74	6,208.92	6,595.38	12,804.30	44.60	0.35
E	3,308.50	6,153.94	6,663.77	12,817.71	58.01	0.45

Table 4.18 – Total operation cost for the ERM of 1000_EV_ERM_FrSa.

It is possible to conclude that the undertaking simulation for 48 hours (scenario A) decreases the operation cost of the two days (day *D* and *D+1*). The use of this approach helps the VPP achieving the best operation cost including EVs in the network. The biggest difference in the operation cost is between scenario A and E, because scenario E considers a simulation period of 24 hours. So, this scenario obtains the optimal scheduling of day *D* without considering the influence of day *D+1* in terms of the required energy to travel in the next day. This is a difference of 0.45% between these two scenario costs. This difference is reduced when a large simulation horizon is used to simulate and then obtain

the energy stored at the end of hour 24 of day *D*. This result is used as the initial value of the batteries state for the next day *D+1*. The lowest difference in the operation is between scenario A and B, due to the fact that scenario B simulates with 42 hours and scenario A considers the simulation with 48 hours. Therefore, in these 2 scenarios the simulation time differs in 6 hours.

Figure 4.28 depicts the resulting energy resource scheduling over 48 hours for scenario A.

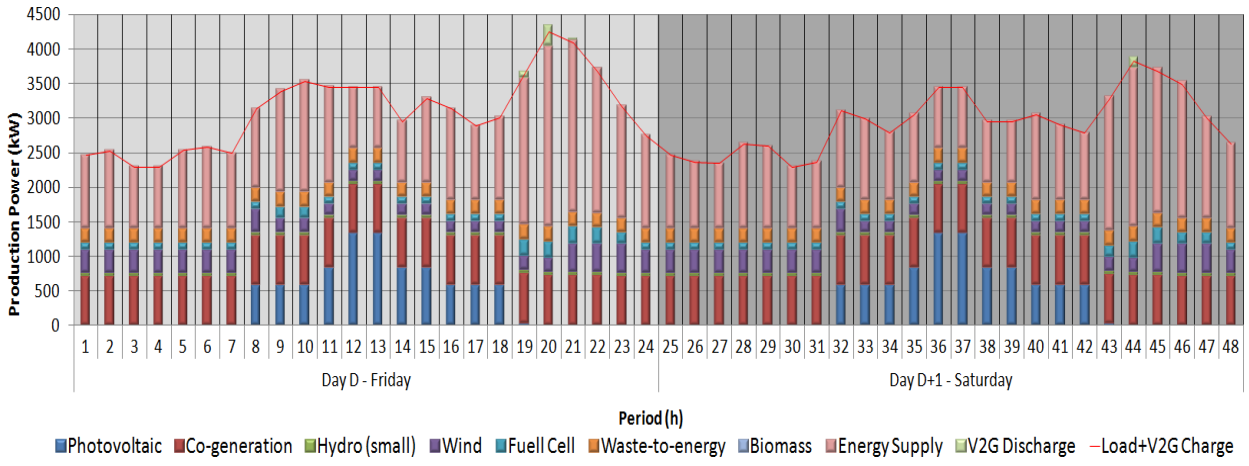

Figure 4.28 – Energy resource scheduling for the scenario with 48 hours of 1000_EV_ERM_FrSa.

Figure 4.28 presents the resources used to supply the required load demand and EV charges. In this case study, the EVs have been more discharged in hours 19 and 20 of day *D*. Figure 4.29 illustrates the load diagram and the total V2G charge for the 48 hour periods of scenario A.

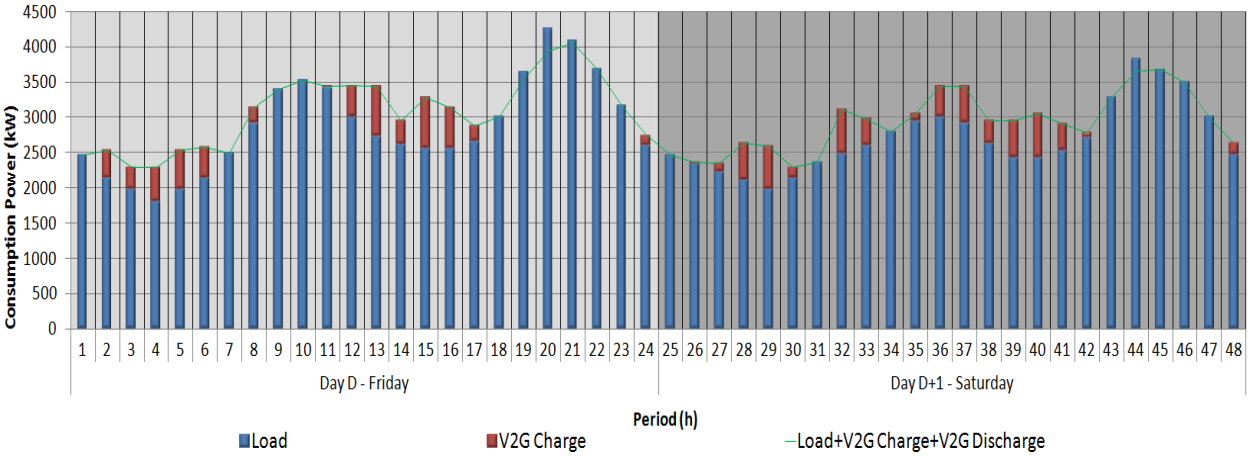

Figure 4.29 – Load diagram for the scenario with 48 hours of 1000_EV_ERM_FrSa.

The solid line represents the resulting load diagram considering the demand, EV charge and the load reduction effect achieved through the use of EV discharge. In scenario A, the EVs have been more allocated to charge in the off-peak hours of day *D* (Friday). Day *D+1* the EV charges are more dispersed into the periods of this Saturday.

Figure 4.30 shows the total EV charge and discharge results obtained for scenario A, being possible to see the amount of energy that is used to discharge in each considered price step (step A, B and C).

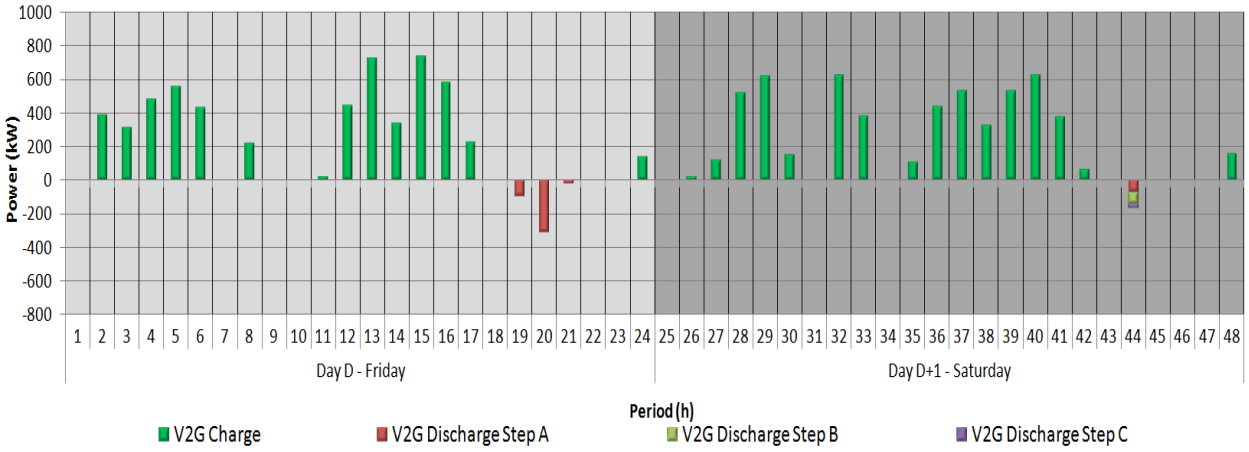

Figure 4.30 – Total charge and discharge profile for the scenario with 48 hours of 1000_EV_ERM_FrSa.

4.5.3. Sunday to Monday Transition

In this case study Sunday and Monday are considered to obtain the optimal scheduling of these two days. Five scenarios have been used in the same way as sub-sections 4.5.1 and 4.5.2. The consumer behavior and EVs trip profile have been adjusted to this case study. Figure 4.31 depicts the load diagram of Sunday (day *D*) and Monday (day *D+1*). The load diagram on Monday (day *D+1*) follows the same behavior as a typical working day. The load diagram was based on the data from the Portuguese transmission operator[10] between the 20th and 21st of March 2011.

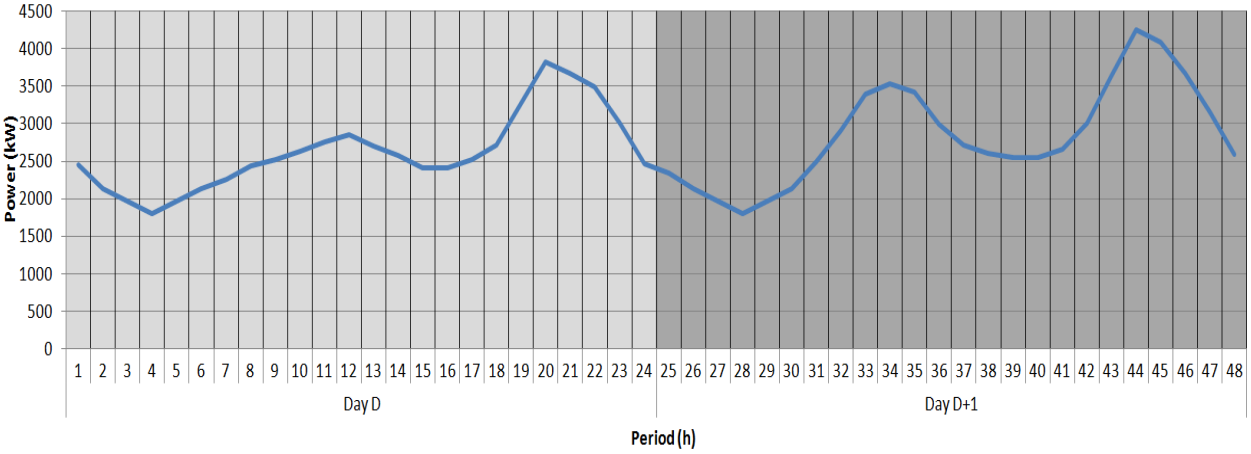

Figure 4.31 – Total load diagram for the 1000_EV_ERM_SuMo case study.

[10] Consulted in October 2011: http://www.centrodeinformacao.ren.pt/en/Pages/CIHomePage.aspx

The same strategy to adapt the EVs trip profile presented in the previous sub-section has been used, and the trip profile for this case study is shown in Figure 4.32. This case study uses the same requirements used in the two other case studies. The EVs start with 30% charge of their battery capacity, and it is imposed at the end of the day *D+1* a global value on 30% of the EVs battery capacity.

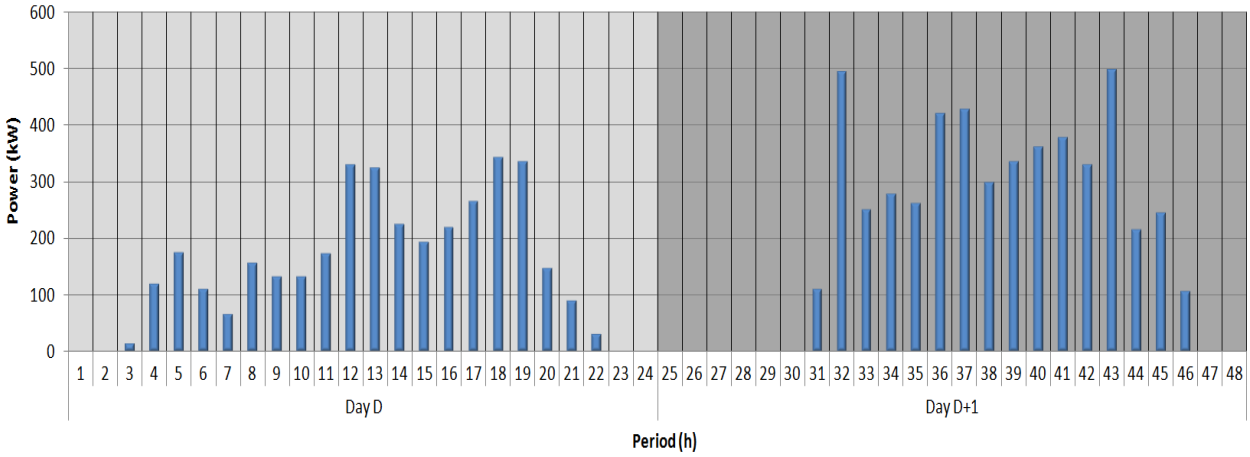

Figure 4.32 – Total energy with trips for the 1000_EV_ERM_SuMo case study.

The operation costs for days *D* and *D+1* are presented in Table 4.19. In day *D+1* the initial state of EV batteries is equal to the result of the batteries state at the end of the 24th hour of day *D*.

Sc.	Day D					
	DG and External suppliers cost (m.u.)	Discharge Cost (m.u.)			Operation cost (m.u.)	24th hour EVs battery state (%)
		Step A (100-70 %)	Step B (70-40 %)	Step C (40-20 %)		
A	6,015.29	6.39	1.09	0	6,022.77	39.28
B	5,638.92	3.90	5.87	46.66	5,695.35	16.61
C	5,593.50	1.62	2.97	68.27	5,666.36	13.42
D	5,502.19	0	0	81.26	5,583.45	7.24
E	5,502.45	0	0	81.76	5,584.21	7.20
Sc.	**Day D+1**					
A	6,365.19	5.63	11.23	5.19	6,387.24	30
B	6,776.11	0	2.66	0	6,778.77	30
C	6,828.44	0.96	4.58	0.96	6,834.94	30
D	6,933.19	2.28	5.97	2.28	6,943.72	30
E	6,939.24	0.58	4.58	0.96	6,945.36	30

Table 4.19 – Results comparison for the ERM of 1000_EV_ERM_SuMo.

As happened in the previous case studies, scenario A achieved the highest operation cost in day *D*, but the lowest cost in the next day *D+1*. In this case study the differences in the operation cost between scenario A and the other four scenarios are higher than for the other two case studies. This fact is related to the load diagram and trip profile considered for this case study, and it will be explained ahead in detail. Again, the remaining energy stored in the 24th hour is an important factor to the difference of the operation cost between the five scenarios. In scenario A, the EVs battery state finished with 39.28%, and in scenario B it finished with 16.61% at the end of day *D*. The difference was bigger because in this case study day *D+1* required more in terms of charging energy to maintain the considered trip profile than in the other two case studies.

Table 4.20 presents the operation costs for days *D* and *D+1* of each scenario. It shows the difference in terms of operation cost, with scenario A considered as reference because this scenario has the lowest operation cost.

Sc.	Execution time (s)	Operation cost (m.u.)			Difference cost	
		Day *D*	Day *D+1*	Total	m.u.	%
A	9,471.10	6,022.77	6,387.24	12,410.01	-	-
B	6,675.06	5,695.35	6,778.77	12,474.12	64.11	0.52
C	5,717.54	5,666.36	6,834.94	12,501.30	91.29	0.74
D	2,997.21	5,583.45	6,943.72	12,527.17	117.16	0.94
E	2,627.58	5,584.21	6,945.36	12,529.57	119.56	0.96

Table 4.20 – Total operation cost for the ERM of 1000_EV_ERM_SuMo.

As it happened in the other two case studies, scenario A achieved the minimum operation cost, since it considers the total simulation horizon of 48 hours. Scenario A obtains a feasible solution for the considered days, with a cost of 12,410.01 m.u. in 9,471.10 seconds, and the other scenarios did not achieve a better operation cost for the two days. The operation cost differences in the five scenarios are higher than in the other two case studies. For instance, the difference between scenario A and E is approximately 1%.

Figure 4.33 depicts the resulting energy resource scheduling over 48 hours for scenario A.

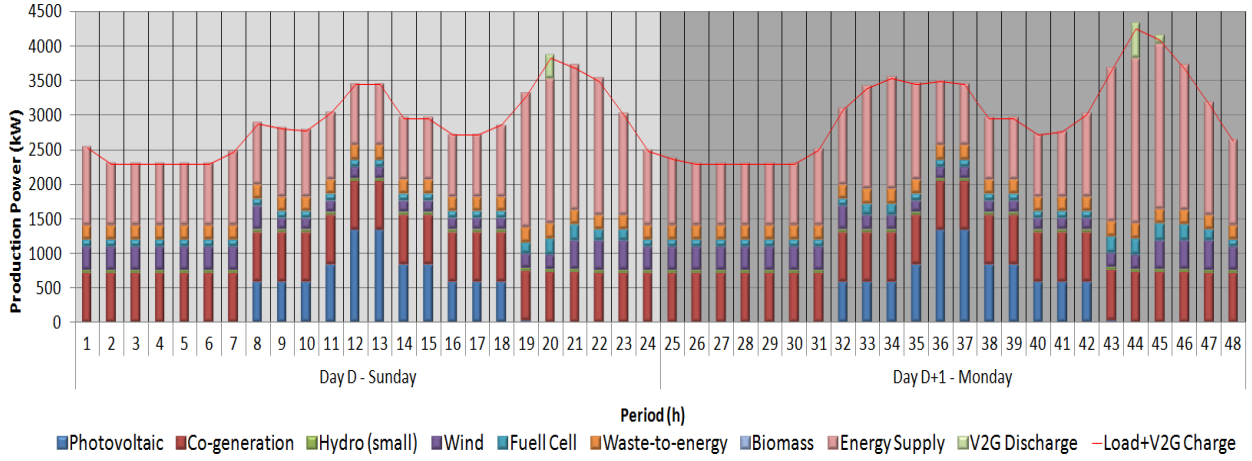

Figure 4.33 – Energy resource scheduling for the scenario with 48 hours of 1000_EV_ERM_SuMo.

The EVs discharges are more used in day *D+1* than in day *D*. It is possible to see the use of EVs discharge in hour 20 of day *D* and; in day *D+1* it is used in hours 44 and 45.

Figure 4.34 illustrates the load diagram and the total V2G charge for the 48 hour periods of scenario A.

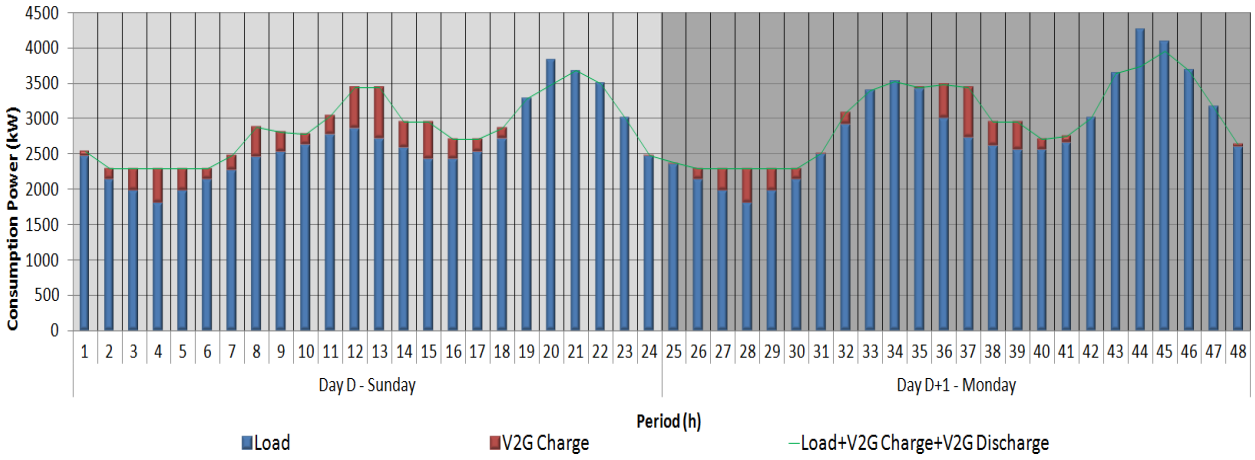

Figure 4.34 – Load diagram for the scenario with 48 hours of 1000_EV_ERM_SuMo.

The EV charges were allocated with more intensity in the off-peak periods of day *D*. This is related to the load diagram of day *D;* in this load diagram the off-peak periods (between hours 1 to 7 of day *D*) have a lower load consumption that in the same periods of day *D+1*. If the EVs charge were more located in the day *D+1* instead of the day *D*, the VPP will be obligated to use the generators more expensive in these off-peak periods. The use of EVs to charge in the day *D+1* could increase the operation cost, because EVs charge is other additional load that would require the use of more expensive energy resources.

In day *D*, at midday some EVs charges appear due to the fact that the photovoltaic generators are totally dispatched and VPP is obligated to buy the energy from these generators. VPP uses that available energy to charge the EVs in hours 12, 13, 14 and 15 of day *D*. In terms of EVs charge management, the VPP tries to allocate more EVs to charge in

day *D* in order to sustain the trip distance of day *D* and *D+1*. In the next day *D+1*, the off-peak periods have higher load consumption than in day *D*, and there are less energy resources with a low operation cost. The VPP will allocate the EVs charge in these periods to use in the peak periods of day *D+1* the EVs to discharge, instead of using expensive energy resources in peak periods.

Figure 4.35 shows the total EV charge and discharge results obtained for scenario A, being possible to see the amount of energy that is used to discharge in each considered price step (step A, B and C).

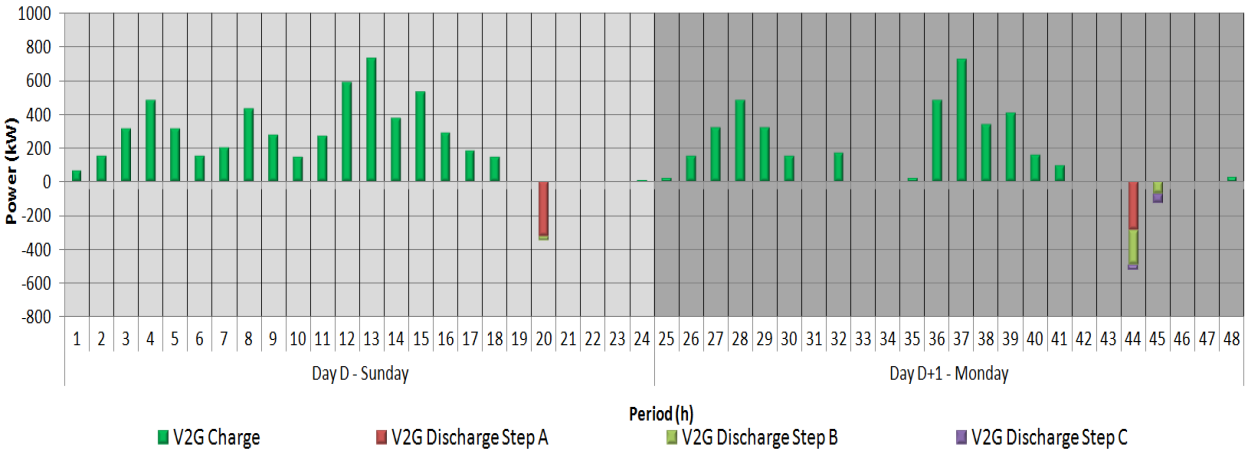

Figure 4.35 – Total charge and discharge profile for the scenario with 48 hours of 1000_EV_ERM_SuMo.

4.6. Conclusions

The case studies presented in this chapter support the demonstration of the proposed methodology's advantages in improving VPPs' management of networks with intensive use of EVs. Furthermore, the presented tests and the achieved results show that the applicability of such a methodology is possible and attainable, being able to provide the means for a full and adequate handling of EVs characteristics, so that the higher possible advantages can be taken from this type of vehicles' management.

Some studies regarding the complexity of the ERM problem are presented in section 4.3, where the influence of the number of decision variables into the increasing of the execution time is demonstrated. When a large number of EVs is connected into the network, the result is an exponential growth of the execution time to obtain the optimal scheduling. The execution time is largely affected by the number of decision variables in the ERM problem, i.e. when a higher number of EVs is considered, this will affect the performance of the MINLP approach in finding an optimal solution. In some cases, the MINLP approach takes more than one day to solve the ERM problem. For instance, in a scenario with 3000 EVs, the MINLP approach takes 74.32 hours to solve the problem, which is unacceptable to solve the scheduling for the next day. In order to be acceptable it should always take below 24 hours, as the scheduling horizon is the following day.

Considering this kind of problem, three different approaches have been proposed with the purpose of reducing the execution time. These approaches' reduction in execution time influences the solution quality of the ERM problem. The first approach is the testing of the MINLP approach using relaxation in some network constraints. The second approach considers a MINLP approach with EVs clustering. Finally, the third approach is based on an adaptation of the simulated annealing metaheuristic. For instance, considering the scenario with 3000 EVs, the basis approach (using MINLP) took approximately 3 days to solve this problem. Using each of the three proposed approaches, the execution time drops drastically but reduces the solution quality of the scheduling.

In section 4.4 the scheduling is evaluated considering different control modes of EVs: uncoordinated charging, smart charging and V2G. Uncoordinated charging of EVs is impracticable, as it leads to highly critical situations in what concerns the capability of supplying the required demand. Using the uncoordinated charging mode means charging indiscriminately the EVs until the charge reaches the specific value indicated by the user. In this case the operation cost is much higher than on the case considering smart charging. For instance, in the 3000_EV_UnC scenario, the operation cost achieved 7,709.13 m.u., while in the case of 3000_EV_SC the operation cost is reduced to 7,405.47 m.u.. The difference between the two costs is approximately 4 %, representing a significant reduction when using the smart charging mode. The V2G mode increases the flexibility of the scheduling, and enables the VPP to use a certain amount of energy stored in EVs in peak periods, instead of using more expensive generators to supply the load. In the 3000_EV_V2G scenario, the operation cost is 7,317.85 m.u.. This value represents a visible reduction in operation costs when compared to the other two scenarios. However, when compared directly with the 3000_EV_SC scenario, the cost is not reduced in the same level as from uncoordinated charging to smart charging. In this case, the difference in cost between 3000_EV_SC and 3000_EV_V2G is approximately 1 %. The results of the V2G mode (presented in sub-section 4.4.3) show this methodology's adequate performance when taking advantage on EVs' potentialities as storage systems, providing the means for charging and discharging when it is most advantageous for the network, from both the VPP's and the individual EV's user perspectives.

In section 4.5 a case study is presented considering several simulation time horizons, namely 24, 30, 36, 42 and 48 hours. This approach considers the influence of EV trips for successive days. The influence of successive days presents a big impact in the operation cost. When a smaller simulation horizon is considered, *e.g.* 30 or 24 hours, the operation cost increases because the VPP does not gather enough information about the requirements for the next day. A higher impact is verified when a transition between Sunday to Monday is simulated. In this case, the ERM for 48 hours finds the lowest operation cost: 12,410.01 m.u. for the two days, because it incorporates the whole

information about the trip profile in Monday. On the other hand, scenario E (considering 24 + 24 hours independently) achieved an operation cost of 12,529.57 m.u.; the difference between these costs is 0.96%.

These results support the applicability of intelligent methodologies in enriching VPP's management of energy resources with the use of EVs, while pointing out the need for such approaches to be quickly considered for adoption in real cases, envisaging the widespread propagation of EVs all around the world in upcoming years.

Chapter 5

Conclusions and Future Research

5. Conclusions and Future Research

5.1. Main Conclusions and Contributions

The work developed in the scope of this thesis has been motivated by the introduction of Electric Vehicles (EVs) as alternative solution to the conventional vehicles used in the transportation sector. The possibility of connecting EVs to the electric network brings new challenges to power system management. It is important to have adequate methods to improve the management when it has to with a large amount of Distributed Energy Resources (DERs). The thesis is centered on the management of an electric network with intensive use of electric vehicles including Vehicle-to-Grid (V2G). Virtual Power Players (VPPs) require these methods and tools to cope with the new operation challenges that arise due to electric vehicle use mainly in the smart grid environment.

The methodologies proposed in the scope of this thesis are integrated in the Energy Resource Management in Smart grid (ERMaS) tool, to help the decision making of VPP concerning the management of aggregated DERs.

During the development of this thesis the EV technical and business model have been improved, mainly in what concerns the mathematical formulation and input data. In terms of input data of electric vehicles, adequate data from automobile manufacturers and standardization charging modes were used when possible; some parts of the EV business and technical model can be discussed, but at this stage there is no consensual opinion on some parameters of electric vehicles, namely discharge rates. These improvements make the Energy Resource Management (ERM) more suitable to be adopted by a VPP in a smart grid environment.

A deterministic and a Simulated Annealing (SA) based techniques have been proposed to solve the energy resource management in the scope of the ERMaS tool, based on two objectives. The first objective was the solution quality that both methodologies should achieve in different scenarios. The case studies presented in chapter 4 prove the effectiveness of both methodologies in terms of solution quality. The differences in the operation cost were minimal. The second objective was the required execution time to determine the optimal scheduling. Regarding the second objective, the results achieved in the case studies indicate that SA is more suitable to solve energy resource management when the main requirement is to solve the problem in a low execution time, since the proposed deterministic technique can take several minutes or even hours to solve the problem. On the other hand, the SA technique takes only seconds or, in extreme scenarios, a few minutes to solve the energy resource management problem. The objective was to develop methodologies that could combine the solution quality and execution time to meet both goals without introducing a large degradation in each objective.

Considering the case study presented in section 4.3, namely the scenario with 3000 EVs in the 32 bus distribution network, the ERMaS tool with the deterministic approach took approximately 3 days to solve the problem. With the SA, the same problem takes only a few minutes to be solved (approximately 2 minutes). In this situation the SA presents itself as a suitable technique to be used by the ERMaS tool. Solving the same problem using the deterministic technique required to use simplifications in the ERM problem, namely reducing the number of variables. The considered approach was changing from 3000 EVs to its equivalent in clusters of 10 vehicles - 300 clusters. Using this EV cluster approach made it possible to reduce the execution time but resulting in a degradation of the solution quality.

The proposed methodologies were also tested in several case studies in section 4.4. The tests presented in this section consider three control modes: uncoordinated charging, smart charge and V2G. The first control mode presents the biggest impact in the energy resource management, because it does not allow controlling the power and timings of the charging for each electric vehicle for the next day. The smart charging decreases the operation cost of the energy resource management when compared to the uncoordinated charging. The V2G control mode increases the flexibility of VPPs, and enables them to use a certain amount of energy stored in the EVs in peak periods, instead of using more expensive generators to supply the load. With these new control modes it is possible to control the charging and select the best periods to charge EVs - the cheapest periods. The extra energy stored in the batteries can be used in peak periods to supply the electric network. It is possible to conclude that the V2G is the best control mode to minimize the VPP operation cost. As mentioned before, some automobile manufacturers are currently presenting EV models to commercialize soon. With the developments in charging modes (see sub-section 2.6.2) it is possible to control the charging of electric vehicles. In the future, V2G capability will most probably be incorporated in electric vehicles.

The proposed SA methodology presented good performance using the three control modes; the results are presented in section 4.4 for three scenarios, namely considering 1000, 2000 and 3000 EVs. The SA methodology presented a low execution time when compared with the deterministic technique. The SA obtained similar results to the ones achieved by the deterministic technique in terms of operation cost. The deterministic technique required clustering EVs in groups that contained 10 vehicles, therefore three scenarios were solved, with 100, 200 and 300 EV clusters. In section 4.3 it has been proved that the EV cluster approach implies some degradation in the operation cost, but it has been necessary to accelerate the execution time of the deterministic technique. When using the SA methodology it was not needed to use such approach, resulting in a more suitable methodology to be used.

Another contribution of the developed work is supported by the case study presented in section 4.5. The energy resource management for several simulation horizons was

solved, namely 24, 30, 36, 42 and 48 hours. This approach considers the influence of vehicle trips of successive days. The influence of successive days presents an impact in the operation cost. When a smaller simulation horizon is considered, e.g. 24 or 30 hours the operation cost increases because the VPP does not gather enough information about the requirements for the next day. The proposed methodology proved its effectiveness in considering the influence of the successive days scheduling, mainly in cases of a transition from a Friday to Saturday or from Sunday to Monday. This results in a decrease of the operation cost when full information about the following day is considered.

Concluding, the proposed methodology, and its inclusion in the ERMaS tool has proven to be successful, as supported by the achieved results and enhanced by the scientific publications it has originated. It is as well a baseline for many equally relevant future developments in the energy resource management field. The ERMaS tool enhanced by the developed work in the scope of this thesis, is not only an adequate supporting system to determine ERM in operation context of power systems, but it also incorporates some approaches to evaluate the impact of EVs in power systems, such as the influence of several EV penetration levels, the implementation of different EV control strategies, and the influence of successive days in energy resource management.

5.2. Future Work Suggestions

Considering the purpose of ERMaS, it is possible to include a more detailed model regarding the energy resource management of a VPP. In the case of ERMaS, the objective is to obtain the optimal scheduling of available DERs for the VPP, typically for the next day. However, the scheduling for the next day is not enough to improve the management of the VPP for the following day. It is possible to include further features in the ERMaS tool in order to improve the response of a VPP for the following day. The architecture of the decision support system that incorporates the proposed ERMaS tool, while aiming at improving the decision making of the VPP is presented in Figure 5.1. The objective is to incorporate further capabilities regarding the electric network management in the scheduling problem, such as ancillary services and dynamic network simulation.

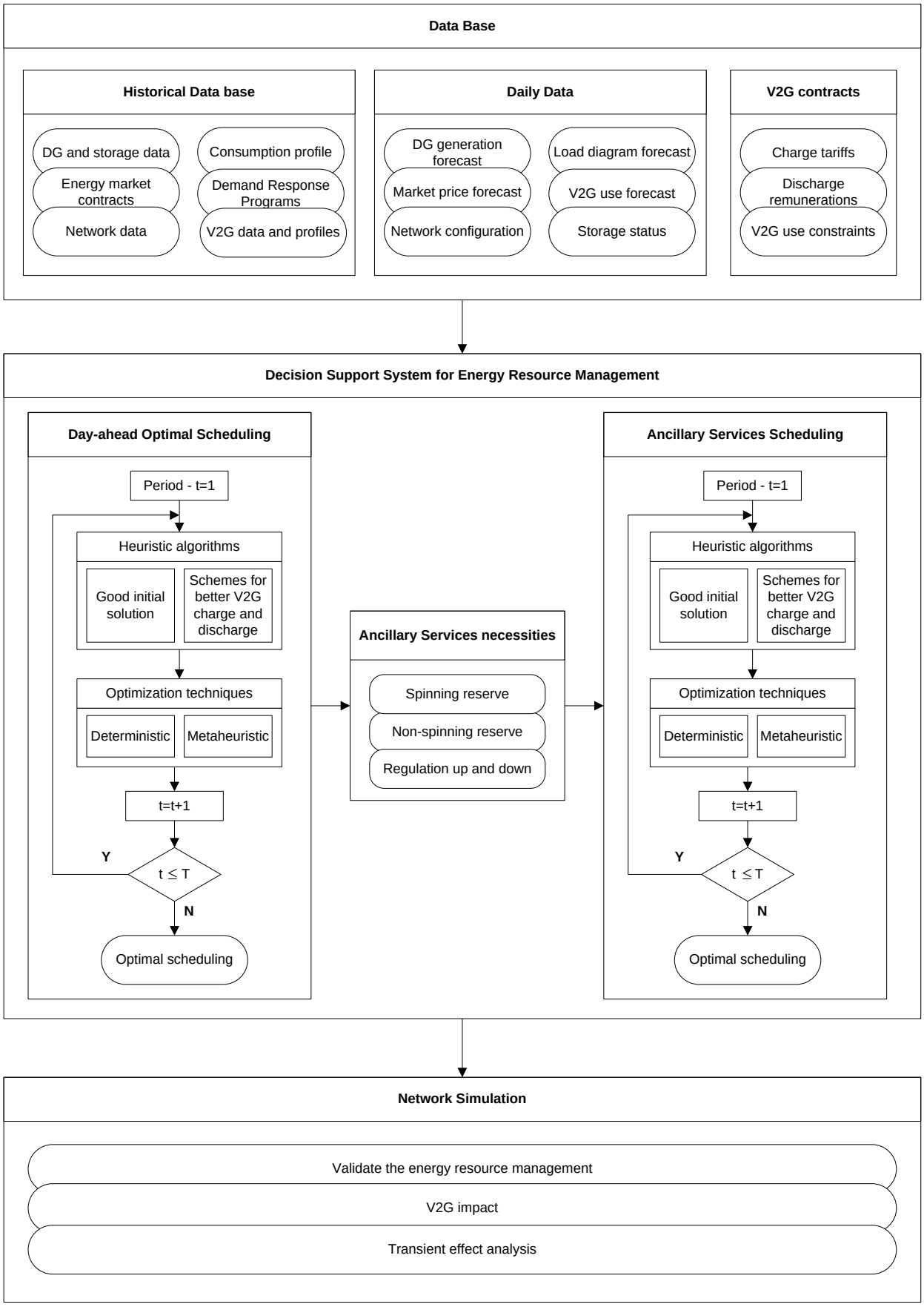

Figure 5.1 – Architecture of the proposed decision support system.

The proposed decision support system has the objective of creating a system able to effectively help in the decision making process of a VPP in what concerns the DER management, considering other characteristics than the energy resource management problem.

The decision support system for the energy resource management is divided in 3 phases (see Decision Support System for Energy Resource Management block in Figure 5.1). The first phase is represented by the ERMaS tool, developed in the scope of this thesis, and it is illustrated in Figure 5.1 as the "Day-ahead Optimal Scheduling" block, located the left of the figure.

After the day-ahead optimal scheduling is finished, using a deterministic or metaheuristic technique to find a satisfactory solution with low execution time, it is necessary to determine the requirements that the VPP needs to ensure the network stability and security (see Ancillary Services necessities block in Figure 5.1), such as spinning reserve, non-spinning reserve and regulation up/down.

The final phase is to solve the ancillary services scheduling for the current day, considering the necessities identified in the previous phase (see Ancillary Services Scheduling block in Figure 5.1).

Using these three blocks it is possible to have a more detailed model about the energy resource management problem. After the results of the decision support system, it will be used the "Network Simulation" block to validate the results and evaluate the transient effect in the electric network.

During the development of this work, several issues that could be solved in the field of the ERMaS tool have been identified. Although the proposed ERMaS tool responds to a lack of the management in smart grid regarding an intensive use of electric vehicles it is possible to consider the following topics to improve the developed work:

- To incorporate even stricter technical and business models of electric vehicles, namely considering a more accurate model in what concerns the charging and discharge rates. In the literature it is pointed out that the charge rate depends on the level of energy stored in the battery (state of charge), the charge rate cannot be constant in all periods, due to the state of charge. It is verified that the efficiency can also depend on the state of charge of the battery. The degradation of batteries should be considered in the ERM problem, through the objective function and constraints of the proposed mathematical formulation. Including a cost that is dependent on the level of degradation of the battery, i.e. if the battery is used several times to charge or discharge, represents an increasing cost and influences negatively the objective function value, because a minimization of the cost is assumed;

- To include a proposal of charge and discharge contracts between electric vehicles and VPPs; this will improve the ERMaS tool because it is predicted that EV users will establish contracts with VPPs, guaranteeing certain amounts of remuneration from charge and discharge processes. The objective is to establish clauses in the contract to use the battery to charge and discharge. For instance, the establishment of a contract that indicates the minimum required energy for a certain period, minimum power to charge, the minimum number of periods that an electric vehicle will be connected to the network to discharge, a minimum profit that EV user is expecting, and the periods in which the EV user is available to charge or discharge. In this field there are several topics that could be considered to establish a contract between electric vehicles and virtual power players;
- To include the greenhouse gas emissions as a component in the ERM problem, considering an topic for these emissions in the objective function and several constraints regarding the greenhouse gas emissions;
- Applications of electric vehicles to ancillary services, as energy resource for spinning reserve or to control the voltage and frequency;
- To use the Power System Computer Aided Design (PSCAD) simulation tool to technically validate the results from the ERMaS tool and other models;
- To study the impact of EVs in the network considering different objectives to manage electric vehicles, such as the maximization of low factor of a load diagram or maximization of the users profits and the evaluation of the impact of EVs management in locational marginal pricing. Finally, the use of the PSCAD simulation tool for the results technical validation;
- To improve the ERMaS tool and develop the required tools to be included in the decision support system architecture that has been presented in Figure 5.1;
- To use the discharge of electric vehicles as reactive energy in order to support some ancillary services;
- To improve the two proposed methodologies in order to be adapted to several scenarios and respond with a reasonable execution time. Including heuristic approaches to reduce the execution time. It could be applied to determine a good initial solution or generate neighbor solution in a metaheuristic technique. In the case studies several scenarios considering a large amount of EVs are presented. If the energy resource management is solved without considering the network constraints, the determinist technique can take just a few seconds to solve the optimal scheduling. This simplification decreases dramatically the execution time. Considering this simplification could be a

good initial solution for the deterministic and SA techniques. Using this strategy, the execution time could be reduced;

- To use other metaheuristic techniques or hybrid techniques to solve the same energy resource management problem;
- To explore other types of deterministic techniques that could solve the energy resource management problem in less execution time;
- To use data mining techniques to cluster electric vehicles in several clusters, depending on the location of EVs, the similarity of the trip profile and similarity in battery characteristics;
- To use data mining techniques to predict the trip profile after a historical data about travels.

The continuous development of this work is a relevant part of the core of some recently approved FCT projects, which come to give continuity to the projects already mentioned in the introductory chapter; namely the following:

- IMaDER – Intelligent Short Term Management of Distributed Energy Resources in a Multi-Player Competitive Environment (PTDC/SEN-ENR/122174/2010).

It is important to refer that the mentioned future work will continue in the PhD thesis that will be supported by a scholarship (reference SFRH/BD/81848/2011) in the scope of the "*Doutoramento e Pós-Doutoramento 2011*" (Phd and post-doctoral 2011) program of FCT "*Fundação para a Ciência e a Tecnologia*". This scholarship proves the interest on the energy resource management theme, considering an intensive use of electric vehicles, and it should continue the improvements of the ERMaS too in order to obtain as main objective the decision support system presented in Figure 5.1.

References

References

[1] Z. Vale, H. Morais, M. Silva, *et al.*, "Towards a future SCADA", *IEEE Power & Energy Society General Meeting,* vol. 1-8, pp. 1894-1900, 2009.

[2] Directive 2009/28/EC, "On the promotion of the use of energy from renewable sources and amending and subsequently repealing Directives 2001/77/EC and 2003/30/EC", European Parliament and Council, 2009.

[3] European Comission, "Analysis of options to move beyond 20% greenhouse gas emission reductions and assessing the risk of carbon leakage", 2010.

[4] R. Castro, "*Uma introdução às energias renováveis: Eólica, fotovoltaica e mini-hídrica*", IST Press, 2011.

[5] U. S. Department of Energy, "Smart grid system report", 2009.

[6] European Comission, "European smart grids technology platform - Vision and strategy for Europe's electricity networks of the future", 2006.

[7] IEEE, "*IEEE & Smart Grid*", Consulted: September 2011, Available: http://smartgrid.ieee.org/about-smartgrid/ieee-and-smartgrid.

[8] P. Hove, "EU research programmes: Future prospects through the SET plan and FP7", *3rd International Conference on Integration of Renewable and Distributed Energy Resources*, Nice, France, 2008.

[9] National Institute of Standards and Technology, "NIST framework and roadmap for smart grid interoperability standards release 1.0 (draft)", U.S. Department of Commerce, 2009.

[10] European Comission, "Expert group 3: Roles and responsibilities of actors involved in the smart grids deployment", 2011.

[11] Z. Vale, H. Morais, P. Faria, *et al.*, "Distributed energy resources management with cyber-physical SCADA in the context of future smart grids", *Melecon 2010 - 2010 15th IEEE Mediterranean Electrotechnical Conference,* pp. 431-436, 2010.

[12] OECD and IEA, "*The urban electric vehicle: policy options, technology trends, and market prospects*", Organisation for Economic Co-Operation and Development, International Energy Agency, Swedish National Board for Industrial and Technical Development, 1992.

[13] C. Chan, "The state of the art of electric, hybrid, and fuel cell vehicles", *Proceedings of the IEEE,* vol. 95, pp. 704-718, 2007.

[14] H. Morais, P. Kádár, P. Faria, *et al.*, "Optimal scheduling of a renewable micro-grid in an isolated load area using mixed-integer linear programming", *Renewable Energy,* vol. 35, pp. 151-156, 2010.

[15] H. Morais, "Gestão de recursos energéticos nas SmartGrids", Master degree thesis, Polytechnic of Porto, Portugal, 2010.

[16] E. Lightner and S. Widergren, "An orderly transition to a transformed electricity system", *IEEE Transactions on Smart Grid,* vol. 1, pp. 3-10, 2010.

[17] European Comission, "European smart grids technology platform - Vision and strategy for Europe's electricity networks of the future", 2010.

[18] H. Morais, M. Cardoso, H. Khodr, *et al.*, "Virtual power producers market strategies", *5th International Conference on European Electricity Market* pp. 1-6, 2008.

[19] H. Ren, W. Zhou, K. Nakagami, *et al.*, "Multi-objective optimization for the operation of distributed energy systems considering economic and environmental aspects", *Applied Energy,* vol. 87, pp. 3642-3651, 2010.

[20] Z. Vale, H. Morais, H. Khodr, *et al.*, "Technical and economic resources management in smart grids using heuristic optimization methods", *IEEE Power and Energy Society General Meeting*, pp. 1-7, 2010.

[21] W. Kempton and J. Tomic, "Vehicle-to-grid power fundamentals: Calculating capacity and net revenue", *Journal of Power Sources,* vol. 144, pp. 268-279, 2005.

[22] J. Soares, T. Sousa, H. Morais*, et al.*, "An optimal scheduling problem in distribution networks considering V2G", *2011 IEEE Symposium on Computational Intelligence Applications In Smart Grid (CIASG)*, pp. 1-8, 2011.

[23] T. Sousa, H. Morais, Z. Vale*, et al.*, "Intelligent energy resource management considering vehicle-to-grid: A simulated annealing approach", *Accepted for Publication on IEEE Transaction on Smart Grid, Special Issue on Transportation Electrification and Vehicle-to-Grid Applications,* 2011.

[24] Nissan, "*Nissan Leaf - 100% electric, zeros gas, zero tailpipe*", Consulted: August 2011, Available: http://www.nissanusa.com/leaf-electric-car/index#/leaf-electric-car/index.

[25] Toyota, "*Prius plug-in*", Consulted: August 2011, Available: http://www.toyota.com/prius-plug-in/.

[26] European Union, "Regulation (EC) no 715/2007 of the european parliament and of the council of 20 June 2007", European Parliament ed, 2007.

[27] A. Bandivadekar, "*Evaluating the impact of advanced vehicle and fuel technologies in U.S. light duty vehicle fleet*", Massachusetts Institute of Technology, Engineering Systems Division, Technology, Management, and Policy Program, 2008.

[28] BERR&DfT, "Investigation into the scope for the transport sector to switch to electric vehicles and plug-in hybrid vehicles", Department for Business Enterprise and Regulatory Reform: Department for Transport, 2008.

[29] IEA, "Technology roadmap: Electric and plug-in hybrid electric vehicles", International Energy Agency, 2011.

[30] A. Bose, "Smart Transmission Grid Applications and Their Supporting Infrastructure", *IEEE Transactions on Smart Grid,* vol. 1, pp. 11-19, 2010.

[31] N. Hatziargyriou, A. Dimeas, and A. Tsikalakis, "Centralized and decentralized control of microgrids", *International Journal of Distributed Energy Resources, Technology & Science Publishers,* vol. 1, pp. 197-212, 2005.

[32] IEA, "Technology roadmap smart grids", International Energy Agency, 2011.

[33] European Comission, "European smart grids technology platform - strategic deployment document for Europe's electricity networks of the future", 2010.

[34] P. Oliveira, T. Pinto, H. Morais*, et al.*, "MASCEM - An electricity market simulator providing coalition support for virtual power players", *15th International Conference on Intelligent System Applications to Power Systems, ISAP*, pp. 1-6, 2009.

[35] LE Law & Your Environment, "*Laws on the climate change*", Consulted, Available: http://www.environmentlaw.org.uk/rte.asp?id=54.

[36] T. Ackermann, G. Andersson, and L. Soder, "Distributed generation: A definition", *Electric Power Systems Research,* vol. 57, pp. 195-204, 2001.

[37] D. Kirschen, "Demand-side view of electricity markets", *IEEE Transactions on Power Systems,* vol. 18, pp. 520-527, 2003.

[38] U. S. Department of Energy, "Benefits of demand response in electricity markets and recommendations for achieving them", 2006.

[39] P. Faria and Z. Vale, "Demand response in electrical energy supply: An optimal real time pricing approach", *Energy,* vol. 36, pp. 5374-5384, 2011.

[40] Z. Vale, T. Pinto, H. Morais*, et al.*, "VPP's multi-level negotiation in smart grids and competitive electricity markets", *IEEE Power and Energy Society General Meeting*, pp. 1-8, 2011.

[41] S. Awerbuch and A. Preston, "*The virtual utility: Accounting, technology & competitive aspects of the emerging industry*", Kluwer Academic Publisher, 1997.

[42] K. Dielmann and A. van der Velden, "Virtual power plants (VPP) - A new perspective for energy generation?", *Modern Techniques and Technologies, 2003. MTT 2003. Proceedings of the 9th*

International Scientific and Practical Conference of Students, Post-graduates and Young Scientists, pp. 18-20, 2003.

[43] H. Morais, M. Cardoso, L. Castanheira*, et al.*, "A decision-support simulation tool for virtual power producers", *International Conference on Future Power Systems (FPS),* pp. 529-534, 2005.

[44] H. Morais, S. Ramos, Z. Vale*, et al.*, "MV producers and consumers agents characterization with DSM techniques", *IEEE Bucharest Powertech,* vol. 1-5, pp. 1395-1402, 2009.

[45] W. Kempton and J. Tomic, "Vehicle-to-grid power implementation: From stabilizing the grid to supporting large-scale renewable energy", *Journal of Power Sources,* vol. 144, pp. 280-294, 2005.

[46] A. Y. Saber and G. K. Venayagamoorthy, "Efficient utilization of renewable energy sources by gridable vehicles in cyber-physical energy systems", *IEEE Systems Journal,* vol. 4, pp. 285-294, 2010.

[47] P. Bates, J. Hermessen, L. Hommel*, et al.*, "Electrically driven vehicles", *Transactions of the American Institute of Electrical Engineers,* vol. XIV, 1897.

[48] M. Ehsani, Y. Gao, and A. Emadi, "*Modern electric, hybrid electric, and fuel cell vehicles: Fundamentals, theory, and design*", CRC Press, 2009.

[49] A. Khaligh and H. Li, "Battery, ultracapacitor, fuel cell, and hybrid energy storage systems for electric, hybrid electric, fuel cell, and plug-In hybrid electric vehicles: State of the art", *IEEE Transactions on Vehicular Technology,* vol. 59, pp. 2806-2814, 2010.

[50] W. Kempton and S. Letendre, "Electric vehicles as a new power source for electric utilities", *Transportation Research Part D-Transport and Environment,* vol. 2, pp. 157-175, 1997.

[51] Paul tan's automotive news, "*Mitsubishi i MIEV research electric vehicle*", Consulted: August 2011, Available: http://paultan.org/2006/10/13/mitsubishi-i-miev-research-electric-vehicle/.

[52] K. Chau and Y. Wong, "Overview of power management in hybrid electric vehicles", *Energy Conversion and Management,* vol. 43, pp. 1953-1968, 2002.

[53] K. Bayindir, M. Gözüküçük, and A. Teke, "A comprehensive overview of hybrid electric vehicle: Powertrain configurations, powertrain control techniques and electronic control units", *Energy Conversion and Management,* vol. 52, pp. 1305-1313, 2011.

[54] A. Srivastava, B. Annabathina, and S. Kamalasadan, "The challenges and policy options for integrating plug-in hybrid electric vehicle into the electric grid", *The Electricity Journal,* vol. 23, pp. 83-91, 2010.

[55] A. Veziroglu and R. Macario, "Fuel cell vehicles: State of the art with economic and environmental concerns", *International Journal of Hydrogen Energy,* vol. 36, pp. 25-43, 2011.

[56] H. Happ, "Optimal power dispatch - A comprehensive survey", *IEEE Transactions on Power Apparatus and Systems,* vol. 96, pp. 841-854, 1977.

[57] A. Mahor, V. Prasad, and S. Rangnekar, "Economic dispatch using particle swarm optimization: A review", *Renewable & Sustainable Energy Reviews,* vol. 13, pp. 2134-2141, 2009.

[58] P. Denholm and W. Short, "An evaluation of utility system impacts and benefits of optimally dispatched plug-in hybrid electric vehicles", National Renewable Energy Laboratory, 2006.

[59] K. Jansen, T. Brown, and G. Samuelsen, "Emissions impacts of plug-in hybrid electric vehicle deployment on the US western grid", *Journal of Power Sources,* vol. 195, pp. 5409-5416, 2010.

[60] A. Y. Saber and G. K. Venayagamoorthy, "Plug-in vehicles and renewable energy sources for cost and emission reductions", *IEEE Transactions on Industrial Electronics,* vol. 58, pp. 1229-1238, 2011.

[61] R. Green, L. Wang, and M. Alam, "The impact of plug-in hybrid electric vehicles on distribution networks: A review and outlook", *Renewable & Sustainable Energy Reviews,* vol. 15, pp. 544-553, 2011.

[62] A. Ford, "Electric Vehicles and the Electric Utility Company", *Energy Policy,* vol. 22, pp. 555-570, 1994.

[63] F. Andrew, "The impacts of large scale use of electric vehicles in southern California", *Energy and Buildings,* vol. 22, pp. 207-218, 1995.

[64] T. Ikeya, M. Iwasaki, S. Takagi*, et al.*, "Collaborative investigation on charging electic-vehicle battery systems for night-time load levelling by Japanese electric power companies", *Journal of Power Sources,* vol. 69, pp. 103-111, 1997.

[65] K. Clement-Nyns, E. Haesen, and J. Driesen, "The Impact of Charging Plug-In Hybrid Electric Vehicles on a Residential Distribution Grid", *IEEE Transactions on Power Systems,* vol. 25, pp. 371-380, 2010.

[66] K. Clement-Nyns, E. Haesen, and J. Driesen, "The impact of vehicle-to-grid on the distribution grid", *Electric Power Systems Research,* vol. 81, pp. 185-192, 2011.

[67] N. Hartmann and E. Ozdemir, "Impact of different utilization scenarios of electric vehicles on the German grid in 2030", *Journal of Power Sources,* vol. 196, pp. 2311-2318, 2011.

[68] E. Sortomme, M. Hindi, S. MacPherson*, et al.*, "Coordinated charging of plug-in hybrid electric vehicles to minimize distribution system losses", *IEEE Transactions on Smart Grid,* vol. 2, pp. 198-205, 2011.

[69] E. Sortomme and M. El-Sharkawi, "Optimal charging strategies for unidirectional vehicle-to-grid", *IEEE Transactions on Smart Grid,* vol. 2, pp. 131-138, 2011.

[70] J. Rand, R. Woods, and R. Dell, "*Batteries for electric vehicles*", Research Studies Press, 1998.

[71] A. Burke, "Batteries and ultracapacitors for electric, hybrid, and fuel cell vehicles", *Proceedings of the IEEE,* vol. 95, pp. 806-820, 2007.

[72] B. Sovacool and R. Hirsh, "Beyond batteries: An examination of the benefits and barriers to plug-in hybrid electric vehicles (PHEVs) and a vehicle-to-grid (V2G) transition", *Energy Policy,* vol. 37, pp. 1095-1103, 2009.

[73] B. Scrosati and J. Garche, "Lithium batteries: Status, prospects and future", *Journal of Power Sources,* vol. 195, pp. 2419-2430, 2010.

[74] A. Dinger, R. Martin, M. Xavier*, et al.*, "Batteries for electric cars: Challenges, Opportunities, and the Outlook to 2020", The Boston Consulting Group, 2010.

[75] F. Zhan, L. Jiang, B. Wu*, et al.*, "Characteristics of Ni/MH power batteries and its application to electric vehicles", *Journal of Alloys and Compounds,* vol. 293, pp. 804-808, 1999.

[76] C. Van Bael, "Electric vehicles market study and simulations", Master of Science, Departement Industriële en Biowetenschappen, Högskolan i Halmstad University, Halmstad, Sweden, 2011.

[77] C. H. Dustmann, "Advances in ZEBRA batteries", *Journal of Power Sources,* vol. 127, pp. 85-92, 2004.

[78] Th!nk, "*Th!nk - Batteries*", Consulted: September 2011, Available: http://www.thinkev.com/The-THINK-City/Charging/Batteries.

[79] N. Omar, J. Van Mierlo, B. Verbrugge*, et al.*, "Power and life enhancement of battery-electrical double layer capacitor for hybrid electric and charge-depleting plug-in vehicle applications", *Electrochimica Acta,* vol. 55, pp. 7524-7531, 2010.

[80] R. Dougal, S. Liu, and R. White, "Power and life extension of battery-ultracapacitor hybrids", *IEEE Transactions on Components and Packaging Technologies,* vol. 25, pp. 120-131, 2002.

[81] A. Baisden and A. Emadi, "ADVISOR-based model of a battery and an ultra-capacitor energy source for hybrid electric vehicles", *IEEE Transactions on Vehicular Technology,* vol. 53, pp. 199-205, 2004.

[82] F. Gagliardi and M. Pagano, "Experimental results of on-board battery-ultracapacitor system for electric vehicle applications", *Proceedings of the IEEE International Symposium on Industrial Electronics, ISIE*, pp. 93-98 vol.1, 2002.

[83] L. Rosario, "Power and energy management of multiple energy storage systems in electric vehicles", Department of Aerospace Power & Sensors, Cranfield University, United Kingdom, 2007.

[84] K. Cheng, B. Divakar, H. Wu*, et al.*, "Battery-management system (BMS) and SOC development for electrical vehicles", *IEEE Transactions on Vehicular Technology,* vol. 60, pp. 76-88, 2011.

[85] S. Venkat and N. John, "Design and optimization of a natural graphite/iron phosphate lithium-ion cell", *Journal of The Electrochemical Society,* vol. 151, pp. A1530-A1538, 2004.

[86] M. Kromer and J. Heywood, "*Electric powertrains: Opportunities and challenges in the US light-duty vehicle fleet*", Massachusetts Institute of Technology, Engineering Systems Division, Technology and Policy Program, 2007.

[87] A. Kraytsberg and Y. Ein-Eli, "Review on Li–air batteries - Opportunities, limitations and perspective", *Journal of Power Sources,* vol. 196, pp. 886-893, 2011.

[88] J. Fergus, "Recent developments in cathode materials for lithium ion batteries", *Journal of Power Sources,* vol. 195, pp. 939-954, 2010.

[89] J. Lehtinen, "Electric vehicle charging systems in the Helsinki region", Master of Science, Department of electrical engineering, Aalto University, 2010.

[90] P. Van den Bossche, "The electric vehicle: raising the standards", Doctor of Philosophy, Vrije Universiteit Brussel, 2003.

[91] P. Van den Bossche, F. Van Mulders, J. Van Mierlo*, et al.*, "The evolving standardization landscape for electrically propelled vehicles", *The World Electric Vehicle Journal,* vol. 2, pp. 41-48, 2008.

[92] International Electrotechnical Comission, "Electric vehicle conductive charging system – Part 21: Electric vehicle requirements for conductive connection to an a.c./d.c. supply", 2001.

[93] International Electrotechnical Comission, "Electric vehicle conductive charging system – Part 22: AC electric vehicle charging station", 2001.

[94] P. Van den Bossche, J. Van Mierlo, C. Yonghua*, et al.*, "Evolution of international standardization of electrically propelled vehicles", *European Ele-Drive*, Bruxelles, Belgium, 2007.

[95] EMSD, "Technical guidelines on charging facilities for electric vehicles", Electrical and Mechanical Services Department, Hong Kong.

[96] J. Francfort, "Electric vehicle charging levels and requirements overview", Idaho National Laboratory, 2010.

[97] Society of Automotive Engineers, "Electric vehicle and plug in hybrid electric vehicle conductive charge coupler", First published 1996, revised 2009.

[98] C. Botsford and A. Szczepanek, "Fast charging vs. slow charging: Pros and cons for the new age of electric vehicles", *EVS 24 International Battery, Hybrid and Fuel Cell Electric Vehicle Symposium*, Stavanger, Norway, 2009.

[99] DAIMLER, "Standards activities in Europe", *Business of Plugging-In Conference*, 2010.

[100] International Electrotechnical Comission, "Plugs, socket-outlets, vehicle couplers and vehicule inlets – Conductive charging of electric vehicles – Part 1: Charging of electric vehicles up to 250 A a.c. and 400 A d.c.", 2003.

[101] International Electrotechnical Comission, "Plugs, socket-outlets and couplers for industrial purposes", 2005.

[102] R. Oestreicher, W. Preuschoff, and R. Bogenberger, "E-mobility infrastructure standardization 2009 ZEV technology symposium Sacramento, CA", 2009.

[103] EFACEC, "*Challenges and opportunities for the electric vehicle society*", Consulted: September 2011, *150th Anniversary of the Treaty of Amity and Commerce Portugal - Japan*, Available: http://www.portugalglobal.pt/PT/geral/Paginas/PortugalJapan150yearsElectricalVehicleSeminar.aspx.

[104] Better place, "*Battery switch stations*", Consulted: September 2011, Available: http://www.betterplace.com/the-solution-switch-stations.

[105] A. Saber and G. Venayagamoorthy, "Intelligent unit commitment with vehicle-to-grid: A cost-emission optimization", *Journal of Power Sources,* vol. 195, pp. 898-911, 2010.

[106] M. Tawarmalani and N. Sahinidis, "*Convexification and global optimization in continuous and mixed-integer nonlinear programming: Theory, algorithms, software, and applications*", Kluwer Academic Publishers, 2002.

[107] K. Lee and M. El-Sharkawi, "*Modern heuristic optimization techniques: Theory and applications to power systems*", IEEE Press, 2008.

[108] S. Boyd and L. Vandenberghe, "*Convex optimization*", Cambridge University Press, 2004.

[109] Z. Vale, "Intelligent power system", *Wiley Encyclopedia of Computer Science and Engineering*, ed: John Wiley & Sons, Inc., 2009.

[110] Z. Vale, "Knowledge-based systems techniques and applications in power systems control centers", *Intelligent Systems Technologies and Applications*. vol. 6, Cornelius T. Leondes, Ed., ed: CRC Press, 2002.

[111] F. Glover and G. Kochenberger, "*Handbook of metaheuristics*", Kluwer Academic Publishers, 2003.

[112] MathWorks, "*MATLAB - The language of technical computing*", Consulted: October 2011, Available: http://www.mathworks.com/products/matlab/.

[113] GAMS, "*GAMS home page*", Consulted: October 2011, Available: http://www.gams.com/.

[114] J. Grainger and W. Stevenson, "*Power system analysis*", McGraw-Hill, 1994.

[115] P. Venkatesh, R. Gnanadass, and N. Padhy, "Comparison and application of evolutionary programming techniques to combined economic emission dispatch with line flow constraints", *IEEE Transactions on Power Systems,* vol. 18, pp. 688-697, 2003.

[116] M. Shahidehpour, H. Yamin, and Z. Li, "*Market operations in electric power systems: forecasting, scheduling, and risk management*", Institute of Electrical and Electronics Engineers, Wiley-Interscience, 2002.

[117] X. Yang, "*Introduction to mathematical optimization: From linear programming to metaheuristics*", Cambridge International Science Publishing, 2008.

[118] I. Grossmann, J. Viswanathan, A. Vecchietti*, et al.*, "GAMS/DICOPT user's notes", Washington. DC, 2001.

[119] A. Drud, "GAMS/CONOPT user's notes", Washington. DC, 2001.

[120] GAMS Development Corporation, "GAMS/CPLEX 12 user's notes", Washington. DC, 2007.

[121] S. Kirkpatrick, C. Gelatt, and M. Vecchi, "Optimization by simulated annealing", *Science,* vol. 220, pp. 671-680, 1983.

[122] P. Laarhoven and E. Aarts, "*Simulated annealing: Theory and applications*", Dordrecht, Lancaster, Reidel, 1987.

[123] N. Metropolis, A. Rosenbluth, M. Rosenbluth*, et al.*, "Equation of state calculations by fast computing machines", *The Journal of Chemical Physics,* vol. 21, pp. 1087-1092, 1953.

[124] M. Fleischer, "Simulated annealing: Past, present, and future", *Winter Simulation Conference Proceedings,* pp. 155-161, 1995.

[125] G. Zäpfel, R. Braune, and M. Bögl, "*Metaheuristic search concepts: A tutorial with applications to production and logistics*", Berlin, Springer, 2010.

[126] R. Tavares, T. Martins, and M. Tsuzuki, "Simulated annealing with adaptive neighborhood: A case study in off-line robot path planning", *Expert Systems with Applications,* vol. 38, pp. 2951-2965, 2011.

[127] E. Aarts and J. Korst, "*Simulated annealing and Boltzmann machines: A stochastic approach to combinatorial optimization and neural computing*", Wiley, 1989.

[128] E. Bonabeau, M. Dorigo, and G. Theraulaz, "*Swarm intelligence: from natural to artificial systems*", New York, Oxford, Oxford University Press, 1999.

[129] B. Hajek, "Cooling schedules for optimal annealing", *Math. Oper. Res.,* vol. 13, pp. 311-329, 1988.

[130] Y. Nourani and B. Andresen, "A comparison of simulated annealing cooling strategies", *Journal of Physics A: Mathematical and General,* pp. 8373-8385, 1998.

[131] M. Keikha, "Improved simulated annealing using momentum terms", *2nd International Conference on Intelligent Systems, Modelling and Simulation*, 2011.

[132] T. Sousa, J. Soares, Z. Vale*, et al.*, "Simulated annealing metaheuristic to solve the optimal power flow", *IEEE Power and Energy Society General Meeting*, pp. 1-8, 2011.

[133] U. Eminoglu and M. Hocaoglu, "Distribution systems forward/backward sweep-based power flow algorithms: A review and comparison study", *Electric Power Components and Systems,* vol. 37, pp. 91-110, 2009.

[134] U. Eminoglu, T. Gozel, and M. Hocaoglu, "DSPFAP: Distribution Systems Power Flow Analysis Package Using Matlab Graphical User Interface (GUI)", *Computer Applications in Engineering Education,* vol. 18, pp. 1-13, 2010.

[135] D. Shirmohammadi, H. Hong, A. Semlyen*, et al.*, "A compensation-based power flow method for weakly meshed distribution and transmission networks", *IEEE Transactions on Power Systems,* vol. 3, pp. 753-762, 1988.

[136] D. Thukaram, H. M. W. Banda, and J. Jerome, "A robust three phase power flow algorithm for radial distribution systems", *Electric Power Systems Research,* vol. 50, pp. 227-236, 1999.

[137] C. Cheng and D. Shirmohammadi, "A three-phase power flow method for real-time distribution system analysis", *IEEE Transactions on Power Systems,* vol. 10, pp. 671-679, 1995.

[138] D. Rajicic, R. Ackovski, and R. Taleski, "Voltage correction power flow", *IEEE Transactions on Power Delivery,* vol. 9, pp. 1056-1062, 1994.

[139] A. Augugliaro, L. Dusonchet, S. Favuzza*, et al.*, "A new backward/forward method for solving radial distribution networks with PV nodes", *Electric Power Systems Research,* vol. 78, pp. 330-336, 2008.

[140] Y. Zhu and K. Tomsovic, "Adaptive power flow method for distribution systems with dispersed generation", *IEEE Transactions on Power Delivery,* vol. 17, pp. 822-827, 2002.

[141] S. Khushalani, J. Solanki, and N. Schulz, "Development of three-phase unbalanced power flow using PV and PQ models for distributed generation and study of the impact of DG models", *IEEE Transactions on Power Systems,* vol. 22, pp. 1019-1025, 2007.

[142] P. Faria, Z. Vale, and J. Ferreira, "DemSi - A demand response simulator in the context of intensive use of distributed generation", *IEEE International Conference on Systems Man and Cybernetics (SMC) 2010*, pp. 2025-2032, 2010.

[143] M. Baran and F. Wu, "Network reconfiguration in distribution systems for loss reduction and load balancing", *IEEE Transactions on Power Delivery,* vol. 4, pp. 1401-1407, 1989.

[144] P. Faria, "Demand response in future power systems management – A conceptual framework and simulation tool", Master degree thesis, Polytechnic of Porto, Portugal, 2011.

[145] Mitsubishi, "*Mitsubishi i-MiEV Technical Specifications*", Consulted: January 2011, Available: http://www.mitsubishi-motors.com/special/ev/whatis/index.html.

[146] Citroen, "*Citroen C-Zero Technical Specifications*", Consulted: January 2011, Available: http://www.c-zero.citroen.com/#/ie/my-life-in-c-zero.

[147] Renault, "*Renault Fluence Z.E.*", Consulted: January 2011, Available: http://www.renault-ze.com/z.e.-range/fluence-z.e./presentation-1935.html.

[148] Nissan, "*Nissan Leaf Technical Specifications*", Consulted: January 2011, Available: http://www.nissan.co.uk/vehicles/electricvehicles/leaf.htm#vehicles/electricvehicles/leaf/leaf-engine/specifications.

[149] Renault, "*Renault Kangoo Z.E. Technical Specification*", Consulted: January 2011, Available: http://www.renault.com/en/vehicules/renault/pages/kangoo-express-ze.aspx.

[150] Renault, "*Renault ZOE Z.E. Technical Specification*", Consulted: January 2011, Available: http://www.renault.com/en/innovation/l-univers-du-design/pages/show-car-zoe-preview.aspx.

[151] Peugeot, "*Peugeot iOn Technical Specification*", Consulted: January 2011, Available: http://www.peugeot.com/en/products/concepts-cars-and-future-models/ion.aspx.

[152] U. S. Department of Transportation, "Summary of travel trends: 2009 national household travel survey", 2011.

[153] J. Soares, "Modified PSO for day-ahead distributed energy resources scheduling including vehicle-to-grid", Master degree thesis, Polytechnic of Porto, Portugal, 2011.

Annexes

Annex A

Input Data for the Case Studies

Table A.1 shows the resistance, inductive reactance, capacitive susceptance and the thermal limit.

Branch number	Bus Out	Bus In	R (Ohm)	X_L (Ohm)	B_C (Siemens)	Thermal limit (MVA)
1	0	1	0.1332	0.0471	0	5.5
2	1	2	0.7122	0.2517	0	5.5
3	1	18	0.2699	0.0954	0	5.5
4	2	3	0.3890	0.1048	0	4.29
5	2	22	0.6039	0.2134	0	5.5
6	3	4	0.1911	0.0515	0	4.29
7	4	5	0.7262	0.1957	0	4.29
8	5	6	1.0514	0.2833	0	4.29
9	5	25	1.0656	0.2872	0	4.29
10	6	7	0.2007	0.0541	0	4.29
11	7	8	0.3822	0.1030	0	4.29
12	8	9	1.4984	0.4038	0	4.29
13	9	10	0.5528	0.1488	0	4.29
14	10	11	0.6033	0.1626	0	4.29
15	11	12	0.7618	0.2053	0	4.29
16	12	13	1.3157	0.3546	0	4.29
17	13	14	0.7472	0.2014	0	4.29
18	14	15	0.3280	0.0884	0	4.29
19	15	16	3.0084	0.8107	0	4.29
20	16	17	0.8190	0.2207	0	4.29
21	18	19	1.0241	0.3620	0	5.5
22	19	20	0.6518	0.2304	0	5.5
23	20	21	1.2973	0.4585	0	5.5
24	22	23	1.2944	0.4575	0	5.5
25	23	24	0.1497	0.0529	0	5.5
26	25	26	0.2901	0.0782	0	4.29
27	26	27	1.0810	0.2913	0	4.29
28	27	28	0.8209	0.2212	0	4.29
29	28	29	0.5180	0.1396	0	4.29
30	29	30	0.9946	0.2680	0	4.29
31	30	31	0.3169	0.0854	0	4.29
32	31	32	0.3481	0.0938	0	4.29

Table A.1 – Branch data of the 32 bus distribution network.

Table A.2 shows the information of all the DG technology used in the case studies.

DG technology	Number of units	Total installed power (kW)	Mean Daily operation hours (h)	Price Scheme (m.u./kWh)		
				Maximum	Mean	Minimum
Photovoltaic	32	1,320	6	0.254	0.1872	0.11
Wind	5	505	12	0.136	0.091	0.06
Small Hydro	2	80	24	0.145	0.117	0.089
Biomass	3	350	24	0.226	0.2007	0.186
WTE[11]	1	10	24	-	0.056	-
CHP[12]	15	725	24	0.105	0.0753	0.057
Fuel Cell	8	440	24	0.2	0.055	0.01
Total of DG	66	3,430				
Upstream connection	-	-	-	-	-	-
External suppliers	10	5,800	24	0.15	0.105	0.06
Total	76	9,230	-	-	-	-

Table A.2 – Distributed generation profile.

Table A.3 presents the demand in each bus in the hour 20, corresponding to the peak period of the load diagram.

Bus number	Active power (kW)	Reactive power (kVAr)	Bus number	Active power (kW)	Reactive power (kVAr)
1	88.51	26.55	**17**	110.00	33.00
2	79.66	23.90	**18**	120.00	36.00
3	106.20	31.86	**19**	79.66	23.90
4	53.12	15.94	**20**	120.00	36.00
5	53.10	15.94	**21**	120.00	36.00
6	177.00	53.10	**22**	79.66	23.90
7	177.00	53.10	**23**	450.00	135.00
8	53.17	15.93	**24**	500.00	150.00

[11] Waste to Energy
[12] Combined Heat and Power or Co-generation

Bus number	Active power (kW)	Reactive power (kVAr)	Bus number	Active power (kW)	Reactive power (kVAr)
9	70.00	21.00	**25**	100.00	30.00
10	80.00	24.00	**26**	53.11	15.93
11	90.00	27.00	**27**	60.00	18.00
12	70.00	21.00	**28**	200.00	60.00
13	170.00	51.00	**29**	250.00	75.00
14	70.00	21.00	**30**	132.77	39.83
15	70.00	21.00	**31**	300.00	90.00
16	70.00	21.00	**32**	100.00	30.00
-	--	-	**Total**	4,252.90	1,275.9

Table A.3 – Demand power for each bus.

Table A.4 shows the number of consumers for the 6 groups: Domestic (DM), Small Commerce (SC), Medium Commerce (MC), Large Commerce (LC), Medium Industrial (MI) and Large Industrial (LI).

Bus number	Number of consumers						
	DM	SC	MC	LC	MI	LI	Total
1	-	2	2	1	-	-	**5**
2	2	5	-	-	-	-	**7**
3	4	4	-	-	-	-	**8**
4	7	2	-	-	-	-	**9**
5	8	-	-	-	-	-	**8**
6	4	1	-	2	-	-	**7**
7	-	1	1	-	-	4	**6**
8	9	1	-	-	-	-	**10**
9	8	-	-	-	-	-	**8**
10	4	-	-	2	-	-	**6**
11	6	1	-	-	-	-	**7**
12	7	-	-	-	-	-	**7**
13	5	2	2	-	-	-	**9**
14	6	-	-	-	-	-	**6**
15	7	1	-	-	-	-	**8**
16	5	2	-	-	-	-	**7**
17	2	4	1	-	-	-	**7**

Bus number	Number of consumers						
	DM	SC	MC	LC	MI	LI	Total
18	-	-	2	2	-	-	**4**
19	3	-	3	1	-	-	**7**
20	-	4	4	-	-	-	**8**
21	-	2	2	1	-	-	**5**
22	2	5	-	-	-	-	**7**
23	2	1	-	-	-	4	**7**
24	-	1	-	-	2	4	**7**
25	7	-	-	-	-	-	**7**
26	5	1	-	-	-	-	**6**
27	7	-	-	-	-	-	**7**
28	2	2	3	-	-	-	**7**
29	-	1	1	-	3	-	**5**
30	-	1	-	-	3	1	**5**
31	-	-	2	4	-	-	**6**
32	5	-	-	-	-	-	**5**
Total	**117**	**44**	**23**	**13**	**8**	**13**	**218**

Table A.4 – Consumer location and types.

Annex B

Sensitivity Analysis of Proposed SA Methodology

The sensitivity analysis has been made to the proposed SA methodology considering two EVs heuristics in the Neighborhood scheme, because these EVs heuristics influence the behavior of the SA methodology.

The SA methodology has been run several times with different parameter values, until the SA algorithm obtained a constant low value for the fitness function. The SA methodology will be tested regarding the following parameters:

- Initial Temperature (T_0);
- Cooling rate (α);
- Number of iterations (*MaxIter*);
- Number of iterations at constant temperature (L).

For each test, the SA methodology has been run 50 times. The SA methodology with consecutive EVs allocation solved an optimal scheduling for 1000 EVs, and the SA with intelligent EVs allocation solved an optimal scheduling for 2000 EVs.

This analysis starts with the change of the initial temperature from 1 until 5000. Figure B.1 shows the results for the SA methodology considering the consecutive EVs allocation and intelligent EVs allocation. Figure B.1 a) shows the evolution of the objective function and execution time for the SA methodology with consecutive EVs allocation, and Figure B.1 b) presents the results for the SA methodology with intelligent EVs allocation.

a)

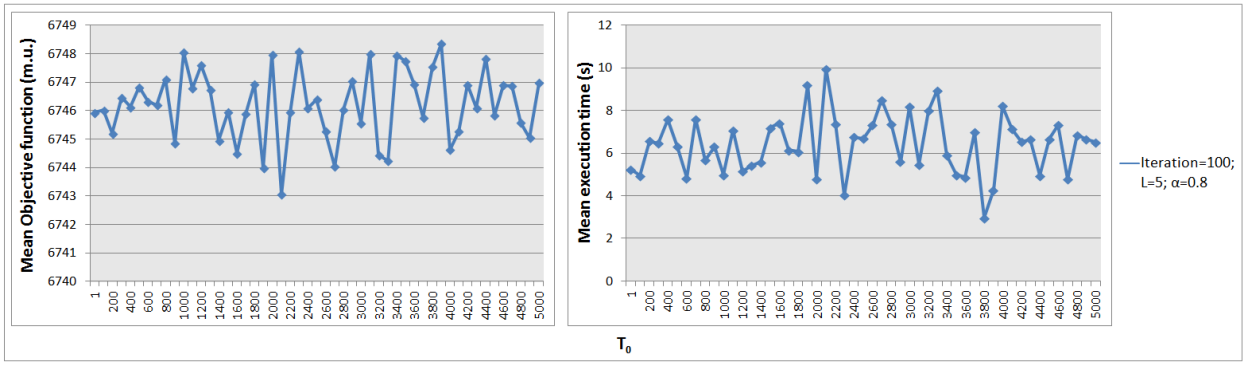

b)

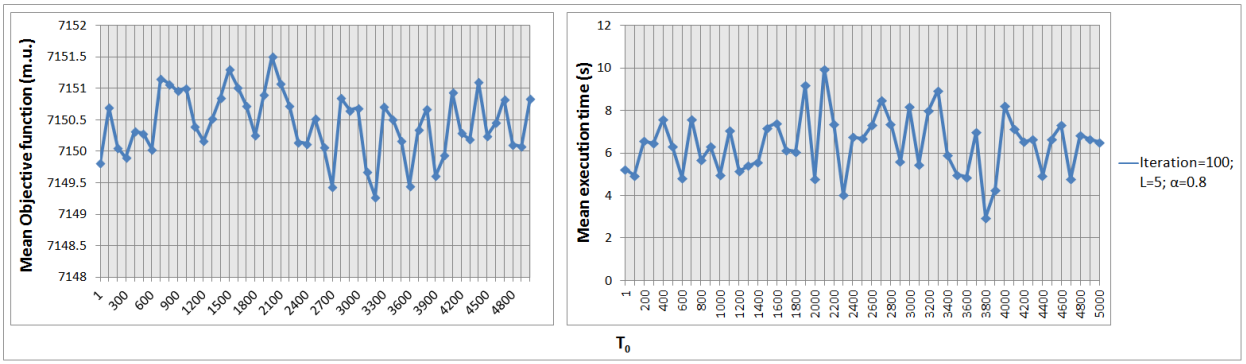

Figure B.1 – Sensitivity regarding the initial temperature with: a) consecutive EVs allocation, b) intelligent EVs allocation.

In Figure B.1 a) 2100 is presented as the best value for the initial temperature concerning the minimization of objective function. The change in the initial temperature did not result in a big difference in the execution time. In Figure B.1 b) 3200 is presented as the best value for the initial temperature in terms of objective function.

One can deduce from these two analyses that a high initial temperature represents good results in terms of objective function, because the acceptance probability increase and the SA could avoid more the local optima.

The second analysis had the purpose to test different values for the cooling rate. In this analysis it is considered the initial temperature value of the previous analysis. It has been tested the SA considering a cooling rate from 0.02 until 1. Figure B.2 illustrates the results for the SA methodology considering the consecutive EVs allocation and intelligent EVs allocation.

a)

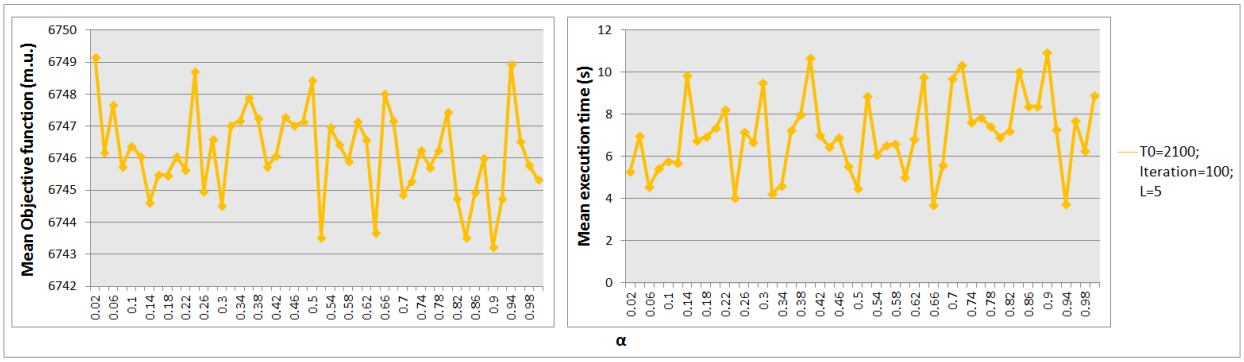

b)

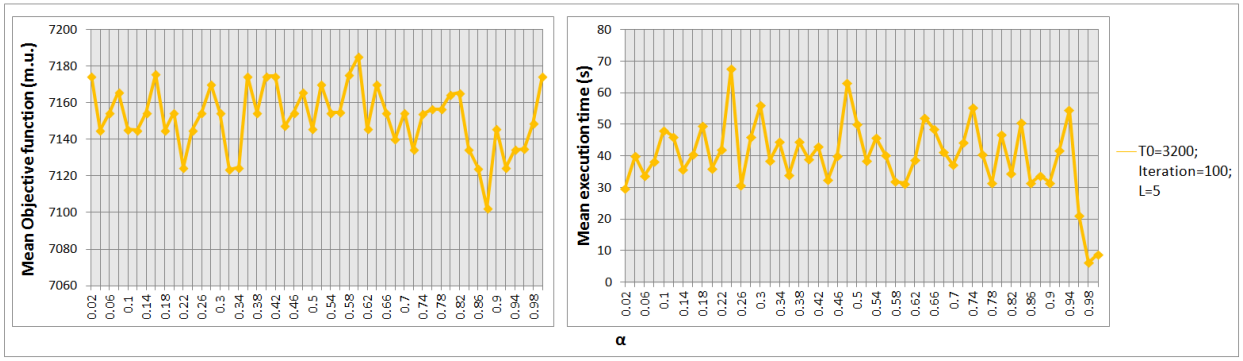

Figure B.2 – Sensitivity regarding the cooling rate with: a) consecutive EVs allocation, b) intelligent EVs allocation.

In Figure B.2 a) 0.9 is presented as the best value for the cooling rate in terms of objective function. In Figure B.2 b) 0.88 is presented as the best value for the cooling rate concerning the minimization of objective function.

In the third analysis the number of iterations has been changed from 1 until 100. In this analysis it is considered the initial temperature and cooling rate values of the previous analyses. Figure B.3 depicts the results for the SA methodology considering the consecutive EVs allocation and intelligent EVs allocation.

a)

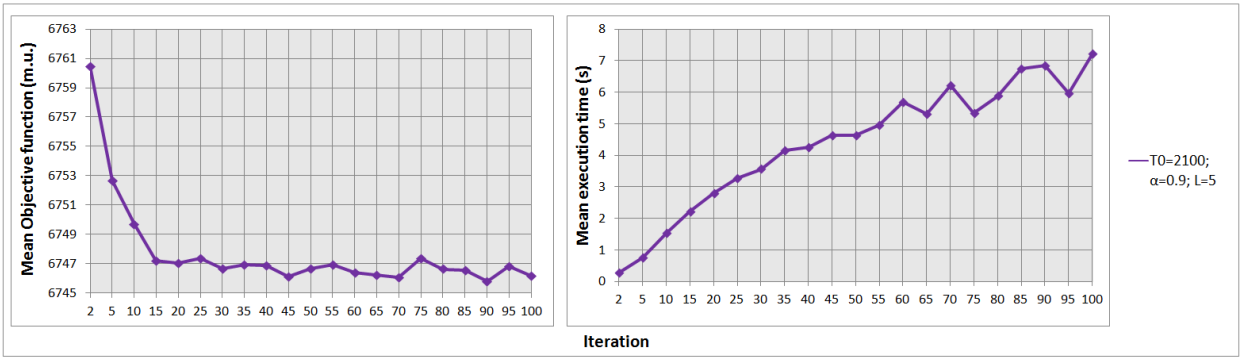

b)

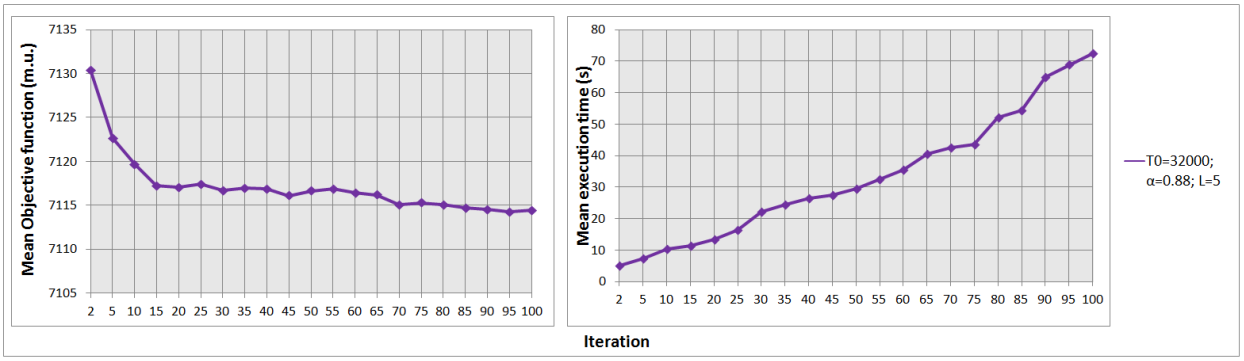

Figure B.3 – Sensitivity regarding the number of iterations with: a) consecutive EVs allocation, b) intelligent EVs allocation.

In Figure B.3 a) 90 is presented as the best value for the number of iterations in terms of objective function. The use of 90 iterations does not represent a significant increase in the execution time. In Figure B.3 b) 70 is presented as the best value for the number of iterations. It can be deduced from these two analyses that a high number of iterations helps finding more solutions for the SA methodology and it will influence directly the execution time.

In the fourth analysis the number of iterations at constant temperature has been changed from 1 until 50. In this analysis it is considered the initial temperature, the cooling rate and the number of iterations values of the previous analyses. Figure B.4 depicts the results for the SA methodology considering the consecutive EVs allocation and intelligent EVs allocation.

a)

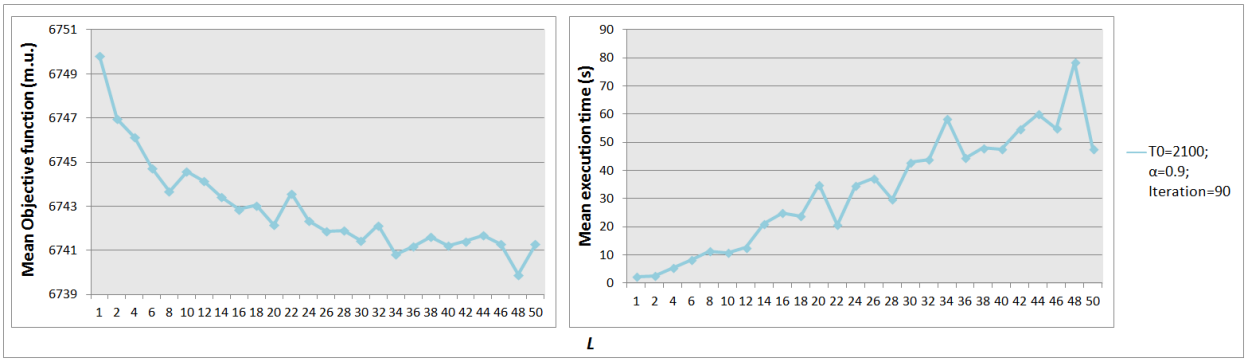

b)

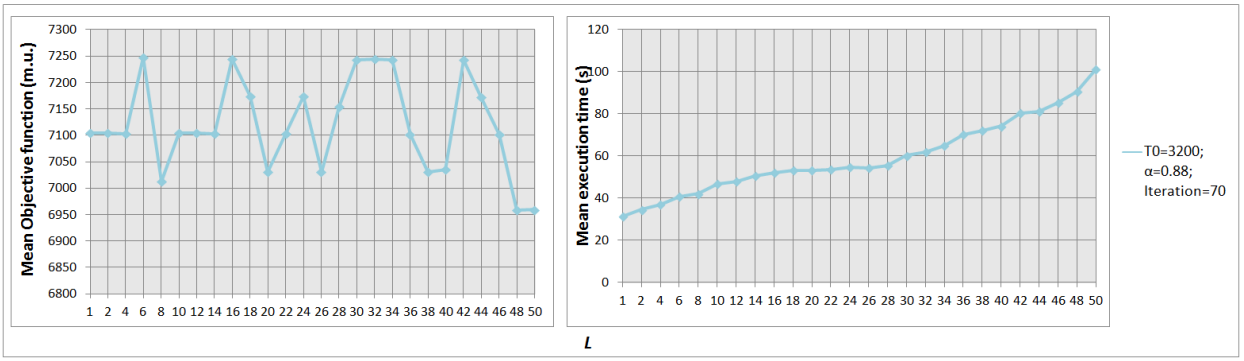

Figure B.4 – Sensitivity regarding the number of iterations at constant temperature with: a) consecutive EVs allocation, b) intelligent EVs allocation.

In Figure B.4 a), the value 8 has been selected as the best value for the number of iterations at a constant temperature. The best value should be the 48 iterations, but it will result in a much higher execution time. If the difference in terms of objective function between is analyzed between the 8 and 48, this difference is much lower than the different in terms of time. With a *L* of 8 the objective function is approximately of 6744 m.u. and the execution time is approximately of 10 seconds. With a *L* of 48 the objective function is approximately of 6741 m.u. and the execution time is around 80 seconds. The number of iterations at a constant temperature improves the probability of finding a new solution. So, with the purpose to maintain a good quality in terms of objective function but also maintains a low execution time would be better to use a *L* of 8.

In Figure B.4 b) 10 is presented as the best value for the number of iterations at a constant temperature for the same reasons explained before.

Table B.1 shows the best values for the SA parameters tested in the sensitivity analysis.

SA parameters	SA methodology	
	Consecutive EVs allocation	Intelligent EVs allocation
T_0	2100	3200
α	0.90	0.88
MaxIter	90	70
L	8	10

Table B.1 – Best values for the SA parameters.

Considering that is possible to use the consecutive and intelligent EVs allocation in the proposed SA approach, it is easier to demonstrate when is possible to use one heuristic or another. Using the proposed SA approach with the two EVs allocation several scenarios since 500 until 3000 EVs have been solved.

Table B.2 shows the execution time and operation cost for the SA approach considering the consecutive and intelligent EVs allocation heuristic. The first one is suitable for scenarios with a small number of EVs, such as 500 and 1000 EVs. In these two scenarios the consecutive EVs allocation presents a closer solution when compared with the SA approach using intelligent EV heuristic. These two heuristics show similar results in terms of objective function but the consecutive presents a low execution time in 500 and 1000 EVs.

Number of EVs	Operation cost (m.u.)		Execution time (seconds)	
	Consecutive EVs allocation	Intelligent EVs allocation	Consecutive EVs allocation	Intelligent EVs allocation
500	6,373.50	6,338.7	9.64	18.45
1000	6,591.90	6,484.90	10.25	29.20
2000	7,526.30	7,154.45	8.98	54.47
3000	7,954.35	7,686.10	24.54	74.54

Table B.2 – Results of SA approach with consecutive and intelligent EVs allocation.

In opposite the SA approach with intelligent EVs allocation is more suitable for a large number of EVs, and the consecutive EVs allocation is suitable for a small number of EVs. The consecutive EV allocation should be used for scenarios of less than or closer to 1000 EVs, and the intelligent EVs allocation should be adopted for the other scenarios with more than 1000 EVs.

Annex C

Evaluation of Uncoordinated Charging

Figure C.1 and Figure C.2 shows the load diagram and EVs charge in each hour for the 1000_EV_UnC and 2000_EV_UnC. It is possible to identify the hours with higher demand power in both scenarios.

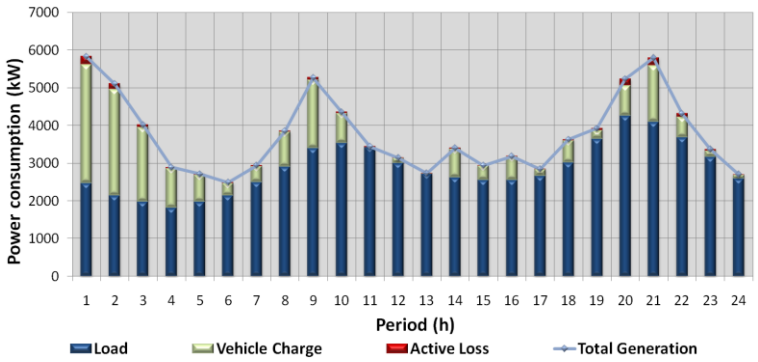

Figure C.1 – Load and EVs charging power of uncoordinated mode for 1000_EV_UnC.

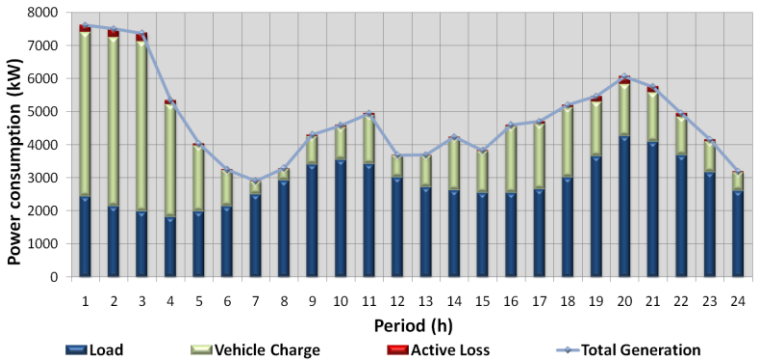

Figure C.2 – Load and EVs charging power of uncoordinated mode for 2000_EV_UnC.

Figure C.3 shows the generation power that VPP bought from the external suppliers. The VPP used the external suppliers' offers until reach the thermal line limit between bus 0 and 1, mainly it has been used with more intensity in the 2000_EV_UnC. Using the LMP information is possible to identify the hours with higher price due to the large amount of energy to charge the EVs. For instance, in the 2000_EV_UnC the LMP achieve the maximum value of 0.15 m.u./kWh in the hours with the biggest energy required the EVs. The LMP achieves the maximum of 0.15 m.u./kWh because the VPP had to use all the external suppliers, even the more expensive one with a offer of 0.15 m.u./kWh.

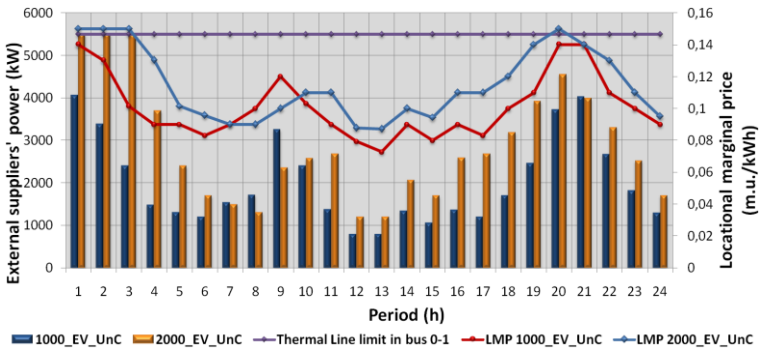

Figure C.3 – External suppliers' power for the uncoordinated charging.